A STUDY OF TWENTY-ONE SHARP-LINED NON-VARIABLE COOL PECULIAR A STARS

Thesis by

Saul Joseph Adelman

In Partial Fulfillment of the Requirements

for the Degree of Doctor of Philosophy

California Institute of Technology

Pasadena, California

1972

(Submitted December 17, 1971)

בראשית

ACKNOWLEDGEMENTS

The author wishes to express his most sincere thanks and appreciation to his advisor, Dr. George W. Preston, III, for his interest, continued guidance, and invaluable advice without which this research could not have been completed.

I thank the mountain staffs of Mt. Wilson and Palomar Observatories especially the night assistants for their cooperation and hospitality and the Director of the Hale Observatories for my observing time.

The author appreciates the efforts of Caltech's Astro-electronics Laboratory, especially Larry Blakeé, Maynard Clark, and Gene Longbrake, on his behalf.

For their help and advice, I thank the faculty and my fellow students of the Department of Astronomy at Caltech and of Hale Observatories, especially Drs. James E. Gunn, A. R. Hyland, and W. L. W. Sargent. I acknowledge the fellowship of the Robinson third basement, my fellow graduate students and our local expert, Dr. Dorothy Davis Locanthi, who has been a constant source of encouragement, information, and cheer.

My financial support came from an NDAE Title IV Fellowship (1966-1969), ARCS Foundation Fellowship (1970-1971), the California Institute of Technology (Graduate Research Assistantship - summers and 1970-1971 and a Graduate Teaching Assistantship 1969-1970), and my parents Mr. and Mrs. Benjamin Adelman.

I am indebted to my father Mr. Benjamin Adelman who introduced me to astronomy and has encouraged my interest for the past twenty-odd years.

My deepest gratitude belongs to my wife Carol for her sacrifices and encouragement. She helped with a variety of time consumming tasks, typing, and lots of tender loving care. Without her help, this work would not have been completed so quickly.

ABSTRACT

Elemental abundance analyses have been performed for twenty-one cool Ap stars, also known as SrCrEu stars, which are not known to be spectrum variables and whose projected rotational velocity is not greater than 10 km/sec. Zeeman and thermal Doppler broadening are the basic line intensification mechanisms considered. Effective temperatures estimated initially from UBV photoelectric data are modified by requiring that the iron abundances derived from both neutral and singly-ionized lines be equal. Log g has been assumed to be 4.0. In addition, two normal stars have been included in this study for comparison.

The cool Ap stars, in general, have normal or over-abundances with respect to hydrogen for every element studied. The iron abundance is found to increase with effective temperature. Similar dependences are found for chromium, manganese, neodymium, gadolinium, and, perhaps, several other elements. The abundances are not dependent on the apparent rotational velocity or magnetic field strength.

The elemental abundances are similar to those of the SrCrEu spectrum variables and agree reasonably well with the results of other studies of cool Ap stars. Comparisons with Mn and Si stars are similar to but not identical with those of other investigators. Substantial differences in certain abundance ratios are found which distinguish Am and cool Ap stars. The results of low dispersion classification spectroscopy correlate better with the appearance than with the derived

abundances. The agreement between photometric indices and abundances is poor. Several stars are found whose properties are similar to those of Si stars studied by Sargent, Searle, and Lungershausen except with regard to their [Cr/Fe] values. Thus, in addition to the fact that both types have magnetic fields, the abundances indicate that the Si and cool Ap stars are probably closely related.

The theories to account for the Ap star elemental abundances have difficulties in explaining the results of this study. The diffusion mechanism and the magnetic accretion hypothesis of Havnes and Conti cannot explain several features, for example, the abundance ratios of certain adjacent elements, and are at best incomplete. On the basis of the latter theory, it is hard to understand why the abundances are not correlated with magnetic field strength. Some features of the abundance anomalies are similar to those produced by the r- and by the s-processes. Theories which require mixing of the Ap star or binary companions are excluded.

TABLE OF CONTENTS

Table of Contents (continued)

I. INTRODUCTION

The study of A-type stars with peculiar spectra began at the turn of the century (Maury 1897, Cannon 1901, Lockyer and Baxandall 1906). During the next few years, unusual enhanced lines in these abnormal stars were identified, for example, Baxandall (1913) found lines of EuII in α^2 Canum Venaticorum. Many years later Morgan (1933) showed that the brighter early type stars with spectral pecularities formed a well-defined group whose members showed spectral anomalies that seemed to be correlated with surface temperature.

The colors of Ap stars are similar to those of normal stars in UBV photometry, but for some, substantial differences can be found using Strömgren photometry (Cameron 1966). They are young objects (Jaschek and Jaschek 1967) and are intrinsically slow rotators (Searle and Sargent 1967).

Abundance analyses of peculiar A stars date back to at least 1940 when Bunker studied eight of them. Since that time other investigators have shown by analyses of individual stars and by surveys of selected elemental abundances that the overabundances inferred from the enhanced lines are real and added details about the abundances of the elements, especially those whose lines can be detected only on high dispersion spectrograms.

On the other hand, certain authors believe that the observed abundances are not real, but caused by mechanisms such as non-LTE

effects (Underhill 1969). Others have not realized that Zeeman intensification due to the magnetic fields enhances some lines with respect to others. However, peculiar A stars possess atmospheres similar to those of normal stars (Hyland 1967, Durrant 1970a, Mihalas and Henshaw 1966, Baschek and Oke 1965, Jugaku and Sargent 1968) since the continuous energy distributions and the profiles of the Balmer lines of these two types of stars are indistinguishable. In addition, peculiar A and normal stars with similar energy distributions and Balmer line profiles have the same degree of ionization when the SiIII/SiII ratio is used as a test (Sargent and Searle 1967). The abundance analyses of the Ap stars show that all lines of an ion give similar abundances. On this basis, the magnetic fields of Ap stars do not greatly affect the atmospheric structure. These facts imply that the abundances are real.

Each major subgroup of the Ap stars, Mn, Si, and cool Ap stars, has its own pattern of abundance anomalies (Sargent and Searle 1967). The explanation of these anomalies is a very controversial subject. Four basic types of theories have been developed: they invoke surface nuclear reactions, interior nuclear reactions, diffusion processes, and selective magnetic accretion.

The phenomenon of spectrum variability was also found early (Lundendorff 1906, Belopolsky 1913) as was that of light variability (Guthnick and Prager 1914). The archetype star was α^2 CVn. In spectrum variables lines of certain elements periodically vary in strength in a manner not compatible with temperature or electron pressure changes.

Often the spectrum variations are accompanied by those of light and radial velocity with the same period. The extrema of light and spectrum variations coincide in phase. All elements do not participate to the same degree and in some stars there are elements which vary in antiphase with others (Preston 1971c).

In 1946, Babcock (1947) first detected a stellar magnetic field in the Ap star 78 Vir (HD118022). In the following years, Babcock surveyed many kinds of stars especially those of A-type. This work led to a catalog (Babcock 1958, 1960) with approximately 90 entries of which 70 are Ap stars. He found that most Ap stars possess measurable magnetic fields if their lines are not greatly broadened by rotation and that all stellar magnetic fields are variable, some being periodic. These magnetic periods are the same as those of light and spectrum variability. Several models have been formulated to explain magnetic phenomenon, the most successful of which has been the oblique rotator model (Stibbs 1950, Deutsch 1954, 1958) which received strong support from the discovery that the line widths of periodic Ap stars tend to vary inversely with their periods (Deutsch 1956).

The properties of the Mn subgroup and the Si and SrCrEu subgroups are different in regard to 1) magnetic properties, the Mn stars being non-magnetic, 2) abundance anomalies, 3) spectrum, light, and magnetic variability, none found for Mn stars, and 4) incidence of spectroscopic binaries, the Mn stars having a significantly higher rate than the other Ap stars. On these bases, it is suggested that they form two subdivisions of the Ap stars (Preston 1971c, Sargent and Searle 1967,

Guthrie 1969a). The separation of the magnetic Ap stars into the Si and SrCrEu stars may be an effect of the effective temperature.

I have chosen to study elemental abundances of the cool Ap stars (SrCrEu, SrCr, Cr, Sr, SrCr, and EuCr stars) which have very interesting although complex spectra in the photographic region. This group is defined approximately as those for which $B-V \gtrsim 0.0$. There are only a few coarse and fine analyses of them. Surveys have been restricted to a few elements in limited samples of these stars. A study of many of the elemental abundances would unite this work and provide a good basis of comparison with other types of stars and with the predictions of the theories of abundance anomalies for Ap stars.

For this survey, I excluded spectrum variables. Without detailed study, it is not known which phase, if any, is representative of the surface as a whole. Furthermore, the probable non-uniformity of the abundance distributions complicates the analyses of the spectra observed in integrated light.

I restricted my attention to sharp-lined stars because sharp lines simplify the process of line identification, especially those of line blends, and allow the detection of weak lines. I chose to study the 21 non-variable cool Ap stars with apparent rotational velocities not greater than 10 km/sec for which estimates of the surface magnetic field strengths are available (Preston 1971a). In most previous studies, a microturbulent velocity parameter has been derived in the abundance analysis and is in some instances inconsistent with the estimates of the line widths. By assuming that Zeeman and thermal Doppler

broadening are the major sources of line intensification, I calculate an effective microturbulent velocity parameter that differs from line to line. If the shape of the curve of growth and the amount that its axes shift with microturbulent velocity are known, all equivalent widths can be reduced to a common effective microturbulent velocity.

The wavelength region studied was restricted to part of the photographic region of the spectrum where many important elements have lines. In addition to the Ap stars listed in Table I-1, I included two normal sharp-lined A stars, ν Cap and o Peg, as a control on the methods of analysis. From these basic considerations I formulated the problems to be solved based on the results of the abundance analyses.

The purpose of this study is to analyze the elemental abundances of these twenty-one sharp-lined cool Ap stars and to ascertain

a) the dependence of the abundances on effective temperature, magnetic field strength, and apparent rotational velocity,

b) how these results compare with those of low dispersion classification spectroscopy and of photometric criterion derived from Strömgren photometry, and, most importantly

c) if these results, when compared with those deduced for normal late B and early A type stars, the sun, spectrum variables, other non-variable Ap stars, and metallic lined stars can be understood in the context of the diffusion hypothesis, nuclear theories, and the magnetic accretion hypothesis which purport to explain the derived abundances.

In this paper, I adopt a few conventions. If the star is one of the twenty-one sharp-lined cool Ap stars studied, it will be referred to by its number in the Henry Draper catalog while the two normal stars will be referred to by name. The units are in the cgs system except when noted; for example, the wavelength is always given in Angstroms. The cool Ap stars will also be referred to as SrCrEu stars.

Table I-1 is the observational data on the 21 cool Ap stars studied. Columns 1 and 2 give the HD number and name, column 3 the apparent rotational velocity in km/sec from Preston (1971a), columns 4, 5, and 6 the UBV colors from studies by Abt and Golson (1962), Cowley, Cowley, Jaschek, and Jaschek (1969), Eggen (1967), Osawa (1965), and Stepien (1968), column 7 the Ap subclass from Cowley et al. (1969) or Preston (1971a), and column 8 the surface magnetic field strength, H_s, in kG from Preston (1971a). HD81009 is a visual binary whose components are too close to be easily separated. It was analyzed as if it were a single star.

TABLE I-1: OBSERVATIONAL DATA FOR THE SrCrEu STARS

HD	Name	v sin i	V	B-V	U-B	Ap Class	H_s
(1)	(2)	(3)	(4)	(5)	(6)	(7)	(8)
2453		≤6	6.9	+0.08	+0.03	SrCrEu	3.8
5797		≤6	8.6	+0.24	+0.15	SrCr	1.8
8441		≤6	6.6	0.00	+0.13	SrCrEu	0.0
12288		≤6	7.9	+0.09	+0.03	Cr	7.0
18078		≤6	8.2	+0.21	+0.17	SrCrEu	3.8
22374	9 Tau	7	6.7	+0.13	+0.11	CrSr	0.5
50169		<10	9.0	0.00	-0.03	SrCr	5.6
81009	HR3724	<10	6.5	+0.22	+0.09	SrCrEu	7.9
89069		7	8.1			SrCrEu	2.3
110066	HR4816	≤6	6.3	+0.07	+0.02	SrCrEu	3.6
111133	HR4854	10	6.4	-0.05	-0.06	SrCrEu	3.7
118022	78 Vir	10	5.0	+0.03	0.00	SrCr	2.9
137909	β CrB	≤3	3.7	+0.27	+0.11	SrCrEu	5.5
137949	33 Lib	10	7.2	+0.38	+0.14	SrCrEu	4.6
165474		≤6	7.4			SrCrEu	6.6
176232	10 Aql	≤6	5.9	+0.25	+0.09	SrCr	2.1
191742		≤6	7.8	+0.22	+0.20	SrCrEu	1.8
192678		≤6	7.3	-0.02	-0.01	Cr	4.6
201601	γ Equ	≤3	4.8	+0.26	+0.10	SrCrEu	1.8
204411	HR8216	≤6	5.3	+0.09	+0.15	CrEu	0.5
216533		7	7.9	+0.08	+0.10	SrCr	2.3

II. ELEMENTAL ABUNDANCE DETERMINATIONS

A. Introduction

In the magnetic Ap stars, each line is broadened by its particular Zeeman pattern. In a coarse analysis such broadening can be treated to first approximation as a pseudo-microturbulence that is peculiar to each line. For these stars, I have assumed that there are no sources of classical microturbulence, i.e., mass motions of turbulent elements whose size is small respect to the mean free path of a photon. This treatment, which differs from most previous ones, is suggested by high dispersion studies of HD137909, HD188041, and HD201601 (Preston 1967a, 1967b; Wolff 1968; Preston and Cathey 1968; Evans 1966) which show that the Zeeman effect is responsible for most of the line broadening in these objects.

Rotation and macroturbulence, which results from mass motions of elements whose size is large with respect to the photon mean free path, affect the profiles but not the equivalent widths of the lines. Line broadening mechanisms (Aller 1963) include: 1) radiation damping due to the finite lifetimes of the excited states, 2) thermal broadening due to the random kinetic motions of the atoms, 3) Stark broadening which results from the interaction of the absorber with electrons and ions, and 4) Van der Waals broadening which results from the interaction of the absorber with neutral atoms, especially H and He, or molecules of a different kind.

To simplify the analysis, I determined what measured equivalent width would result if the magnetic fields were turned off. This requires calculation of the factor by which the equivalent width of a line with a given pseudo-microturbulent velocity must be divided to reduce its value to the case of zero microturbulence. This factor can be found by shifting the axes of the curve of growth and comparing the results at a given abundance.

To obtain the abundances requires that we know the proper effective temperature and gravity. The value of the latter has been assumed to be log g=4.0 which is based on studies by other investigators. I require that the adopted mean Fe abundances deduced from both FeI and FeII lines be the same. This condition is used to modify the effective temperatures initially estimated from UBV photoelectric data. My calculations resulted in plots of effective temperature vs. equivalent width with contours of constant abundance. By use of these plots, the abundances are determined.

B. Generation of the Grid of Model Atmospheres

The computer program ATLAS (Kurucz 1969a,b) generated the model atmospheres used in this research. The resultant models include opacities due to the hydrogen lines except the Lyman series, Rayleigh scattering from H and He, and the following elements and ions: HI, HeI, HeII, H^-, SiI, MgI, AI, C, N, and O. Radiative, hydrostatic, and local thermodynamic equilibrium as well as a uniform composition were assumed. A grid of eight model atmospheres with effective temperatures

between 7500°K and 11000°K were calculated for two values of the gravity, log g = 3.5 and 4.0. The primary abundance determinations were done for the latter value. Tables II-1 and II-2 give physical properties of the models for τ_{5000}=.316 where T_{eff} is the effective temperature; T, the temperature at the level considered; θ = 5040/T; P, the pressure; N_e, the electron density; P_e, the electron pressure; κ, the opacity; and the height of the level above optical depth unity. In most models, there exists a thin convective region in the uppermost layers of the atmosphere which was treated as one in radiative equilibrium in this study.

For some program stars, the Hγ profile can be measured fairly accurately. However, for others, a great line density makes this determination very difficult. Wolff (1967a) by use of Hγ profiles found that the normal and peculiar A stars have similar values for their gravities. Sargent, Strom, and Strom (1969) found a value of log g = 4.3 for the cool Ap star HD204411. Popper (1959) used four eclipsing systems of two detached A-type stars to determine that the main sequence stars in this temperature range have values of log g between 4.0 and 4.4. This result agrees with those of Schild, Peterson, and Oke (1971) who found that log g = 4.05 for Vega and log g = 4.35 for Sirius. In addition, Adelman (1972) found log g =3.75 for ν Cap and Conti and Strom (1968b) found values between log g = 3.7 and 4.0 for four field A stars. Thus, the value of log g for main sequence stars, must be close to 4.0 and, by implication from Wolff's results, also for the Ap stars.

TABLE II-1: PHYSICAL CONDITIONS FOR LOG g=4.0 MODEL ATMOSPHERES WITH SOLAR METALS ABUNDANCE AT τ_{5000}=.316

T_{eff}	T	θ	P	N_e	P_e	log P_e	κ	log κ	height(km)
7500	6989.0	0.721	1.73×10^{4}	5.97×10^{13}	5.76×10	1.760	.543	-.266	1.25×10^{2}
8000	7628.5	0.661	1.01×10^{4}	1.21×10^{14}	1.27×10^{2}	2.104	1.05	.021	1.13×10^{2}
8500	8320.4	0.606	5.75×10^{3}	2.10×10^{14}	2.41×10^{2}	2.382	2.28	.358	1.06×10^{2}
9000	8926.5	0.565	3.16×10^{3}	2.78×10^{14}	3.42×10^{2}	2.534	4.62	.665	1.27×10^{2}
9500	9442.8	0.534	1.83×10^{3}	2.95×10^{14}	3.84×10^{2}	2.584	7.76	.890	2.03×10^{2}
10000	9870.7	0.511	1.14×10^{3}	2.63×10^{14}	3.58×10^{2}	2.554	9.86	.994	3.70×10^{2}
10500	10258.1	0.491	8.21×10^{2}	2.24×10^{14}	3.17×10^{2}	2.501	10.20	1.009	6.02×10^{2}
11000	10622.2	0.474	6.79×10^{2}	1.97×10^{14}	2.89×10^{2}	2.461	9.50	.978	8.16×10^{2}

TABLE II-2: PHYSICAL CONDITIONS FOR LOG g=3.5 ATMOSPHERES WITH SOLAR METALS ABUNDANCE AT τ_{5000}=.316

T_{eff}	T	θ	P	N_e	P_e	log P_e	κ	log κ	height(km)
7500	7065.7	0.713	7.33×10^{3}	4.47×10^{13}	4.36×10	1.64	.419	-.38	3.72×10^{2}
8000	7722.3	0.653	4.32×10^{3}	8.84×10^{13}	9.42×10	1.97	.883	-.05	3.12×10^{2}
8500	8387.5	0.601	2.31×10^{3}	1.40×10^{14}	1.62×10^{2}	2.21	2.01	.30	3.19×10^{2}
9000	8967.5	0.562	1.21×10^{3}	1.64×10^{14}	2.03×10^{2}	2.31	4.00	.60	4.77×10^{2}
9500	9430.0	0.534	6.96×10^{2}	1.52×10^{14}	1.98×10^{2}	2.30	5.77	.76	9.24×10^{2}
10000	9851.2	0.512	4.52×10^{2}	1.26×10^{14}	1.71×10^{2}	2.23	6.24	.80	1.72×10^{3}
10500	10229.2	0.493	3.57×10^{2}	1.07×10^{14}	1.51×10^{2}	2.18	5.82	.76	2.51×10^{3}
11000	10597.5	0.476	3.22×10^{2}	9.84×10^{13}	1.44×10^{2}	2.16	5.30	.72	3.07×10^{3}

The rigid rotator model requires that a major fraction of the Ap stars have radii exceeding those of the zero-age main sequence by a factor around two (Preston 1970b) although the youngest association with a classical Ap star Lac OB1 (Adelman 1968) has a λ4200-Si star slightly below its main sequence. Doubling R decreases g by a factor of four and log g by .60. So if we believe the predictions of the rigid rotator model, the zero-age main sequence in the region under consideration must lie near log g=4.5 while most of the observed stars have values of log g near 4.0. Sirius must be the least evolved A star of those cited above. The mass of Sirius A is 2.1 $M_\odot$ (Harris, Strand, and Worley 1963). A 2.25 $M_\odot$ model (Iben 1967a) has log g=4.47 on the zero-age main sequence. Log g decreases by .06 dex in the next 10^8 years of evolution which is more time than that required for a 5 $M_\odot$ star to complete its evolution to the white dwarf stage (Iben 1967b). The width of the main sequence is about .43 dex in log g which implies that ν Cap is probably somewhat evolved.

C. Determination of Microturbulent Velocities

The microturbulent velocities observed in the cool Ap stars are assumed to have been caused primarily by Zeeman broadening. For stars with large magnetic fields, the addition of one km/sec or so of microturbulence would not greatly change the derived abundances. Nevertheless, it would in stars with small magnetic fields such as HD201601. However, Preston and Cathey (1968) set an upper limit of 3.3 km/sec on its microturbulent velocity while Evans and Elste (1971) suggest a

third of that value at most. For the lines examined in this star, the pseudo-microturbulent velocity is usually between 0.5 and 2 km/sec. For the normal stars, I used 3 km/sec. This estimate is based on the following values: 2.75 km/sec for ν Cap (Adelman 1972), 2.5 to 3.0 km/sec for four field A stars (Conti and Strom 1968b), 2.9 km/sec for α CMi (Danziger 1966), and 3.1 km/sec for α Lyr (Baschek and Searle 1969) (see also Baschek and Reimers 1969).

The stellar magnetic fields given in Table I-1 are from Preston (1971a) except for HD12288 whose value was determined from the splitting of FeII(27) λ4385.38 which is a resolved doublet on the coudé plate Pb11997. The value of the magnetic field strength used is the mean surface field, H_s, which is insensitive to aspect and whose derived values are based on resolved doublets for stars with large values of H_s and on differential Zeeman broadening for stars with small values of H_s. The errors in the derived values are estimated to be 1 kG or more for those stars with $H_s \lesssim 3$kG.

For allowed Zeeman components in LS coupling, the wavelength displacement in Å, $\Delta\lambda_H$ is given as (Bray and Loughhead 1965):

$$\Delta\lambda_H = 4.667 \times 10^{-13}[(g_1-g_2)M_1 - g_2(M_2-M_1)]\lambda^2 H \qquad \text{(II-1)}$$

where g is the Landé factor, M the magnetic quantum number, H the magnetic field strength in Gauss, and 2 and 1 refer to the upper and lower levels, respectively. The selection rule is $\Delta M = M_2 - M_1 = 0$ for the π components and $\Delta M = \pm 1$ for the σ components.

The symbol z is used to designate the mean value of the bracket in equation (II-1) weighted by the components relative strengths, i.e., z is the centroid of the σ components of the Zeeman pattern. If we equate $\Delta\lambda_H$ with the Doppler half-width, then

$$\Delta\lambda_H = 4.667 \times 10^{-13}\ z\lambda^2 H = \lambda v/c \qquad \text{(II-2)}$$

and

$$v = 1.40 \times 10^{-4}\ z\lambda H \qquad \text{(II-3)}$$

where H is in kG, λ in Å, v in km/sec, and c is the speed of light. Formula (II-3) is used as a crude algorithm to calculate the pseudo-microturbulent velocity v due to Zeeman broadening.

For most lines the term classifications are taken from the Revised Multiplet Table (Moore 1945) and the Zeeman patterns from Kiess and Meggers (1928). For some lines I used the techniques given in this last source to calculate them. As an aid in determining z, I used Russell's (1927) rule. A few z values are from Preston (1970a). The following ions required additional sources: MnII-term classifications (Curtis 1952; Auer, Mihalas, Aller, and Ross 1966), GaII-term classifications (Bidelman and Corliss 1962), SmII-Landé g values (Albertson 1936), OsI-term classifications (Meggers, Corliss, and Schribner 1961), and UII-Landé g values (Osman 1966).

D. Choice of Spectroscopic Plates

The spectrograms used in this study are 4.5Å/mm IIa-O coudé plates obtained by Preston primilarily for use in his study of

rotational velocities of peculiar A stars either at Lick or Palomar Observatories. The plates of ν Cap, measured previously for a fine analysis (Adelman 1972), were obtained at Palomar by Deutsch and at Mt. Wilson by Searle (Ce 15468 and Ce 15469 at 10 Å/mm) and by the author. There is some variation in plate quality. For six of the fainter stars, there was just one plate available. For some of the brighter stars, 2Å/mm plates could have been used, but they were not in order to have survey uniformity. Table II-3 lists the plates used and the dates of observation.

E. Line Identification Techniques

The spectra of many of the program stars are complicated and difficult to interpret due to much blending. In normal A-type stars, for example ν Cap, the last point, longward of the Balmer jump where the true continuum is seen, occurs between Hε and Hδ. On the other hand, it probably occurs between Hδ and Hγ in some of the cool Ap stars. In general above the Balmer jump, the shorter the wavelength examined on a IIa-O plate of a cool sharp-lined Ap stars, the worse the line blending problem becomes.

In a major survey it is expedient to choose the smallest wavelength range which yields the largest number of useable lines of the most elements. I initially chose $\lambda\lambda$4200-4635. The long wavelength end point was selected by the following considerations: 1) the Lick coudé plates used extend to about λ4650 and the plate ends tend to be of lower quality than plate centers, 2) the number of interesting lines

TABLE II-3: SPECTROGRAMS USED IN THIS STUDY

Star	Plate	Date of Observation
HD2453	Pb11256	August 26/27, 1969
HD5797	Pb11412	October 30/31, 1969
HD8441	Pb11272	August 28/29, 1969
HD12288	Pb11997	October 20/21, 1970
HD18078	Pb11421	October 31/1, 1969
HD22374	Pb11414	October 30/31, 1969
HD50169	Pb11697	March 23/24, 1970
HD81009	Pb11689	March 21/22, 1970
HD89069	Pb11746	May 14/15, 1970
HD110066	ECZ6561	May 3/4, 1968
HD111133	Pb11699	March 23/24, 1970
HD118022	ECZ6562	May 3/4, 1970
HD137909	ECZ5021	June 2/3, 1966
HD137949	Pb11695	March 21/22, 1970
HD165474	Pb11247	August 25/26, 1969
HD176232	Pb11260	August 27/28, 1969
HD191742	Pb11271	August 28/29, 1969
HD192678	Pb11153	July 1/2, 1969
HD201601	Pb11261	August 27/28, 1969
HD204411	Pb11254	August 26/27, 1969
HD216533	Pb11255	August 26/27, 1969
ν Cap	Ce15468	June 7/8, 1962
	Ce15469	June 7/8, 1962
	Ce19935	September 3/4, 1969
	Pb9376	May 5/6, 1966
	Pb10235	August 19/20, 1967
	Pb10237	August 19/20, 1967
	Pb10248	August 21/22, 1967
o Peg	Pb11265	August 27/28, 1969

beyond λ4635 is few, and 3) the number of measured oscillator strengths for Fe peak elements is relatively small for lines in this region. To include some important elements in this study and to ascertain whether lines of PmII, OsI, OsII, PtII, ThII, and UII were present, I investigated lines in other selected regions on the plates.

Guided by these considerations, I measured all plates on the Grant Machine between λ3850 and λ3870 and between λ3968 and the long wavelength end of the plate. I used an intensity mode microphotometer tracing of the spectra with a dispersion of 2 Å/inch as a guide in measuring the features. As I made a measurement, I annotated the tracing. In this manner, I recorded what was measured. For complicated features, I measured various subparts. With the Grant Machine, one can theoretically measure a position to better than one micron or to within .005 Å on a 4Å/mm plate.

The comparison lines were used to determine the wavelengths of the features in the stellar spectra. I used the hydrogen lines to obtain a crude radial velocity which was refined using line identification lists of normal A stars (Wright, Lee, Jacobson, and Greenstein 1964) supplemented by those of HD188041 (Bidelman 1971a).

The primary source of line identifications is the Revised Multiplet Table (Moore 1945). I used the two lists mentioned above as well as Meggers et al. (1961) and some for specific elements. Line intensities and excitation potentials were used as a guide to identification. By measuring positions in assymetric features, I determined the identity of many blend components. For the normal

stars, I used the line identifications from Adelman (1972) for ν Cap and from Maestre and Deutsch (1961) for o Peg.

This paper includes no line identification lists for the peculiar A stars studied because they are far too long, their accuracy needs to be checked by analyzing additional lines and by measuring additional plates, and they are in fairly good agreement with those that are already available, namely a) HD111133 (Wolff 1971), b) HD137909 (Hiltner 1945), c) HD176232 (Auer 1964), d) HD201601 (Bidelman 1971b), and e) HD204411 (Sargent et al. 1969). This agreement is a function of the completeness and the quality of the comparable studies. Auer's list is only for unblended lines while the others are more complete. Disagreements occur mainly in the identification of weaker features. However, there exist a fair number of moderately strong lines without good identifications.

After I completed the line identifications, I decided that the best way to choose a set of lines for equivalent width measurement was to determine which lines in the region studied had reasonably good profiles and oscillator strengths in several program stars, primarily, HD2453, HD5797, HD22374, HD110066, and HD191742. From this list, I chose for abundance determinations those lines which had the best line quality in the majority of stars. These decisions were tempered by the desirability of obtaining elemental abundances in the normal stars and of having several lines per ion.

F. Measurement of the Equivalent Widths

For use in this study I produced two types of intensity mode tracings, one for line identifications and the other for equivalent width measurements. The spectra were calibrated every 200 Å. Considerable overlap was allowed between sections of the spectra run with different calibrations. For equivalent width measurements, I made two tracings of the spectra with dispersions of 4 Å/inch and 1 Å/inch and one of the clear plate with a chart dispersion of 15 Å/inch for each calibration region. The tracings covered λλ3840-4650.

For each calibration region, I drew a line through the clear plate tracing that best represented its variation with wavelength which was required to be a smooth function. Then this determination was drawn under the 1 Å/inch spectrum.

In order to establish the continuum level, I examined the 4 Å/inch spectral tracings. The three highest points were averaged for every 1 inch interval for the 4140 Å, 4340 Å, and 4540 Å regions. These averages were then used as a guide for drawing the continuum which was transferred to the 1 Å/inch spectrum where it was adjusted if it seemed necessary. The continuum placement started with the 4540 Å calibration region. As there is an overlap with the 4340 Å calibration, I transferred the continuum from the 4540 Å 4 Å/inch spectra to that of the 4340 Å region in order to insure continuity. If adjustments were necessary, I worked with both continua to obtain it. The continuum near Hγ had to be such that both wings of this line had

the same profile. I used a similar transfer procedure from the 4340Å to the 4140 Å region. For lines measured in the 3940 Å calibration region, I drew the best local pseudo-continuum.

Measured half-widths vary from line to line in stars with strong magnetic fields. This is quite important when line profiles are drawn, especially for stars such as HD12288 and HD81009. Using the line cores and the wavelength measurements, I constructed symmetric profiles. For strong lines, I tried to include the line wings. It was often difficult to complete the profiles of the weakest and strongest lines.

When I drew the line profiles, I estimated the probable error in the equivalent width as described by what I call the line quality. Although this quantity depends on the continuum placement and on the quality of the spectroscopic plate, it has been used as a guide in determining the mean elemental abundances. My system follows:

A = The line is not weak and has a virtually complete and symmetric profile. There appears to be only a small error possible in the equivalent width measurement.

B = The line is intermediate in quality between A and C.

C = The line profile is better than two-thirds defined. A reasonable number of lines of this quality should result in a good abundance determination.

D = Less than one-half of the line profile is defined. This quality is used for weak lines whose equivalent width is seriously affected by continuum placement.

E = The line profile is partially blended. These measurements are

slightly worse than C but better than D quality.

G = Same as E except that the line is blended with another of the same multiplet. If one component of a blend is labeled G and the other is not, the one labeled G is the weaker.

Q = The line identification is questionable.

W = This is a wild guess.

In order to determine the equivalent widths, I normally measured positions on the line profiles. Only the equivalent widths of the strongest lines were measured using a planimeter. By use of an acetate sheet printed with a twenty line to the inch grid, I read the distance from the continuum to the clear plate and measured the position of the line profile with respect to clear plate every .10" except for those lines with broad profiles in which case the spacing was .15".

To convert the profile measurements into equivalent widths, I determined for each measured point the residual intensity, the intensity at that point divided by the continuum intensity. The residual intensities were converted into an equivalent width by use of Simpson's Rule. The first and last points on the measured line profile were assumed to be at the continuum.

G. The Behavior of Line Strengths

In the cool Ap stars, each line has its own value of the microturbulent velocity while all lines in the normal stars have the same value. I have reduced all measured equivalent widths to the values that they would have if the microturbulent velocities were reduced to

zero, i.e., the magnetic fields were turned off. The procedure is described in the next section. By means of the computer program WIDTH4, which incorporates the methods of Strom, Gingerich, and Strom (1966), I constructed diagrams showing how the equivalent width is a function of effective temperature and of elemental abundance for the case of no microturbulent velocity. By use of the reduced equivalent widths, I have determined by interpolation the proper abundances for each line. These diagrams were not constructed for all lines, but only for those representative of the lines under consideration. Abundances were derived for the other lines by use of the diagrams and scaling factors determined from the axes of the curve of growth. I normally used the same diagram for all lines measured in a multiplet. In these cases I ignored the variation of the opacity with wavelength since over the limited wavelength range which most multiplets cover the opacity variation is usually less than .02 dex.

For most lines the shape of the curve of growth was rather similar. This minimized the number of reduction factor calculations to a maximum of two per element. In addition the shifts in the curve of growth due to microturbulence are similar for adjacent elements in the periodic table. Thus reduction factors were generated for representative lines of the various elements.

Curves of growth were made with the axes as log equivalent width and log elemental abundance with respect to hydrogen for selected lines by solving the Saha and Boltzman equations given the structure of the atmosphere and atomic constants. By means of a grid of model

atmospheres with the same parameters except effective temperature, Figure II-1 was constructed for FeI(41) λ4404.75. The curve labeled log Fe/H = -4.40 has the solar value. The equivalent width changes very rapidly for those effective temperatures below 8500°K compared with those above 9000°K.

The shape of the contours of constant abundance depends on the atomic damping constants, the atmospheric structure, the line's excitation potential, the ionization potentials, and the partition functions. The partition functions are those of Drawin and Felenbok (1965) and for some elements not included therein from Aller (1963). However, there are additional elements whose partition functions have never been calculated for the temperature range of the cool Ap stars, especially the rare earths and the heavier elements. In these cases, an educated guess has been made, for example, the statistical weight of the ground state. The partition function enters the calculations in two ways: 1) the Saha equation where its ratio with that of an adjacent stage of ionization is important and 2) the abscissa of the curve of growth. For the rare earths, in the first case the log of the ratio is near zero since the atomic structures of the rare earth ions are somewhat similar at least for neutral and singly-ionized ions although there are differences with regard to the number and distribution of levels. Singly-ionized rare earth lines are mostly in the violet-blue region while doubly-ionized lines are in the ultraviolet. In the second case the partition function behaves similarly to an oscillator strength. The only extensive calculations of rare earth partition

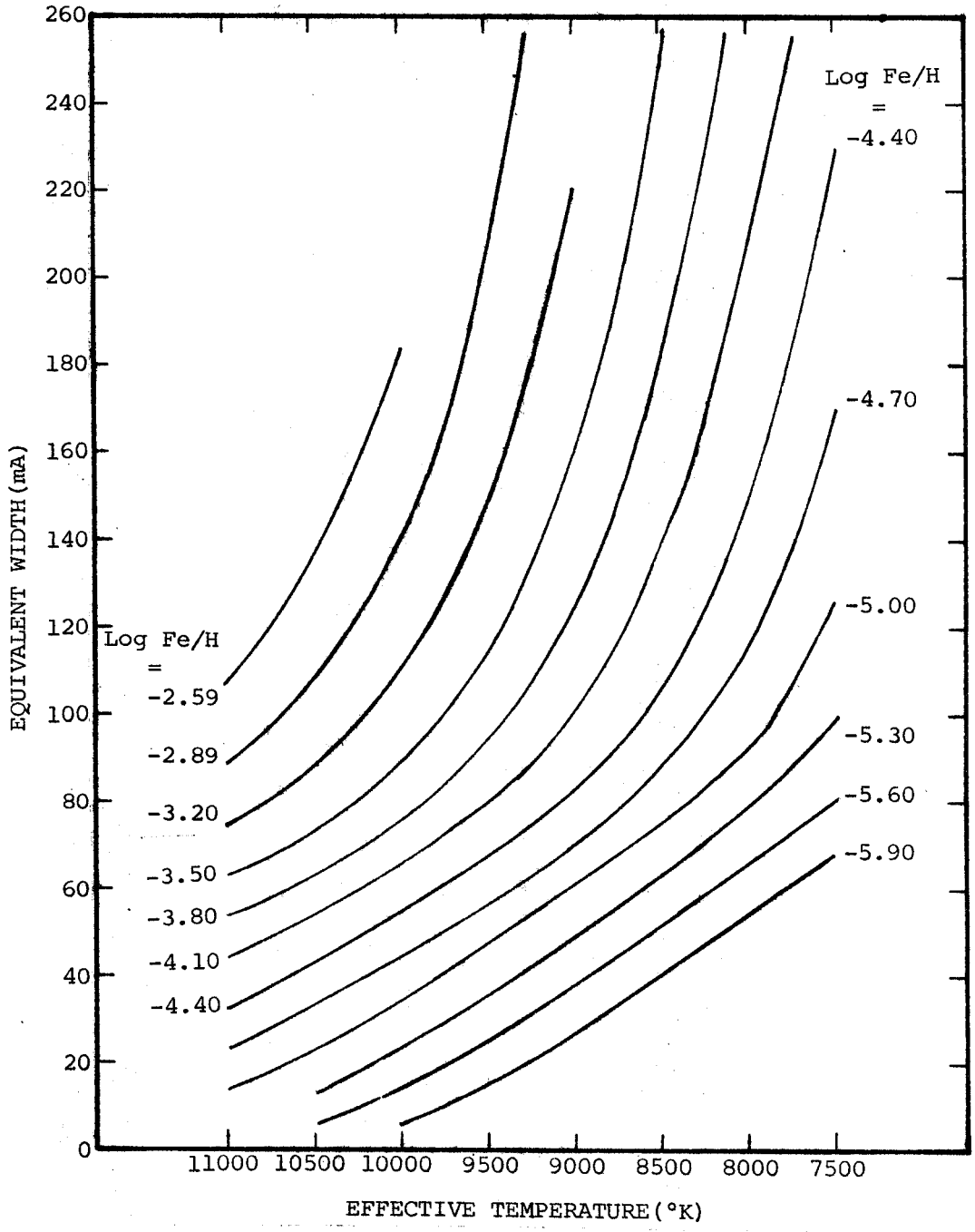

Figure II-1: The equivalent width of FeI(41) λ4404.75 vs. effective temperature diagram. The solid lines are contours of constant log Fe/H. This diagram was constructed using model atmospheres with log g=4.0 and no microturbulent velocity.

functions were made for LaI and LaII (Cayrel and Jugaku 1963). They indicate that the values of the partition functions are approximately 100. Those of Corliss (1962) for other rare earths when scaled by means of the La values indicate similar values for typical stellar temperatures.

The atomic damping constants for most lines are poorly known. The assumption made when either the Stark or Van der Waals damping coefficient is not known is that the damping constant is equal to ten times the classical radiative one. This assumption is not important except for strong lines.

For lines with known Stark broadening coefficients, I used formula (7-55) in Aller (1963) to calculate the Van der Waals damping constant C_6.

$$C_s = 1.61 \times 10^{-33} \left(13.5\, Z/\chi_r - \chi_{r,s}\right)^2 \qquad \text{(II-4)}$$

where Z is the effective nuclear charge, χ_r the ionization potential of the ion and $\chi_{r,s}$ the excitation potential of level s. The interaction constant C_6 for a transition from s to s' is $C_s - C_{s'}$. Using the tables in Griem (1964), I derived the Stark broadening constant C_4 for SiII(1) λ3854 and λ3862; CaI(2) λ4227; and CaI(4) λ4425, λ4435, λ4436, and λ4455. The appropriate formula is

$$C_4 = \left(\alpha^{4/3}\, \omega/F_o^2\right) \left(N_e/N_e'\right)^{2/3} \qquad \text{(II-5)}$$

where

$$F_o = 2.61\, e\, N^{2/3} \qquad \text{(II-6)}$$

and α and ω are tabulated quantities given as a function of temperature,

N_e the electron density, $N_e' = 10^{16}$ cm^{-3}, e the charge of the electron, and N the number density of the perturbing ion. For MgII(4) λ4481, C_4 comes from the values of Chapelle and Sahal-Bréchot (1970).

To compare the results calculated using a model atmosphere with curve of growth techniques, we can write the Planck function B as

$$B = B_0 + B_1\tau \qquad \text{(II-7)}$$

Then for a grey body temperature distribution (Aller 1963)

$$B_0/B_1 \simeq 8/3(\kappa_\lambda/\bar{\kappa})\ (kT_o/h\nu) \qquad \text{(II-8)}$$

where T_o is the boundary temperature, h the planck constant, ν the frequency, $\bar{\kappa}$ the mean absorption coefficient, and κ_λ the absorption coefficient at wavelength λ. I considered three log g - 4.0 model atmospheres with effective temperatures of 8000, 9000, 10000°K and found B_o/B_1 = .585 to .687 for 5000 Å if $\kappa_\lambda/\bar{\kappa} = 1$. Then I compared a number of curves of growth with those computed by Wrubel (1950) for the Milne-Eddington model with $B_0/B_1 = 2/3$. The resulting values of log a were usually between -1.4 and -1.8 except for CaI(2) λ4226 which agreed best with -2.2. The quantity a is the ratio of the damping constant to the Doppler width (Aller 1963). The fit was made using primarily the flat and damping portions of the curve of growth since the adopted curves of growth fit Wrubel's very poorly in the linear section.

H. Generation of Reduction Factors

The major line intensification mechanism which has been considered in the Ap stars is Zeeman broadening. We need to calculate what the equivalent width of a line of given microturbulent velocity would be if the magnetic field were turned off and the microturbulent velocity were zero.

After selecting a line and a model atmosphere, I made curves of growth for a series of microturbulent velocities. In Figure II-2, I have shown the result for FeI(41) λ4404.75 using a model atmosphere with an effective temperature of 9000°K, log g = 4.0, and solar elemental abundances. Only a few velocities are shown for clarity. The normal grid was 0.0, 0.5, 1.0, 1.5, 2.0, 2.5, 3.0, 4.0,...km/sec.

The ordinate of the curve of growth (Aller 1963) is log $W_\lambda V/\lambda c$ where W_λ is the equivalent width, λ the wavelength, c the velocity of light and

$$V = \sqrt{(2kT/M)^2 + \xi^2} \qquad \text{(II-9)}$$

where ξ is the microturbulent velocity, M the atomic weight of the atom in question, T the temperature, and k Boltzmann's constant. The abscissa is

$$\log \eta_o = -1.824 + \log N_r + \log gf\lambda - \theta\chi_{r,s} - \log Vu(T) - \log \kappa_\lambda \qquad \text{(II-10)}$$

where η_o is the ratio of the line to continuous opacity, N_r the ionic abundance, g the statistical weight of the lower level, f the

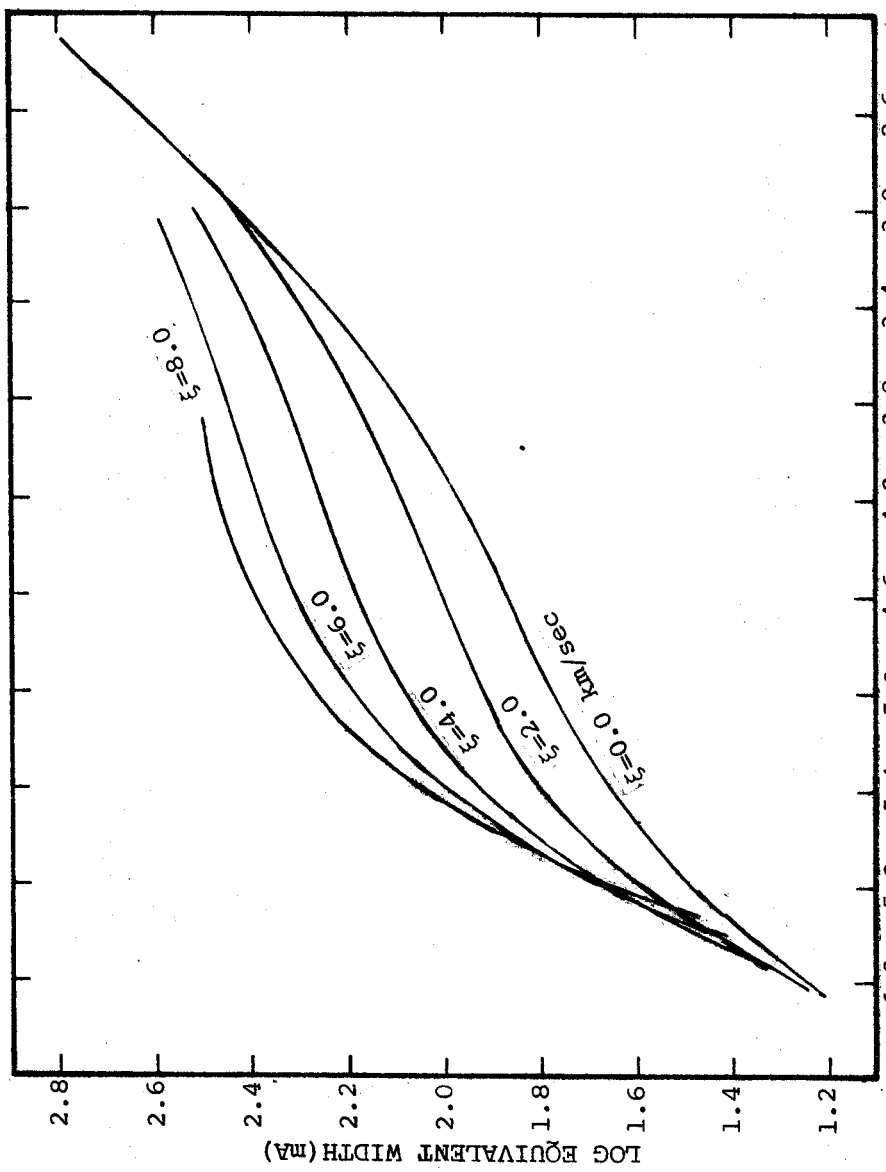

Figure II-2: Curves of growth for FeI(41) λ4404.75 for different microturbulent velocities. The model atmospheres had T_{eff}=9000°K, log g=4.0, and solar elemental abundances. Each curve is labeled by its value of the microturbulent velocity in km/sec.

oscillator strength, $\theta = 5040/T$, $\chi_{r,s}$ the excitation potential, $u(T)$ the partition function, and κ_λ the continuous opacity.

If we leave all factors unchanged except ξ, then as ξ increases so does V and the ordinate. At the same time, the value of log V increases and the abscissa shifts. These effects are seen in Figure II-2.

For selected points on each curve of growth, I determined at a given abundance the ratio of the equivalent width to that for zero microturbulent velocity. These ratios are plotted as functions of equivalent width as in Figure II-3 which shows part of the figure used for Fe. By interpolation in such a diagram, one can determine the proper reduction factors to zero microturbulent velocity. The curve for each microturbulent velocity rises and then falls as the equivalent width increases. The figure also shows that the abscissa of the curve of growth shifts as the microturbulent velocity increases.

By assigning a different microturbulent velocity to each line, we also ascribe a different error to each derived abundance. There is an error in measuring an equivalent width due to photographic calibration of the plate and the placement of the continuum and clear plate levels. In reducing the measured equivalent width to that which the line would have if its microturbulent velocity were zero, we modify the error. To illustrate what happens, let us examine Figure II-3.

Suppose that the microturbulent velocity is 4 km/sec and the true equivalent width is 80 mÅ. If instead we measure 70 mÅ, the reduction factor is diminished and hence the reduced equivalent width has a

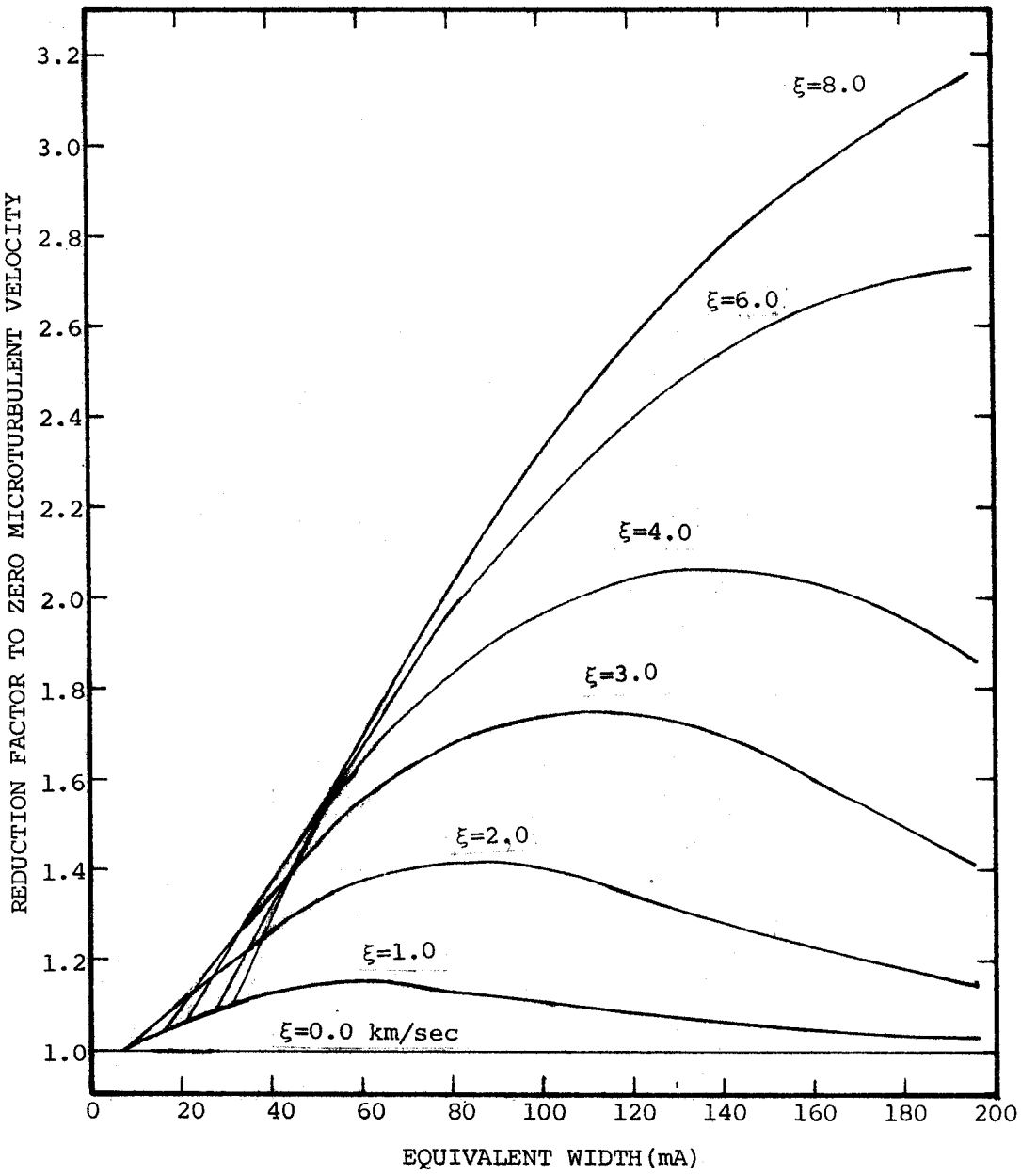

Figure II-3: Reduction factors generated for FeI(41) λ4404.75. The curves of growth used were those of figure II-2. Each curve is labeled by its value of microturbulent velocity in km/sec.

smaller error than the measured equivalent width. This happens, in general, when the reduction factors increase with equivalent width. When the reduction factors decrease with increasing equivalent width, the reduced equivalent widths will have larger errors than the measured ones.

I. Solar Abundances

By including normal stars, those whose elemental abundances are similar to the sun's, in this program we can by comparison of their abundances and those of cool Ap stars derive the abundance anomalies. Errors in the oscillator strengths cancel to first order in these comparisons. However, for some elements, no comparable lines appear in the spectra of normal stars and a zero point is needed to determine the anomalies. It is also desirable to compare the abundances of the normal stars with the solar values. For these reasons, I have compiled a list of solar abundances in Table II-4.

J. Effective Temperatures and Fe Abundances

The only unspecified parameters for the abundance analyses are the effective temperatures which are estimated initially from UBV photoelectric data and modified by requiring that the Fe abundances as derived from FeI lines be the same as from FeII lines. This requirement was applied to the logarithmic rather than the arithmetic mean in order to minimize errors.

TABLE II-4: SOLAR ABUNDANCES

Element	Abundance	Source
H	.900	
He	.100	
	Log Abundance	
C	-3.49	Lambert (1968)
N	-4.11	Lambert (1968)
O	-3.27	Lambert (1968)
Ne	-3.49	= C
Na	-5.82	Lambert and Warner (1968a)
Mg	-4.56	Lambert and Warner (1968b)
Al	-5.64	Lambert and Warner (1968b)
Si	-4.49	Lambert and Warner (1968c)
P	-6.57	Lambert and Warner (1968a)
S	-4.79	Lambert and Warner (1968a)
K	-6.95	Lambert and Warner (1968a)
Ca	-5.76	Lambert and Warner (1968b) and Goldberg *et al.* (1960)
Sc	-9.07	Warner (1968) and Goldberg *et al.* (1960)
Ti	-7.32	Goldberg *et al.* (1960)
V	-8.19	Warner (1968) and Goldberg *et al.* (1960)
Cr	-6.59	Warner (1968) and Goldberg *et al.* (1960)
Mn	-7.11	Warner (1968) and Goldberg *et al.* (1960)

TABLE II-4 (continued)

Fe	-4.40	Garz et al. (1969)
Co	-7.30	Aller (1968)
Ni	-6.09	Goldberg et al. (1960)
Ga	-9.49	Müller (1966)
Sr	-9.18	Lambert and Warner (1968b)
Y	-8.80	Müller (1966)
Zr	-9.35	Müller (1966)
Mo	-9.70	Aller (1968)
Ba	-9.90	Goldberg et al. (1960)
La	-9.97	Müller (1967)
Ce	-10.22	Müller (1967)
Pr	-10.55	Müller (1967)
Nd	-10.07	Müller (1967)
Sm	-10.38	Müller (1967)
Eu	-11.04	Müller (1967)
Gd	-10.87	Müller (1967)
Dy	-11.00	Müller (1967)
Yb	-10.47	Müller (1967)
U	-12.30	Aller (1960)

For initial estimates of the effective temperatures, I used those derived by Preston (1971d) (Table II-6). The UBV colors were corrected for reddening by means of the color excesses of B-type stars in the same direction (Crawford 1963). Then the main sequence in a two-color diagram was parameterized as follows:

$$(U-B) = t(B-V) \qquad \text{(II-11)}$$

where

$$t = 1.77 - 10.0(B-V)+14.3(B-V)^2 \qquad \text{(II-12)}$$

and t~0 at spectral type F0. This method works because when B-V is greater than 0.0, the Paschen continuum is temperature sensitive while when U-B is less than 0.0, the Balmer jump is temperature sensitive. The intrinsic colors of the cool Ap stars were chosen to be those at the intersection of a normal from this main sequence through the unreddened position of the star. Deviations are attributed to blanketing effects. The values of t were converted into effective temperatures by comparison with the results of Wolff, Kuhi, and Hayes (1968) which are similar to those of Schild et al. (1971). There are two stars without UBV photometry, HD89069 and HD165474. In these cases the initial estimates of effective temperatures were simply guessed.

Some sources of error in determining the Fe abundances are the equivalent width measurements, the magnetic field measurements, the applied reduction factors, the oscillator strengths, and the degree that the model atmosphere represents that of the true star (see Comparison of Effective Temperature Results). The equivalent width

measurements are based only on one plate except for ν Cap. The result of measuring additional plates and lines is to reduce errors. We are mainly limited in the addition of more lines due to a paucity of good oscillator strengths for some elements and the desirability of using only blend-free lines.

The magnetic fields have been determined by comparing Fe peak neutral and singly-ionized lines with large and small values of z. These values should be fairly representative for the lines under consideration unless the field is quite patchy which is unlikely (Preston 1971c). The reduction factors are based on z values which, if anything, overestimate the effects of the field.

Errors in the oscillator strengths influence the absolute abundances and the effective temperature determinations. However, such systematics should affect all stars in approximately the same way and should mostly cancel when the abundances are made relative to the normal stars. For FeI lines, there are three basic sets of recent determinations, Garz and Kock (1969), Bridges and Wiese (1970), and Wolnik, Berthel and Wares (1970). They are in reasonably good agreement with one another and disagree with the older determinations such as those of Corliss and Bozman (1962). Because of errors in the older determinations, the more recent measurements are preferred.

Baschek, Garz, Holweger, and Richter (1970) using the same arc as Garz and Kock (1969), measured oscillator strengths of FeII lines on the absolute scale of Garz and Kock. They also presented correction factors for FeII oscillator strengths of other authors. Their solar

value of log Fe/H was -4.37 which compares with -4.40 determined by Garz, Holweger, Kock, and Richter (1969) from FeI lines. These determinations are supported by values of -4.5 from solar [FeII] lines (Grevesse and Swings 1969) and -4.45 from the meteoric Fe abundance (Urey 1967).

On the other hand, Cowley (1970) and Ross (1970) after considering the damping of FeI lines have proposed lower Fe abundances with -4.8 as an upper limit. Wolnik, Berthel, and Wares (1971) have measured FeII oscillator strengths which are approximately 1.6 times greater than those of Baschek et al. (1970). They imply a solar Fe abundance of -4.60.

Because of this discrepancy, I determined the Fe abundances and effective temperatures for two cases: 1) the Baschek et al. (1970) scale is correct for the FeII lines and 2) the Wolnik et al (1971) scale is correct. In addition, to show how changing the gravity affects the results, I calculated the Fe abundances and effective temperatures using the Baschek et al. (1970) FeII oscillator strengths and a series of model atmospheres with log g = 3.5 (case 3) instead of log g = 4.0 used for cases 1 and 2. For elements other than Fe, the abundance calculations are performed only for cases 1 and 2. The adopted atomic constants for the FeI and FeII lines are given in Table A-1. For case 2, add .20 dex to all log gf values for FeII.

To determine the effective temperatures and Fe abundances, it is necessary to make initial estimates of the effective temperatures, for example, those determined from UBV photoelectric data. Then from the

derived Fe abundances from FeI and FeII lines improved estimates can be made for the effective temperatures. Within two or three iterations, convergence can be achieved. Furthermore I determined the effective temperatures to the nearest 50°K.

Table II-5 contains the final Fe abundance determinations while the effective temperatures are in Table II-6. As an example, let us derive the values of the abundances for multiplet 41 for HD2453, case 1, as given in Table A-2. Using formula (II-3) and a magnetic field of 3.8 kG, the microturbulent velocity for λ4404 is 2.93 km/sec and for λ4415, 2.75 km/sec. After dividing the respective equivalent widths, 145.6 and 107.1 mÅ by the reduction factors, 1.62 and 1.67, which are determined by use of Figure II-3, we find 89.9 and 64.1 mÅ for the case of no microturbulence. By entering these values in Figure II-1 at an effective temperature of 10350°K, we find the resultant values for the abundances are -3.23 and -3.85, respectively. For λ4415, however, we must adjust the abundance due to the oscillator strength. This amounts to .41 dex by use of the values in Table A-1. Thus the final values are -3.23 for λ4404 and -3.44 for λ4415.

If the effective temperature is reduced by 100°K, the derived Fe abundances from FeI lines decrease by .073 dex and that from FeII lines by .023 dex. If we diminish the gravity by .10 dex, the derived Fe abundance decreases by .047 dex while the effective temperature decreases by 100°K in order to keep the derived Fe abundance from both stages of ionization in agreement.

TABLE II-5: LOG Fe/H VALUES

Star	Case 1	Case 2	Case 3
HD2453	-2.91	-3.19	-3.12
HD5797	-2.58	-2.90	-2.82
HD8441	-3.31	-3.56	-3.56
HD12288	-3.20	-3.48	-3.45
HD18078	-2.96	-3.26	-3.24
HD22374	-3.58	-3.87	-3.82
HD50169	-2.99	-3.25	-3.27
HD81009	-4.01	-4.30	-4.29
HD89069	-3.28	-3.60	-3.55
HD110066	-2.86	-3.14	-3.12
HD111133	-3.24	-3.51	-3.51
HD118022	-2.78	-3.10	-3.06
HD137909	-3.04	-3.31	-3.32
HD137949	-3.42	-3.73	-3.71
HD165474	-3.94	-4.23	-4.25
HD176232	-4.10	-4.37	-5.39
HD191742	-3.26	-3.59	-3.54
HD192678	-2.85	-3.11	-3.09
HD201601	-3.98	-4.23	-4.21
HD204411	-3.28	-3.56	-3.56
HD216533	-3.36	-3.64	-3.63
ν Cap	-4.44	-4.73	-4.71
o Peg	-4.24	-4.53	-4.50

TABLE II-6: COMPARISON OF EFFECTIVE TEMPERATURES

	Effective Temperatures (°K)				
Star	a	b	c	d	e
HD2453	9420	10350	9950	9850	
HD5797	9250	9600	9200	9150	
HD8441	9840	10200	9800	9650	
HD12288	9840	10600	10150	10000	
HD18078	9300	10050	9700	9550	
HD22374	9300	9450	9100	9050	
HD50169	10200	10150	9800	9600	
HD81009	8300	9300	8900	8900	
HD89069		9950	9500	9400	
HD110066	9600	10100	9700	9550	10100-W
HD111133	10580	10650	10150	10000	9700-W
HD118022	9900	10000	9550	9450	9700-W,10250-MH,9350-SS, 10750-JS
HD137909	8020	9750	9450	9300	8850-W,7300-MH,8000-H1, 8700-JS,B0
HD137949	7960	8850	8450	8450	
HD165474		9150	8750	8750	
HD176232	8100	8200	7800	7800	7900-W,7400-MH
HD191742	8600	8900	8500	8450	
HD192678	10140	10400	10000	9850	
HD201601	8100	8150	7750	7750	7900-W,7500-MH,7600-H2, 7550-SL
HD204411	9250	9550	9150	9050	8750-S3,9175-MH,8550-SS, 9200-SL
HD216533	9780	10400	9950	9800	

TABLE II-6 (continued)

ν Cap	10500	10050	9950	10200-A,11200-SS,12300-SL
o Peg	10150	9750	9600	9500-CS,11200-SL

Effective Temperatures: a = initial estimates from UBV photometry (Preston 1971d).

b,c,d = cases 1,2,3 respectively.

e = from other sources indicated as follows:

A = Adelman (1972)
BO = Baschek and Oke (1965)
CS = Conti and Strom (1968b)
H1 = Hack (1958)
H2 = Hack (1960)
JS = Jugaku and Sargent (1968)
MH = Mihalas and Henshaw (1966)
S3 = Sargent et al. (1969)
SL = Searle et al. (1966)
SS = Searle and Sargent (1964)
W = Wolff (1967a,b)

For HD12288, I measured the equivalent widths of both Zeeman components of FeII(27) λ4385 and derived the Fe abundance from them separately. They gave a value about 0.1 dex smaller than the method normally used in this study.

The run of equivalent width with effective temperature and Fe abundance for FeI λ4404.75 is given in Figure II-1 where log g = 4.0. The corresponding figure for log g = 3.5 model atmospheres is virtually identical. Figure II-4 is a similar diagram for FeII λ4385.38 when log g = 4.0. For log g = 3.5 the values of the contours of constant abundance are made smaller by .30 to .40 dex compared with log g = 4.0 models.

Table II-7 gives the fractional Fe abundances at τ_{5000}=.32 using the parameters in Table II-1 for log g = 4.0 model atmospheres and Table II-2 for log 3.5 model atmospheres. This table also shows a quantity log r which is the variable quantities in the abscissa of the curve of growth less a constant.

In both series of model atmospheres, most of the Fe is singly-ionized while at the high temperature end of the sequence Fe begins to become doubly-ionized. At a given effective temperature, an FeII line of a given equivalent width will require a greater abundance if log g = 4.0 rather than log g = 3.5. These calculations show that an opposite effect should occur for FeI lines. However, we are not examining a typical level in either case for FeI lines which are formed higher in the atmosphere where the temperature is lower and the amount of FeI is greater. The table also gives the approximate

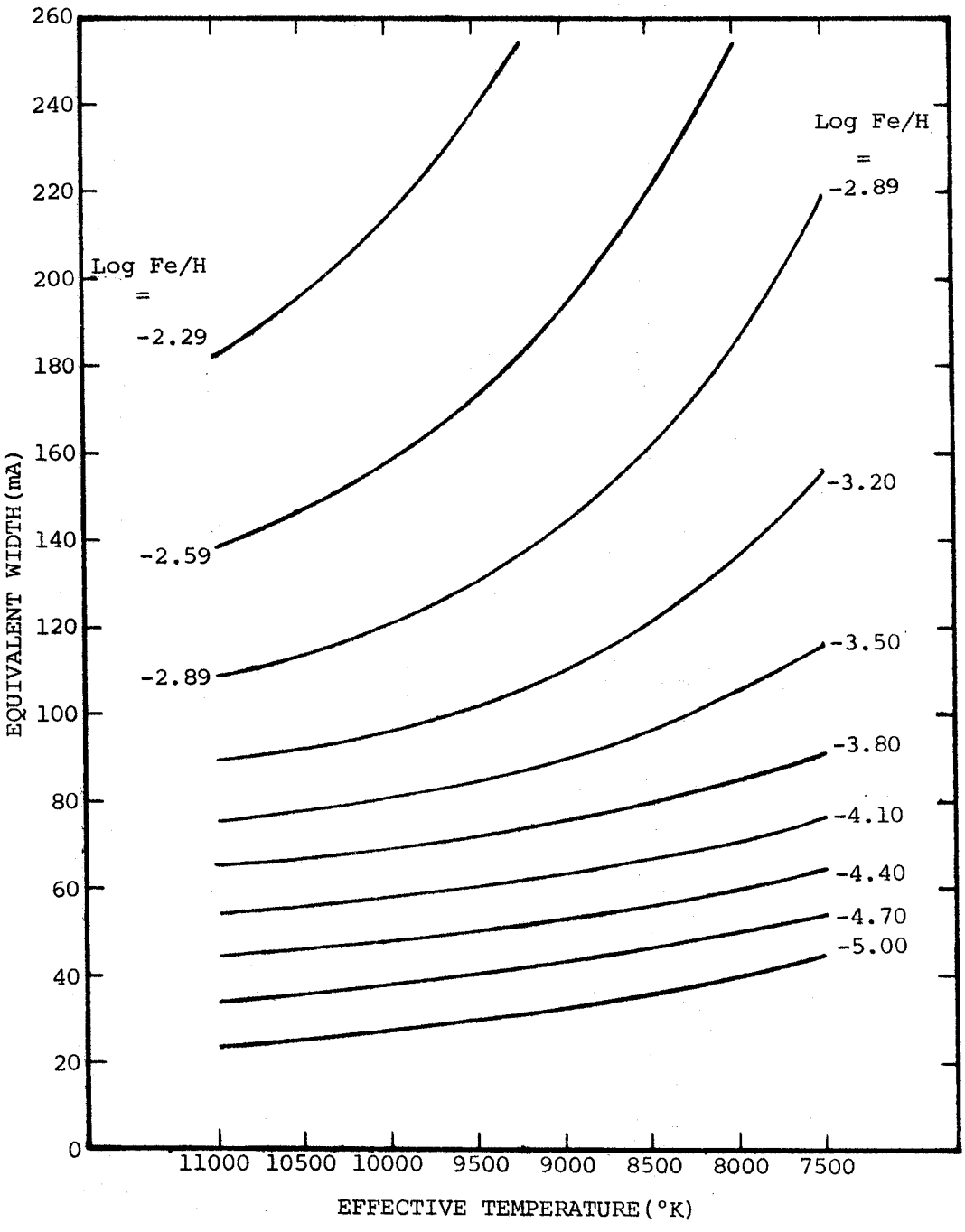

Figure II-4: The equivalent width of FeII(27) λ4385.38 vs. effective temperature diagram. The solid lines are contours of constant log Fe/H. This diagram was constructed using model atmospheres with log g=4.0 and no microturbulent velocity.

TABLE II-7: PHYSICAL CONDITIONS AT τ_{5000}=.32 FOR Fe IONS

	Effective Temperature	Log Fe/H Fractions FeI	Log Fe/H Fractions FeII	Log r FeI λ4404	Log r FeII λ4385
Log g = 3.5 Models	7500	-2.33	0.00	-4.62	-3.30
	8000	-2.55	0.00	-5.11	-3.48
	8500	-2.78	0.00	-5.65	-3.70
	9000	-3.05	0.00	-6.20	-3.92
	9500	-3.30	-0.01	-6.61	-4.02
	10000	-3.51	-0.03	-6.85	-4.04
	10500	-3.88	-0.08	-7.18	-4.01
	11000	-4.16	-0.17	-7.43	-4.02
Log g = 4.0 Models	7500	-2.13	0.00	-4.54	-3.43
	8000	-2.34	0.00	-5.07	-3.57
	8500	-2.58	0.00	-5.52	-3.78
	9000	-2.50	0.00	-6.03	-3.99
	9500	-3.05	-0.01	-6.49	-4.15
	10000	-3.29	-0.02	-6.82	-4.22
	10500	-3.55	-0.05	-7.10	-4.22
	11000	-3.81	-0.10	-7.34	-4.21

shape of the contours of constant abundance (log r). The contours for the dominant species are less steep than the ones for those which have a low fractional abundance.

The sensitivity of the abundance determinations to variations in atmospheric parameters can be summarized in a set of simple algebraic expressions, e.g., the Boltzmann and Saha equations. I found the dependence of the continuous opacity κ and the electron pressure P_e on θ for τ_{5000}=.32 of log g = 4.0 model atmospheres. For θ>.52

$$\log \kappa = -6.90\ \theta; \tag{II-13}$$

Otherwise

$$\log \kappa \simeq 1.00. \tag{II-14}$$

Thus, the continuous opacity behaves similarly to a 7 eV line for most of the temperature range. For θ>.54

$$\log P_e = 5.38 - 5.00\ \theta; \tag{II-15}$$

Otherwise

$$\log P_e = -1.12 + 2.80\ \theta. \tag{II-16}$$

Let us consider a 100°K temperature change between 9000 and 9100°K, i.e., θ = .560 to .554. FeII(27) λ4385.38 is a 2.77 eV line. FeII is the dominant ionic species. Thus

$$\log \ell = \log N_{r,s} + \log \alpha_o \tag{II-17}$$

$$\log \ell = \log N_r - \theta\chi_r + \text{constants} \tag{II-18}$$

where $N_{r,s}$ is the abundance of level s of ionization state r, N_r the

abundance of ion r, α_o the fictitious absorption coefficient at the line center, ℓ the line absorption coefficient, and the other quantities have their normal meanings. Since most of the Fe is in the singly-ionized state, log N_r for this ion is approximately constant.

$$\log \ell \propto - 2.77\ \theta \qquad \text{(II-19)}$$

$$\log \eta = \log \ell/\kappa \propto + 4.13\ \theta \qquad \text{(II-20)}$$

Hence, a 100°K shift in temperature changes log η by .024 dex. FeI(41) λ4404.75 is a 1.55 eV line. If I is the ionization potential, we can express the line absorption coefficient ℓ for a line of an element which is mostly ionized to the next stage of ionization as

$$\log \ell \propto (I-\chi_r)\theta + \log P_e \qquad \text{(II-21)}$$

$$\log \ell \propto + 6.32\ \theta - 5.00\ \theta \qquad \text{(II-22)}$$

$$\log \eta \propto + 8.22\ \theta \qquad \text{(II-23)}$$

Thus, a 100°K change alters log η by .049 dex. These amounts are similar to those found by comparing the results of cases 1 and 2. There is an additional effect due to the shape of the curve of growth that is not calculated here.

K. Comparison of Effective Temperature Results

Table II-6 gives the effective temperature determinations derived with the Fe abundances for cases 1, 2, and 3 along with the initial estimates of effective temperature derived from UBV photometry and the results of other studies. First, I will intercompare the first four

sets of results and discuss the effects of line blanketing. Then the other estimates will be compared with those from case 1.

The ordering of the stars by the effective temperatures of case 1 is essentially the same as those of cases 2 and 3. There are, however, discrepancies between case 1 values and initial estimates. Figure II-5 shows them plotted against each other. On the average, case 1 effective temperatures are 490°K hotter (those of case 2 are 80°K hotter and those of case 3 are 10°K cooler) than those based on UBV photometry. There are, nevertheless, several groups: a) those where the difference is less than 200°K, HD22374, HD50169, HD111133, HD118022, HD176232, and HD201601, b) those where the difference is greater than group a but less than 550°K, HD5797, HD8441, HD110066, HD191742, HD192678, and HD204411, and c) those where the difference is greater than 700°K, HD2453, HD12288, HD18078, HD81009, HD137909, HD137949, and HD216533. The agreement for group a is excellent while for group c there are problems.

Metallic line blanketing is in general greater for B than for V. Hence line blanketing makes the star appear cooler as judged by the B-V index. Wolff (1967a) concluded that the differential effects due to line blanketing on B and V are small except for the coolest stars. Thus, the initial estimates and the case 1 effective temperatures should agree, but they do not for many stars. There are five stars in common: HD111133, HD118022, HD137909, HD176232, and HD201601. Only HD137909, which belongs to group c, has corrections due to line blanketing large enough so that the effective temperature derived

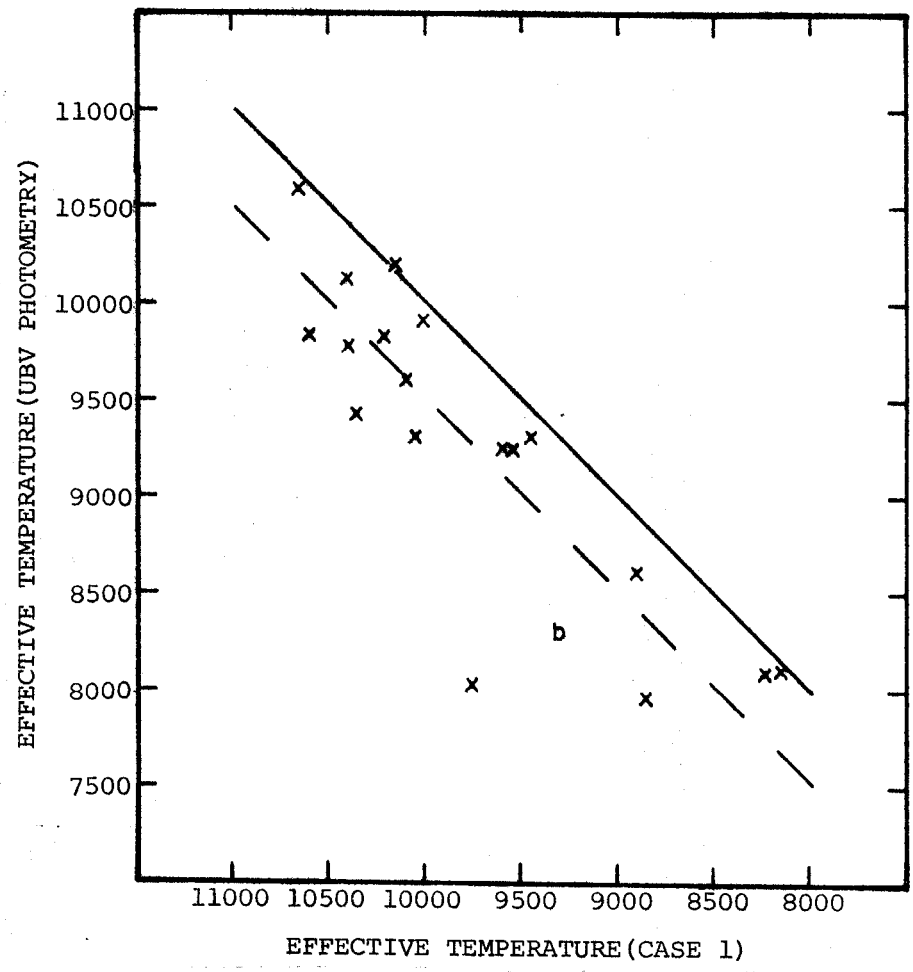

Figure II-5: The initial estimates of effective temperatures derived from UBV photometry vs. effective temperatures derived in case 1 diagram. The solid line is when they are equal. The dashed line is when the effective temperatures of case 1 are greater by 500°K. b represents the position of HD81009 while the x's represent the other cool Ap stars.

from continuum energy scans has to be corrected for this effect. The other stars belong to group a. This suggests that we are observing a sequence caused in part by line blanketing.

Line blanketing causes a change in the emergent flux due to the modification of the stellar temperature distribution resulting from the energy absorbed in the lines (Code 1960). The effect of the line absorption will be negligible when the ratio of the total energy absorbed in discrete transitions to the total integrated flux is small.

The model atmospheres used in this study include hydrogen line blanketing except for the Lyman series. The line blanketing we are concerned with is metallic line blanketing and the ratio of it to hydrogen line blanketing. When this ratio is small, then the model atmospheres used are a good representation. For stars such as HD137909, metallic line blanketing is quite important.

The requirement that the deduced Fe abundance be the same from both FeI and FeII lines means that the effective temperatures are determined by a fit to the model atmospheres at an optical depth which is typical of where the lines are formed. The UBV and Strömgren photometric colors, if they were not influenced by line blanketing, would fit the star at an optical depth typical of the formation of the continuum.

We will consider a simplified treatment of line blanketing. In the outer layers of the atmosphere, line absorption is important and acts as an additional source of opacity, reducing the boundary temperature. The flux returned to the atmosphere increases the

temperature gradient. The temperature is somewhat higher than that of the corresponding depth in an unblanketed atmosphere. The radiation field can be considered to consist of flux in the continuum and that in the lines ΔF.

If the energy removed by the lines appears between them and is distributed in wavelength in the same manner as for a model with a higher effective temperature, T_e^*, then

$$\sigma T_e^4 = \sigma T_e^{*4} - \Delta F \qquad \text{(II-23)}$$

where σ is the Stefan-Boltzmann constant and T_e the unblanketed effective temperature.

Strom and Strom (1969) showed that the opacity arising from the bound-free transitions for SiI which has an absorption edge at $\lambda 1527$ can significantly affect the emergent flux and the hydrogen line profiles for A and late B stars. If this effect is ignored as has been done for this study, the effective temperatures and surface gravity are overestimated for Si rich stars with effective temperatures above 10000°K while for cooler stars the surface gravities are overestimated if the Balmer jump, Paschen continuum, and Hγ profiles are used to determine the fundamental atmospheric parameters. Thus for the stars under consideration, this effect will basically show up as a correction to the gravity which will amount to at most 0.2 dex in log g.

Peterson (1970) showed that the other abundant species particularly Fe can cause similar effects. Elements which can have important

contributions to the ultraviolet opacity are C at normal abundances, and O, Mg, Si, and Fe with overabundances of ten. Other elements, such as Cr, will require overabundances of 100. Peterson points out that the effects of CI and NI absorption in the ultraviolet at solar abundances reduce the magnitude of the Si effect.

Wolff and Wolff (1971) noted that discrete absorption by rare earth lines in $\lambda\lambda$2000-3000 could have similar effects in cool Ap stars. Dieke, Crosswhite, and Dunn (1961) called attention to the large number of doubly-ionized rare earth lines in this region where the emergent flux of A-type stars is large. The rare earths are largely doubly-ionized in the cool Ap stars and, in spite of this, the abundances of certain rare earths appear to increase with effective temperature. Because of the survey nature of this study and the coarse analysis employed, such difficulties are ignored.

Wolff (1967a) has proposed that the strength of the EuII lines, the average value of the line blocking coefficient, the Strömgren metal index m_1, and the apparent rotational velocity are correlated. The values of m_1 determined by Cameron (1966) and this study's Eu abundances are poorly correlated. However, one can determine by comparison of the colors of the cool Ap stars and the means of the standards (Crawford and Barnes 1970 and sources cited within that paper) an index Δm_1 which represents the excess metal index of the Ap stars. Δm_1 is loosely correlated with the Eu abundance. This diagram is more convincing than the one with m_1. A similar result is found between m_1 and ΔT, and Δm_1 and ΔT, where ΔT is the difference

between the effective temperatures derived from UBV photometry and those of case 1. This indicates that this effective temperature difference is somewhat dependent on the amount of line blanketing.

The above diagrams suggest that we consider other elemental abundance vs. Δm_1 diagrams. I examined the better determined rare earths and found that log Ce/H vs. Δm_1 has a somewhat believable correlation while those for log Nd/H and log Gd/H vs. Δm_1 are scatter diagrams. If one computes A for each star, where A = log Nd/H + log Eu/H + log Gd/H, then A vs. Δm_1 is a diagram which has a weak correlation.

Previous discussions indicated that the effects of Si and Fe abundances might be connected with the line blanketing. I attempted similar correlations with these elemental abundances and with B = log Cr/H + log Mn/H + log Fe/H for Δm_1. The resulting diagrams basically show scatter. I also tried correlations of ΔT vs. these elemental abundances and A and B, but none exist.

Most continuum energy distributions published in the last few years use the calibration of Oke (1964) rather than that of Oke and Schild (1970) which is in good agreement with that of Hayes (1970). Thus the resulting effective temperature determinations are based on continuum scans which contain errors in the slope of the Paschen continuum and in the size of the Balmer jump.

The value of T_{eff}=10200°K for ν Cap (Adelman 1972) is based on the new determination. If the case 1 and 3 effective temperatures are interpolated for a value of log g = 3.75, then the result differs by

75°K with that of the fine analysis. Wolff (1967a, 1967b) used continuum scans in the system of Oke (1964) supplemented by line blanketing corrections. The photometric corrections of Oke and Schild (1970) will make all the continua bluer. The value for HD110066 is marked uncertain. Jugaku and Sargent (1968) and Baschek and Oke (1965) worked in the older system. The high value for HD118022 is most likely due to the calibration error in the Balmer jump.

Conti and Strom (1968b) used model fitting techniques to obtain their temperature of o Peg. Their result for the microturbulent velocity is affected by the oscillator strengths as is their check on the effective temperature and gravity using the FeII/FeI ionization. The results of Hack (1958, 1960) come from standard curve of growth techniques.

Searle and Sargent (1964) used $\theta_e = (B-V) + 0.45$ based on a determination which uses the model atmospheres of Mihalas (1965). The results of Mihalas and Henshaw (1966) are based on estimates derived from Searle and Sargent and similar relations, the strength of SiIII λ4552, and Strömgren photometry. They also used the model atmospheres of Mihalas (1965) which do not allow for blanketing due to the Balmer lines. Except for HD118022, their results are systematically low with respect to the temperatures derived in case 1. The method of determination of effective temperatures in Searle, Lungershausen, and Sargent (1966) involves curve of growth techniques.

The effective temperature for HD204411 was determined in several ways by Sargent et al. (1969). Their final result, however, is

affected by the choice of FeI and FeII oscillator strengths. The value for case 1 is approximately the highest effective temperature that they believe would be possible. Thus, the best previous effective temperature determinations support the values adopted in this study.

L. Line Identification Criteria and Abundance Determinations

The elemental abundances of the other elements have been determined relative to H. As a convention, abundance means log elemental abundance by number with respect to H. Most of the identification criteria are deduced from the Revised Multiplet Table (Moore 1945), known as the RMT. This source can be assumed if none is given. Another major source, especially for the heavier elements, is Meggers et al. (1961), known as NBS 32. The ionization potentials except as noted are from Moore (1958), Sugar and Reader (1965, 1966), and NBS 32 (see also Table III-10). Every ion with lines in the RMT and NBS 32 was searched for in the region studied.

Criteria are required in order to accept the line identifications and the quality of the abundance determinations based on them. Ions listed in the RMT and NBS32 for which there are no identified lines in the region λλ3850-3870 and λλ3990-4635 will not be discussed except for those seen in other Ap stars. For other unidentified ions, lines from the RMT and NBS32 which occur in this region which are not mentioned can be assumed to be blended or absent. Comments on some elements are omitted when sufficiently strong lines from the RMT are found in cool Ap stars and abundances are deduced in this paper. The atomic

constants for those lines used to derive the abundances are given in Table A-1 and the abundance determinations for individual lines are in Tables A-2 to A-57.

Table II-8 gives the amount that log N/H is decreased if the effective temperature is decreased by 100°K. It is computed by comparing the results determined using the effective temperatures of cases 1 and 2. Hence, it depends on the size of the equivalent widths measured.

Simple rules can be given based on the continuum κ and line ℓ absorption coefficients which give similar results. For Ca through Ni, the form of these rules for deriving this type of relation is the same as those given for Fe, (II-21) for neutral lines and (II-19) for singly-ionized lines. Table II-9 gives the fractional abundances of Mg ions at τ_{5000}=.32 for model atmospheres with log g = 4.0. Between the 7500° and the 11000°K models, the ionic state of Mg changes from being mostly singly-ionized to becoming partially doubly-ionized. From the relations given in the discussion of Fe for the lines of the dominant ion at 9000°K which is MgII

$$\log \eta \simeq - \chi\theta - \log \kappa + \text{constants} \qquad \text{(II-25)}$$

For λ4481

$$\log \eta \propto - 1.93\ \theta \qquad \text{(II-26)}$$

So a 100°K shift in the temperature changes log η by .01 dex. λ4481 is temperature insensitive since the dependence of ℓ is similar to that of κ on θ, i.e., the lower levels of MgII are analogous to the opacity producing

TABLE II-8: AMOUNTS BY WHICH LOG N/H IS DECREASED IF THE EFFECTIVE TEMPERATURE IS REDUCED BY 100°K

Element	Abundance Determinations From Neutral Lines	Singly-ionized Lines	The Adopted Mean
Fe	.073	.023	
Mg		.010	
Si		.002	
Ca	.120		
Sc		.057	
Ti	.082	.044	
V	.090	.035	
Cr	.079	.022	.054
Mn	.071	.028	
Co	.079		
Ni	.062	.011	.012
Sr		.076	
Y		.068	
Zr		.060	
Ba		.084	
La		.056	
Ce		.060	
Pr		.076	
Nd		.079	
Sm		.078	
Eu		.097	
Gd		.070	
Hf		.022	
U		.052	

TABLE II-9: ABUNDANCE FRACTIONS AT τ_{5000}=.32 FOR Mg, Y, AND Ce IONS

Model Atmosphere Effective Temperature	Abundance Fractions					
	MgII	MgIII	YII	YIII	CeII	CeIII
7500	1.000	0.000	0.965	0.035	0.591	0.409
8000	1.000	0.000	0.909	0.091	0.360	0.640
8500	0.994	0.006	0.780	0.220	0.180	0.821
9000	0.973	0.023	0.574	0.426	0.085	0.915
9500	0.935	0.066	0.360	0.641	0.038	0.961
10000	0.845	0.154	0.212	0.788	0.019	0.982
10500	0.691	0.309	0.111	0.890	0.010	0.990
11000	0.494	0.506	0.061	0.939	0.004	0.991

Paschen levels of H in terms of excitation and ionization potentials (Searle & Sargent 1964). The SiII lines have a similar dependence.

Table II-9 contains the abundance fractions for Y at τ_{5000}=.32 for log g = 4.0 model atmospheres. The ionic state of Y changes from singly-ionized to doubly-ionized in the temperature range considered. For crude calculations of the effect of temperature changes, also for Sr and Zr, it is probably best to consider the element as basically doubly-ionized. Thus for a typical line near a temperature of 9000°K similarly to equation (II-20)

$$\log \eta \propto (I-\chi_r)\ \theta + \log P_e - \log \kappa \qquad \text{(II-27)}$$

For YII(5) λ4398.02

$$\log \eta \propto 14.00\ \theta \qquad \text{(II-28)}$$

so changing the temperature by 100°K alters log η by .084 dex.

In addition Table II-9 shows that the ionic state of Ce is basically doubly-ionized. This conclusion also holds for the other rare earth elements and U. Similarly to Y for 9000°K, equation (II-27) holds. For CeII(1) λ4628.16

$$\log \eta \propto 11.90\ \theta \qquad \text{(II-29)}$$

Thus by changing the temperature by 100°K diminishes log η by .071 dex.

Temperature sensitivities (Table II-8) of adjacent elements in the periodic chart of the elements have similar values. Abundances determined from singly-ionized lines have less sensitivity than those from neutral lines. The temperature sensitivities of the singly-ionized rare earth lines are similar to those of neutral Fe peak lines.

Figures II-1 and II-4 show how the equivalent widths of typical FeI and FeII lines depend on log Fe/H and the effective temperature. These figures also give an idea of the abundance error due to equivalent width measurement. In general, these errors for medium strength lines are less serious than those of weak lines. The accuracy of the best abundance results is about .4 dex while that of the worse determinations is 1.0 dex and marked uncertain. As a general rule, .5 dex will be used as a mean accuracy. Two stars with an abundance difference of this amount in some element will be considered to have different abundances.

Figure II-6 shows the relative insensitivity of MgII λ4481 equivalent widths to effective temperature. The contours of constant abundance have relatively little dependence on the effective temperature as expected from the value in Table II-8. For the SiII lines studied, the comparable contours have even less temperature dependence.

Figure II-7 shows the relative sensitivity of the Ca abundances from λ4227. The diagrams for the other Ca lines have similar but slightly less steep contours. Compared with the determinations for the other elements, Ca has the greatest temperature sensitivity. The contours of constant abundance are steeper than those of FeI (Figure II-1) since the ionization and excitation potentials are both lower.

Figure II-4 for FeII is similar to those for ScII and TiII lines except that the slopes of constant abundance are steeper due to lower ionization and excitation potentials. The equivalent width vs. effective temperature diagrams for TiI, VI, and CrI lines have

Figure II-6: The equivalent width of MgII λ4481 vs. effective temperature diagram. The solid lines are contours of constant log Mg/H. This diagram was constructed using model atmospheres with log g=4.0 and no microturbulent velocity.

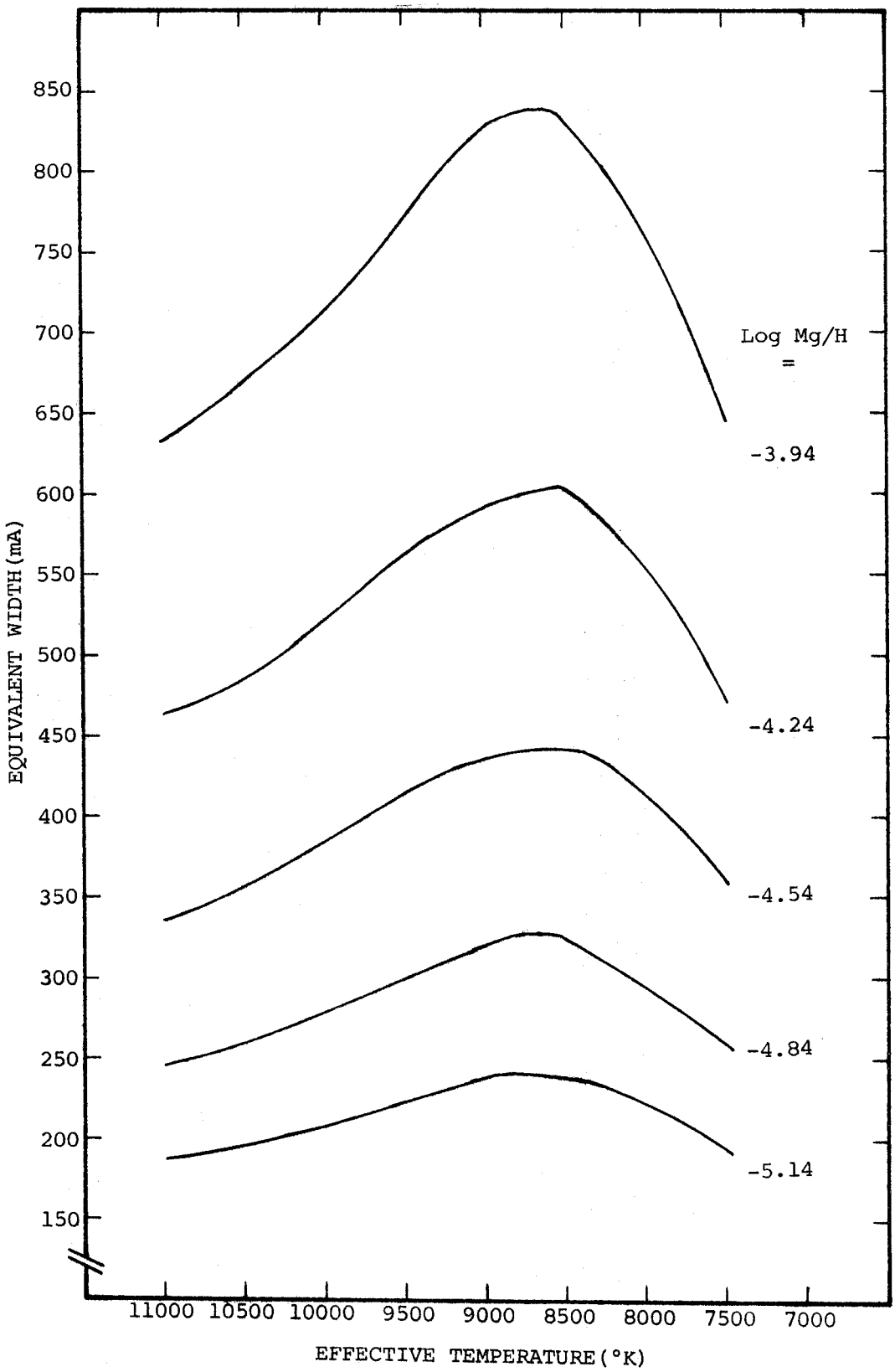
850
800
750
700
650
600
550
500
450
400
350
300
250
200
150
EQUIVALENT WIDTH (mA)
Log Mg/H =
-3.94
-4.24
-4.54
-4.84
-5.14
11000 10500 10000 9500 9000 8500 8000 7500 7000
EFFECTIVE TEMPERATURE (°K)

Figure II-7: The equivalent width of CaI(2) λ4226.73 vs. effective temperature diagram. The solid lines are contours of constant log Ca/H. This diagram was constructed using model atmospheres with log g=4.0 and no microturbulent velocity.

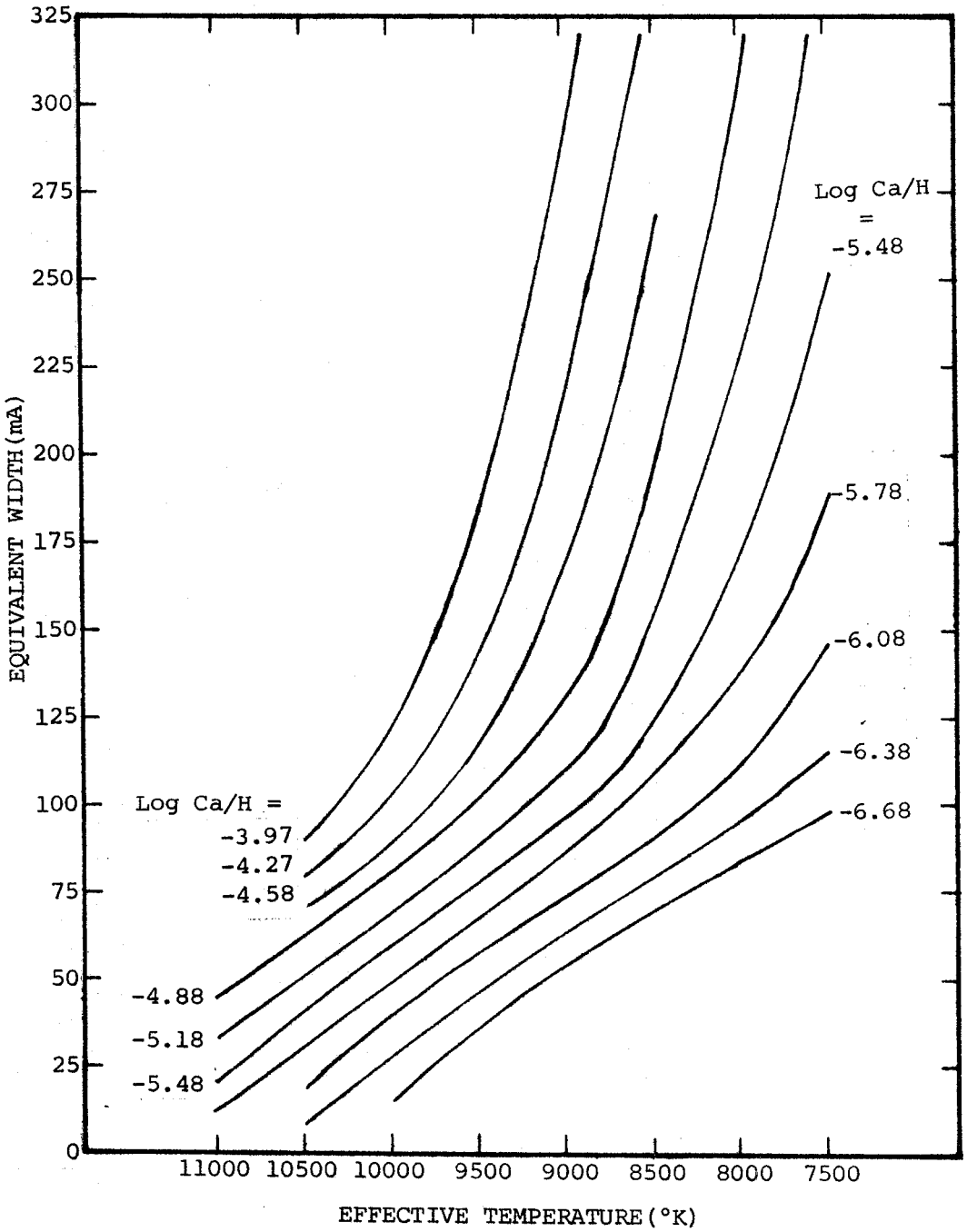
EQUIVALENT WIDTH (mA)
325
300
275
250
225
200
175
150
125
100
75
50
25
0
11000 10500 10000 9500 9000 8500 8000 7500
EFFECTIVE TEMPERATURE (°K)
Log Ca/H =
-3.97
-4.27
-4.58
-4.88
-5.18
-5.48
Log Ca/H = -5.48
-5.78
-6.08
-6.38
-6.68

contours of constant abundance with nearly identical slope. The slope of the analogous contours for VII are slightly flatter than those of TiII due to higher ionization and excitation potentials while those for CrII have the mean slope of those for FeII. The higher excitation and ionization potentials of Mn, Co, and Ni lines result in less temperature sensitivity than those of Fe.

The contours of constant abundance for SrII(3) λ4161.80 (Figure II-8) in the equivalent width vs. effective temperature diagram are slightly steeper than those for FeI (Figure II-1). The corresponding figure for YII(5) λ4398.02 is quite similar while that for ZrII(40) λ4317.32 has similar contours which are less temperature dependent due to the higher ionization potential.

The contours of constant abundance for BaII(1) λ4554.03 (Figure II-9) are steeper than those of FeI (Figure II-1) for the same relative overabundance but slightly less for nearly solar abundances. Figure II-10 is the diagram for CeII(1) λ4628.16 whose comparable contours have similar slope to those of the diagram for LaII(40) λ3988.51. Those for PrII(4) λ4408.84 and NdII(10) λ4303.57 are intermediate in slope between those of CeII and those of EuII (Figure II-11). SmII(37) λ4262.69 has contours of constant abundance which are somewhat steeper than those for EuII(4) λ4435. Due to its higher excitation potential, the analogous contours for GdII(82) λ4582.38 are less temperature sensitive than most other rare earth elements in equivalent width vs. abundance diagrams. The contours are less steep for UII(-) λ3859.58 than those of GdII(82) λ4582.38.

Figure II-8: The equivalent width of SrII(3) λ4161.80 vs. effective temperature diagram. The solid curves are contours of constant log Sr/H. This diagram was constructed using model atmospheres with log g=4.0 and no microturbulent velocity.

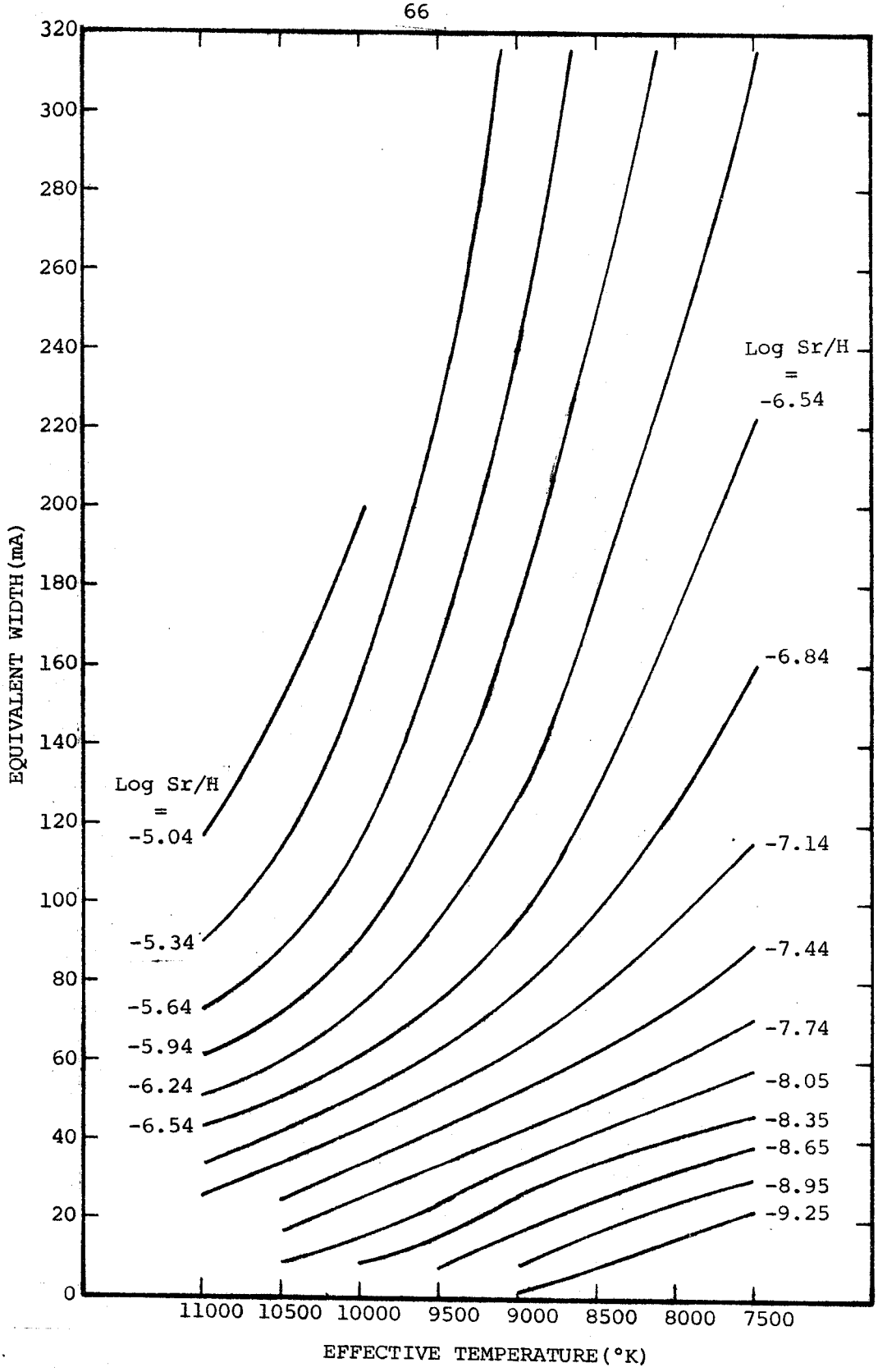
EQUIVALENT WIDTH (mA)
320
300
280
260
240
220
200
180
160
140
120
100
80
60
40
20
0
Log Sr/H = -5.04
-5.34
-5.64
-5.94
-6.24
-6.54
Log Sr/H = -6.54
-6.84
-7.14
-7.44
-7.74
-8.05
-8.35
-8.65
-8.95
-9.25
11000 10500 10000 9500 9000 8500 8000 7500
EFFECTIVE TEMPERATURE (°K)

Figure II-9: The equivalent width of BaII(1) λ4554.03 vs. effective temperature diagram. The solid curves are contours of constant log Ba/H. This diagram was constructed using model atmospheres with log g=4.0 and no microturbulent velocity.

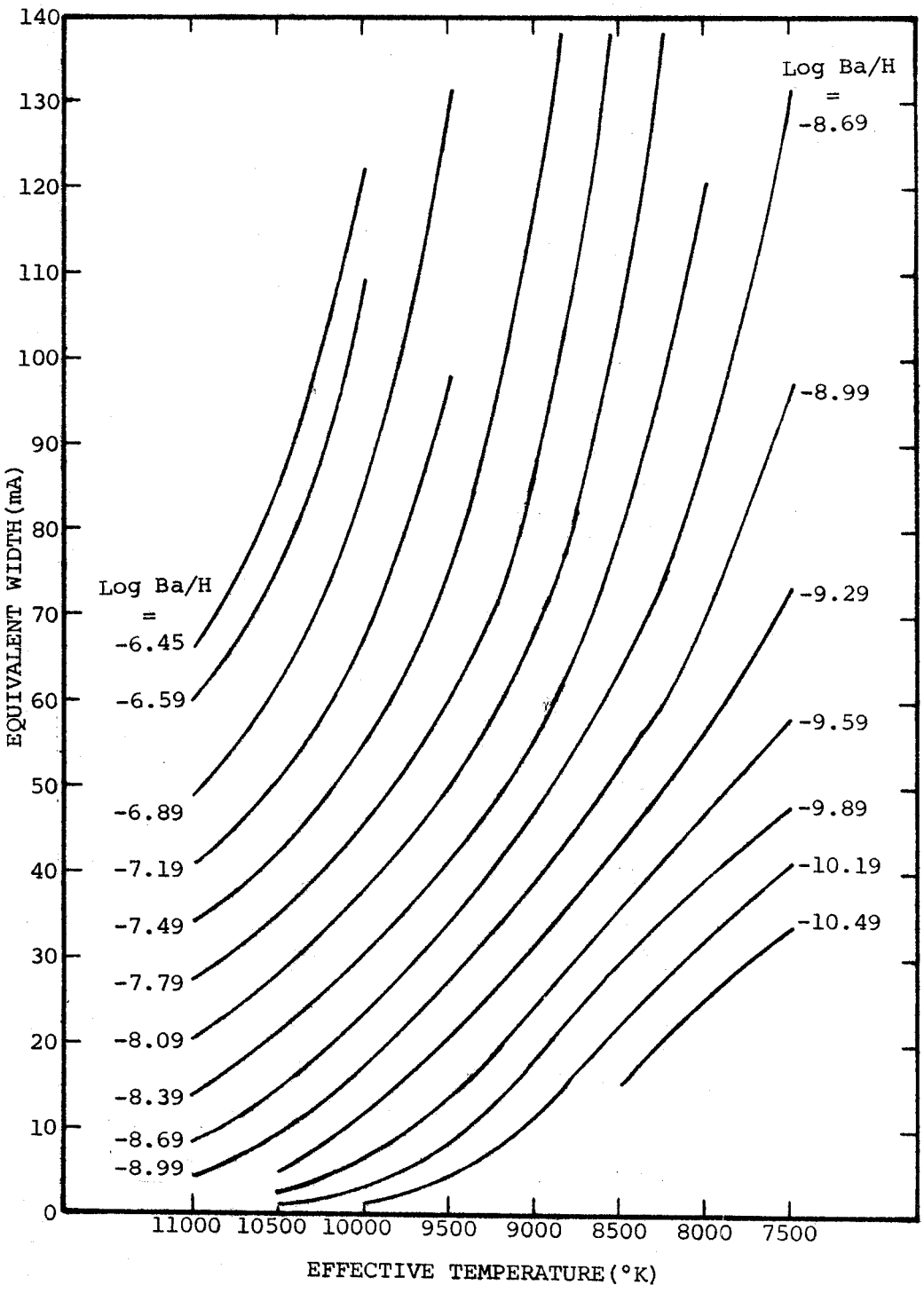
140
130
120
110
100
90
80
70
60
50
40
30
20
10
0
EQUIVALENT WIDTH (mA)
Log Ba/H
=
-6.45
-6.59
-6.89
-7.19
-7.49
-7.79
-8.09
-8.39
-8.69
-8.99
Log Ba/H
=
-8.69
-8.99
-9.29
-9.59
-9.89
-10.19
-10.49
11000 10500 10000 9500 9000 8500 8000 7500
EFFECTIVE TEMPERATURE (°K)

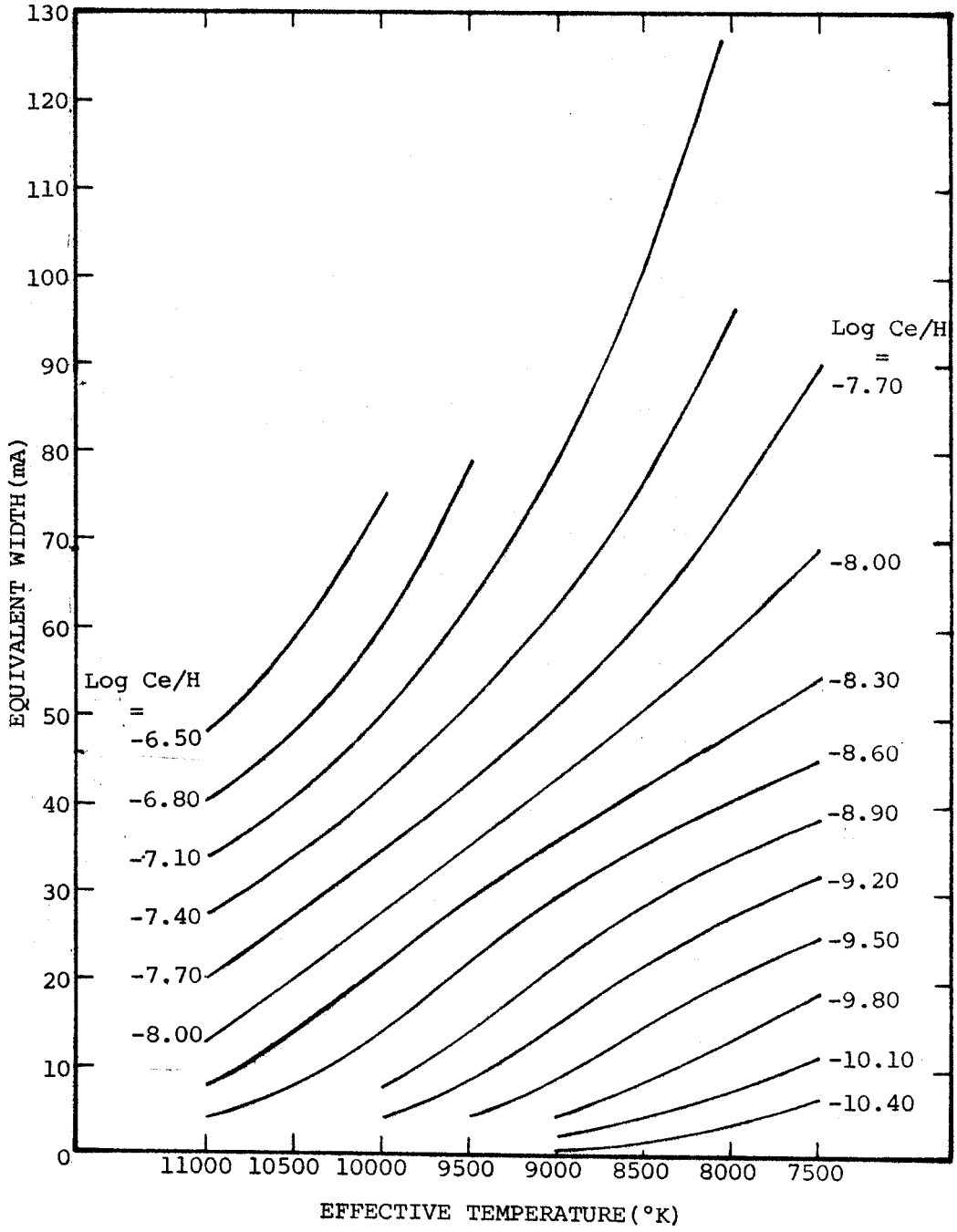

Figure II-10: The equivalent width of CeII(1) λ4628.16 vs. effective temperature diagram. The solid lines are contours of constant log Ce/H. This diagram was constructed using model atmospheres with log g=4.0 and zero microturbulent velocity.

Figure II-11: The equivalent width of EuII(4) λ4435.56 vs. effective temperature diagram. The solid curves are contours of constant log Eu/H. This diagram was constructed using model atmospheres with log g=4.0 and no microturbulent velocity.

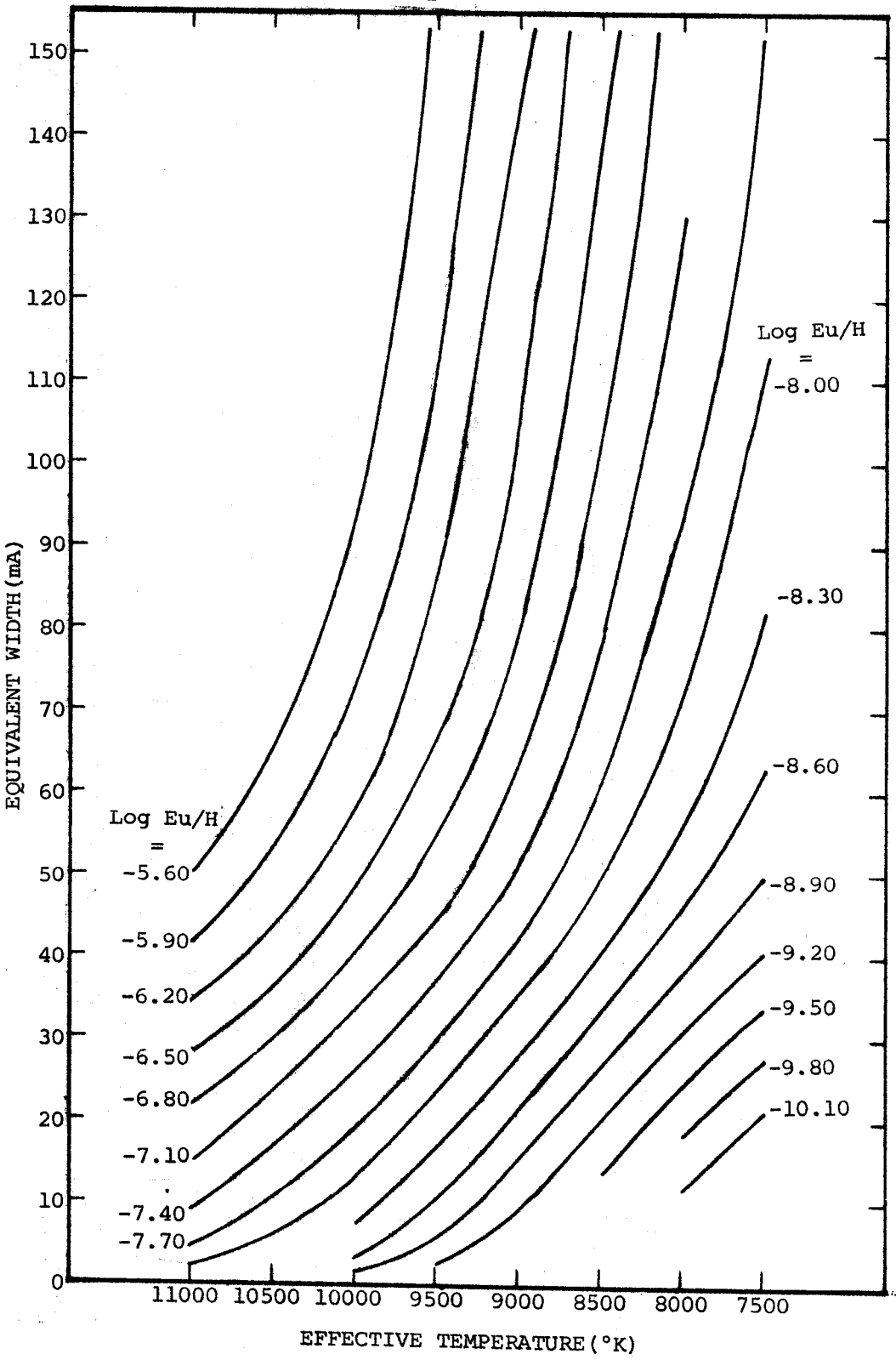
EQUIVALENT WIDTH (mA)
150
140
130
120
110
100
90
80
70
60
50
40
30
20
10
0
11000 10500 10000 9500 9000 8500 8000 7500
EFFECTIVE TEMPERATURE (°K)
Log Eu/H =
-5.60
-5.90
-6.20
-6.50
-6.80
-7.10
-7.40
-7.70
Log Eu/H =
-8.00
-8.30
-8.60
-8.90
-9.20
-9.50
-9.80
-10.10

We will now discuss the criteria for the identification of the individual elements.

Helium

The strongest HeI lines which can be detected using a IIa-O plate are λ4471.48 and λ4026.19. The latter, the weaker line, is normally blended with CrI(37) λ4026.17. In the cool Ap stars, there are no detectable features near λ4471.48 except for HD201601 where there is a line at λ4471.52 probably due to a weak CoI line at λ4471.52. As to the normal stars, λ4471 is absent in o Peg while it has an equivalent width of 70.8mÅ in ν Cap.

The strongest line of HeI is λ10830. Zirin (1968) has examined HD137909 and found that this line is absent (less than 35 mÅ).

Since most cool Ap stars are cooler than ν Cap, we do not expect the HeI lines. The absence of the line at λ4471 indicates that He is probably deficient in those stars which have effective temperatures near that of ν Cap, namely HD2453, HD12288, HD111133, HD192678, and HD216533.

Lithium and Beryllium

Most of the program stars are too hot to show the LiI resonance line at λ6707. No LiII lines have been observed in stars (Wallerstein Conti 1969) due to this ion's high excitation potential. Wallerstein and Merchant (1965) reported the presence of LiI lines in HD188041 (HR7575) and HD201601. These magnetic stars show a very high Li^6 content (Li^6/Li^7 = 0.5) implying spallation processes. Li might be present in HD137909. However, this is rather controversial

(Wallerstein and Hack 1964, Garstang 1964).

Wallerstein (1968) gives the following [Li/H] abundances:

HD137909 < 1.4

HD176232 < 1.9

HD201601 2.2

BeII, which has strong lines in the far ultraviolet, has been seen in stars (Wallerstein and Conti 1969), for example, α^2CVn (Bonsack 1961) and some Mn type Ap stars (Sargent, Searle, and Jugaku 1962). In SrCrEu stars, strong line blending prevents the identification of BeII lines.

Carbon

There are no strong CI lines in the region examined. The multiplet near λ4771 has been observed in a number of early A-type stars (Conti and Strom 1968a) and weakly in HD201601 (Bidelman 1966).

The strongest lines of CII are at λ4267.02 and λ4267.27. The former lies close to FeI(273) λ4266.97 which appears in most of the program stars. The CII lines are absent in o Peg and have a combined equivalent width of 20.3mÅ in ν Cap.

Twelve program stars have no measurable features near λ4267.27. The others have weak features whose equivalent widths are uncertain. These stars, equivalent widths (in mÅ), and line qualities follow: HD8441-11.0 D, HD81009 - 14.6 D, HD118022 - 5.6 W, HD137909 - 38.2 E, HD137949 - 41.3 E, HD176232 - 10.6 W, HD192678 - 13.3 D, HD201601 - 12.7 D, and HD216533 - 11.8 D. CII λ4267 is seen in stars as hot as

ν Cap (Searle and Sargent 1964). Thus, HD192678 and HD216533 might have normal C abundances while HD2453 and HD111133 may be deficient. HD12288 has broad lines due to its strong magnetic fields which makes it difficult to measure weak lines. The C abundances for the other cool Ap stars are unknown.

Nitrogen

The lowest excitation potential of any NI (I.P. = 14.53 eV) line in the region studied is 10.29 eV. Kohl (1964) claims to have seen NI lines between λ7423 and λ8719 in Sirius but he did not find multiplet 6 near λ4140. Sargent et al. (1962) tried to detect the infrared NI lines in four bright Ap stars. They did not although they are easily visible at the same dispersion for A and B type stars of the same temperature. N may well be deficient with respect to H in these stars although the absence of NI lines in the region observed in both the normal and cool Ap stars is as expected.

Oxygen

The strongest OI multiplet near the region studied is close to λ3947. Kohl (1964) claims that it is blended but present in Sirius. It is not, however, in o Peg (Maestre and Deutsch 1961), ν Cap (Adelman 1972), and HD204411 (Sargent et al. 1969). It is in an area of the plates which was not measured on the Grant Machine except for HD8441 for which the maximum equivalent width of the strongest line is about 5 mÅ.

Searle and Sargent (1962) examined the strongest OI lines, the infrared blends of multiplets 1 and 3, in peculiar and normal A stars. They found eight cool Ap stars have weak or undetectable OI lines. Their values for [O/H] for the stars in common with this study are:

HD118022	<-2.0
HD137909	<-1.8
HD176232	-0.9
HD201601	<-1.7
ν Cap	+0.1
o Peg	-0.2

Thus the sharp-lined cool Ap stars can have O/H deficiencies by factors greater than eight.

Neon and Aluminum

A. Sargent, Greenstein, and Sargent (1969) searched for NeI in the hotter Ap stars and found that the λ4200-Si stars are Ne deficient while the Mn stars may be marginally so. They found no NeI lines in ν Cap. Since the cool Ap stars are not much hotter than ν Cap, NeI lines are not expected to be observed.

The strongest lines of AlI are in a region not examined for this study at λ3944.01 and λ3961.52. They are present in the normal stars o Peg (Maestre and Deutsch 1961) and ν Cap (Adelman 1972). In the latter star the equivalent widths are 50.8 and 48.4 mÅ, respectively. The lines are absent in HD204411 (Sargent et al. 1969), but present in HD176232 (Auer 1964).

Magnesium

The strongest expected MgI line on most of the plates I examined was λ4702.98. However, it falls beyond the end of the spectrograms taken at Lick Observatory. Thus, in order to use the same line for all stars I chose the best remaining line λ4167.26 which is, unfortunately, normally blended with a weak GdII line λ4167.16 whose upper level is an unclassified term. In determining the unblended equivalent width, a correction has been applied for this blend component (see Ba for details) treating the GdII line as a null line. Consequently, the abundances deduced from λ4167 may be considered as upper limits.

The strongest MgII line is λ4481. This blend is treated as a single line which has an oscillator strength equal to the sum of those of its components and no Zeeman intensification. An exact treatment is complicated since it is a three component blend, two of which coincide in wavelength. In some program stars, lines from multiplet 10 can be identified. However, as they are often blended, they have not been used to derive abundances.

By comparing the abundances derived from MgI and MgII (Table A-25), we observe that the abundances from MgI are larger. This occurs even for normal stars. If this is a problem in the scale of oscillator strengths, depending whether case 1 or 2 abundances are preferred, the abundances from MgI should be decreased by .28 or .08 dex, respectively, to get agreement from both stages of ionization for the normal stars. This correction still leaves six stars with very poor agreement, i.e., 0.70 dex or greater.

TABLE II-10: MEAN Mg, Si, AND Ca ABUNDANCES

Star	Mg Abundance		Si Abundance		Ca Abundance	
	(1)	(2)	(1)	(2)	(1)	(2)
HD2453	-4.18	-4.23	-4.37	-4.39	-4.77	-5.79
HD5797	-4.13	-4.18	-3.81	-3.83	-5.38	-5.79
HD8441	-4.84	-4.91	-4.88	-4.89	-5.83	-6.33
HD12288	-4.44	-4.50	-3.68	-3.69	-4.64	-5.13
HD18078	-4.64	-4.69	-4.17	-4.18	-5.32	-5.78
HD22374	-5.05	-5.09	-4.44	-4.46	-6.23	-6.59
HD50169	-4.57	-4.63	-3.27	-3.29	-4.99	-5.37
HD81009	-4.69	-4.72	-4.44	-4.43	-5.59	-5.97
HD89069	-4.41	-4.47	-4.33	-4.34	-5.58	-6.08
HD110066	-4.46	-4.52	-3.63	-3.64	-4.88	-5.21
HD111133	-4.49	-4.56	-4.25	-4.26	-5.78	-6.30
HD118022	-4.34	-4.41	-4.85	-4.85	-4.90	-5.37
HD137909	-4.46	-4.50	-4.59	-4.60	-4.13	-4.42
HD137949	-4.74	-4.74	-4.44	-4.45	-4.42	-4.77
HD165474	-5.03	-5.06	-4.64	-4.65	-5.44	-5.82
HD176232	-4.74	-4.67	-4.56	-4.51	-5.12	-5.38
HD191742	-4.64	-4.65	-3.95	-3.97	-4.49	-4.84
HD192678	-4.78	-4.82	-3.47	-3.48	-5.00	-5.31
HD201601	-4.59	-4.50	-4.40	-4.34	-5.11	-5.37
HD204411	-4.56	-4.62	-4.48	-4.48	-4.39	-4.84
HD216533	-4.33	-4.40	-4.20	-4.21	-4.73	-5.21
ν Cap	-4.46	-4.52	-4.64	-4.65	-5.89	-6.25
o Peg	-4.51	-4.57	-4.83	-4.84	-5.63	-6.08

There are no suggested additional blending components in the line lists to which I had access for λ4167. Mg in the temperature range under consideration begins a transition from the singly-ionized to the doubly-ionized state at τ_{5000}=0.32. Thus λ4167 is extremely temperature sensitive. Changing the stellar gravity would also change the ionic abundances. As to line quality, of the worse cases of agreement only HD5797 has a λ4167 line marked E. Thus, the equivalent width may have been overestimated. It is possible that some of equivalent widths of λ4481 are underestimated. But even fairly large errors cannot significantly change the abundances derived from it. As to the damping constants errors, a small change in the slope of the damping part of the curve of growth can cause a larger change in the deduced abundance at a given equivalent width. Since λ4481 is relatively insensitive to atmospheric structure at the effective temperatures considered, I have chosen its deduced abundances as the preferable values (Table II-8) to those based on λ4167.

Silicon

SiI has many strong lines in its spectrum, most of which are in the red. Only λ3905.53 is in the region which the plates cover. However, it is seriously contaminated by CrII(167) λ3905.64 which is often stronger.

SiII has two strong multiplets in the region studied. Multiplet 3 at λ4128 and λ4131 is in a region of strong line blending for most cool Ap stars. Multiplet 1 has lines at λ3856, λ3863, and λ3854.

The strongest line λ3856 has an equivalent width which is difficult to determine due to nearby strong lines. The other two lines are suitable for equivalent width measurement.

In some of the hotter stars, especially those with relatively high Si abundances, SiII λ4200.66 and λ4200.90 (Moore 1965) can be seen as blend contributors. In addition the strongest line of SiIII, λ4552.56 may appear weakly in these stars.

Phosphorus

The original source of the data for the RMT's line list of PII (I.P. = 19.72 eV) contains errors of over 0.1Å in wavelength (Martin 1959). In Table II-11, I have listed the strongest PII lines, their intensities, and possible blend contaminants. Their excitation potentials are at least 11 eV so that for a given P abundance these lines would become easier to detect as the effective temperature increases for the stars under consideration. No identifications were made using the four best lines. Thus, its abundance is unknown. In some Si stars, P has a normal abundance while it is found in large excesses in some Mn stars (Sargent and Searle 1967).

Chlorine and Argon

ClII lines are found in α^2 CVn (Cohen 1970) and in τ Cap and HR6870 (Bidelman 1966). Jugaku, Sargent, and Greenstein (1961) found Ar lines in 3 Cen A. HD34452 has lines from both elements (Tomley,

TABLE II-11: THE STRONGEST PII LINES BETWEEN λ3600 AND λ4800

Wavelength(A)	Intensity	Possible Blends
4420.71	400	ScII(14) λ4420.67
4588.04	500	CrII(44) λ4588.22*
4589.86	500	CrII(44) λ4589.89*
4602.08	600	FeI(39) λ4602.01
4626.70	300	CrI(209) λ4626.81
4658.31	300	

Notes: Wavelengths and Intensities from Martin (1959)

Possible Blends from Moore (1945)

*Indicates the line is not useable for line identifications.

Wallerstein, and Wolff 1970). No lines of these elements were found in the program stars.

Calcium

The resonance line of CaI λ4226.73 is present in all program stars. In most of them, lines from multiplets 4 and 5 are also seen. In some of the hotter stars, λ4227 gives a smaller abundance than the higher excitation lines. However, it is the only CaI line from which abundances can be deduced from the normal stars. The derived abundance may not be correct because the assumed structure of the outer parts of the atmosphere is incorrect.

CaII has two strong lines at λ3933.66 and λ3968.47. The latter is near the core of Hε and blended with it. The former, the K line, is often suitable for abundance determinations in normal late B and early A stars. However, in some cool Ap stars this line is so strong that it is difficult to determine its equivalent width while in others where the line is weaker, it is badly blended by nearby lines. For these reasons, I have not derived Ca abundances from the K line. Its measured equivalent widths (Table A-55) which should be regarded as rather crude estimates tend to correlate with the abundances deduced from the CaI lines. Stars having the largest Ca abundances have the largest K line equivalent widths and conversely.

TABLE II-12: MEAN Sc, V, and Co ABUNDANCES

Star	Sc Abundances		V Abundances		Co Abundances	
	(1)	(2)	(1)	(2)	(1)	(2)
HD2453	-8.08	-8.32	-8.08:	-8.20:	-5.99:	-6.29:
HD5797	-8.07	-8.30	-7.82	-7.94	-4.13	-4.45
HD8441	-9.24	-9.48	-7.84	-7.98	-6.75:	-7.10:
HD12288	-7.92	-8.19	-7.90ul	-8.07ul	-6.03ul	-6.57ul
HD18078	-8.64	-8.84	-7.64	-7.77	-5.43	-5.71
HD22374	-8.86	-8.99	-8.27ul	-8.39ul	-6.90ul	-7.21ul
HD50169	-8.78	-8.99	-8.13:	-8.22:	-5.56	-5.83
HD81009	-8.43	-8.66	-7.86:	-8.00:	-6.41:	-6.78:
HD89069	-8.68	-8.96	-7.67:	-7.89:	-5.40	-5.77
HD110066	-8.17	-8.43	-7.62	-7.76	-5.45	-5.76
HD111133	-8.93	-9.23	-7.74:	-7.92:	-5.26	-5.60
HD118022	-8.67	-8.94	-8.12ul	-8.23ul	-5.82	-6.19
HD137909	-7.19	-7.35	-7.48:	-7.59:	-5.65:	-5.89:
HD137949	-7.52	-7.73	-7.29	-7.41	-6.31	-6.64
HD165474	-8.63	-8.84	-8.10:	-8.24:	-7.16ul	-7.45ul
HD176232	-9.71	-9.91	-7.81	-8.04	-6.18	-6.52
HD191742	-8.54	-8.75	-7.46	-7.60	-6.49:	-6.92:
HD192678	-8.38	-8.56	-7.28	-7.38	-4.98	-5.20
HD201601	-9.41	-9.60	-7.20	-7.45	-6.34	-6.65
HD204411	-8.64	-8.86	-8.06:	-8.20:	-6.01	-6.37
HD216533	-8.82	-9.10	-7.89:	-8.05:	-6.17ul	-6.50ul
ν Cap	-9.16	-9.43	-8.48	-8.63	-6.31ul	-6.64ul
o Peg	-9.18	-9.42	-8.03	-8.15	-6.57ul	-6.89ul

Notes: V Upper Limits (ul) based on the equivalent width of λ4183 = 15mÅ.

Co Upper limits (ul) based on the equivalent width of λ3995 = 15mÅ.

Titanium

Nine lines of TiI and fourteen of TiII are used for the abundance determinations. They include the strongest easily accessible TiI line λ4533.24. Two lines of TiII multiplet 61 near λ4409 are sometimes blended together. When this occurs, I divide the blended equivalent width in half and derive an abundance using the mean line parameters.

Only for HD5797 and HD137909 are the TiI lines sufficiently strong so that their derived abundances compare in accuracy with those from the TiII lines. The agreement in these cases is fair to good. For these two stars, I averaged the results from both stages of ionization using the number of lines measured as weights to obtain the mean Ti abundance (Table II-13). For the other stars I used the abundances derived from the TiII lines as the mean Ti abundance.

Vanadium

VI has only strong multiplet in the region studied. It includes the ultimate line at λ4379.24 which, however, can be measured in only two stars HD176232 and HD201601. In the latter, λ4389.97 can also be measured.

Most of the strong lines of VII are shortward of the Balmer jump or in regions which I did not reduce. However, I measured the two strongest lines of multiplet 23, λ4005.71 and λ4023.39. The other lines I used were λ4178.39, λ4183.44, and λ4202.35 which was usually blended with a possible GdIII line. The results obtained from

TABLE II-13: MEAN Ti ABUNDANCE DETERMINATION

Star	From TiI Lines		From TiII Lines		Adopted Ti Abundance	
	(1)	(2)	(1)	(2)	(1)	(2)
HD2453	-5.01:	-5.37:	-6.02	-6.21	-6.02	-6.21
HD5797	-4.64	-5.00	-4.72	-4.91	-4.69	-4.94
HD8441	n.m.	n.m.	-6.79	-6.97	-6.79	-6.97
HD12288	-5.29:	-5.64:	-5.77	-5.97	-5.77	-5.97
HD18078	-5.08:	-5.39:	-6.50	-6.67	-6.50	-6.67
HD22374	-6.44:	-6.75:	-6.83	-6.98	-6.83	-6.98
HD50169	n.m.	n.m.	-6.40	-6.59	-6.40	-6.59
HD81009	-6.10:	-6.44:	-6.63	-6.79	-6.63	-6.79
HD89069	n.m.	n.m.	-6.34	-6.53	-6.34	-6.53
HD110066	-4.95:	-5.30:	-6.32	-6.47	-6.32	-6.47
HD111133	-5.32:	-5.76:	-6.50	-6.70	-6.50	-6.70
HD118022	n.m.	n.m.	-6.16	-6.34	-6.16	-6.34
HD137909	-5.36	-5.55	-5.65	-5.80	-5.55	-5.72
HD137949	-6.51:	-6.89:	-6.33	-6.52	-6.33	-6.52
HD165474	-6.13:	-6.47:	-6.64	-6.79	-6.64	-6.79
HD176232	-7.13:	-7.45:	-6.82	-6.97	-6.82	-6.97
HD191742	-6.46:	-6.72:	-6.43	-6.59	-6.43	-6.59
HD192678	-5.07:	-5.32:	-5.97	-6.12	-5.97	-6.12
HD201601	-7.06:	-7.34:	-6.93	-7.11	-6.93	-7.11
HD204411	-5.82:	-6.17:	-5.99	-6.16	-5.99	-6.16
HD216533	-4.69:	-5.06:	-6.21	-6.41	-6.21	-6.41
ν Cap	n.m.	n.m.	-7.18	-7.39	-7.18	-7.39
o Peg	n.m.	n.m.	-6.94	-7.11	-6.94	-7.11

multiplet 23 are substantially different from those of the other lines. This I attribute to difficulties in placing the continuum. I have omitted these results except for ν Cap.

Chromium

Of the strongest CrI lines in the region studied only λ4274.80 is suitable for equivalent width measurement in many program stars. There are many suitable lines for measurement between λ4200 and λ4635. However, I used the oscillator strengths of Wolnik et al. (1968, 1969) which restricted this selection process. I measured λ4275 to derive abundances for the normal stars. Its oscillator strength is an atomic beam measurement of Lawrence, Link, and King (1965) which agrees quite well with that of Corliss and Bozman (1962).

CrII has two strong multiplets between λ4200 and λ4635, numbers 31 and 44. The latter has very strong lines in many program stars and due to a desire to avoid using lines on the damping part of the curve of growth, no lines of this multiplet were included in the abundance determinations. In addition to five lines of multiplet 31, I selected CrII(18) λ4217.07, which for a few stars is blended with GdII(49) λ4217.20, and CrII(162) λ4224.85.

In many stars, there is a discrepancy of about a factor of ten between the result derived from the ground term line CrI λ4275 and the other CrI lines which have excitation potentials near one electron volt. There are two basic types of explanations: oscillator strength and model atmosphere problems. As for CaI(2) λ4227, the latter is

TABLE II-14: MEAN Cr ABUNDANCE DETERMINATIONS

Star	From CrI Lines		From CrII Lines		Adopted Cr Abundance	
	(1)	(2)	(1)	(2)	(1)	(2)
HD2453	-3.12	-3.43	-3.68	-3.78	-3.34	-3.57
HD5797	-2.52	-2.84	-3.51	-3.63	-2.78	-3.08
HD8441	-3.66	-3.99	-3.77	-3.87	-3.71	-3.93
HD12288	-3.24	-3.58	-3.19	-3.30	-3.21	-3.42
HD18078	-3.55	-3.83	-3.88	-3.98	-3.68	-3.90
HD22374	-3.81	-4.08	-4.24	-4.32	-3.97	-4.18
HD50169	-3.54	-3.83	-3.76	-3.86	-3.64	-3.84
HD81009	-4.58	-4.91	-4.74	-4.82	-4.65	-4.86
HD89069	-3.82	-4.19	-4.00	-4.10	-3.90	-4.14
HD110066	-3.18	-3.53	-3.58	-3.70	-3.35	-3.61
HD111133	-3.72	-4.08	-4.01	-4.11	-3.91	-4.09
HD118022	-3.68	-4.04	-3.91	-3.98	-3.78	-4.01
HD137909	-3.91	-4.16	-4.35	-4.42	-4.08	-4.27
HD137949	-4.65	-4.98	-4.39	-4.47	-4.57	-4.65
HD165474	-4.71	-5.06	-4.93	-5.00	-4.81	-5.03
HD176232	-5.24	-5.54	-5.13	-5.17	-5.18	-5.36
HD191742	-3.56	-3.88	-3.98	-4.08	-3.72	-3.97
HD192678	-2.88	-3.12	-3.67	-3.73	-3.12	-3.34
HD201601	-5.28	-5.58	-5.27	-5.31	-5.27	-5.42
HD204411	-3.97	-4.28	-4.47	-4.56	-4.15	-4.40
HD216533	-3.26	-3.62	-3.80	-3.90	-3.45	-3.74
ν Cap	-5.94	-6.27	-6.04	-6.12	-5.99	-6.19
o Peg	-5.82	-6.11	-5.96	-6.03	-5.88	-6.07

more likely. Nevertheless, including λ4275 in the average only changes the value slightly.

The difference between the abundances deduced from CrI and CrII lines is around 0.20 dex for case 1 effective temperatures on the average. In Table II-14, the adopted Cr abundances are given. They are the mean of those determined from CrI and CrII lines.

Manganese

The strongest lines of MnI are due to the ground term multiplet near λ4030. When I measured lines in the region which included them, I already knew about the problems with resonance lines and skipped them. Between λ4200 and λ4635, the strongest lines belong to multiplets 22, 23, and 28. Two lines of multiplet 23 are blended with each other λ4235.14 and λ4235.29. When I needed an additional line to improve the abundance determination, I used this blend. In this case, I used one-half of the equivalent width and the mean parameters of the blend components.

MnII has many strong lines in the primary region studied (Velasco, Iglesias, Gullon, and Diago 1963 and the RMT). I could find only five lines for abundance determinations since there are only a limited number of oscillator strengths available (Warner 1967). To include MnII lines from the normal stars, it is necessary to observe the ultraviolet region (Searle et al. 1966).

The value of log Mn/H for the normal stars has been assumed to be solar since it was not determined for them. Table II-15 contains

TABLE II-15: MEAN Mn ABUNDANCE DETERMINATIONS

Star	From MnI Lines		From MnII Lines		Adopted Mn Abundance	
	(1)	(2)	(1)	(2)	(1)	(2)
HD2453	-5.05	-5.29	-5.21	-5.26	-5.14	-5.27
HD5797	-4.89	-5.20	-4.00	-4.05	-4.25	-4.32
HD8441	-5.82:	-6.10:	-5.55	-5.60	-5.60	-5.69
HD12288	n.m.	n.m.	-5.68:	-5.73:	-5.68:	-5.73:
HD18078	-5.23	-5.47	-5.13	-5.19	-5.19	-5.31
HD22374	-6.21	-6.47	-5.63	-5.70	-5.84	-5.93
HD50169	-5.34:	-5.57:	-5.53	-5.58	-5.46	-5.58
HD81009	-6.00	-6.31	-5.62	-5.67	-5.71	-5.80
HD89069	-5.22	-5.53	-4.48	-4.54	-4.71	-4.80
HD110066	-5.24	-5.52	-5.22	-5.28	-5.23	-5.37
HD111133	-5.07	-5.37	-5.04	-5.10	-5.06	-5.17
HD118022	-5.46	-5.84	-5.42	-5.48	-5.43	-5.57
HD137909	-5.43	-5.65	-5.36	-5.41	-5.41	-5.55
HD137949	-6.10	-6.39	-5.30	-5.36	-5.79	-5.92
HD165474	-6.39:	-6.77:	-5.81:	-5.85:	-6.01:	-6.10:
HD176232	-6.80	-7.10	-6.07	-6.10	-6.48	-6.59
HD191742	-6.08	-6.39	-5.38	-5.40	-5.68	-5.76
HD192678	-5.35	-5.53	-5.43	-5.48	-5.40	-5.50
HD201601	-6.69	-6.93	-5.88	-5.91	-6.12	-6.28
HD204411	-5.90	-6.21	-5.92	-5.96	-5.91	-6.11
HD216533	-5.17	-5.45	-5.12	-5.19	-5.14	-5.30
ν Cap	n.m.	n.m.	n.m.	n.m.	n.m.	n.m.
o Peg	n.m.	n.m.	n.m.	n.m.	n.m.	n.m.

the derivation of the mean Mn abundance from both MnI and MnII line averages with the number of lines used as weights. In general, the agreement from both stages of ionization is good. However, for a few stars it is poor. The difference is a factor of 14 for HD5797 which probably results from unknown blending constituents in the MnII lines.

Iron

The Fe abundances have been determined previously from FeI and FeII lines. Wright et al. (1964) indicate that in early B-type stars in the region which they studied λ4419.60 is the strongest FeIII line. If we use this line and the next two weaker members of FeIII(4) λ4431.01 and λ4395.75, as a guide to identification, then this ion is present in HD8441 and HD12288 and possibly in HD18078 and HD111133.

Cobalt

No CoI lines between λ4190 and λ4635 are suitable for equivalent width measurement. The abundances are based on λ3873.12 and λ3995.31. The continuum levels are more uncertain than for lines longward of their positions.

The RMT lists CoII lines only between λ3350 and λ3622. The spectrum of HD201601 contains several of these lines. Thus without suitable plates, the only lines that can be used are from CoI.

Nickel

NiI has several moderately strong lines between λ4200 and λ4635 of which only λ4462.46 and λ4470.48 can be measured for equivalent widths. The oscillator strengths used are from Garz, Heise, and Richter (1970) which are more accurate than those of Corliss and Bozman (1962). Unfortunately this list is rather limited and no value is given for NiI(32) λ3858.30 which can be measured in most cool Ap stars.

NiII has its strongest lines in the ultraviolet. The strongest accessible lines above λ4000 are normally blended except for λ4244.80. The mean Ni abundances adopted (Table II-16) are the smaller abundances from the NiI and NiII lines unless the derived abundances are nearly equal. The upper limits are based on the equivalent widths of NiI(86) λ4470.48 and NiII(9) λ4244.80 equal to 15 mÅ.

Copper

Between λ3800 and λ4635, there are two unblended lines of CuII (I.P. = 20.29 eV), λ4506.00 and λ4043.50. Neither was identified in any of the stellar line lists consulted. Thus the latter feature was not looked for. As to the former, no features were close enough for tentative identification in the cool Ap stars except possibly in HD5797 and HD191742.

Guthrie (1969a) has discussed the detection of neutral and singly-ionized lines for elements with Z>30. No lines are expected from elements whose isotopes are all radioactive and have half-lives short

TABLE II-16: MEAN Ni ABUNDANCE DETERMINATIONS

Star	From NiI Lines		From NiII Lines		Adopted Ni Abundance	
	(1)	(2)	(1)	(2)	(1)	(2)
HD2453	-4.42	-4.67	-5.73	-5.75	-5.73	-5.75
HD5797	-5.21ul	-5.47ul	-5.49	-5.55	-5.49	-5.55
HD8441	-4.86ul	-5.10ul	-5.99ul	-6.02ul	-5.99ul	-6.02ul
HD12288	-4.64ul	-4.88ul	-6.00ul	-6.00ul	-6.00ul	-6.00ul
HD18078	-4.59	-4.83	-6.00ul	-6.03ul	-6.00ul	-6.03ul
HD22374	-5.31ul	-5.56ul	-6.07ul	-6.12ul	-6.07ul	-6.12ul
HD50169	-4.88ul	-5.09ul	-5.94:	-5.97:	-5.94	-5.97
HD81009	-5.38:	-5.65:	-6.09ul	-6.16ul	-6.09ul	-6.16ul
HD89069	-4.79	-5.06	-5.80	-5.86	-5.80	-5.86
HD110066	-4.57	-4.82	-5.72	-5.76	-5.72	-5.76
HD111133	-4.15:	-4.44:	-6.00ul	-6.00ul	-6.00ul	-6.00ul
HD118022	-4.93:	-5.20:	-5.94:	-6.00:	-5.94:	-6.00:
HD137909	-4.74	-4.96	-5.51	-5.55	-5.51	-5.55
HD137949	-5.38	-5.66	-6.17ul	-6.24ul	-6.17ul	-6.24ul
HD165474	-5.31:	-5.59:	-6.10ul	-6.18ul	-6.10ul	-6.18ul
HD176232	-6.16:	-6.38:	-6.28ul	-6.34ul	-6.28ul	-6.38:
HD191742	-5.28	-5.53	-5.30	-5.36	-5.29	-5.44
HD192678	-4.09	-4.27	-6.00ul	-6.00ul	-6.00ul	-6.00ul
HD201601	-6.04	-6.27	-6.29ul	-6.35ul	-6.29ul	-6.35ul
HD204411	-5.09:	-5.38:	-6.01:	-6.07:	-6.01:	-6.07:
HD216533	-4.50	-4.77	-5.41	-5.46	-5.41	-5.46
ν Cap	-4.90ul	-5.14ul	-6.80	-6.86	-6.80	-6.86
o Peg	-5.09ul	-5.32ul	-5.99	-6.02	-5.99	-6.02

compared with the age of the peculiar A stars (~10^8 to 10^9 years). The strongest lines of neutral and singly-ionized atoms for elements beyond the Fe peak (Meggers 1941) show a general correlation with ionization potential. Neutral lines will be difficult to detect since the ionization potentials are usually between 4.8 and 7.6 eV. Thus these atoms are usually singly-ionized. The wavelengths of the strongest lines for atoms with the higher ionization potentials are usually less than λ3300. For singly-ionized atoms there is a similar decrease in the wavelength of the strongest lines with increase in ionization potential. It is longward of λ3300 only when the ionization potential is less than about 13.4 eV which occurs for Sr, Y, Zr, Ba, the rare earths, and Th.

Gallium and Arsenic

GaII (I.P. = 20.51 eV) (Bidelman and Corliss 1962) has several lines near λ4250 of which only λ4251.11 and λ4251.16 can be used for identification of this ion. They are not the strongest GaII lines. For two stars, HD2453 and HD111133, I measured weak features near λ4251.13. The resulting abundances should be regarded as upper limits (Table A-39). Abundances from GaII lines increase as the effective temperature decreases. Ga lines are observed in Mn type Ap stars (Sargent and Searle 1967).

AsII (I.P. = 18.63 eV) has two lines in the region studied at λ4552.37, which is sometimes blended with TiI(42) λ4552.45, and at λ4352.25, which is reputed to be the stronger. The minimum excitation

potential is 9.77 eV. In some stars, a feature appears at the wavelength of the weaker line, but its strength is inconsistent with the expected intensities.

Selenium and Krypton

The strongest unblended wavelengths of SeII (I.P. = 21.5 eV) in the region studied and their intensities follow (Martin 1935): λ4180.94 - 10, λ4446.02 - 8, λ4467·60 - 8, and λ4604.34 - 7. SeII is probably present in HD2453, HD165474, and HD216533. A more complete analysis is required for positive identification. Bidelman (1966) believes that SeII lines are present in HD188041 (HR7575).

Kr has been identified in Mn type Ap stars (Sargent and Searle 1967).

Strontium

The only strong line of SrI available for study is its resonance line at λ4607.33. There are no known lines close to its position except for a weak AuI line at λ4607.34 (RMT and NBS 32). SrII has four lines to be considered for equivalent width measurement of which λ4161.80 and λ4215.52 are the least bad.

The SrII λ4215.52 oscillator strength is taken from Penkin (1964). It agrees with the Bates-Damsgaard calculation of Goldberg, Müller, and Aller (1960). The value from Corliss and Bozman (1962) is -0.99 dex. If it is believed, all abundance determinations from this line are

TABLE II-17: COMPARISON OF Sr ABUNDANCES

Star	From SrI Lines		From SrII Lines	
	(1)	(2)	(1)	(2)
HD2453	-4.38	-4.85	-6.66	-6.99
HD5797	-4.83	-5.34	-6.15	-6.45
HD8441	n.m.	n.m.	-6.88	-7.17
HD12288	n.m.	n.m.	-8.35	-8.71
HD18078	-4.98	-5.42	-6.47	-6.77
HD22374	n.m.	n.m.	-8.85	-9.23
HD50169	n.m.	n.m.	-5.73	-6.03
HD81009	-6.09:	-6.61:	-7.54	-7.81
HD89069	n.m.	n.m.	-7.77	-8.03
HD110066	-4.71	-5.17	-6.17	-6.54
HD111133	-4.23	-4.81	-5.23	-5.60
HD18022	n.m.	n.m.	-6.77	-7.12
HD137909	-4.91	-5.29	-6.94	-7.17
HD137949	-4.86	-5.31	-6.42	-6.71
HD165474	-5.88	-6.34	-7.22	-7.52
HD176232	-6.47	-6.85	-7.00	-7.20
HD191742	-3.86	-4.45	-5.78	-6.08
HD192678	n.m.	n.m.	-8.33	-8.55
HD201601	-6.25	-6.65	-7.34	-7.54
HD204411	n.m.	n.m.	-8.06	-8.42
HD216533	-4.92	-5.49	-5.34	-5.67
ν Cap	n.m.	n.m.	-9.10	-9.45
o Peg	n.m.	n.m.	-8.48	-8.77

increased by .88 dex. This would increase the disagreement between the results derived from the normal A stars and the solar abundance.

The SrI lines give larger abundances by factors up to 100 compared with those from SrII (see Table II-17). This implies that the equivalent width of λ4607 is not due entirely to SrI in all cool Ap stars. Because of this difficulty, I have adopted the abundances from the SrII lines as the elemental abundances.

Yttrium and Zirconium

Between λ4100 and λ4700, the only YII line suitable for equivalent width measurement is λ4398.02. In order to improve the abundance determinations, I measured λ3965.35 and λ3982.59.

ZrII has most of its strongest lines below λ4100. For the region I examined, I could only find two blend free lines λ4179.81 and λ4317.32. In addition to those stars for which equivalent widths were measured, ZrII can be detected in HD18078 and probably in HD2453.

Niobium and Molybdenum

NbII (I.P. = 14.32) has three strong lines in the region studied of which only λ4527.65, although it is in the far wing of a CrI, is usuable for line identification. NbII is probably present in the spectra of HD22374 and HD201601.

MoI (I.P. = 7.10 eV) has several lines in the region studied of which only λ3864.12 was possibly identified in HD191742. MoII (I.P. = 16.15 eV) is identified in many cool Ap stars by use of the

TABLE II-18: MEAN Y, Ce, AND Nd ABUNDANCES

Star	Y Abundances		Ce Abundances		Nd Abundances	
	(1)	(2)	(1)	(2)	(1)	(2)
HD2453	-8.42	-8.72	-7.97	-8.21	-6.72	-7.04
HD5797	-8.66:	-8.92:	-8.24:	-8.50:	-6.61	-6.95
HD8441	-8.28	-8.56	-9.29:	-9.56:	-7.30	-7.67
HD12288	-8.12	-8.44	-8.48:	-8.75:	-6.43	-6.78
HD18078	-8.15	-8.40	-8.21:	-8.43:	-7.62	-7.94
HD22374	-8.62	-8.86	-9.42ul	-9.64ul	-8.08	-8.34
HD50169	-8.30	-8.61	-8.48:	-8.72:	-7.42	-7.72
HD81009	-8.48	-8.75	-8.16	-8.36	-8.46	-8.73
HD89069	-8.37	-8.72	-8.47:	-8.75:	-7.34	-7.72
HD110066	-8.42	-8.70	-8.03	-8.29	-6.86	-7.20
HD111133	-8.16	-8.53	-8.70ul	-9.00ul	-7.22	-7.62
HD118022	-8.44	-8.75	-8.30	-8.58	-7.67	-8.08
HD137909	-8.02	-8.18	-7.49	-7.70	-7.67	-7.97
HD137949	-8.16	-8.40	-8.14	-8.34	-7.28	-7.60
HD165474	-8.50	-8.77	-8.46	-8.68	-8.92	-9.27
HD176232	-8.80	-9.03	-9.44	-9.63	-9.87	-10.12
HD191742	-9.22	-9.45	-8.38	-8.58	-7.91	-8.19
HD192678	-8.37	-8.67	-8.84ul	-9.09ul	-6.37	-6.69
HD201601	-8.22	-8.42	-9.12	-9.29	-8.90	-9.09
HD204411	-9.23	-9.50	-9.36ul	-9.60ul	-8.37	-8.67
HD216533	-8.46:	-8.83:	-8.16:	-8.48:	-6.56	-6.93
ν Cap	-8.50ul	-8.75ul	-8.78ul	-9.06ul	-8.16ul	-8.54ul
o Peg	-8.74	-9.00	-9.00ul	-9.24ul	-8.46ul	-8.79ul

Notes: Y upper limit based on an equivalent width of YII λ3950 = 15mÅ.
Ce upper limit based on an equivalent width of CeII λ4187 = 15mÅ.
Nd upper limit based on an equivalent width of NdII λ4303 = 15mÅ.
The solar abundances follow: Y -8.80, Ce -10.22, and Nd -10.07.

TABLE II-19: MEAN Zr, Ba, AND La ABUNDANCES

Star	Zr Abundances (1)	Zr Abundances (2)
HD50169	-7.69:	-7.91:
HD81009	-7.87:	-8.09:
HD89069	-7.45:	-7.72:
HD137909	-7.04	-7.21
HD137949	-7.80:	-8.06:
HD165474	-7.69:	-7.91:
HD201601	-8.71	-8.92

Star	Ba Abundances (1)	Ba Abundances (2)
HD81009	-9.53:	-9.97:
HD118022	-9.32:	-9.52:
HD137909	-7.83	-8.02
HD137949	-7.79	-8.03
HD165474	-9.57	-9.97
HD176232	-10.06	-10.39
HD191742	-8.19	-8.50
HD201601	-8.53	-8.80
HD204411	-7.81	-8.25
HD216533	-6.77	-7.26
ν Cap	-8.77	-9.18
o Peg	-8.04	-8.38

Star	La Abundances (1)	La Abundances (2)
HD2453	-9.30:	-9.53:
HD5797	-8.19	-8.44
HD12288	-8.31	-8.56
HD50169	-8.93	-9.14
HD81009	-8.77	-8.97
HD89069	-9.10:	-9.34:
HD118022	-9.36:	-9.63:
HD137949	-8.21	-8.43
HD176232	-10.24:	-10.44:
HD192678	-8.71	-8.95
HD201601	-8.96	-9.11
HD216533	-8.39:	-8.65:

strongest lines of multiplet 3. In some stars, it was possible to measure the equivalent widths of two of these lines (Table A-56). No oscillator strengths are known. The value for HD111133 is very questionable while HD22374 and HD50169 are other stars likely to have MoII lines in their spectra.

Palladium, Cadmium, and Xenon

PdI (I.P. = 8.33 eV) has only one line above λ3800, λ4212.95 which was not observed. I found several strong PdI lines in the ultraviolet spectrum of HD201601 on 2 Å/mm plates. Both PdI and PdII lines appear in HR465 (Bidelman 1967).

CdI (I.P. = 8.99 eV) has no lines between λ3614 and λ4678. The line at λ4678 is present in HD201601 (Bidelman 1971b) as is the line at λ4800 which is blended. These lines are not identified in HD204411 (Sargent et al. 1969) although there are features within .04Å of both wavelengths. Lines of XeI are seen in two Mn stars, κ Cnc and 112 Her (Bidelman 1967).

Barium

The resonance line of BaII at λ4554.03 is blended with CrI(276) λ4553.95 and possibly with ZrII(130) λ4553.96 which will be ignored. Of the other strong lines only λ4166.00 is blend-free. Unfortunately, its equivalent width is measurable in only four stars. In order to obtain crude abundance estimates, I have measured the equivalent width of the blend of BaII(1) λ4554 with CrI(276) λ4554. Then using

the mean Cr abundances and magnetic field strengths, I predicted the equivalent width of the CrI contribution. Then I found the difference d between the blend's and the CrI line's equivalent width. As a correction factor, I used 1/3 of the equivalent width of the CrI line or $\frac{1}{2} d$ whichever was smaller. The resulting equivalent widths, I treated in the standard manner. In addition to the blending problem, the deduced abundances also have problems associated with resonance lines.

Cerium

CeII is well represented in the spectra of some cool Ap stars. The strongest lines of multiplets 1 and 2, especially λ4186.60, λ4460.21, and λ4562.36, and λ4628.16 were used to make the initial identifications. The excitation potentials are from Corliss and Bozman (1962). The strongest CeII line λ4186.60 often has a poorly defined profile.

The strongest unblended lines of CeIII in the region primarily studied and their intensities are λ4448.32-600, λ4627.60-500, and λ4485.27-500 (Sugar 1965). No identifications were made.

Praseodymium

I used the excitation potentials combined with the oscillator strengths of Corliss and Bozman (1962) to determine the strongest expected PrII lines of which four were suitable for equivalent width measurement. Abundances from the weakest of these lines should be

TABLE II-20: Pr AND Sm ABUNDANCES

Star	Pr Abundances		Star	Sm Abundances	
	(1)	(2)		(1)	(2)
HD8441	-7.74:	-8.07:	HD2453	-7.02	-7.35
HD50169	-8.51	-8.81	HD5797	-7.46	-7.83
HD110066	-8.36	-8.72	HD18078	-7.10	-7.45
HD111133	-8.20:	-8.56:	HD110066	-7.03	-7.31
HD118022	-8.24	-8.67	HD137909	-6.71	-7.00
HD137909	-7.21:	-7.44:	HD137949	-7.37	-7.73
HD137949	-7.63	-7.90	HD176232	-8.33	-8.65
HD165474	-8.68	-8.95	HD191742	-8.21:	-8.47:
HD201601	-8.25:	-8.46:	HD201601	-8.33	-8.60
HD216533	-8.48:	-8.83:			

regarded as uncertain unless determinations from the stronger lines are available, e.g., HD8441 and HD137909. There are lines of PrIII in χLupi (Bidelman 1967). By analogy with CeIII, these lines are not expected in the cool Ap stars. Sugar (1961, 1969) has studied this ion.

Promethium

Aller and Cowley (1970) claim to have tentatively identified lines of PmII (I.P. = 10.90 eV) in HR465. There are no identifications in the program cool Ap stars of this ion by use of those lines which have laboratory intensities greater or equal to 80 (Meggers, Schribner, and Bozman 1951). My choice of region examined excluded some lines. λ3877.63 was included in some stellar line searches. To be fair, I did not measure λ3919.09 which Aller and Cowley claim is the strongest blend-free PmII line. However, I suggest that this feature in HR465 is due to FeI(430) λ3919.07 and CrI(23) λ3919.16. The latter line was given by Bidelman (1971a) as the identification of a feature at λ3919.12 in HR7575. All Pm isotopes are radioactive. The longest known half-life is 18 years (Weast 1968).

Europium

EuII has several strong lines in the region of interest which can be measured. Most of them are blended. I chose the easiest to deal with: λ4205.05, blended with GdII(46) λ4204.86 and VII(37) λ4205.08, and λ4435.58, blended with CaI(4) λ4435.69. These lines I treated similarly to BaII(1) λ4554.03. In addition, I measured the equivalent

width of λ3907.10 which fell in a region of the spectrum only measured with the Grant Machine for HD8441. I compared microphotometer tracings of the spectra of the other stars with HD8441 in order to find this line. This method is less accurate than direct measurement.

Gadolinium

Nine lines of GdII between λ4200 and λ4635 are suitable for equivalent width measurement. Crosswhite (1968) measured the wavelengths and intensities of some GdIII lines. Those between λ4150 and λ4650 and their intensities and blend components are given in Table II-21. If we regard those coincidences with lines marked as GdII(-) as really being the same line, then by use of this list GdIII is probably present in HD2453, HD5797, HD8441, HD18078, HD81009, HD110066, HD111133, HD137909, HD191742, and HD216533. I measured the equivalent width of λ4202.52 when it was not too badly blended with VII(25) λ4202.35 (Table A-57). Although there is no alternative identification, I doubt that this feature is entirely due to GdIII.

Terbium and Dysprosium

The best unblended lines of TbII (I.P. = 11.52 eV) (NBS 32) in the region studied are λ4144.26 intensity 100 and λ4278.52 intensity 70. In HD2453, HD12288, and HD216533 at least the strongest line is present.

The strongest lines of DyII (I.P. = 11.67 eV) in the region of the plates measured on the Grant Machine are λ4000.48, which is blended with FeI(426) λ4000.47, and λ3872.13. The next strongest lines are

TABLE II-21: GdIII LINES IN λ4150 - λ4650

λ(Å)	Intensity	Blend Components
4202.521	41	VII(25) λ4202.350
4205.375	39	MnII(2) λ4205.40
4212.000	44	GdII(15) λ4212.001
4238.777	43	GdII(-) λ4238.782 and others
4253.603	42	GdII(-) λ4253.612
4341.277	43	Hγ and others
4397.505	44	GdII(-) λ4397.51
4548.007	39	FeI(755) λ4547.851
4563.010	40	CrI(246) λ4563.245
4579.593	40	FeII(-) λ4579.523
4606.641	40	

TABLE II-22: MEAN Eu, Gd, AND U ABUNDANCES

Star	Eu Abundance		Gd Abundance		U Abundance	
	(1)	(2)	(1)	(2)	(1)	(2)
HD2453	-5.78	-6.16	-7.34	-7.54	-8.90	-9.09
HD5797	-5.98	-6.47	-6.78	-7.07	-8.04	-8.25
HD8441	-7.31	-7.65	-6.95	-7.25	-8.76	-8.97
HD12288	-7.42	-7.85	-7.02	-7.34	-9.53ul	-9.73ul
HD18078	-7.81	-8.08	-7.26	-7.53	-9.09	-9.26
HD22374	-8.44	-8.82	-7.15	-7.41	-9.12	-9.31
HD50169	-7.47	-7.79	-6.76	-7.02	-9.04	-9.22
HD81009	-7.19	-7.62	-7.91	-8.19	-9.69	-9.91
HD89069	-6.49	-6.93	-7.94	-8.29	-9.09	-9.32
HD110066	-6.34	-6.77	-7.12	-7.46	-9.09	-9.30
HD111133	-7.47	-7.89	-6.68	-7.05	-9.60	-9.83
HD118022	-6.32	-6.74	-7.23	-7.54	-9.27	-9.51
HD137909	-5.43	-5.73	-7.14	-7.33	-8.81	-8.94
HD137949	-6.77	-7.20	-7.49	-7.74	-9.97	-10.20
HD165474	-7.05	-7.50	-8.12	-8.40	-10.15	-10.37
HD176232	-8.89	-9.27	-8.74	-8.97	-10.20	-10.38
HD191742	-7.38	-7.82	-7.97	-8.17	-8.86	-9.07
HD192678	-7.44:	-7.79:	-6.81	-7.10	-9.09	-9.30
HD201601	-8.19	-8.54	-8.91	-9.11	-10.65	-10.85
HD204411	-8.84:	-9.07:	-8.42	-8.66	-9.88	-10.12
HD216533	-6.89	-7.28	-7.12	-7.47	-7.94	-8.16
ν Cap	-8.08ul	-8.48ul	-7.74ul	-8.09ul	-9.56ul	-9.78ul
o Peg	-8.39ul	-8.76ul	-8.01ul	-8.33ul	-9.73ul	-9.94ul

Notes: Eu upper limit based on an equivalent width of EuII λ4205 = 15mÅ.
Gd upper limit based on an equivalent width of GdII λ4215 = 15mÅ.
U upper limit based on an equivalent width of UII λ3859 = 15mÅ.
The solar abundances follow: Eu -11.04, Gd -10.87, and U -12.30.

considerably weaker. Using these two lines as a guide, this ion is possible in all the cool Ap stars except HD8441, HD89069, and HD12288. Further study is needed to confirm the identification.

Holmium and Erbium

In the region studied, the four strongest lines of HoII (I.P. = 11.80 eV) are sometimes blended. Only two stars HD176232 and HD201601 have possible identifications.

ErI (I.P. = 6.10 eV) has its strongest line at λ4007.97 (NBS 32). There are features near this position in several stars but, except for HD176232, the identification of the ErII lines is doubtful.

ErII (I.P. = 11.93 eV) has three moderately strong lines in the region measured on the Grant Machine which are not seriously blended, λ3858.39, λ4419.62, and λ4142.92. Possible identifications are made for HD50169, HD137949, and HD176232. The lines used are much weaker than the strongest lines.

Thulium

TmII (I.P. = 12.05 eV) has a very strong line at λ3848.02 which is just shortward of the start of measurement of many plates on the Grant Machine and a less strong line at λ4242.15. In HD12288, HD111133, and HD204411 the strong line is missing while in HD176232 and HD201601 it was present. Stars having features within .04 Å of λ4242.15 which is usually weak and the line at λ3848.02 was not measured include HD2453, HD18078, HD89069, HD110066, HD118022,

HD137909, HD137949, and HD192678. Ho, Er, and Tm are present in HD101065 (Przybiski 1966).

Ytterbium and Hafnium

The resonance line of YbII (I.P. = 12.17 eV) is λ3694.19. On a 2 Å/mm plate of HD201601, I found this line. The strongest line (NBS 32) in the region studied is λ4180.82, which is far weaker than the resonance line. However, by use of this criterion, uncertain identifications were made for HD137909, HD165474, and HD176232.

HfII (I.P. = 14.9 eV) has several strong lines in the region of study. λ4232.43 had its equivalent width measured in HD110066. Since other strong HfII lines were not measured, it would be best to regard this value as an upper limit (Table A-52).

Osmium

OsI (I.P. = 8.7 eV) has two strong lines in the region studied λ4260.85 and λ4420.47. For two stars I measured the equivalent widths of the latter line. The deduced abundances (Table A-53) should be regarded as upper limits. Guthrie (1969b) has observed OsII (I.P. ≃ 17 eV) in 73 Dra which Jaschek and Malaroda (1970) confirm. The strongest unblended lines from Van Kleef's (1960) list were λ4399.27, λ4608.77, and λ4824.44. I used the first two lines as a criterion to identify this ion.

Os was definitely present in HD5797 in both stages of ionization. In several other stars lines from both stages were possible: HD2453,

HD50169, and HD118022. There are several other stars with lines of possibly one stage of ionization present.

Brandi and Jaschek (1970) claim to have found Os in HD2453 and HD137909 while they do not believe that it is found in HD191742 and HD216533. Their work is not as accurate for these stars except for HD216533 because they compared tracings. Examination of Hiltner's (1945) line list of HD137909 shows that OsI is not present. One has to be extremely careful that a feature is not noise or a Zeeman component of a nearby line. A second good plate greatly aids the line identification process.

Platinum

PtII (I.P. = 18.56 eV) lines has been observed in some Ap stars (Dworetsky 1969). By use of the line list of Shenstone (1938), I searched for these lines in cool Ap stars. Some of the stronger lines are partially blended. PtII lines are definitely present in HD5797. Other PtII identifications were possible for HD12288, HD18078, HD111133, HD118022, HD165474, HD192678, and HD216533. Confirmation requires more careful study. In some stars without the strongest lines present, there is a feature near λ4288.40, a medium strength PtII line. This means that it is caused by another ion. Brandi and Jaschek (1970) believe that contrary to my results that PtII lines are found in HD2453 and HD137909. They also get null results for HD191742 and HD216533. Hiltner (1945)'s line list of HD137909 has a feature near the strongest PtII line, but the next strongest line is absent.

Gold

AuI (I.P. = 9.22 eV) has only weak lines in the region studied (NBS 32). No identifications were made. Jaschek and Malaroda (1970) claim to have seen the four strongest lines of AuI in 73 Dra. The strongest two lines are λ4607.34, which coincides with SrI(2) λ4607.33, and λ4065.08, with TiI(80) λ4065.09 and VII(215) λ4065.07(NBS 32).

Mercury

HgI (I.P. = 10.43 eV) has accessible lines at λ4046.56 and λ4358.34. No identifications were made. In the past some misidentifications have been made of the former line (Dworetsky 1969, Bidelman 1967). HgII (I.P. = 18.75 eV) has a strong feature near λ3984. Due to its complexity and the problem of blending, identification is very difficult in cool Ap stars (see, for example, Preston 1971b).

Thorium

The longest half-life of any Th isotope is 1.39×10^{10} years (Weast 1968) which is much greater than the main sequence lifetimes of A stars. ThII (I.P. ≃ 12 eV) has its resonance line at λ4019.14 which is a region relatively free from other lines. It is possible only in three stars: HD18078, HD81009, and HD165474. These identifications should be checked using additional plates.

Uranium

U has two isotopes with half-lives greater than 10^8 years (Weast 1968). Brandi and Jaschek (1970) claim that UII lines are present in HD2453, HD137909, and HD216533. The ionization potential of UI is about 6 eV which means that for the stars considered, U is at least singly-ionized. The strongest features which were not expected to be blended are λ3859.58, λ3854.66, and λ4241.67 (NBS 32). λ3854.66 is, however, most probably blended with some unknown constituent and is not reliable as a guide to the presence of UII lines. λ3859.58 is in the wing of FeI(4) λ3859.91 which makes equivalent width measurements difficult and perturbs its measured wavelength. The line profile was drawn after making allowance for the stronger line. λ4241.67 tends to be quite weak. The isotopic shifts between the lines of isotopes 235 and 238 are less than 0.01 Å for λ3859.58 and for λ4241.67 (Diringer 1965). Table A-58 gives the measured wavelengths for all three features.

The U identifications, I believe, are reasonable, but not conclusive. Better measurements of the features at λ3860 and λ4242 are needed. The abundances are determined assuming that the features are due to U. There are uncertainties due to poorly determined excitation potential and partition functions.

Trans-uranium Elements

Np and Pu have isotopes with the longest half-lives of the trans-uranium elements, 2.20×10^6 and 7.6×10^7 years (Weast 1968). Kuchowicz (1970) and Sargent and Burbidge (1970) have suggested looking for Pu lines in peculiar A stars. The former's list of strongest lines did not coincide with the one I examined. Tomkins and Fred (1949) give the wavelengths of the neutral lines of both elements. Fred (1971) sent me a list of the strongest lines between λ3800 and λ4700 for Pu^{240} and their isotopic shifts. The most sensitive PuI lines are in the infrared with PuII best in the ultraviolet. The isotope shifts can be appreciable.

The longest lived isotope is Pu^{244}. I have made some preliminary comparisons of the line lists between λ4200 and λ4635 for two stars with large U abundances. There are a small number of coincidences with the strongest lines, but to prove that this is due to more than chance will require a careful examination of the spectrum in great detail and is beyond the scope of this research.

III. ELEMENTAL ABUNDANCE SYSTEMATICS

A. Introduction

In this chapter an overview of the absolute abundances and the abundance anomalies and a review of the sources of error are given. Then, the results of this study are compared with those of other investigators for normal stars; the sun; Si, Mn, and cool Ap stars; Am stars; and spectrum variables. We interpret the abundances, consider their dependences on the physical properties of the stars, and compare these results with the predictions of the theories of the origins of the chemical composition anomalies. Finally, a summary of the major conclusions is given.

B. Overview of the Abundance Determinations

The general characteristics of the abundances of the cool Ap stars provide tests of the theories which purport to explain the origin of these anomalies. Figure III-1 shows as a function of atomic number the elemental abundance anomalies [N/H] which are the logarithmic absolute abundances in units of the solar values. Gaps have been left for missing elements. The mean measured values are indicated by arrows. If abundances were not determined for all cool Ap stars, then another mean was made by assuming that the remaining stars had solar values. This is indicated by a triangle. Closed circles denote Ap

stars with T_{eff}>9500°K; +, HD81009; x's, the other Ap stars; and open circles, the normal stars. Figure III-2, which shows the absolute abundances with respect to H, log N/H,uses diamonds to indicate solar abundances for those elements whose abundances were not determined in the normal stars. The other symbols are the same as those in Figure III-1. The abundances used in this chapter are those derived using case 1 effective temperatures.

Figure III-1 shows that most stars have elemental overabundances with respect to H. Except for Ba, no cool Ap star has an elemental abundance with respect to solar values less than -0.6 dex. Si has a mean overabundance of +0.5 dex compared with Mg's nearly solar value. Between Ca and V, the mean overabundance is near +0.65 dex. At Cr, it jumps to +2.00 dex then drops to +1.06 dex at Fe with Mn in between. It appears to increase at Co and decrease for Ni. Sr has a very large overabundance compared with Y. Zr is very indeterminate, although some stars have greater Zr than Y overabundances. The rare earths show increasing overabundances from La through Eu, the values for Pm being unknown, with those of Gd less than those of Eu. U and Gd have similar overabundances. The individual stars have values which, in general, follow these trends.

Mg and Y are the only elements whose abundances are reasonably well determined which have near solar mean values. If we consider a mean overabundance of .50 as being significant, then those elements for the cool Ap stars as a class which are overabundant follow: Si, Ca, Sc, Ti, Cr, Mn, Fe, Co, Sr, Ce, Nd, Eu, Gd, and U. In addition,

Figure III-1: [N/H] values, the logarithmic abundances with respect to H and relative to solar values, as a function of atomic number. Closed circles represent cool Ap stars with $T_{eff} > 9500°K$; +, HD81009; x's, the other cool Ap stars; and open circles, normal stars. Uncertain values are indicated by bracketing horizontal lines except for HD81009 when * is the symbol. The arrows, →, indicate the mean elemental abundances for those cool Ap stars with deduced abundances. In case all the program's cool Ap stars did not have abundances deduced for an element, a second average was made by assuming that those cool Ap stars without lines measurable for equivalent widths had solar abundance values. These averages are indicated by open triangles. The atomic number for each element with deduced abundances is given below the diagram while the corresponding chemical symbol is above it.

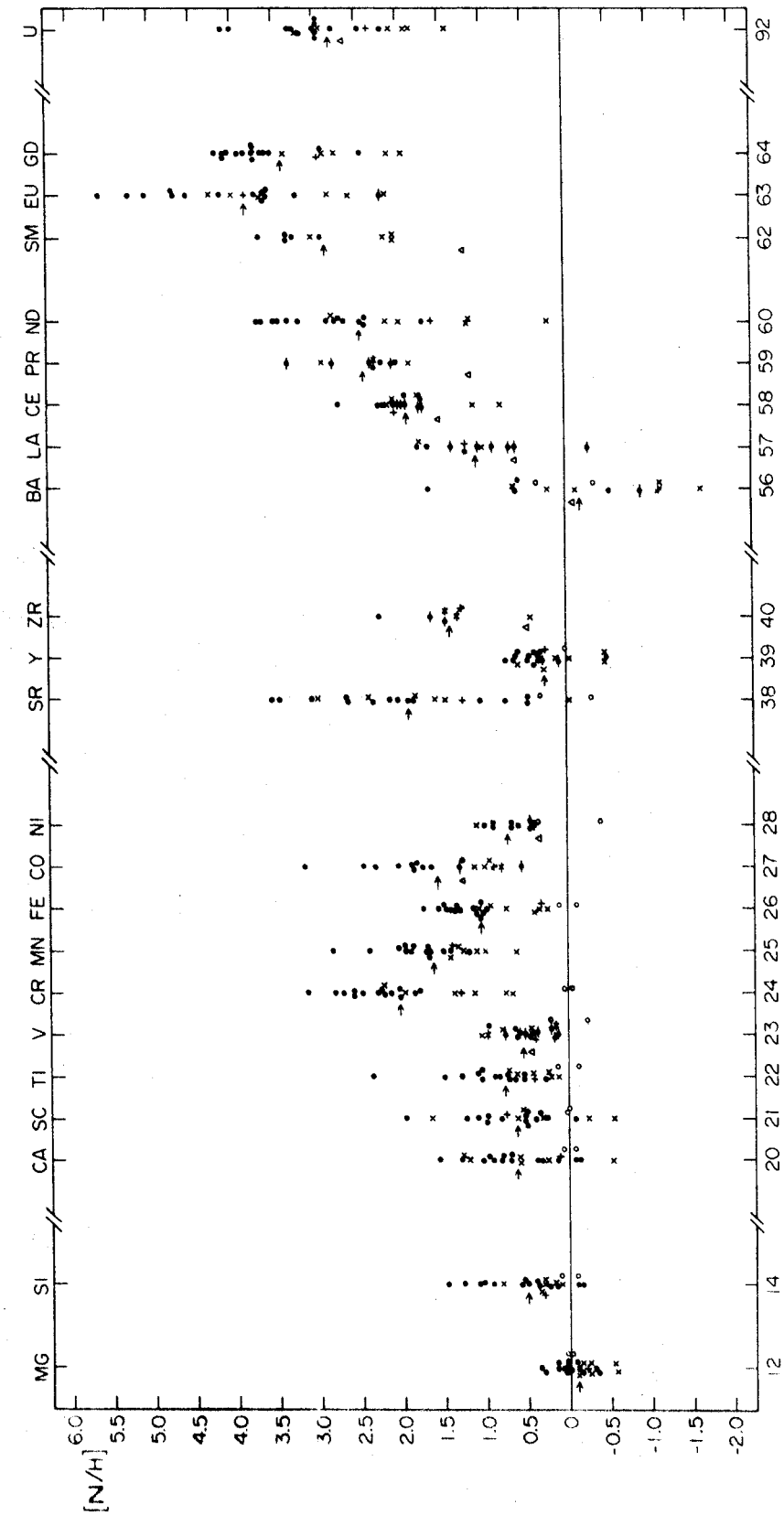
MG SI CA SC TI V CR MN FE CO NI SR Y ZR BA LA CE PR ND SM EU GD U
12 14 20 21 22 23 24 25 26 27 28 38 39 40 56 57 58 59 60 62 63 64 92
[N/H]
6.0 5.5 5.0 4.5 4.0 3.5 3.0 2.5 2.0 1.5 1.0 0.5 0 -0.5 -1.0 -1.5 -2.0

V, Ni, Zr, La, Pr, and Sm may be. For Cr and Mn, the minimum stellar overabundance is 0.6 dex while for Gd and Eu, it is 2.0 dex. These elements are overabundant in all cool Ap stars. Since the maximum Mg overabundance for any cool Ap stars is 0.35 dex, then the Cr, Mn, Gd, and Eu overabundances are always greater.

Similar results come from examining the abundances of individual stars. The most interesting and certain of which follow: The Cr and Mn overabundances are always greater than those of Si, Ti, and Fe. Except for HD81009, HD111133, HD89069, and HD201601, the Cr overabundance is greater than the Mn. For the first two stars, the difference is less than .1 dex. The Si overabundance is less than that of Fe except for HD50169 and HD201601 in which they are equal, of Gd, and of Eu. The Sr overabundance is greater than that of Y except for HD12288 and HD22374. The Y overabundance is less than that of Cr, Mn, Eu, and Gd. The Eu overabundance is always greater than that for Nd. Except for HD12288 and HD192678, Gd has a greater overabundance than Nd.

In Figure III-2, the Fe-peak elements with odd values of Z have lower absolute abundances than adjacent elements with even values of Z. Adjacent elements in the [N/H] diagram show no such effects. Thus, the process responsible for the overabundances does not fill in the valleys of the cosmic abundances. Sr has a significantly greater abundance than Y although their solar abundances are not that dissimilar.

Figure III-2: Log N/H values, the absolute abundances, as a function of atomic number. Closed circles represent cool Ap stars with T_{eff}>9500°K; +, HD81009; x's, the other cool Ap stars; and open circles, normal stars. Uncertain values are indicated by bracketing horizontal lines except for HD81009 when * is the symbol. The arrows, →, indicate the mean elemental abundances for those cool Ap stars with deduced abundances. In case all the program's cool Ap stars did not have abundances deduced for an element, a second average was made by assuming that those cool Ap stars without lines measurable for equivalent widths had solar abundance values. These averages are indicated by open triangles. The elements whose abundances were not determined in normal stars have their solar abundances indicated by open diamonds except for U which has a solar value of log U/H = -12.30. The atomic number for each element with deduced abundances is given below the diagram while the corresponding chemical symbol is above it.

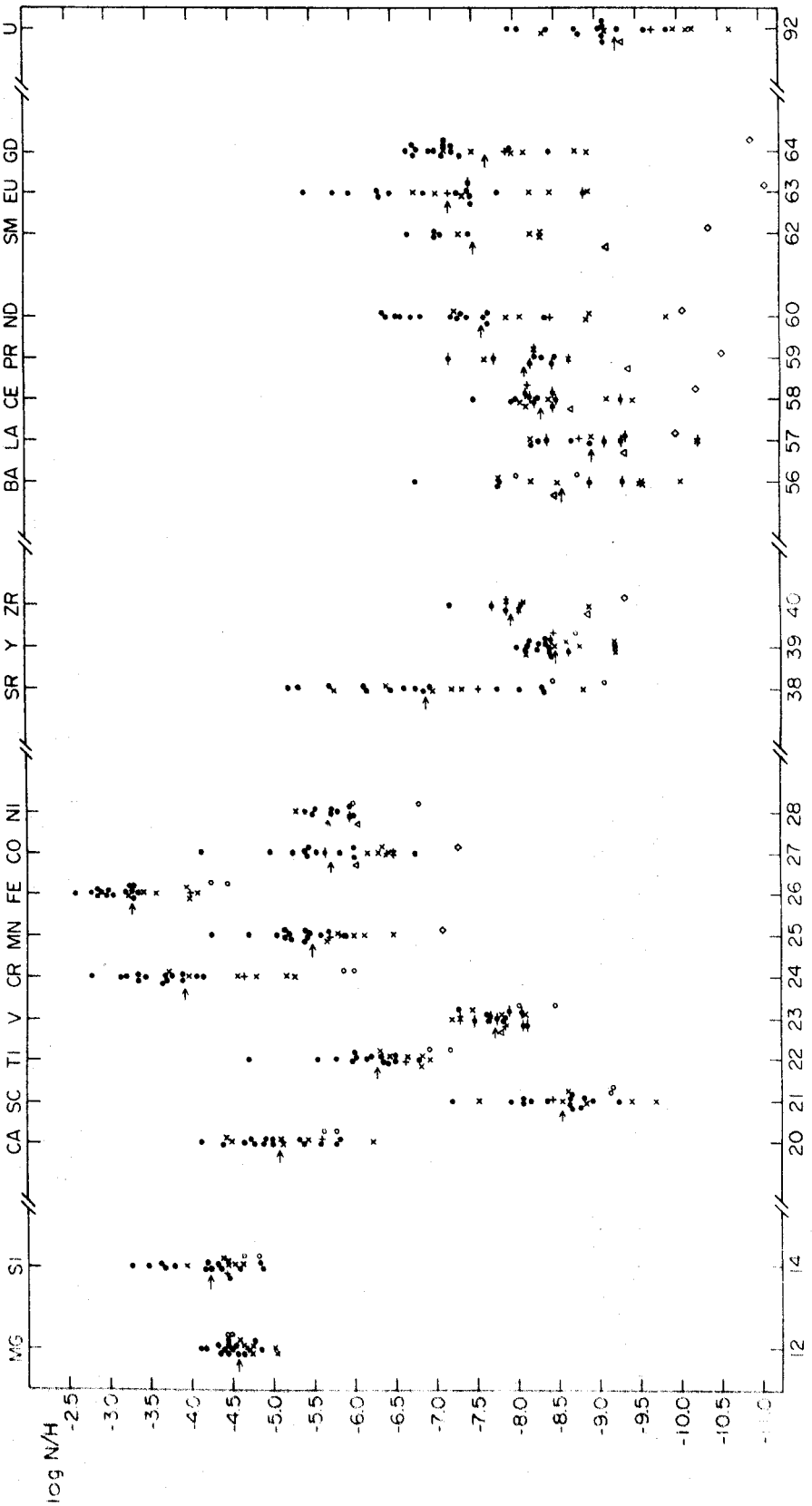
MG SI CA SC TI V CR MN FE CO NI SR Y ZR BA LA CE PR ND SM EU GD U
12 14 20 21 22 23 24 25 26 27 28 38 39 40 56 57 58 59 60 62 63 64 92
log N/H
-2.5 -3.0 -3.5 -4.0 -4.5 -5.0 -5.5 -6.0 -6.5 -7.0 -7.5 -8.0 -8.5 -9.0 -9.5 -10.0 -10.5

For the program Ap stars the following inequalities about absolute abundances can be derived by using Figure III-2 and by examining a few stellar abundances (only elements with at least 10 good determinations have been considered):

Ti > Y, Ce, U

Cr, Fe > Ca, Ti

Mg, Si, Cr, Fe > Ni, Sr, Eu

Mg, Si, Cr, Fe, Ni > Nd

Mg, Si, Ca, Cr, Mn, Fe, Co, Ni > Sc, V, Y, Ce, Gd, U

There is a possible decline from Z = 26 to Z = 56 in abundance. Among the rare earths, the absolute abundances tend to increase with atomic number except for Gd. This trend is more clearly seen in Figure III-3 in which I have included only those stars with six or seven rare earth abundance determinations. The arrows indicate the derived mean abundances of these stars. By comparing the individual stellar abundances we find that those for

HD5797, HD137909, and HD137949 > HD176232 and HD201601

HD2453, HD50169, HD110066, and HD118022 > HD176232

HD216533 > HD201601.

Between La and Eu, the total increase in absolute abundance is over 2.00 dex. Any theory of Ap stars must explain this rise from La to Sm, the sudden increase at Eu, and the decline at Gd in absolute abundances. It must also predict the unknown Pm abundances.

The absolute abundances and overabundances indicate that the cool Ap stars must have somewhat similar abundance anomalies. If we

Figure III-3: The absolute abundances of the rare earth elements for ten cool Ap stars with at least determinations for six of these elements. The arrows, →, represent the mean abundance determinations for these stars. Uncertain values are indicated by bracketing horizontal lines. a = HD2453, c = HD5797, n = HD50169, x = HD110066, r = HD118022, o = HD137909, • = HD137949, u = HD176232, v = HD201601, and z = HD216533. s indicates the solar values.

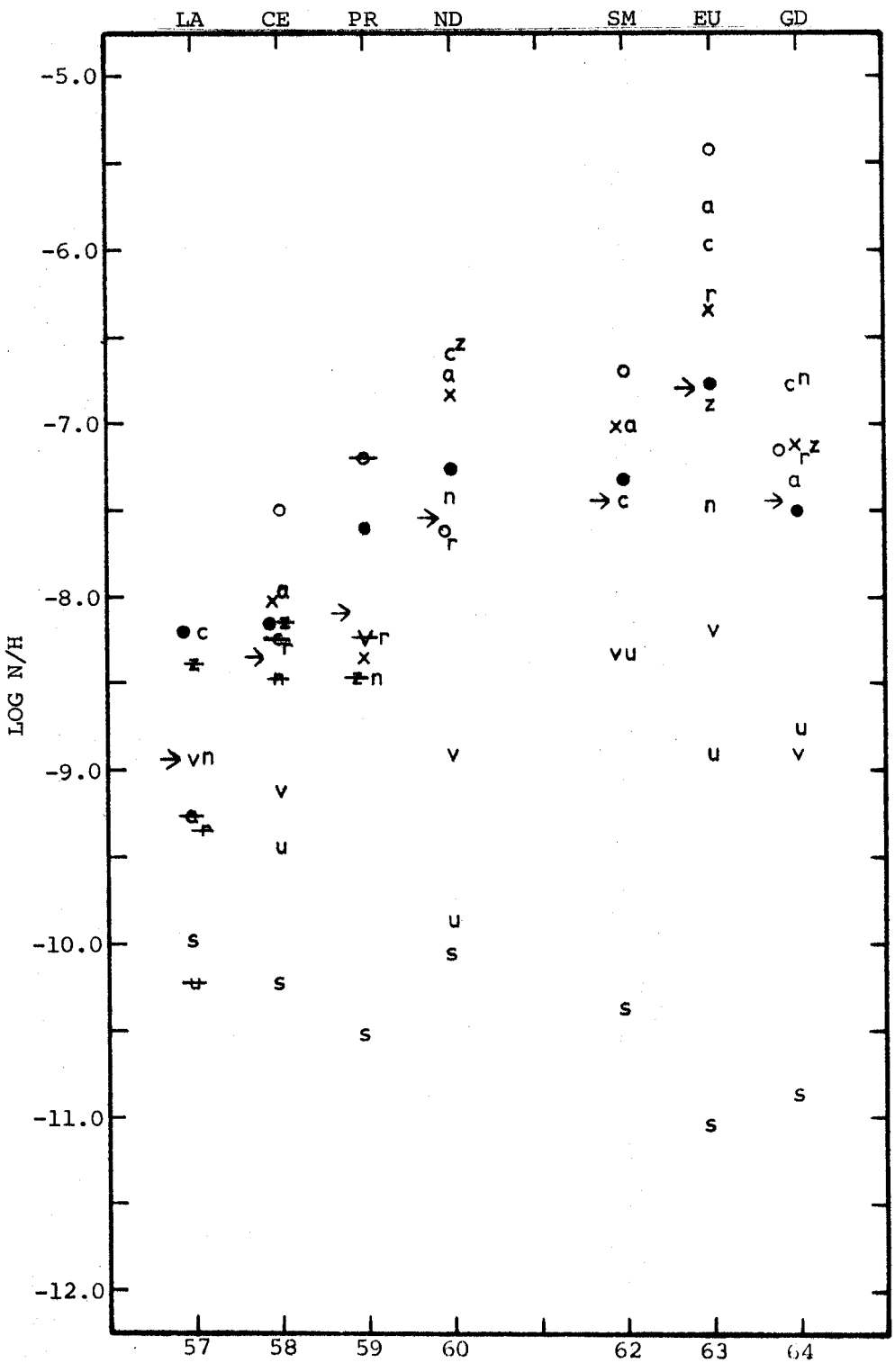
LA
CE
PR
ND
SM
EU
GD
-5.0
-6.0
-7.0
-8.0
-9.0
-10.0
-11.0
-12.0
LOG N/H
57
58
59
60
62
63
64

examine Figure III-2 closely, we observe that for some elements, for example Fe, the x's are below the closed circles. This suggests a temperature dependence. We will examine these dependences later.

For some elements the range of values is less than that for others. One way to judge how closely the stars show the same abundance anomalies is to examine mean deviations. Table III-1 shows the mean log N/H values and their mean deviations, the mean [N/H] values, and the mean [N/Fe] values. The mean values are logarithmic means. Except for Sr, Ba, Nd, and Eu, the mean deviations are similar to or smaller than the acknowledged errors. Hence all cool Ap stars show the same abundance anomalies within a well defined range of values. Consequently any dependence of the abundances on the physical properties of the stars, effective temperature, magnetic field strength, and rotational velocity, must not, in general, be very strong.

There are many remarks in the literature that this star is like that star. I consider two typical examples. Bidelman (1967) says:

> "Gamma Equulei certainly has a much higher strontium and yttrium abundance than β Coronae Borealis; on the other hand, it certainly has considerably weaker lines of manganese and chromium. Furthermore, the differences go further than this. The rare-earth elements present are different in the two cases: β Coronae Borealis has very strong lines of GdII and CeII, while in γ Equulei these lines are much less marked, and the notable rare-earth lines are those of NdII and SmII. Thus there are substantial differences in abundance even for stars which we regard as of approximately the same temperature."

TABLE III-1: MEAN VALUES OF LOG N/H AND ITS MEAN DEVIATION, MEAN VALUES OF [N/H], AND MEAN VALUES OF [N/Fe] FOR THE COOL PECULIAR A STARS

Element	log N/H	[N/H]	[N/Fe]
Mg	-4.58±0.19	-0.10	-1.15
Si	-4.23±0.35	+0.51	-0.55
Ca	-5.08±0.43	+0.62	-0.42
Sc	-8.54±0.41	+0.63	-0.43
Ti	-6.28±0.37	+0.78	-0.28
V	-7.72±0.24	+0.54	-0.52 *
Cr	-3.92±0.51	+2.02	+0.96
Mn	-5.49±0.38	+1.62	+0.56
Fe	-3.28±0.33	+1.06	+0.00
Co	-5.72±0.56	+1.58	+0.46 *
Ni	-5.68±0.21	+0.72	-0.60 *
Sr	-6.90±0.80	+1.89	+0.83
Y	-8.50±0.27	+0.24	-0.82
Zr	-7.96±0.34	+1.39	+0.50 *
Ba	-8.58±0.82	+0.17	-1.05 *
La	-8.96±0.42	+1.08	-0.01 *
Ce	-8.32±0.29	+1.90	+0.73 *
Pr	-8.13±0.36	+2.42	+1.31 *
Nd	-7.60±0.71	+2.47	+1.41
Sm	-7.50±0.51	+2.88	+1.68
Eu	-7.19±0.72	+3.85	+2.79
Gd	-7.64±0.54	+3.40	+2.34
U	-9.26±0.53	+3.04	+1.98

Note: * = not all stars included in the average.

The last comment is true for the cool Ap stars as a class. For some elements the range of abundances at a given temperature is far smaller than the total range, for example Cr, while for other elements, such as Sr, at a given temperature there can be stars with elemental abundances at the extrema. The effective temperatures of HD137909 (β CrB) and HD201601 (γ Equ) are quite different as are their magnetic field strengths. The Sr and Y abundances of HD137909 are .4 and .2 dex greater than those of HD201601 although the equivalent widths of the strongest lines of both elements have the reverse order. Mn, Cr, Ce, and Gd behave as Bidelman says. NdII and SmII have stronger lines in HD137909, but fewer are easily identified than in HD201601.

Van den Heuvel (1971) claims that the spectrum of HD81009 resembles that of HD137909 although it is earlier in type. "Eu and Sr are very strong, Cr is moderately strong. Of the rare earths at least Eu, Gd, La, Ce, and Dy are present". The spectrum of HD137949 resembles the two previous stars. Of the rare earths particularly EuII and SmII are strong while the others are present. HD81009 is a close visual binary. It is not possible to separate the two components. Thus the abundances derived from this star have larger uncertainties than the other cool Ap stars. The visual appearances of both stars generally agree with Van den Heuvel's description.

I compared these three stars looking for differences in [N/H] and [N/Fe] for twenty-three elements. If we use 0.5 dex as a significant difference in these abundance ratios, then HD137909 and HD137949 have seven in each category, while HD137909 and HD81009 have 14 and 6, and

HD81009 and HD137949 have 10 and 9. Hence, HD137909 and HD137949 are closer in abundance than either is with HD81009. Many remarks in the literature describe what is observed and not necessarily something significant about the abundances.

To consider the similarity and degree of abundance anomalies further, I made a simple test. According to the average overabundance for five groups consisting of thirteen elements, I ranked the stars in the following scheme: 1) Mg and Si, 2) Ca, Sc, and Ti, 3) Cr, Mn, and Fe, 4) Sr and Y, and 5) Nd, Eu, and Gd, and then determined a mean rank. The five stars with the lowest ranks, i.e., those with the smallest abundances in the above sense, HD81009, HD165474, HD201601, HD176232, and HD22374, are all rather cool and are near the bottom of the abundance distributions for all five groups, while the top ranked star HD5797 is always near the top of the distributions. The second through fourth ranked stars are also near the top, HD110066, HD2453, and HD216533. On the other hand, HD8441 and HD204411, the fifteenth and sixteenth ranked stars, are near the bottom only for some elements, groups 1 and 2, and groups 4 and 5, respectively. The rest of the stars are fairly well mixed. Thus, the top and the bottom of the range of the observed elemental abundances tend to be occupied by the same stars while the center is better mixed.

I tried to find stars typical of the entire sample by excluding those which had anomalous positions in the correlation diagrams which we will discuss later. The three stars I selected are HD2453, HD18078, and HD110066. Two of them have high rankings in the above average

overabundances. Hence, HD18078 is the most representative cool Ap star of the sample studied.

The conclusions of this research are not likely to be changed by errors in the adopted values of effective temperature, gravity, and abundance. The adopted scale of effective temperatures for the primary abundance determinations is supported by the best determinations of other investigators. The determination for ν Cap suggests an error of 300°K in the effective temperature due to all causes. Most of the results which are based on absolute abundances would be somewhat modified by a 600°K error in effective temperature. However, those which depend on the abundance anomalies or which involve elements whose deduced abundances have similar effective temperature sensitivities would not be. Problems with the rare earth abundance determinations, especially in the use of temperature independent partition functions, may introduce systematic effects between their abundances and those of lighter elements.

Classical microturbulence is not likely to be important and $\log g = 4.0$ is a good assumption. Most estimates of the magnetic field strength have 0.5 kG errors. The values of the equivalent widths measured for this study agree with those of other studies to within 20 per cent except for weak lines. The equivalent widths measured on the Lick, Palomar, and Wilson plates are assumed not to be systematically different from one another.

The abundances of most elements for the normal stars are in good agreement (within 0.3 dex) with the solar values. This suggests that

both the effective temperatures and the derived absolute abundances are well determined. The errors in the best absolute abundances are 0.4 dex, while in the worse cases they are 0.8 to 1.0 dex and marked uncertain. As a mean value, I will use 0.5 dex as the error.

We conclude that all cool Ap stars exhibit the same characteristic abundance anomalies although not all to the same degree, especially the tendency for the mean abundance of the rare earths to increase with atomic number between La and Eu. Significant Cr, Mn, Eu, and Gd overabundances are characteristic of all cool Ap stars. Most deduced elemental abundances are overabundances with respect to solar values. The process that is responsible for the abundance anomalies does not fill in the valleys of cosmic abundances in the Fe peak. The errors in the abundances are not likely to change these conclusions.

C. Comparison of the Normal Star Abundances

The abundances of the normal stars, ν Cap and o Peg, determined in this study are in good agreement with the previous studies of these stars (Adelman 1972, Conti and Strom 1968b). Table III-2 gives the derived abundances for these stars and for the sun. The effective temperatures, gravities, and microturbulent velocities, ξ, in km/sec, which were used in the analyses of these stars are also given.

The results for ν Cap agree well, normally within 0.2 dex, except for the Sr abundance because a different oscillator strength was adopted for SrII λ4215. As for o Peg, the abundances derived in this study are larger for most elements since the adopted effective

TABLE III-2: COMPARISON OF SOLAR AND NORMAL A STAR ABUNDANCES

	log N/H				
	ν Cap		o Peg		The
ion(s)	A(72)	A(71)	CS(68)	A(71)	Sun
FeI,II	-4.6	-4.4	-5.2	-4.2	-4.4
MgII	-4.4	-4.5	-4.3	-4.5	-4.6
SiII	-4.5	-4.6	-4.0	-4.8	-4.5
CaI	-6.0	-5.8	-6.2	-5.6	-5.8
ScII	-9.1	-9.2	-9.5	-9.2	-9.1
TiII	-7.3	-7.2	-7.2	-6.9	-7.3
VII	-8.6	-8.5	-8.4	-8.0	-8.2
CrI,II	-6.1	-6.0	-6.5	-5.9	-6.6
MnII			-6.5		-7.1
NiI			-5.6		-6.1
NiII	-7.2	-6.8	-6.4	-6.0	-6.1
SrII	-8.4	-9.1	-8.3	-8.5	-9.2
YII			-9.3	-8.7	-8.8
ZrII			-8.6		-9.4
BaII	-8.9	-8.8	-8.4	-8.0	-9.9
T_{eff}	10200°	10500°	9500°	10150°	
log g	3.75	4.00	4.00	4.00	
ξ	2.75	3.00	3.00	3.00	

Notes: A(71) = This study
A(72) = Adelman (1972)
CS(68) = Conti and Strom (1968b)

temperature is greater by 650°K. The Si abundance cannot be reconciled in this manner. Conti and Strom used lines of multiplet 4 to obtain the abundance. I suspect a problem with their oscillator strengths.

Except for Cr, Sr, and Ba, the solar and average abundances of ν Cap and o Peg agree to within 0.2 dex. The Cr abundances have been affected by the adoption of improved CrI oscillator strengths. The Sr abundances are higher in the normal stars. The Ba difference is partially due to the use of a blended resonance line. o Peg has overabundances of Sr and Ba and is a moderate Am star according to Conti and Strom (1968b) as is ν Cap (Adelman 1972). Hence, when the solar and the mean abundances from ν Cap and o Peg disagree, this may be due to the mild Am phenomenon which our normal stars exhibit.

D. Comparison with Other Abundance Studies of Non-Variable Cool Ap Stars

There are six relatively recent analyses of cool peculiar A stars: HD137909 (Hack 1958), HD176232 (Auer 1964), HD201601 (Hack 1960, Evans 1966), HD204411 (Sargent et al. 1969), and HD151199 (Burbidge and Burbidge 1956). Except for the last star, these stars are included in this survey. We have discussed the differences in the effective temperature determinations.

Table III-3 gives the derived abundances for Sargent et al.'s study of HD204411 and Evans' study of HD201601 and this study for both stars. The effective temperatures and log g values are also given.

TABLE III-3: COMPARISON OF COOL PECULIAR A STAR ABUNDANCES

	log N/H			
	HD204411		HD201601	
Element	S3	A(71)	E(66)	A(71)
Mg	-4.5	-4.6	-4.1	-4.6
Si	-4.5	-4.5	-3.6	-4.4
Ca	-5.3	-4.4	-4.8	-5.1
Sc	-9.2	-8.6		-9.4
Ti	-7.2	-6.0		-6.9
V	-7.3	-8.1:		-7.2
Cr	-5.8	-4.2	-6.2:	-5.3
Mn	-6.4	-5.9	-6.0	-6.1
Fe	-4.9	-3.3	-4.7	-4.0
Co	-7.3	-6.0		-6.3
Ni	-6.2	-6.0:		
Sr	-8.7	-8.1	-7.4	-7.3
Y	-9.2	-9.2		-9.2
Zr	-8.3			-8.9
Ba	-9.3	-7.8	-8.7	-8.5
Ce	-9.2			-9.1
Nd	-10.2	-8.4	-8.8	-8.9
Gd	-8.7	-8.4		-8.9
Sm			-9.6	-8.3
Eu		-8.8:	-8.4	-8.2
T_{eff}	8750°	9550°	7750°	8150°
log g	4.3	4.0	3.5	4.0

Notes: A(71) = This study

E(66) = Evans (1966)

S3 = Sargent *et al.* (1969)

Sargent et al. used ξ = 3.5 km/sec. Most deduced abundances for this study are higher than their results due to a lower mean microturbulent velocity and a higher effective temperature. The exceptions are V and Mg, while Si has the same value in both studies. The Mg abundance is only 0.10 dex different which results most likely from the additional lines measured. The difference in the V abundance is partially due to the large uncertainty in the equivalent widths used for this study.

Evans employed a model atmosphere in convective equilibrium. There is fair agreement, mostly 0.2 dex or better with some larger discrepancies, between both sets of deduced abundances. These differences often result from the choice of oscillator strengths. Evans and Elste (1971) revised the Fe abundance to a factor of 1.6 greater than the solar value which is in better agreement with the results of this study.

Table III-4 contains the results of the other detailed cool Ap star studies and the comparable values for this work given as abundances with respect to solar values. Hack (1960)'s results for HD201601 are usually larger than mine which I attribute to analysis differences, especially the values used for oscillator strengths, partition functions, and solar abundances. For HD137909, the situation is reversed. Overabundances derived in this study are greater than Hack(1958)'s for most elements which is a reflection of the higher effective temperature as well as those causes cited for her HD201601 study. In Auer(1964)'s analysis of HD176232 the rare earth abundances were determined with respect to those of τ UMa.

TABLE III-4: COMPARISON OF COOL PECULIAR A STAR ABUNDANCE DETERMINATIONS

[N/H]

	HD201601		HD137909		HD176232		HD151199
Element	H(60)	A(71)	H(58)	A(71)	A(64)	A(71)	B(56)
Mg	+1.2	-0.1	+0.2	+0.0	+1.6:	-0.3	+0.1
Si	+0.5	+0.3		+0.2	+0.3	+0.2	+0.1
Ca	+0.7	+0.6	+0.1	+1.6	+0.2	+0.6	+0.4
Sc	+0.7	-0.3	+0.4	+2.0	-1.6:	-0.5	
Ti	+0.2	+0.1	+0.9	+1.5	-0.1	+0.2	
V	+0.8	+1.1	+0.4	+0.8:	-0.4	+0.4	
Cr	+1.3	+0.7	+1.5	+1.9	+0.4	+0.8	+0.3
Mn	+1.8	+1.0	+1.6:	+1.7	+0.6	+0.6	+1.0
Fe	+0.6	+0.4	+0.8	+1.3	+0.0	+0.3	+0.0
Co	+1.7	+1.0	+1.0:	+1.6:	+1.2	+1.1	+1.8
Ni	+1.6		+0.3	+0.9	-0.5		
Sr	+2.6	+1.4	+1.6	+1.8	+1.8	+1.4	
Y	+0.6	-0.5		+0.7	+0.3	-0.6	
Zr	+0.8	+0.4	+2.0	+2.2	-0.2		
Ba	+1.2	+0.5	+0.7	+0.6	-0.8	-1.6	-0.2
La	+2.3	+1.0	+2.8			-0.3:	
Ce	+2.0	+1.1	+2.9	+2.7		+0.8	
Pr	+2.4	+2.3:	+2.7	+2.9			
Nd	+2.3	+1.2	+2.2	+2.4		+0.2	
Sm	+1.7	+2.0	+2.3	+3.7		+2.0	
Eu	+2.6	+2.8	+3.2	+5.6		+2.2	+2.1
Gd	+2.2	+2.0	+2.9	+3.7		+2.1	

Table III-4 (continued)

Notes: A(64) = Auer (1964)
A(71) = This Study
B(56) = Burbidge and Burbidge (1956) and Sargent (1964)
H(58) = Hack (1958)
H(60) = Hack (1960)

He derived the Mg abundance from MgI lines. Allowing for a slight difference in effective temperature, the agreement is reasonable, 0.4 dex or better, except for V, Y, and Ba. The abundance determinations of the first two elements are based on weak lines while the difficulties with Ba abundance determinations have already been discussed.

HD151199 is the only non-variable cool Ap star whose abundances have been studied in detail (Burbidge and Burbidge 1956), but was not included in this survey. Sargent (1964) calculated the overabundances with respect to solar values. Although this analysis uses oscillator strengths different from those of this survey, the overabundances, in general, fall within the range of this study's cool Ap star determinations (see Figure III-2). The agreement for Fe and Cr is fair at an effective temperature of 8700°K. We will see later that these elements have abundances which are functions of the effective temperature. Thus, the results of this study and the six detailed analyses of single stars agree or the differences are understood in a general way.

The relative abundances with respect to Fe of this survey and of Wolff(1967a)'s study agree poorly for the stars in common. The measured equivalent widths are similar. She adopted the solar Fe abundances for the Ap stars and obtained microturbulent velocities by use of the equivalent width of FeII(38) λ4508.28 which has a z value of 0.50. This method of analysis is unfounded for the cool Ap stars and introduces errors into the relative abundances of the other elements. No further discussion of her results will be given.

Sargent and Searle (1962), Searle and Sargent (1964), and Searle et al. (1966) included cool Ap stars in their studies. The results for the stars in common with this study are given in Table III-5. We see that there are possible shifts in the zero points. When comparing both sets of results, we should remember that the errors acknowledged are $\pm$ 0.5 dex for this study and $\pm$ 0.6 dex by Searle and Sargent. The cool Ap stars studied only by Sargent, Searle, and Lungershausen and those in common with this study have similar abundances.

The Mg abundances given here are derived from MgII λ4481 by a method similar to that used by Searle and Sargent. I also determined [Si/H] values by assuming as did Searle and Sargent that all microturbulent velocities were zero. The results were 0.0 for both cool Ap stars in common. Thus the scales for [Mg/H] and [Si/H] values are probably similar.

This study shows that the average cool Ap star has a [Cr/Fe] and perhaps a [Mn/Fe] overabundance with a [Ti/Fe] marginal underabundance while Searle et al. (1966) find that all three ratios have normal ratios. Furthermore, their values of the microturbulent velocity are too large for some cool Ap stars (Preston 1967b, Preston and Cathey 1968, Evans and Elste 1971). The mean z values of the lines of Ti and Cr that they studied are smaller than those of Mn and Fe. The use of a common microturbulent velocity causes a compression of the [Ti/Fe] and [Cr/Fe] values.

Despite these differences, the results show a fair agreement (0.3 dex) in the values derived for the cool Ap stars in common. Hence,

TABLE III-5: COMPARISON OF THE RESULTS OF SARGENT, SEARLE, AND LUNGERSHAUSEN WITH THOSE OF THIS STUDY

Star	SS [Mg/H]	A [Mg/H]	SS [Si/H]	A [Si/H]
HD118022	+0.2	+0.1	-0.6:	-0.1
HD204411	+0.6	-0.1	+0.8	+0.3
ν Cap	+0.2	+0.0	+0.1	-0.1
mean	+0.3	-0.1	+0.3	+0.5
shift	+0.2		0.0	

Star	SLS [Ti/Fe]	A [Ti/Fe]	SLS [Cr/Fe]	A [Cr/Fe]	SLS [Mn/Fe]	A [Mn/Fe]
HD201601	+0.05	-0.23	+0.10	+0.31	-0.16	+0.63
HD204411	+0.22	+0.01	+0.39	+0.73	+0.29	+0.14
mean	0.0	-0.28	0.0	+0.96	0.0	+0.56
shift	+0.25		+0.28		+0.32	

Notes: Shift means the difference of results of SS or SLS with those of A.
SS = Searle and Sargent (1964)
SLS = Searle *et al.* (1966)
A = this study

the comparison with the other abundance studies of cool Ap stars indicates that the stars of this survey have abundances representative of the cool Ap stars as a whole. This is not surprising as they constitute 21 out of the approximately 50 cool Ap stars whose apparent rotational velocities are known.

Si stars have values of [Si/Mg] greater than 1.4 according to Searle and Sargent (1964) and are cleanly separated from the other Ap stars in a [Si/H] vs. [Mg/H] diagram (Figure III-4). Of the nine cool Ap stars that they examined, six had Si/Mg ratios significantly lower than normal, e.g., HD118022, while the remaining stars, including HD204411, had normal Si/Mg ratios. Figure III-5 shows this study's results. Most of the stars studied have normal values of [Si/Mg]. Two stars are in the Si star band, HD50169 and HD192678, while at least four others fall in the gap in Figure III-4, HD12288, HD22374, HD110066, and HD191742. These six stars possess the other properties of the Si stars as given by Searle and Sargent: the equivalent widths of the SiII lines are large (λ3862 has been considered instead of λ4131 since their equivalent widths are similar in ν Cap as is their values of z). The ratios of the equivalent widths of MgII λ4481 to SiII λ3862 are smaller than for the normal A stars. The equivalent widths of SiII λ4200 are similar to those predicted by an empirical result. HeI λ4471 and CII λ4267 lines do not appear because of the stellar B-V values. These results indicate that these stars may be an extension of the Si stars to cooler effective temperatures.

Table III-6 shows the Fe peak elemental abundances of these six cool Ap stars and those of normal Si stars. The [Ti/Fe] values are

Figure III-4: The [Si/H] vs. [Mg/H] diagram from Searle and Sargent(1964). x denotes a normal star; ■ , a Si star; Δ , a Mn star, and o, another type of Ap star. The diagonal lines are those of constant Si/Mg. Line (a) is for [Si/Mg] = -0.5, (b) for +0.5, and (c) for +1.8.

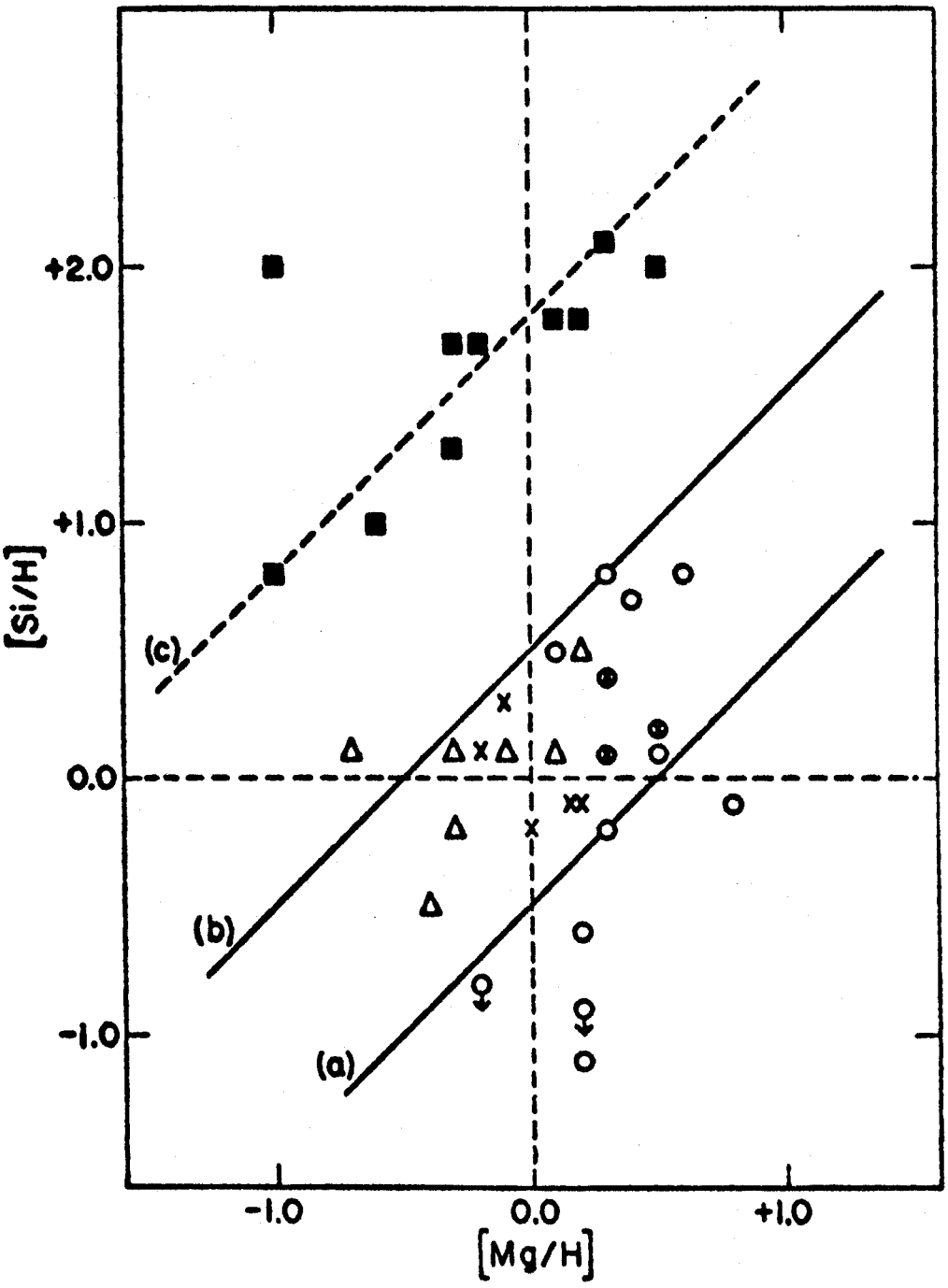
+2.0
+1.0
0.0
-1.0
[Si/H]
(c)
(b)
(a)
-1.0
0.0
+1.0
[Mg/H]

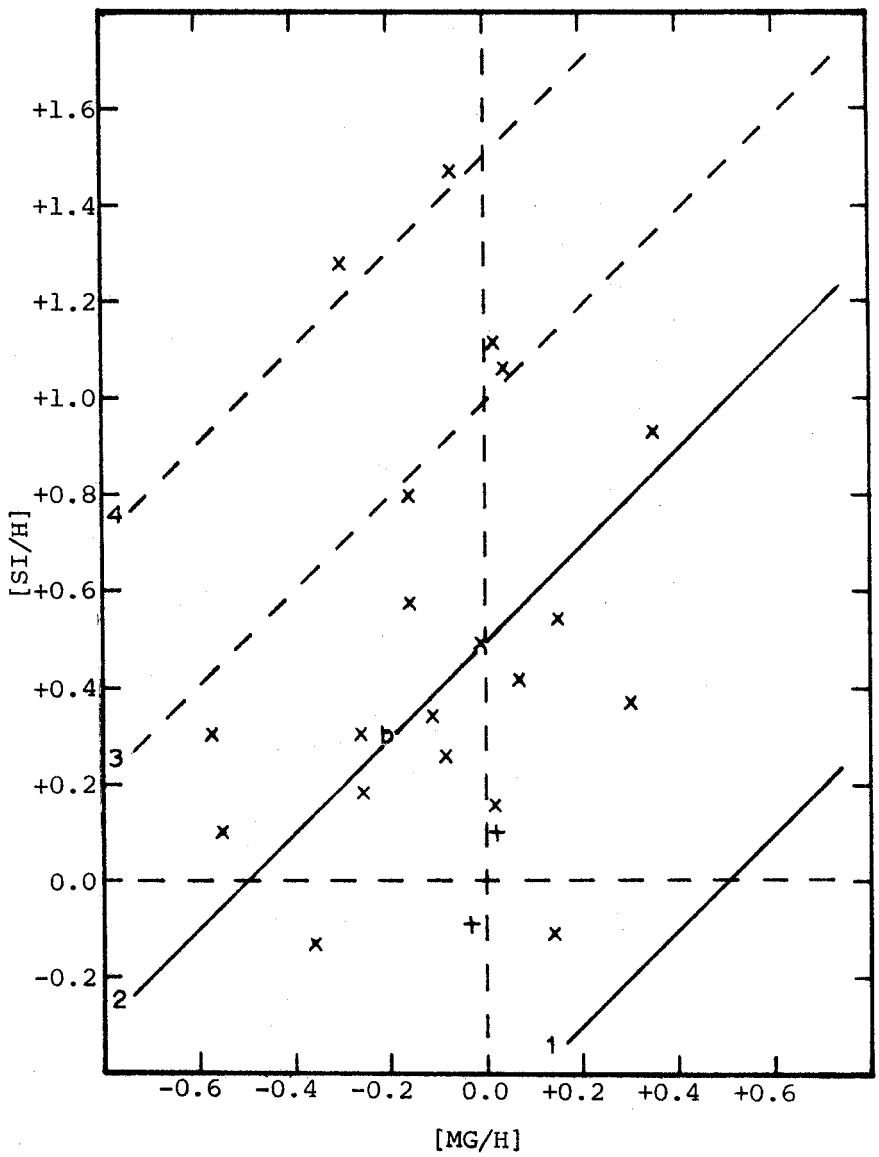

Figure III-5: The [Si/H] vs. [Mg/H] diagram. b denotes HD81009; x's, the other cool Ap stars, and +'s, the normal A stars. Line 1 is for [Si/Mg] = -0.5, 2 for +0.5, 3 for +1.0, and 4 for +1.5.

TABLE III-6: COMPARISON OF IRON PEAK ABUNDANCES FOR THE SI STARS AND THE CANDIDATES FOR THE EXTENSION OF THIS CLASS INTO THE COOL PECULIAR A STARS

Star	[Ti/Fe]	[Cr/Fe]	[Mn/Fe]
Si and λ4200-Si Stars from Searle *et al.* (1966)			
21 Per	-0.09	-0.03	+0.16
41 Tau	-0.37	+0.04	-0.28
11 Ori	-0.64	+0.10	-0.17
49 Cnc	-0.19	-0.28	-0.24
21 Aql	-0.73	-0.77	
Cool Ap Star Si Star Extension Candidates			
HD50169	-0.69	+0.95	+0.30
HD192678	-0.40	+1.33	+0.22
HD12288	+0.15	+1.59	+0.29
HD22374	-0.53	+1.21	+0.51
HD110066	-0.74	+1.11	+0.40
HD191742	-0.45	+1.14	+0.35

similar, those for [Mn/Fe] are marginally higher in a few cool Ap stars, but those for [Cr/Fe] are quite different. Part of the differences may be due to techniques of analysis. There is some overlap in B-V between the two groups in Table III-6. However, 21 Per is a spectrum variable which has unusually strong rare earth lines for its effective temperature which is at least 1000°K greater than any cool Ap star under discussion. We have previously discussed the differences in effective temperatures derived by Searle et al. (1966) and those used in this study, namely their effective temperatures are the lower ones.

This study shows that there exists cool Ap stars whose characteristics including the [Si/Mg] ratio are similar to those of classical Si stars except for their [Cr/Fe] values. The sample of Si stars studied is smaller than that of the cool Ap stars. The abundance anomalies, in general, may be similar for the two types (Sargent and Searle 1967). This suggestion can be tested by an abundance survey similar to this study for the sharp-lined Si stars. If this supposition is correct, then a number of Si stars will be found with values of [Cr/Fe] intermediate between the two cases previously studied. Analyses of individual Si stars in the literature use determinations of the Fe oscillator strengths which contain serious systematic errors which are a function of excitation potential. These studies can give only a weak confirmation of this hypothesis (see for example, Burbidge and Burbidge 1955a). Searle and Sargent (1964) also found three hot peculiar A stars, ν Cnc, 21 Aql, and HD207840, which have normal Si

abundances. Durrant (1970b) measured the equivalent width of SiII λ6347-71 in a large number of A and B type stars. He found that contrary to the results of Searle and Sargent the equivalent width vs. B-V diagram did not show a clear cut separation into normal and anomalous types. These facts strengthen the hypothesis that the Si and cool Ap stars are similar types differentiated by effective temperature.

The presence of singly-ionized rare earth lines in the hottest SrCrEu stars studied requires large overabundances. If the effective temperatures of these stars were increased a few hundred degrees, these lines would disappear. If the Si and cool Ap stars are similar objects, then near the same effective temperature Cr will have to have more normal abundances with respect to Fe. Both elements become doubly-ionized at similar temperatures. If the process which causes these overabundances is related to some property of the singly-ionized ions, then the absence of these ions means that both Fe and Cr will have more nearly solar abundances. In this effective temperature region, large Si overabundances begin to affect the atmospheric parameters. Hence the division of the magnetic stars in cool and Si stars may be an effect of three physical processes which occur in the same region of effective temperature.

Summaries of abundance anomalies are given by Sargent (1964, 1966) and Hack (1968). We will consider that there are three groups of Ap stars, Mn, Si, and SrCrEu or cool, and discuss those elements studied in this survey. Table III-7 shows the compilations.

TABLE III-7: SUMMARY OF ELEMENTAL ABUNDANCES IN PECULIAR A STARS

Element	Mn Stars	Si Stars	SrCrEu Stars	This Study
He	o,-	--	?	?
C	o	-	-,?	?
O	o	-	--,?	?
Mg	o	o,-	o,+	o
Si	o	++,+	o	o,+
Ca	-	--	o	o,+
Ti	o,+	o,+	o,+	o,+(++)
V	-,?	o,+	o	o,+
Cr	o,+	o,+	o,+	+,++
Mn	+,++	o,+	+,++	+,++
Fe	o,+	o,+	o,+	o,+
Sr	+,++	+	++	+,++
Y	+,++	+	+,++	o,+
Zr	++	++	o,+	o,+,?
Ba	+	o	o,+	o,?
rare earths	?	++	++	(+),++

Sources: Sargent (1964, 1966), Hack (1968), and this study.

Notes: o = normal

- = deficient by a factor of 10

-- = deficient by a factor of 100

+ = overabundant by a factor of 10

++ = overabundant by a factor of 100 or more

? = unknown

All abundances are given with respect to solar values.

The results of this survey agree with that of the compilation for SrCrEu stars with these basic differences: Cool Ap stars have larger Si and Cr abundances and smaller Y abundances. In addition this study increased the range of known cool Ap star abundances. Si and cool Ap stars have ranges of abundances which overlap except for Ca and Zr. Although the mean abundances appear to be somewhat different, the abundance anomalies for the two types of stars are similar.

The Mn stars do not show convincing evidence for magnetic fields (Babcock 1958, Conti 1970) in excess of a few hundred Gauss. In addition, they do not exhibit spectrum, light, or magnetic variations as do some of the Si and cool Ap stars (Preston 1971c). Their abundance characteristics are different. No Mn star has any detectable rare earth lines. They do not show the He and O deficiencies (Sargent and Searle 1962, Searle and Sargent 1964). Mn stars also have a larger percentage of companions than Si and cool Ap stars. Thus, a separation of Ap stars into Mn stars and the magnetic stars has been proposed on the basis of magnetic fields, a few abundance characteristics, and binary statistics (Preston 1971c, Sargent and Searle 1967, Guthrie 1969a).

In addition to the aforementioned distinctions, the major abundance differences of the Mn stars compared with the cool Ap stars are Y, Zr, and Hg overabundances and a normal Cr abundance. Mn stars also have lines of a number of peculiar elements some of which may be found in SrCrEu stars when a greater wavelength range is studied.

In this section we have found that the cool Ap stars of this study have abundances that are typical of all cool Ap stars. The

cool Ap stars and the Si stars have similar but not identical abundance anomalies which are different than those of the Mn stars. The two types of magnetic Ap stars may be similar types of stars differentiated by effective temperature.

E. Comparison of the Results with Those of Low Dispersion Spectral Classification and Photometric Indices

Peculiar A-type stars have mostly been studied spectroscopically at much lower dispersions than that employed in this study. In addition, these stars have been examined photoelectrically with both UBV and intermediate band photometry. The UBV results show that Ap stars have colors similar to those of normal stars. They will not be considered further.

Table I-1 gives the cool Ap star subclasses of low dispersion classification spectroscopy: 12 are SrCrEu, 6 SrCr or CrSr, 1 CrEu, and 2 Cr stars. They suggest that all cool Ap stars should have large Cr abundances as we have found. Do the Cr stars, HD12288 and HD192678, and the EuCr star, HD204411, have smaller Sr abundances than the other cool Ap stars studied? Except for HD22374, they do. The survey's stars with the smallest equivalent widths of SrII(1) λ4215.52 are HD12288, HD22374, HD89069, HD192678, and HD204411. The value of log Sr/H for HD89069 is about 0.2 dex greater than that for HD204411 which has abundances greater than the remaining three stars. HD12288 has broader lines than most of the other cool Ap stars due to its strong magnetic field. This makes it relatively difficult to measure the equivalent widths. Thus, the subclasses isolate those stars with Sr

overabundances as well as those with large SrII line equivalent widths. HD22374 is a puzzle. Perhaps this discrepancy is a clue to the variability of this star.

Do the 12 SrCrEu stars and the CrEu star have greater Eu abundances than the other cool Ap stars studied? HD204411, the CrEu star, has the weakest EuII lines of the cool Ap stars studied. This star may be a long period spectrum variable (Preston 1970c). Of the six stars with the greatest Eu abundances four are classified as SrCrEu and two as SrCr stars. The ten stars with the weakest EuII lines include 1 CrEu star, 2 Cr stars, 1 CrSr star, 3 SrCr stars, and 2 SrCrEu stars. The SrCrEu and the SrCr stars are well mixed with respect to effective temperature and Eu abundance. The Cr stars, which are the hottest cool Ap stars studied, are in the below average part of the Eu abundance distribution. The subclasses agree better with the appearance than with the abundances. Thus low dispersion classification spectroscopy records better what is seen rather than what are the abundances.

Cameron (1966) investigated the peculiar A stars by means of photoelectric intermediate band Strömgren and Hβ photometry. He found that if the m_1 index is greater than ≥ 0.21, then the star has a magnetic field. The program cool Ap stars cover most of the range indicated for their subclasses. Table III-8 gives the values of the Strömgren and Hβ indices, whether it is a hot, H, or cool, C, star for Hβ photometry the number of observations, n, and their weight, wt.

TABLE III-8: STRÖMGREN AND Hβ PHOTOMETRY FOR THE COOL PECULIAR A STARS

HD	u-b	b-y	m_1	c_1	β	H or C	n	wt.
2453	-0.013	-0.005	0.271	0.877	2.849	H	2	1.5
5797								
8441	+0.047	+0.022	0.141	1.145	2.833	H	2	1.7
12288	+0.058	+0.034	0.200	1.013	2.883	H	1	0.5
18078	+0.332	+0.087	0.251	1.079	2.831	C	1	0.7
22374	+0.167	+0.073	0.173	1.097	2.878	C	2	1.7
50169	-0.021	-0.024	0.244	0.962	2.804	H	2	1.1
81009								
89069								
110066	-0.004	+0.004	0.256	0.898	2.877	H	3	2.8
111133	-0.089	-0.047	0.204	1.021	2.830	H	3	2.4
118022	-0.048	-0.010	0.231	0.934	2.881	H	3	2.2
137909	+0.135	+0.145	0.264	0.739	2.832	C	3	2.2
137949	+0.157	+0.209	0.302	0.558	2.833	C	2	0.8
165474								
176232	+0.110	+0.139	0.215	0.825	2.806	C	3	2.3
191742	+0.227	+0.114	0.232	0.960	2.884	C	2	1.6
192678	-0.022	-0.060	0.263	0.995	2.884	H	4	3.0
201601	+0.115	+0.157	0.242	0.740	2.814	C	1	0.8
204411	+0.241	+0.052	0.179	1.202	2.894	C	1	0.9
216533	+0.062	+0.014	0.219	1.019	2.896	H	1	0.8

Cameron plots m_1, the metal index, vs. c_1, the Balmer discontinuity index, and examines the [O/H] and [Si/Mg] determinations of Sargent and Searle (1962) and Searle and Sargent (1964) as regard the position of the stars that they studied in this type of diagram. Stars with similar abundance ratios are close together. The cool Ap stars with the largest values of [Si/Mg] do not occupy the same region of the (c_1,m_1) diagram as do the Si stars studied by Searle and Sargent. This study's cool Ap stars are distributed in a band in the (c_1,m_1) diagram. I tried c_1 vs. log N/H correlations for many elements. They are basically scatter diagrams except the one for Cr which suggests that as we go towards hotter stars the Cr abundance increases. Mn, Nd, Gd, and U have diagrams which are basically of the scatter variety although there is some suggestion of correlation. Thus, in (c_1,m_1) diagrams except when one studies the Cr abundances, stars with the greatest abundances are not necessarily close to one another. The effects of line blanketing upon the values of the Strömgren indices may cause part of the scatter. Hence, low dispersion classification spectroscopy and Strömgren photometry pick out the Ap stars, but do not tell us much about their elemental abundances.

F. Comparison of the Cool Ap and Am Star Elemental Abundances

The cool Ap and the Am stars occupy overlapping regions in the H-R diagram. Smith (1971) studied the abundances of sixteen Am stars which he determined are representative of this class as a whole. Figure III-6 shows his results given with respect to Fe relative to

Figure III-6: The relative abundances of the elements for the Am stars from Smith(1970). The ordinate is the logarithmic abundance ratio with respect to Fe and relative to the means of the standards. Dots represent Am stars; crosses, marginal Am stars; circles, standards; and squares, HR906. The more uncertain values are denoted with bracketing horizontal lines.

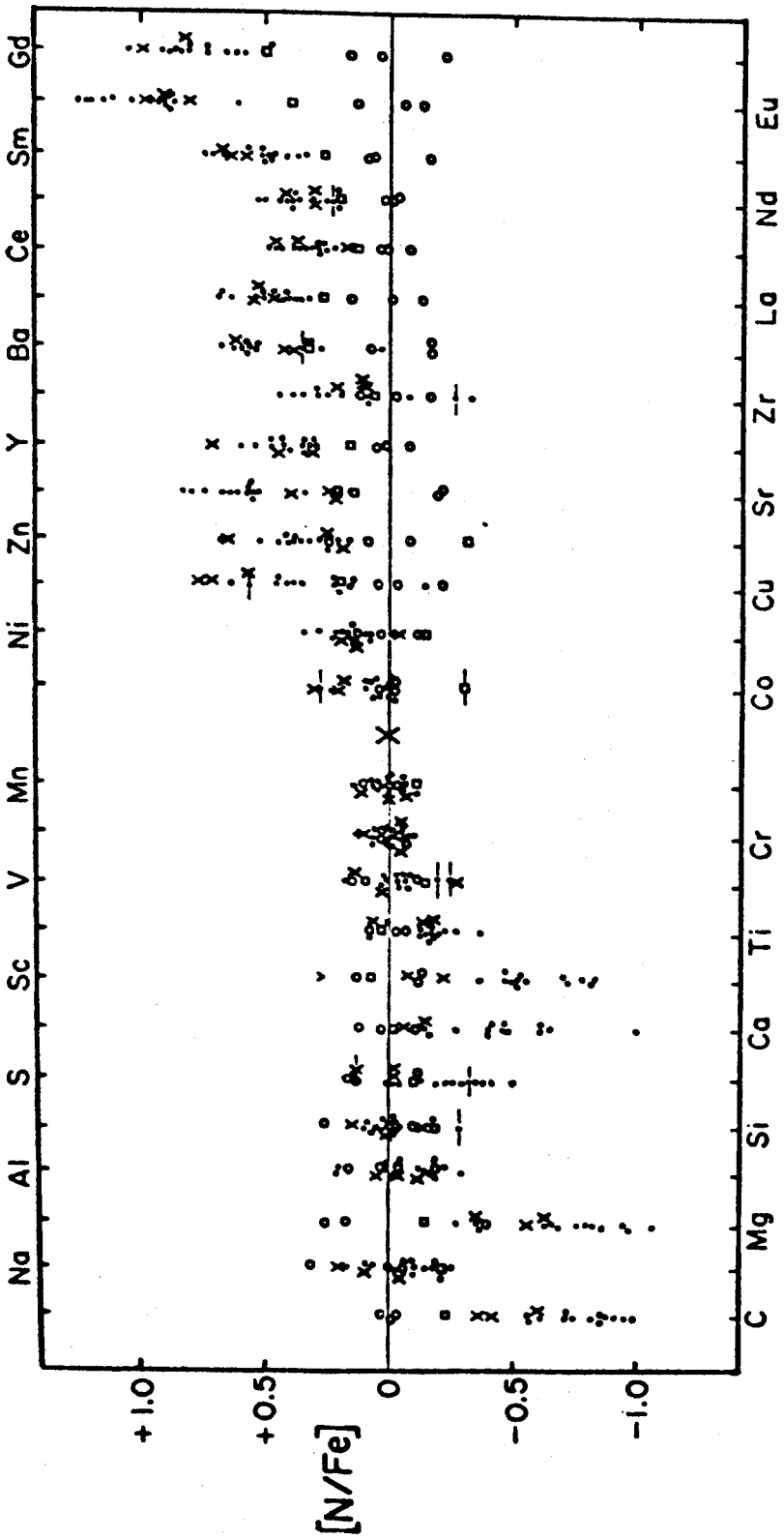
Na Al S Sc V Mn Ni Zn Y Ba Ce Sm Gd
C Mg Si Ca Ti Cr Co Cu Sr Zr La Nd Eu
+1.0
+0.5
0
-0.5
-1.0
[N/Fe]

Figure III-7: [N/Fe] values, the logarithmic abundances with respect to Fe and relative to solar values. Closed circles represent cool Ap stars with T_{eff}>9500°K; +, HD81009; x's, the other cool Ap stars; and open circles, normal stars. Uncertain values are indicated by bracketing horizontal lines except for HD81009 when * is the symbol. The arrows, →, indicate the mean elemental abundances for those cool Ap stars with deduced abundances. In case all the program's cool Ap stars did not have abundances deduced for an element, a vertical bar was attached to the shaft of the arrow. The atomic number for each element with deduced abundances is given below the diagram while the corresponding chemical symbol is above it.

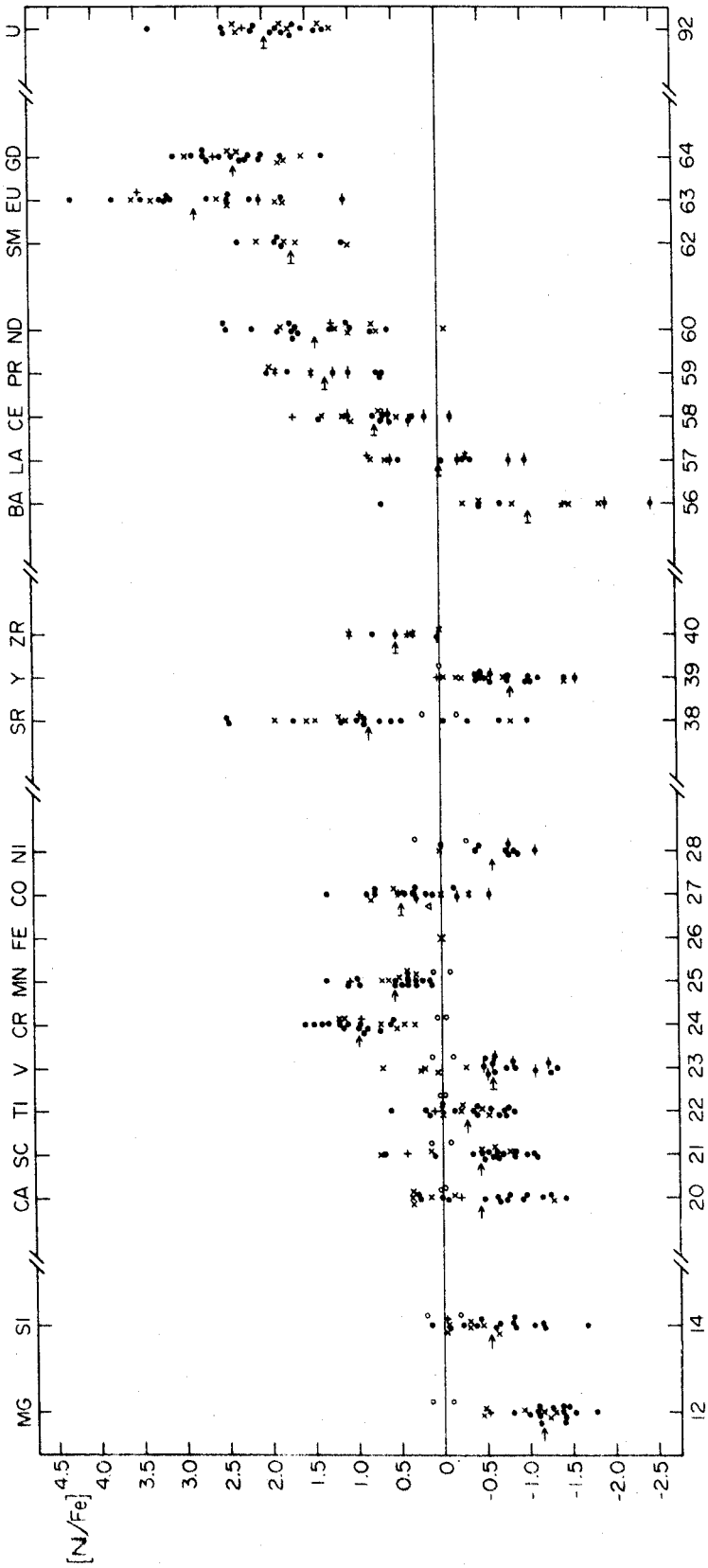
MG SI CA SC TI V CR MN FE CO NI SR Y ZR BA LA CE PR ND SM EU GD U
12 14 20 21 22 23 24 25 26 27 28 38 39 40 56 57 58 59 60 62 63 64 92
[N/Fe]
4.5 4.0 3.5 3.0 2.5 2.0 1.5 1.0 0.5 0 -0.5 -1.0 -1.5 -2.0 -2.5

the means of the standards while Figure III-7 gives the results for the SrCrEu stars presented in the same manner. This way of presenting the data illustrates the character of the Am star abundance anomalies. The values of [N/Fe] generally increase with atomic number except for a few elements. Smith used a less accurate determination of the Fe oscillator strengths than did this study, but his normalization procedure should remove most of this effect.

Smith determined the Mg abundances from MgI rather than MgII lines. There are some differences in the values used for the normal star abundances. For most elements this does not matter due to the normalization procedure. For elements which did not have their abundances determined from the normal stars in this study, the agreement between the solar value and the normal star abundances as determined by Smith is usually within 0.3 dex. If we adjust this study's [N/Fe] values for this effect, these changes would cause only minor modifications to the conclusions which we will deduce.

The range of derived abundances is larger for the SrCrEu stars than for the Am stars. For some elements there is a complete separation of [N/Fe] values. The cool Ap star values are all greater than those of the Am stars for Cr, Nd, Sm, and Gd, while for Y the reverse is true. In addition, there is nearly complete separation for Mn and Eu similar to that in the Cr relative abundances while those for Ba and Ni are similar to Y. The other elements have overlapping abundance ranges, but there are still differences. For the cool Ap stars, the mean value of [Mg/Fe] is -1.15 compared with -0.75

for the Am stars. A similar effect occurs for Si where the cool Ap stars have a mean value of [Si/Fe] of -0.55 while that for the Am stars is 0.0. The means for [Ca/Fe], [Sc/Fe], and [Ti/Fe] are similar with the Ap stars having a much larger range of deduced abundances. The Ap star range is larger for [V/Fe] while the mean value is smaller for the Am stars. This may result from a number of poorly determined values. The cool Ap star [Co/Fe] mean value may be higher than that for the Am stars and its range greater, but this determination is poor. For [Sr/Fe], the range of cool Ap star abundances is larger and the mean value greater than that for the Am stars. [Zr/Fe] is uncertain in the cool Ap stars, but may be similar to values of the Am stars. [La/Fe] has greater range for Ap stars as does [Ce/Fe] which also has a larger mean value for the Ap stars than for the Am stars.

The scatter in the relative abundances for the Am stars is similar to that of the standards. This is not so for the cool Ap stars. For absolute abundances, the scatter is larger than the normal stars for both Am and cool Ap stars. The mechanism which produces the overabundances with respect to Fe for the Am stars does not allow variations from one star to another by more than a factor of two for most elements. The cool Ap star abundance anomaly mechanism permits much greater variations. Cool Ap stars lack the Am stars' relation that the stars with the largest Fe enhancement for their temperature also have the largest Sr/Fe values, and conversely.

A plot of absolute abundances with respect to H as a function of atomic number does not show the Am star abundance anomalies as well as those with respect to Fe. In general, absolute overabundances are not as great for the Am stars as for the cool Ap stars. The Am stars have similar rare earth abundances for all elements. For most elements, the ranges of abundances overlap for the Am and the cool Ap stars. For Cr, Sm, and Gd, there is complete separation with the cool Ap stars having the greater absolute abundances. Ti, Mn, Nd, and Eu show virtually complete separation in the same sense.

Similar to the results for the cool Ap stars, the Fe abundance in the Am stars increases with effective temperature with a similar slope (see the next section). For the Am stars, the abundances of Mg, Ca, and Sc show good, but imperfect correlations with one another both in their absolute and relative abundances with respect to Fe. In the cool Ap stars there are also similar relations between Ca and Sc, while those between Mg and Ca are weak, and those between Mg and Sc are suggested. The cool Ap stars also show similar correlations between many Fe peak elements, Sc and Ti, Cr with Mn and Fe, Fe with Mn, Ti with Fe, and Ti poorly with Cr. The abundances of Sr and Y do not correlate as do those of Gd and Ce. Many elements have abundances which do not correlate with those of Fe. The abundances of elements which do correlate with one another. While for the Am stars, the abundances of all elements correlate reasonably well with one another and with Fe.

The mean value of [Sc/Sr] is -1.26 for the cool Ap stars. Some of them have near solar values while others have very small values

near -3.0. This ratio has been used to detect Am stars (Conti and Strom 1968a). Although some cool Ap stars have values of [Sc/Sr] similar to Am stars, this is just coincidental.

The abundance anomaly characteristics imply that the mechanisms producing the cool Ap and Am stars are different. Am stars do not have substantial magnetic fields (Conti 1969) as do the cool Ap stars. If one theory explains the abundances of one type of star, it will not for the other. Thus, if a diffusion mechanism working in a subsurface elemental separation zone produces the abundance anomalies of Am stars (Watson 1970, Smith 1970), it is unlikely it can do so for the cool Ap stars.

The most clear cut differences between the cool Ap and Am stars appear by use of a few elemental abundance ratios, the most certain of which are [Cr/Fe], [Nd/Fe], [Gd/Fe], [Y/Fe], [Cr/H], and [Gd/H]. [Mn/Fe], [Eu/Fe], [Ti/H], [Mn/H], [Nd/H], and [Eu/H] may also be useful in this regard. Improved values of these abundances may show that there is also complete separation in these ratios. Temperature dependent rare earth partition functions may change the situation somewhat. So by comparing [N/Fe] and [N/H] values for the cool Ap and the Am stars, many differences are found which completely distinguish these types of stars.

G. Dependence of the Abundances on the Physical Properties of the Stars

No convincing case can be made for the dependence of the elemental abundances on the apparent rotational velocity for any of the elements

studied. The range in v sin i for the stars studied is 0 to 10 km/sec. For many stars only an upper limit is known. If one divides these stars into two groups, those with effective temperatures greater and less than 9500°K, then for some elements a tendency exists in each group for the abundance to be a function of v sin i. Unfortunately these group correlations usually are in the opposite sense. Hence for all cool Ap stars studied, no such relations exist.

Correlations between elemental abundance and magnetic field strength are weak or non-existent. This implies either that the magnetic fields are not important in the production of the abundance anomalies or that the time scale for their decay is shorter than the main sequence lifetimes of the Ap stars. In Figure III-18, there is a group of six stars with large values of log Si/H. If we plot these values against the magnetic field strength of these stars, then these quantities tend to increase together. Log Sc/H appears to increase with magnetic field strength despite the large scatter in the individual values. If we consider only those stars with magnetic fields of 2.2 kG or stronger, then log Mn/H decreases with magnetic field strength. These relations are, nevertheless, rather speculative. The magnetic field strength is not a function of effective temperature or apparent rotational velocity.

There are some abundance correlations with effective temperature. In addition, some abundances show peculiar distributions in abundance vs. effective temperature diagrams. I will discuss these cases and illustrate some of them. On the other hand, there are many scatter

diagrams. Table III-9 is a list of those which were tried as a function of effective temperature.

Log Fe/H vs. effective temperature is shown in Figure III-8 for the values derived in case 1. The diagrams for cases 2 and 3 are similar as is the one which uses the values derived from FeII lines for log Fe/H vs. the initial estimates of effective temperature from UBV photometry. In these diagrams the Fe abundance increases with effective temperature. Since the log Fe/H vs. magnetic field strength diagram shows only scatter, this result is independent of the size of the magnetic field. In Figure III-8, the tip of the arrow indicates the position of HD5797 if its value of log g is 3.5 instead of 4.0. The ends of the solid line indicate the sensitivity of the log Fe/H values to a 1000°K change in the effective temperature. Hence errors in log g and effective temperature do not weaken the correlation. HD5797 is the furthest Ap star from the correlation line.

A suggestion that log Fe/H begins to decrease with effective temperatures near 10250°K comes from averaging the mean values deduced from the hottest seven stars (T_{eff}>10150°K), the intermediate seven stars, and the coolest seven stars (T_{eff}<9500°K). I used these mean values to confirm the correlations. For the cool Ap stars, the mean value of log Fe/H is -3.28 compared with -4.34 for the normal A stars and -4.40 for the sun. The cool Ap stars studied have significant Fe overabundances except for four coolest ones which are marginally overabundant.

TABLE III-9: ABUNDANCE RATIOS WHICH AS A FUNCTION OF EFFECTIVE TEMPERATURE ARE SCATTER DIAGRAMS

log Mg/Fe	log Ti/Mn	log Pr/H
log Si/Fe	log Co/H	log Pr/Fe
log Ca/H	log Ni/H	log Sm/H
log Ca/Fe (?)	log Sr/H (?)	log Eu/Fe
log Sc/H	log Sr/Fe	log Ce/Eu (?)
log Sc/Fe	log Sr/Sc	log Eu/Nd (?)*
log Ca/Sc	log Y/Fe	log Gd/Fe (?)
log Ti/H	log Sr/Y	log Gd/Eu
log Ti/Fe	log Zr/H	log Gd/Ce
log V/H	log Ba/H	log Eu/H
log V/Fe	log La/H	log Eu/Fe
log Mn/Fe	log Ce/H	log U/Fe
log Cr/Mn	log Ce/Fe	

Notes: ? = possible weak correlation.

* = possible correlation where the abundance ratio decreases as the effective temperature increases.

Figure III-8: Log Fe/H vs. effective temperature diagram for the values of case 1. The tip of the arrow indicates the position of HD5797 in this diagram if its value of log g is 3.5 instead of 4.0. The ends of the solid line indicate the effect of a 1000°K change in effective temperature on log Fe/H values. This direction is virtually the same as that of the arrow. b denotes HD81009; x's, the other cool Ap stars; and pluses, the normal A stars. The Fe abundances and effective temperatures increase together. The mean log Fe/H value for the cool Ap stars is -3.28; for the normal stars, -4.34; for the sun, -4.40.

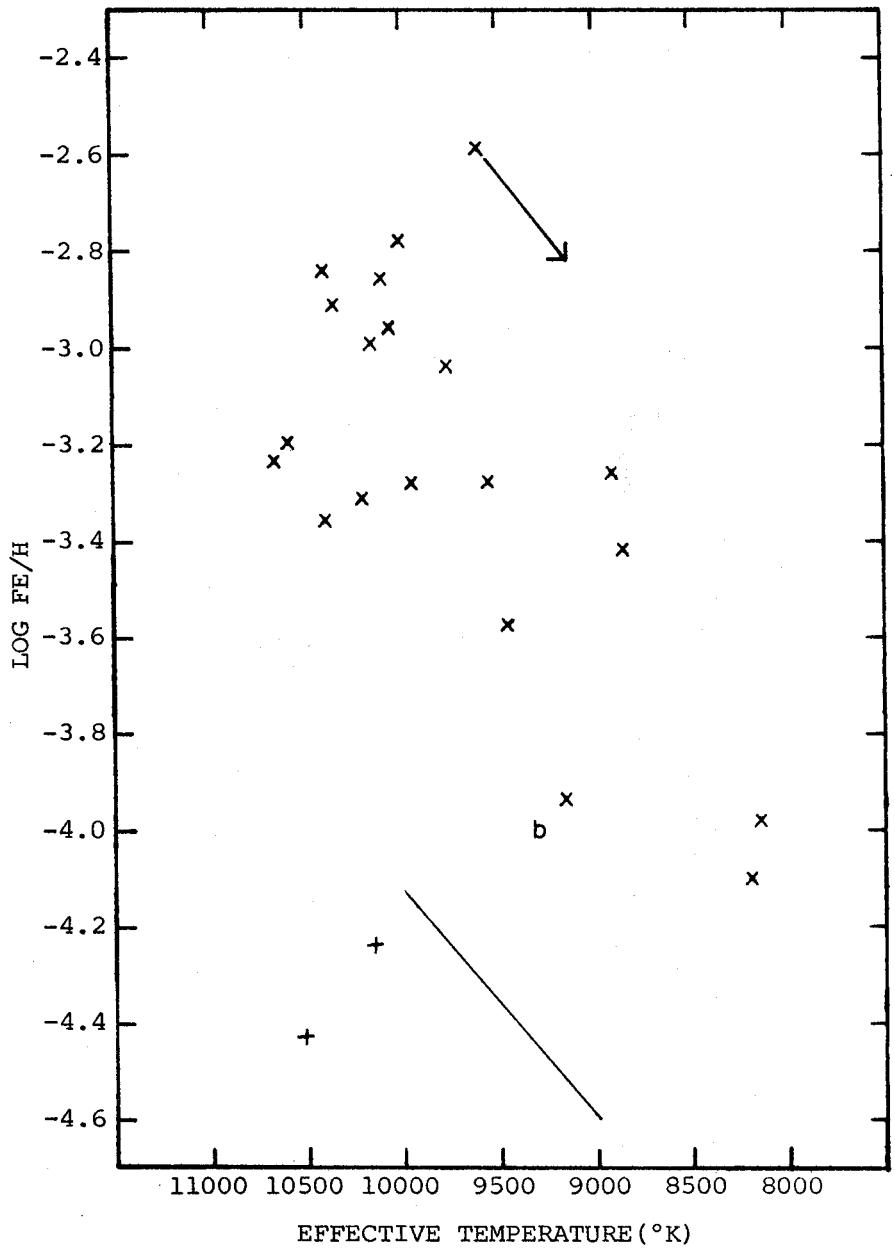
-2.4
-2.6
-2.8
-3.0
-3.2
-3.4
-3.6
-3.8
-4.0
-4.2
-4.4
-4.6
LOG FE/H
b
11000 10500 10000 9500 9000 8500 8000
EFFECTIVE TEMPERATURE(°K)

This is the fundamental correlation. That it occurs with all of the effective temperatures and the derived Fe abundances, and that the correlation line is the one along which errors in the effective temperature and log g would cause, imply that it is real. Errors in oscillator strengths shift the stars with respect to effective temperature but do not change this correlation. At a given effective temperature, there are stars with significantly different Fe abundances. This scatter may be due to errors in log Fe/H and atmospheric parameters. However, I believe that a good part of it is real and should be regarded as a clue to the origin of the abundance anomalies.

Log Cr/H (Figure III-9), log Mn/H (Figure III-10), log Nd/H (Figure III-11), log Gd/H (Figure III-12) and $A' = 1/3$ (log Nd/H + log Eu/H + log Gd/H) are functions of effective temperature. In addition log Mg/H (Figure III-13) may be although the degree of scatter in log Mg/H is large relative to the degree of correlation to make this relation certain. Also in this category are log Y/H (Figure III-14) and log U/H (Figure III-15). In addition, log Cr/Fe (Figure III-16) and log Nd/Fe (Figure III-17) are functions of the effective temperature.

On the log Y/H, log Nd/H, log Gd/H, and log U/H vs. effective temperature diagrams, I have indicated with a solid line what the abundance of a typical line of these elements with a 15 mÅ equivalent width would be. On the other correlation diagrams, the ends of the solid line represent the temperature sensitivity of the abundance ratio to a 1000°K change in effective temperature. The slopes of the log

Figure III-9: Log Cr/H vs. effective temperature diagram. b denotes HD81009; x's, the other cool Ap stars; and pluses, the normal stars. The ends of the solid line represent the effect of a 1000°K change in the effective temperature on log Cr/H values. For the cool Ap stars, log Cr/H increases with effective temperature. Three stars are not on the main relation. HD5797 and HD191742 are above it while HD111133 is below it. All cool Ap stars have significant Cr overabundances which range from .8 to 3.1 dex. The mean value of log Cr/H is -3.92 for the cool Ap stars compared with -5.94 for the normal A stars and -6.59 for the sun. The overabundances are computed relative to the normal A stars rather than relative to the sun in which case they would have been significantly larger.

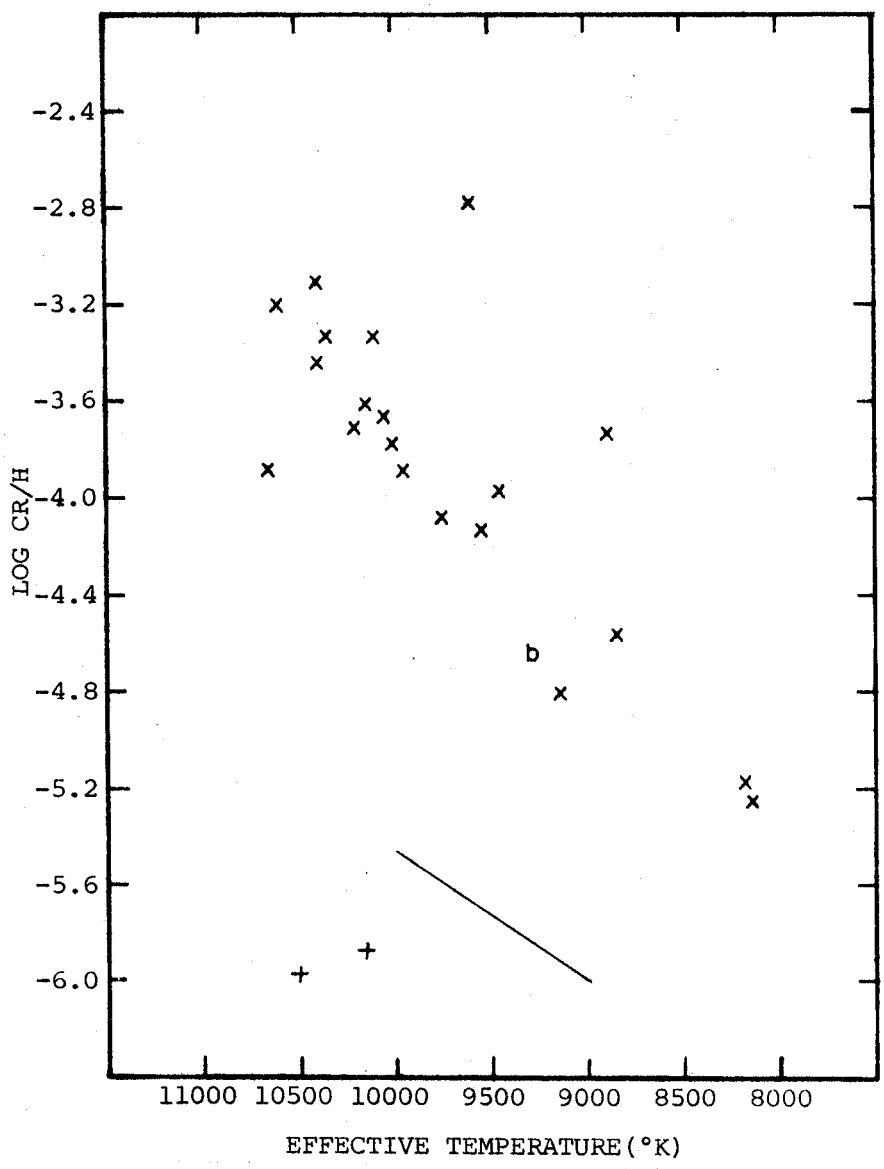
-2.4
-2.8
-3.2
-3.6
-4.0
-4.4
-4.8
-5.2
-5.6
-6.0
LOG CR/H
b
11000 10500 10000 9500 9000 8500 8000
EFFECTIVE TEMPERATURE(°K)

Figure III-10: Log Mn/H vs. effective temperature diagram. Log Mn/H increases with effective temperature. b denotes HD81009 and x's, the other cool Ap stars. The ends of the solid line indicate the effect of a 1000°K change in the effective temperature on log Mn/H values. HD5797 and HD89069 are above the main correlation. The mean value of log Mn/H for the cool Ap stars is -5.49 with the solar value as -7.11.

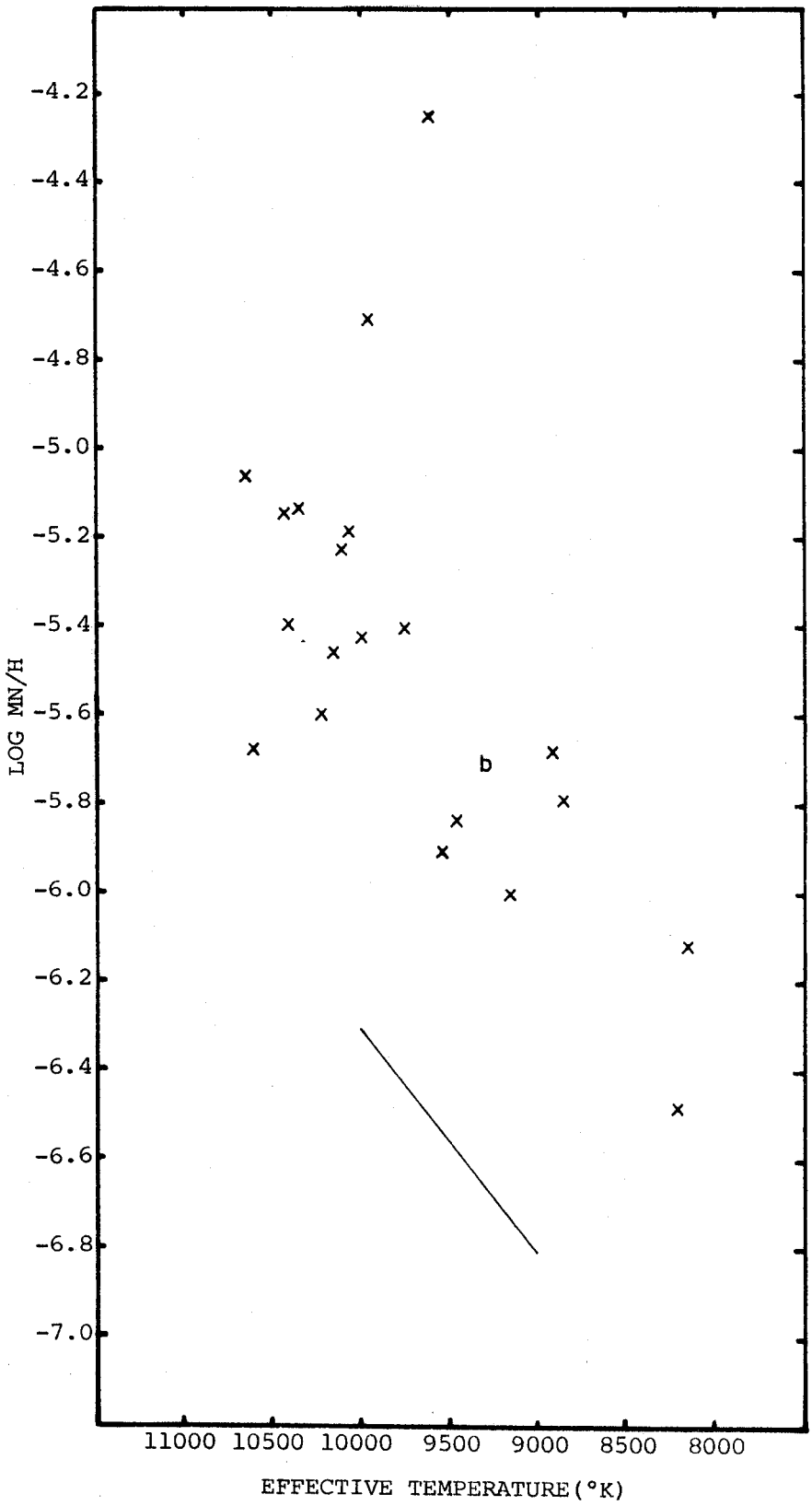
-4.2
-4.4
-4.6
-4.8
-5.0
-5.2
-5.4
-5.6
-5.8
-6.0
-6.2
-6.4
-6.6
-6.8
-7.0
LOG MN/H
b
11000 10500 10000 9500 9000 8500 8000
EFFECTIVE TEMPERATURE(°K)

Figure III-11: Log Nd/H vs. effective temperature diagram. b denotes HD81009 and x's, the other cool Ap stars. The solid line represents the abundance that a 15mA equivalent width of NdII λ4304 would have. Since the correlation of log Nd/H and effective temperature veers away from this line, it is real. The mean value of log Nd/H is -7.06 for the cool Ap stars compared with a solar value of -10.07.

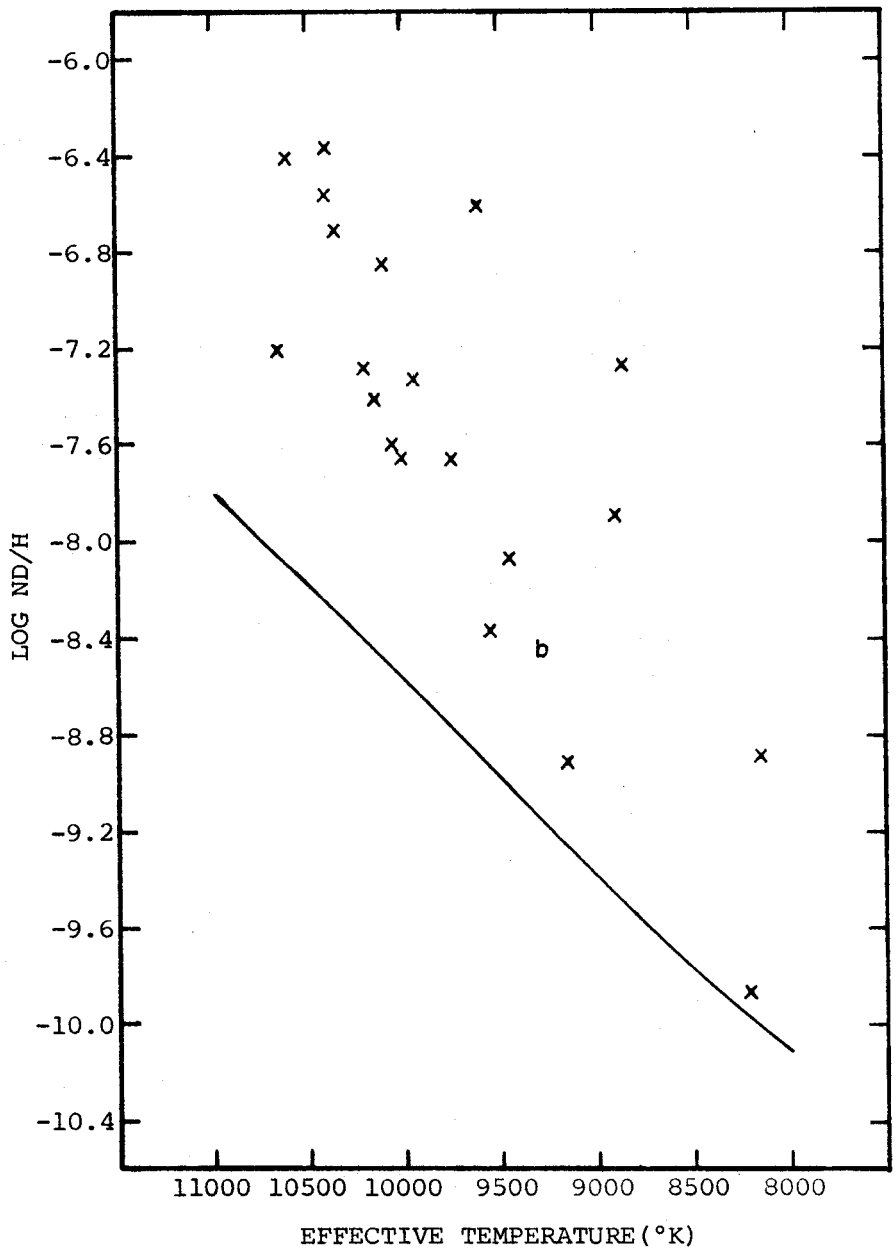
-6.0
-6.4
-6.8
-7.2
-7.6
-8.0
-8.4
-8.8
-9.2
-9.6
-10.0
-10.4
LOG ND/H
b
11000 10500 10000 9500 9000 8500 8000
EFFECTIVE TEMPERATURE (°K)

Figure III-12: Log Gd/H vs. effective temperature diagram. The solid line represents the abundance that a 15mA equivalent width of GdII(32) λ4215 would have. The correlation of log Gd/H and effective temperature is nearly parallel to this line. However, the values are significantly greater that it is real. The mean value of log Gd/H for the cool Ap stars is -7.64 compared with -10.87 for the sun. o's denote members of the lower group in the log Gd/Nd diagram while x's denote the other cool Ap stars except for HD81009 which is denoted by b.

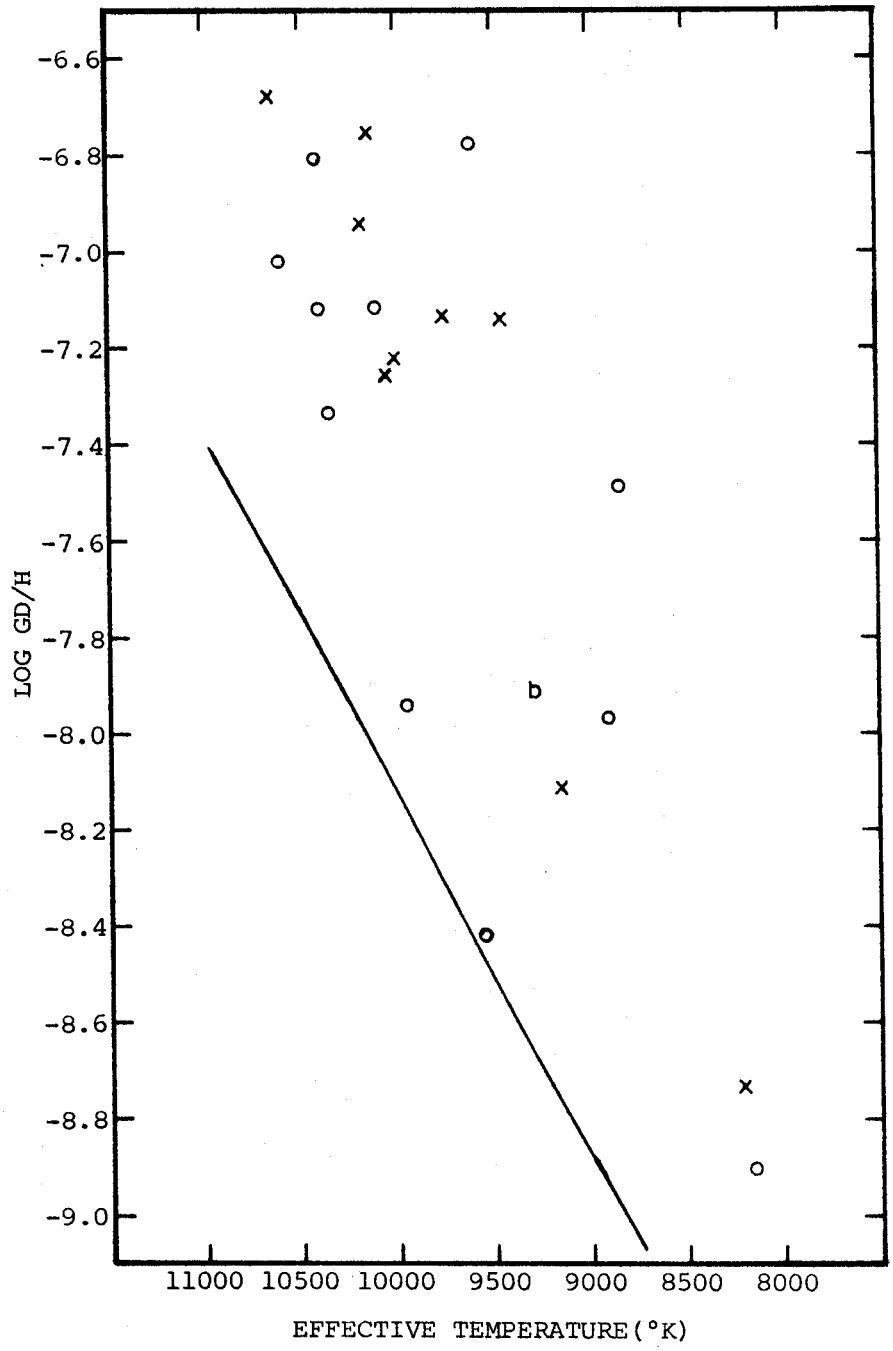
-6.6
-6.8
-7.0
-7.2
-7.4
-7.6
-7.8
-8.0
-8.2
-8.4
-8.6
-8.8
-9.0
LOG GD/H
b
11000 10500 10000 9500 9000 8500 8000
EFFECTIVE TEMPERATURE(°K)

Figure III-13: Log Mg/H vs. effective temperature diagram. b denotes HD81009; x's, the other cool Ap stars; and pluses, the normal stars. The ends of the solid line indicate the effect of a 1000°K change in effective temperature on log Mg/H values. Log Mg/H is a weak function of the effective temperature. The scatter in log Mg/H is too large relative to the degree of correlation to make this relation certain. This correlation would be improved by the removal of HD5797 at -4.13, 9600°K from this diagram. The mean value of log Mg/H is -4.58 for the cool Ap stars compared with -4.48 for the normal stars and -4.56 for the sun.

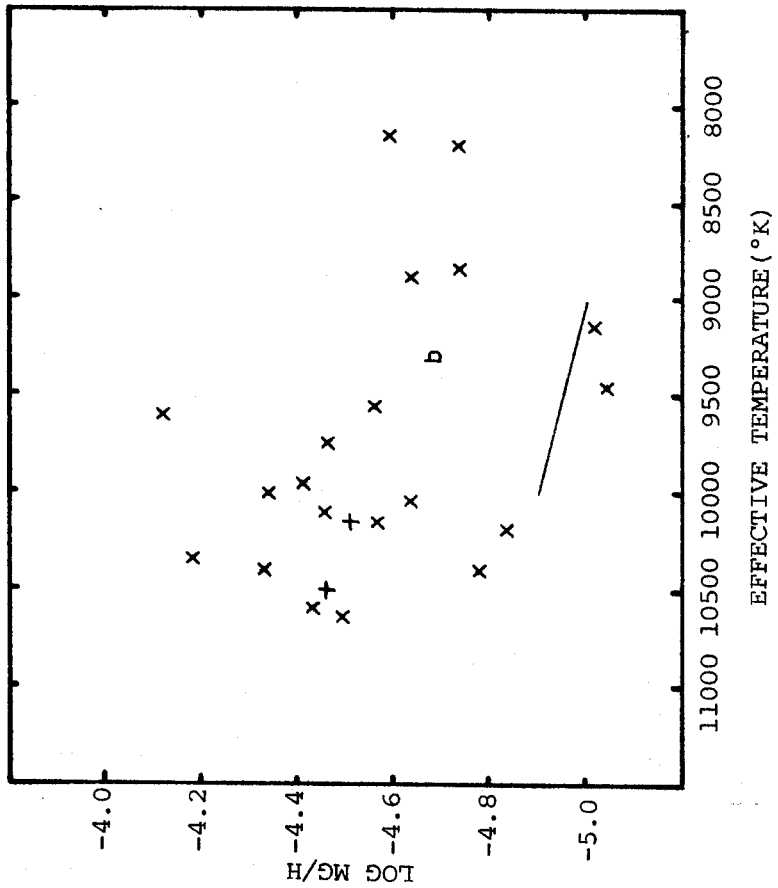
LOG MG/H
-4.0
-4.2
-4.4
-4.6
-4.8
-5.0
11000 10500 10000 9500 9000 8500 8000
EFFECTIVE TEMPERATURE (°K)
b

Figure III-14: Log Y/H vs. effective temperature diagram. b denotes HD81009; x's, the other cool Ap stars; and +, o Peg. Log Y/H may be a function of effective temperature. The solid line represents the abundance that a 15mA equivalent width of YII(6) λ3950 would have. Many deduced abundances fall near this line and the correlation is somewhat parallel. Hence, the above conclusion is a tentative one. The mean value of log Y/H for the cool Ap stars is -8.50 compared with -8.74 for o Peg and -8.80 for the sun.

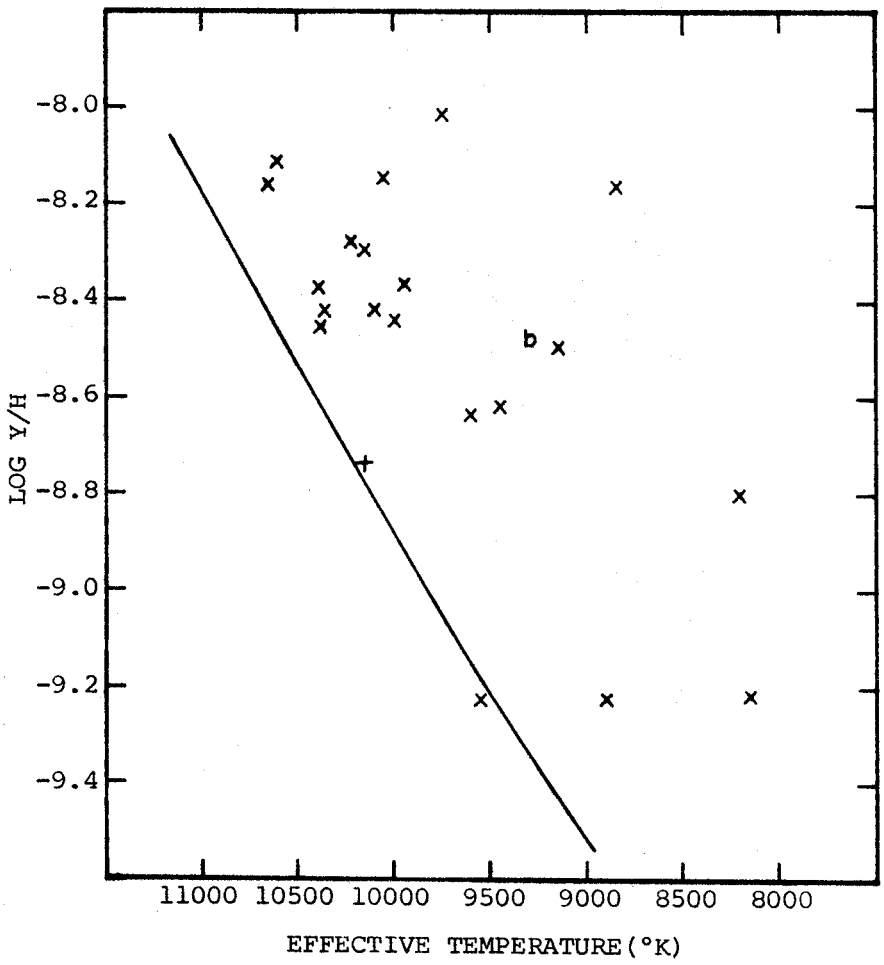
-8.0
-8.2
-8.4
-8.6
-8.8
-9.0
-9.2
-9.4
LOG Y/H
b
11000 10500 10000 9500 9000 8500 8000
EFFECTIVE TEMPERATURE (°K)

Figure III-15: Log U/H vs. effective temperature diagram. The solid line represents the abundance that a 15mA equivalent width of UII(-) λ3860 would have. x's represent the cool Ap stars except for HD81009 which is denoted by b. Log U/H increases with effective temperature. The correlation is tentative due to the large scatter which results from weak and partially blended. HD5797 and HD216533 are far above the other stars. The mean value of log U/H for the twenty cool Ap stars in whose spectra UII line equivalent widths were measured is -9.26 compared with a solar value of -12.30.

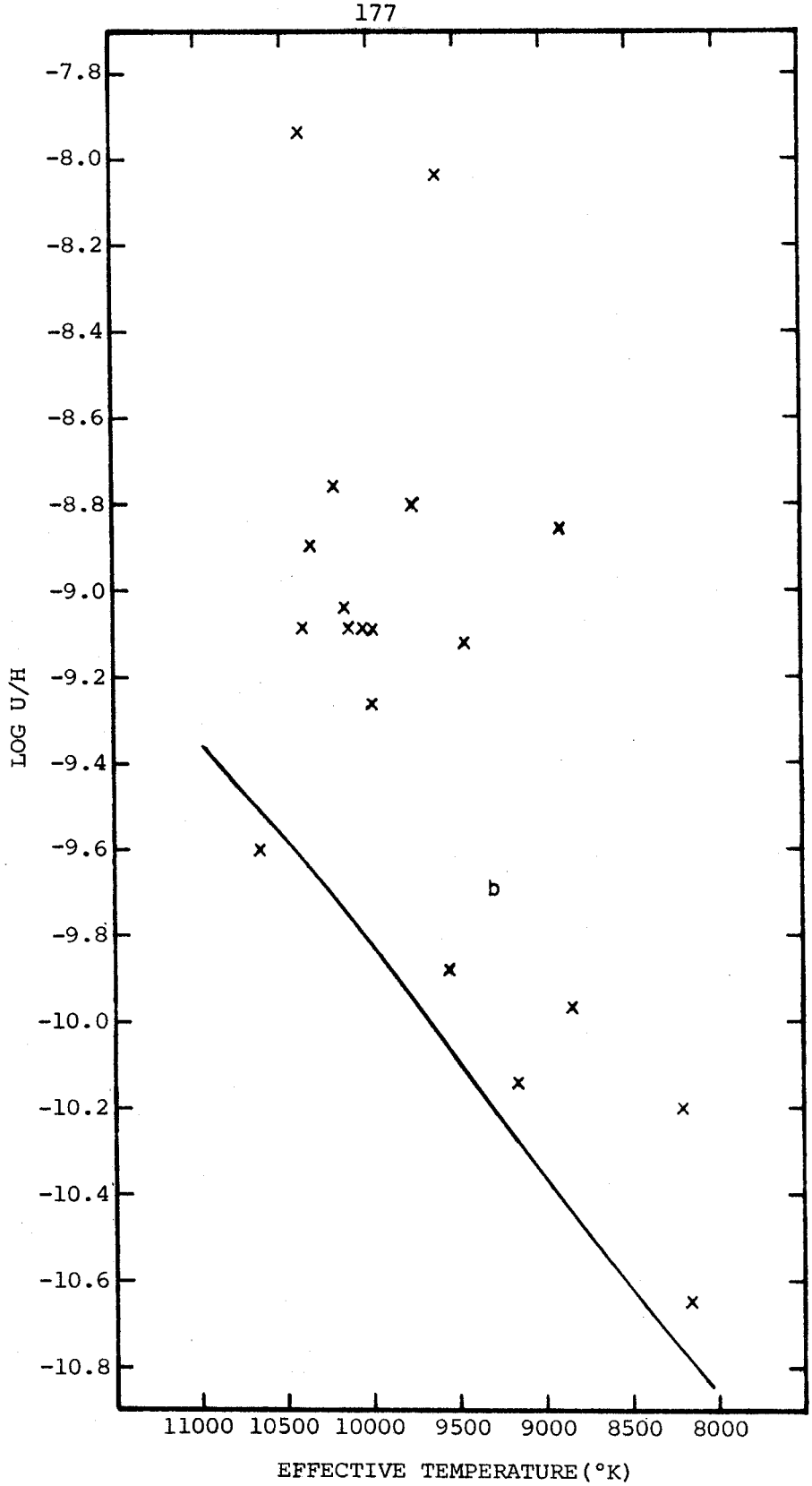
-7.8
-8.0
-8.2
-8.4
-8.6
-8.8
-9.0
-9.2
-9.4
-9.6
-9.8
-10.0
-10.2
-10.4
-10.6
-10.8
LOG U/H
b
11000 10500 10000 9500 9000 8500 8000
EFFECTIVE TEMPERATURE (°K)

Figure III-16: Log Cr/Fe vs. effective temperature diagram. b denotes HD81009; x's, the other cool Ap stars; and pluses, the normal stars. The ends of the solid line represent the effect of a 1000°K change in effective temperature on log Cr/Fe values. Log Cr/Fe and the effective temperature increase together, but this relation is not as tight as that for log Cr/H vs. effective temperature. The mean value of log Cr/Fe for the cool Ap stars is -0.64. The cool Ap stars have definite overabundances of Cr with respect to Fe except for the three coolest ones which have marginal overabundances. So the Cr abundance increases faster with effective temperature than that of Fe for the cool Ap stars.

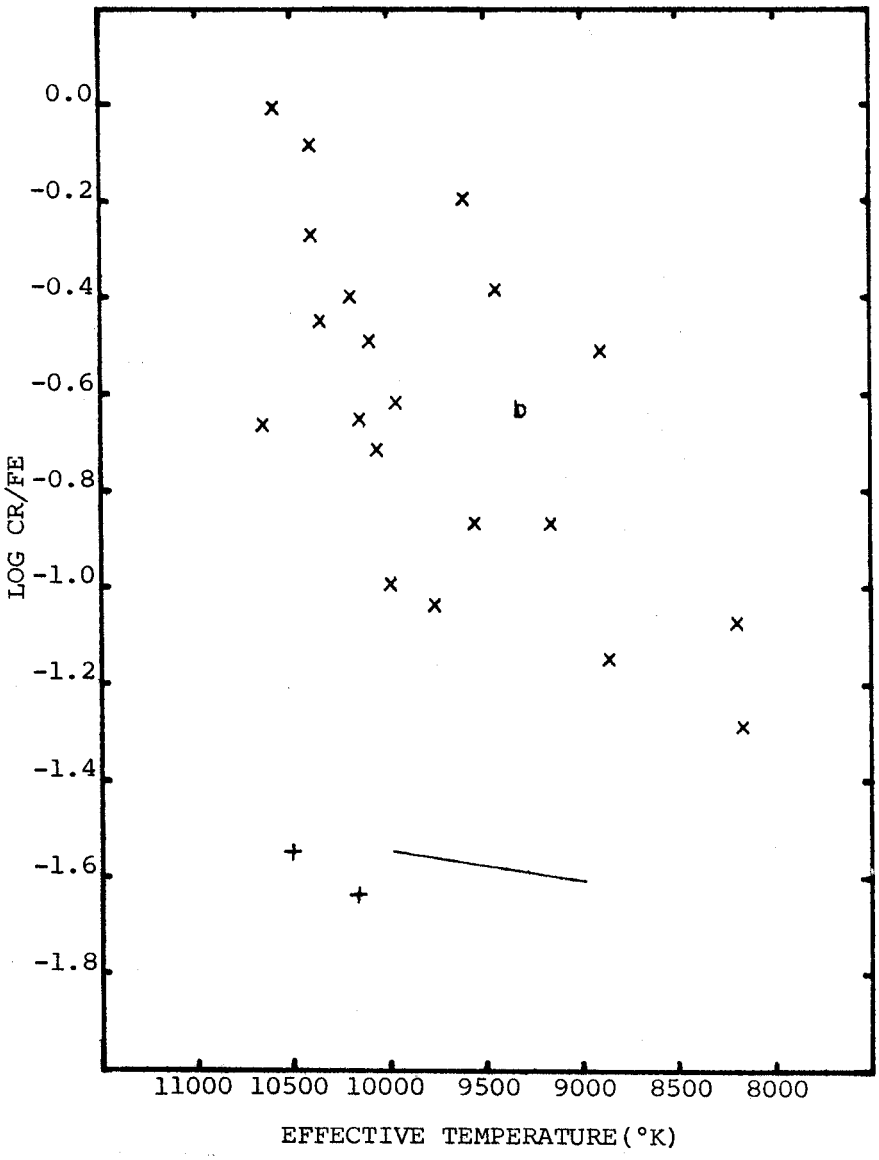
0.0
-0.2
-0.4
-0.6
-0.8
-1.0
-1.2
-1.4
-1.6
-1.8
LOG CR/FE
11000 10500 10000 9500 9000 8500 8000
EFFECTIVE TEMPERATURE(°K)

Figure III-17: Log Nd/Fe vs. effective temperature diagram. b denotes HD81009 and x's, the other cool Ap stars. The mean value of log Nd/Fe is -4.32 for the cool Ap stars compared with a solar value of -5.67. Log Nd/Fe increases with effective temperature. This is a loose correlation with much scatter. HD137949 is not on the relation. The ends of the solid line represent the effect of a 1000°K change in effective temperature on the log Nd/Fe values.

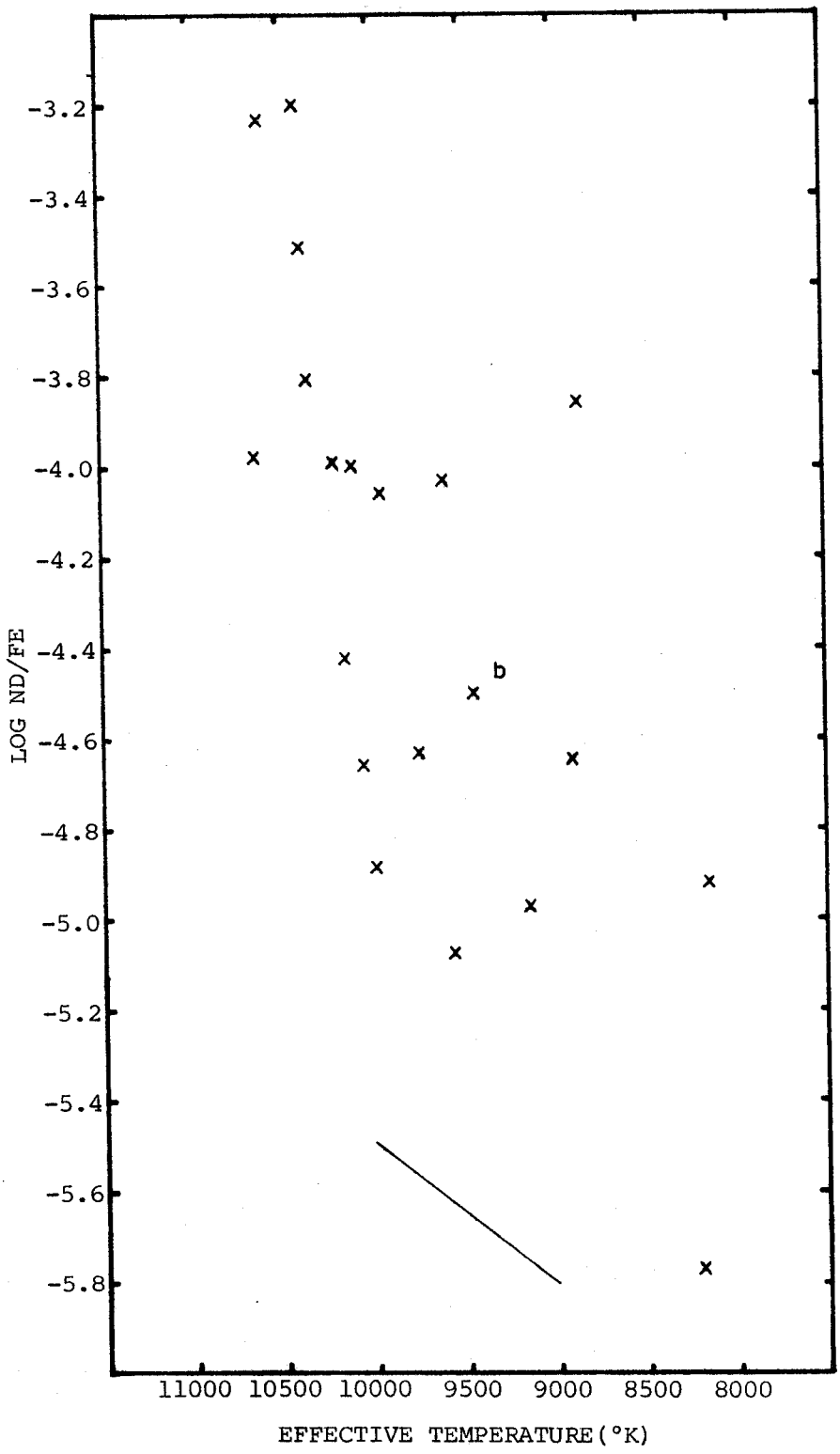
-3.2
-3.4
-3.6
-3.8
-4.0
-4.2
-4.4
-4.6
-4.8
-5.0
-5.2
-5.4
-5.6
-5.8
LOG ND/FE
b
11000 10500 10000 9500 9000 8500 8000
EFFECTIVE TEMPERATURE(°K)

N/H correlation diagrams with effective temperature do not appear to be a function of atomic number.

There are other diagrams which have interesting divisions in the distribution of the abundance ratios. They include:

1) Log Si/H vs. effective temperature (Figure III-18). The sample appears to be divided into two major groups separated in 0.4 in log Si/H. The stars with the larger log Si/H values are HD5797, HD12288, HD50169, HD110066, HD191742, and HD192678.

2) Log Ca/H vs. effective temperature. The most interesting divisions in log Ca/H values are perpendicular to the direction along which errors in effective temperature and gravity would cause. HD137909, HD137949, HD176232, HD191742, HD201601, and HD204411 are to the right of this division if the diagram is drawn similar to Figure III-18.

3) Log Sc/Fe vs. effective temperature. Most cool Ap stars have below solar values due to large Fe abundances. HD137909 and HD137949 have normal values while HD12288, HD81009, and HD165474 have near normal ones.

4) Log Cr/Ti vs. effective temperature (Figure III-19). The cool Ap stars divide into two groups, those with log Cr/Ti<1.98: HD5797, HD81009, HD137909, HD137949, HD165474, HD176232, HD201601, and HD204411; and the others, with log Cr/Ti>2.38. The first group is basically the cooler program Ap stars.

5) Log Sr/Fe vs. effective temperature. There are 3 divisions in the values of log Sr/Fe. HD111133 and HD216533 are well above the

Figure III-18: Log Si/H vs. effective temperature diagram. b denotes HD81009; x's, the other cool Ap stars; and pluses, the normal A stars. The ends of the solid line represent the effect of a 1000°K change in the effective temperature on log Si/H values. The sample of abundances appears to be divided into two groups separated by about 0.4 in log Si/H. The stars with the larger log Si/H values are HD5797, HD12288, HD50169, HD110066, HD191742, and HD192678. The mean value of log Si/H is -4.23 for the cool Ap stars. The normal stars give -4.74 compared with a solar value of -4.49.

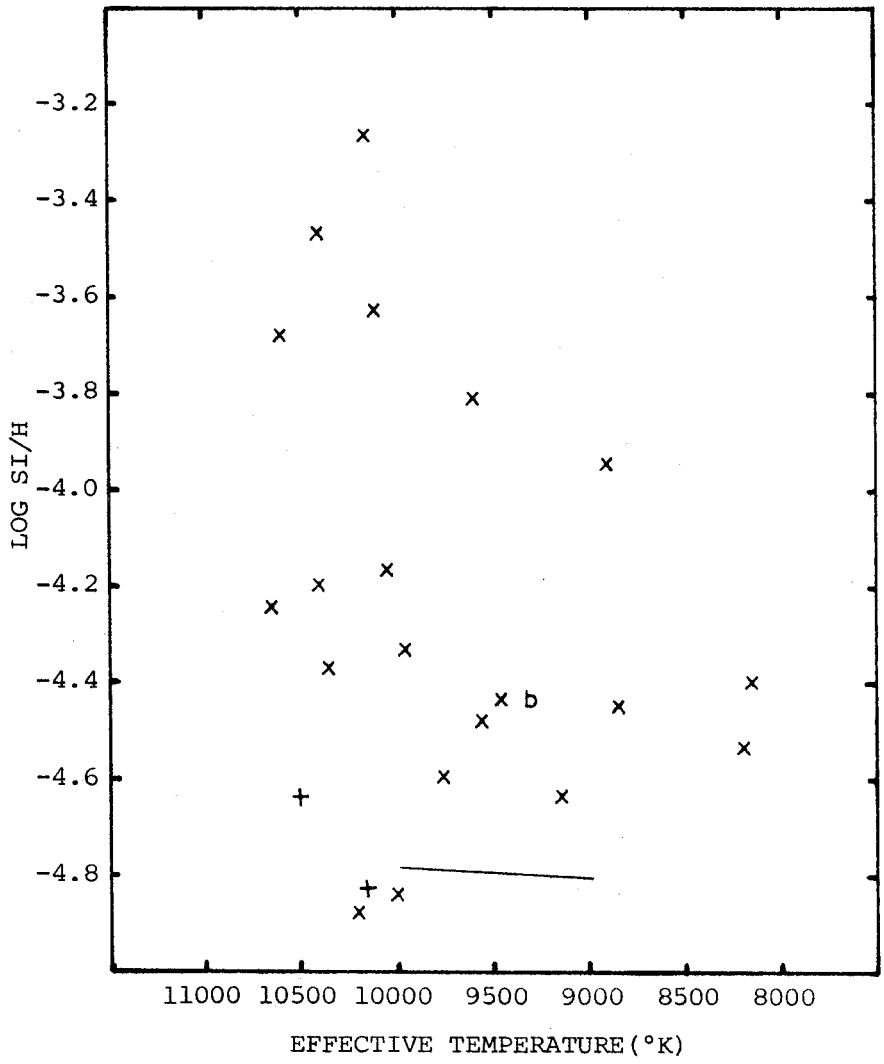
-3.2
-3.4
-3.6
-3.8
-4.0
-4.2
-4.4
-4.6
-4.8
LOG SI/H
b
11000 10500 10000 9500 9000 8500 8000
EFFECTIVE TEMPERATURE(°K)

Figure III-19: Log Cr/Ti vs. effective temperature diagram. b denotes HD81009; x's, the other cool Ap stars; and pluses, the normal A stars. The ends of the solid line indicate the effect of a 1000°K change in effective temperature on log Cr/Ti values. The cool Ap stars are divided into two groups, those with log Cr/Ti < 1.98: HD5797, HD81009, HD137909, HD137949, HD165474, HD176232, HD201601, and HD204411; and the others, with log Cr/Ti > 2.38. The first group is basically the cooler program cool Ap stars.

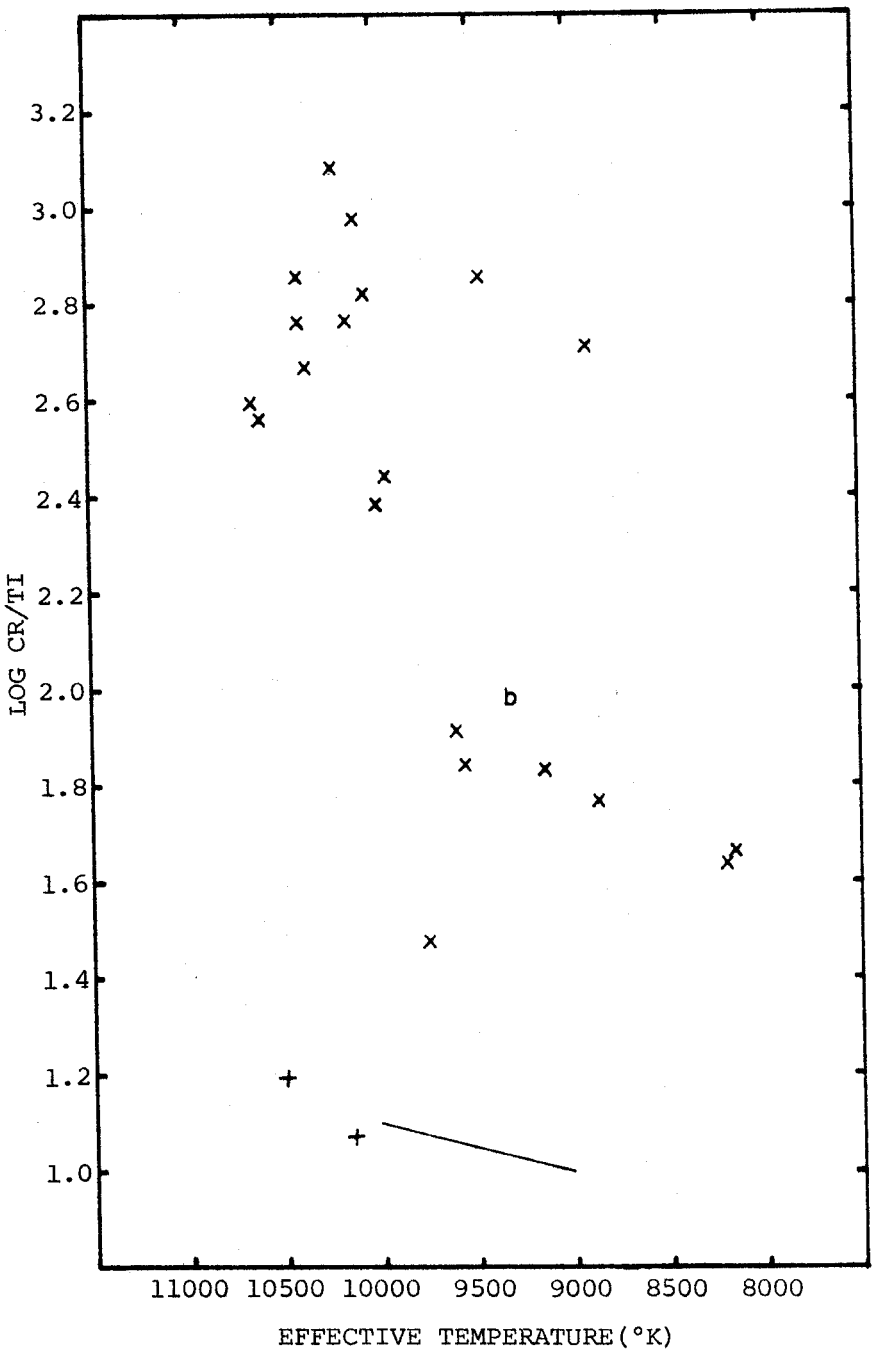
3.2
3.0
2.8
2.6
2.4
2.2
2.0
1.8
1.6
1.4
1.2
1.0
LOG CR/TI
b
11000 10500 10000 9500 9000 8500 8000
EFFECTIVE TEMPERATURE(°K)

main concentration of values while HD89069, HD22374, HD204411, and HD12288 have below normal values.

6) Log Gd/Nd vs. effective temperature (Figure III-20). This diagram shows two groups, both of which have ratios of log Gd/Nd which decrease with increasing effective temperature. The members of the upper group are HD8441, HD22374, HD50169, HD81009, HD111133, HD118022, HD137909, HD165474, and HD176232. In Figure III-12 the members of the two groups are indicated with different symbols. One group has a tighter correlation than the other. In other correlation diagrams, there exist weaker and less perfect relations for these two groups.

In addition, a plot of log Ce/Eu vs. log Gd/Nd shows a weak correlation with a large scatter. As log Ce/Eu increases, log Gd/Nd decreases.

Now let us examine Figure III-3 again. The rare earth with the largest abundance for most stars is Eu. Of the ten stars whose abundances are used in Figure III-3, 7 have maxima at Eu, 1 at Nd-HD216533, 1 at Sm-HD176232, and 1 at Gd-HD50169. Of the seven stars with five rare earth abundance determinations, four have peaks at Eu, 1 at Nd, 1 at Sm, and 1 at Gd. This shift of the maximum rare earth abundance causes scatter in some attempted correlation diagrams. The stars of the upper groups in the log Gd/Nd vs. effective temperature diagram (Figure III-20) have four maxima at Gd, four at Eu, and one at Sm. HD192678 with four determined rare earth abundances is the one star with a maxima at Gd which does not belong to this group.

Figure III-20: Log Gd/Nd vs. effective temperature diagram. The ends of the solid line represent the effect of a 1000°K change in effective temperature on log Gd/Nd values. x's denote the cool Ap stars except for HD81009 which is indicated by b. The solar value of log Gd/Nd is -0.80. This diagram shows two groups,both of which have ratios of log Gd/Nd which decrease with increasing effective temperature. The members of the upper group are HD8441, HD22374, HD50169, HD81009, HD111133, HD118022, HD137909, HD165474, and HD176232.

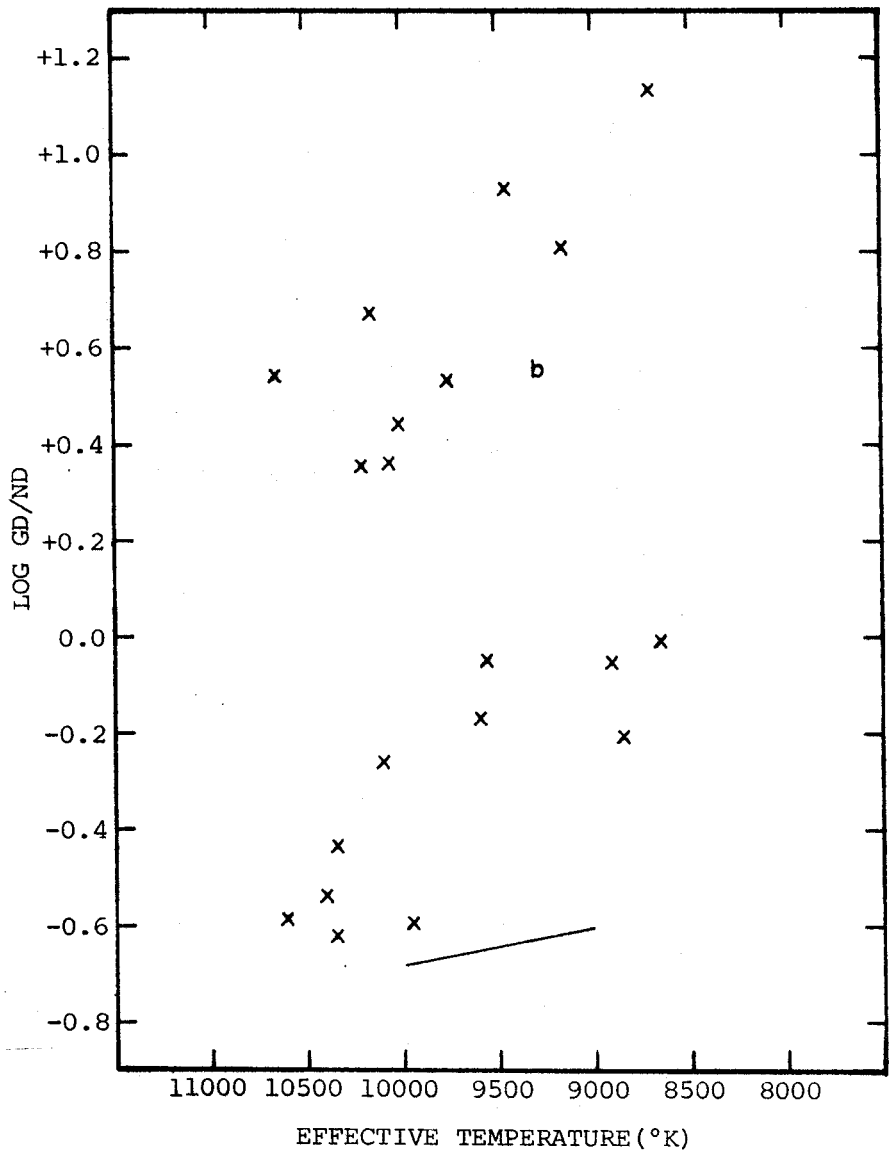
+1.2
+1.0
+0.8
+0.6
+0.4
+0.2
0.0
-0.2
-0.4
-0.6
-0.8
LOG GD/ND
b
11000 10500 10000 9500 9000 8500 8000
EFFECTIVE TEMPERATURE(°K)

In the log Gd/H vs. effective temperature diagram (Figure III-12), the stars with Gd and Eu maxima are towards the top of the scatter while those with Sm and Nd maxima are towards the bottom. In the Eu/H vs. effective temperature diagram, the eleven stars with maxima at Eu form the upper envelope of the values and show an increase of Eu abundance with effective temperature. The other stars show a similar but shifted relation displaced downward by about 1.2 dex with respect to the maximum Eu values. So shifts in the rare earth maximum abundances confuse this correlation diagram.

Thus there are no conclusive correlations with magnetic field strength or apparent rotational velocity. Log Fe/H, log Cr/H, log Cr/Fe, log Mn/H, log Nd/H, log Nd/Fe, and log Gd/H increase with effective temperature. Other less certain correlations with effective temperature with the same sense are log Mg/H, log Y/H, and log U/H. Shifts in the maximum rare earth abundance introduce scatter in some attempted correlation diagrams. If we plot the abundances of any two elements whose abundances increase with effective temperature against one another, they increase together. In addition, curious gaps in the distributions of certain abundance ratios in other diagrams have been found.

H. Comparison of the Abundances with Those of Spectrum Variables

If a line is formed only on part of the stellar surface, then the observed equivalent width is smaller than that we would find if we could only observe the region of formation and the deduced abundance

will be smaller than that in the spot. On the other hand, we want an abundance average over the entire stellar surface. If the magnetic field in the spot region is greater than the mean over the stellar surface, then the degree of Zeeman intensification will be greater than that predicted by the mean field for the line in question. Without a detailed knowledge of the field geometry and the distribution of the local contributions to the equivalent widths, it is impossible to get more than a crude abundance estimate. It is not known whether magnetic intensification can become more important than dilution effects.

Several studies indicate which elements vary together in spectrum variables. For HD125248 (Deutsch 1968), a EuCr star, GdII, CeII, and EuII lines vary together but opposite to those of CrI, CrII, and SrII while FeI, FeII, and TiII lines vary similarly to the first set but with far less amplitude. Pyper (1969) found three groups of elements in α^2CVn, a SiCrEu star, on the basis of equivalent width and radial velocity behavior a) the rare earths, b) the Fe peak elements, Ti, V, Cr, Mn, and Fe, and c) elements whose variations are small, Si, Mg, and Ca. Group c has strong lines that vary together in their values of the effective magnetic field. Groups a and b have dramatically different behaviors. Rice (1970) found in HD173650, a SrCrSi star, that the light and line strength variations for all elements are in phase and that the radial velocity curves for all species becomes most positive 1/4 cycle after the line strength maximum.

73 Dra (Preston 1967a), a SrCrEu spectrum variable, has two groups of lines varying in antiphase 1) Ti, Mn, Sr, Y, Ba, and Eu, and 2) Mg, Cr, Fe, and possibly Sc. The first group has, in general, larger variations than the second. 21 Per (Preston 1969), a SiEuSrCr spectrum variable, has a velocity variation of TiII and MnII resembling those of the rare earths, while the lines of SiII, SrII, and FeII yield velocity curves of small amplitude with a double wave. HD124224 and 56 Ari (Peterson 1966), two Si spectrum variables, have SiII and HeI lines varying out of phase with each other.

HD221568 (Kodaira 1967) has a very complicated spectrum variation. The rare earth lines have a different behavior than those of Sr, Mg, Ti, and Fe while those of Si and Ca have a similar behavior to those of the rare earths but with a less extreme equivalent width amplitude. HD9996, a CrEu star, exhibits spectrum variation in a period of 22-24 years (Preston and Wolff 1970). Cr and Eu lines vary out of phase. Hence spectrum variables have a large range of properties. Only the rare earths appear to always vary together. In the non-variable cool Ap stars the elements tend to become overabundant together. If there are undetected spectrum variables included in this study, their variety of elemental behavior has introduced scatter into these results.

Sargent and Searle (1962)'s study included several spectrum variables. For the three with more than one plate, there are no certain variations in the strengths of the infrared OI and MgII lines. The abundances of the spectrum variables generally agreed with those for the non-variable stars of their peculiarity class. A similar

conclusion is deduced from Searle and Sargent(1964)'s study of SiII and MgII lines. They examined HD34452 at several phases and concluded that a survey using only one plate per star could be used to investigate the gross characteristics of a spectrum variable's atmosphere and composition. Searle et al. (1966)'s study of the Fe peak elements includes the spectrum variable 21 Per which has abundance ratios typical of the λ4200-Si stars. Thus these studies indicate that spectrum variables generally share the same abundance anomalies of other Ap stars of their peculiarity type.

Five spectrum variables have been analyzed 73 Dra (Faraggiana and Hack 1962), α^2CVn (by several authors, most recently by Cohen 1970), HD34452 (Tomley et al. 1970), HD173650 (Rice 1970), and HD221568 (Kodaira 1967). The first study was done using spectra with a dispersion of 35 Å/mm. This star's abundances show a general resemblence with those of α^2CVn (Sargent 1964) and, hence, this study will be ignored because of its low dispersion. The results of the other studies are given in Table III-10. In general, the effects due to inhomogenieties of the surface abundances are ignored.

The abundances for α^2CVn (Cohen 1970) at phases 0.0 and 0.5 are based on a model atmosphere with T_{eff}=12000°K, log g = 4.0, and a Si overabundance of 30 times solar. α^2CVn has overabundances greater than any cool Ap star studied for Si, Ca, V, Y, La, Ce, Pr, Nd, and Sm. Its abundances are approximately the maximum seen in the cool Ap stars except for V where its overabundance is 1.4 dex larger, Y 2.2 dex larger, and Ce 1.0 dex larger. In addition it shows lines of

TABLE III-10: RELATIVE ABUNDANCES, [N/H], OF SPECTRUM VARIABLES COMPARED WITH THE MEAN OF THE COOL AP STARS

Element	Mean Cool Ap Stars	α^2CVn Φ=0.0	Φ=0.5	HD34452	HD173650	HD221568
Mg	-0.1	-0.2:		+1.2		+1.0
Si	+0.5	+1.6	+1.9	+1.9	-0.5:	+1.2
Ca	+0.6	+1.8:				-1.5
Sc	+0.6	+1.9:				
Ti	+0.8	+1.6	+1.3	+2.1	+0.5	+0.7
V	+0.5	+2.5:				
Cr	+2.0	+1.8	+2.3	+2.0	+1.5	+1.0
Mn	+1.6	+3.0:		<+1.4	+2.0	
Fe	+1.1	+1.6	+2.0	+1.7	+1.1	+1.0
Sr	+1.9	+2.0:		+2.7	+2.3	+2.3
Y	+0.2	+2.9	+2.7			
Zr	+1.4:	+2.2	+1.8			+2.3
Ba	-0.2:	<+1.6				
La	+1.1:	+2.5	+2.2			
Ce	+1.9:	+4.2	+3.7			+2.0
Pr	+2.4:	+4.3	+3.5			+3.6
Nd	+2.5	+4.2				+3.2
Sm	+2.9:	+3.9	+3.5			+3.8
Eu	+3.8	+6.2	+5.0	+6.2	+4.0:	+3.5
Gd	+3.4	+4.8	+4.1		<+3.9:	+3.8

Note: All values are approximate for HD221568.

Sources of data: α^2CVn - Cohen (1970)
HD34452 - Tomley *et al.* (1970)
HD173650 - Rice (1970)
HD221568 - Kodaira (1967)

elements not seen in the cool Ap stars some of which may be due to the higher effective temperature. Normal Si stars with similar effective temperatures show only the strongest lines of the rare earths.

The rare earth abundances of α^2CVn average 0.5 dex greater than the maximum of the range of abundances observed in the cool Ap stars. Its temperature is 1500°K greater than the hottest cool Ap star studied, HD111133. If this star were given the effective temperature of α^2CVn, log η would shift by 1.20 dex for a typical rare earth line and the corresponding log W decrease by at least 0.35 to 0.50 dex. Hence, most of the rare earth lines seen would disappear. So α^2CVn has anomalous abundances with respect to the cool Ap stars studied. Perhaps they are responsible for its photometric pecularities (Preston 1971c).

The abundances of HD173650 (Rice 1970) are within the range of the cool Ap stars. They are not particularly phase dependent. The curve of growth analysis used an effective temperature of 10100°K and a boundary temperature of 7500°K. Thus this spectrum variable fits well with this study's cool Ap stars.

HD221568 is a 160 day SrCrEu spectrum variable with very peculiar photometric properties. Kodaira (1967) made a coarse analysis at the bluest phase with atmospheric parameters $\theta \approx 0.50$ and log g = 3.7. HD221568 has abundances which fall in the distribution of the cool Ap stars except for Mg, Ca, Pr, and Sm. The Mg abundance determination uses both MgI and MgII lines while that for Ca is based only on the

CaII K line. These variations cause differences in the final abundances. The Pr and Sm abundances are greater than those of any cool Ap star studied. Both α^2CVn and HD221568 have larger Pr and Sm abundances than the non-variables. Perhaps these abundances differentiate spectrum and non-spectrum variables.

The final spectrum variable considered is HD34452 (Tomley et al. 1970), one of the hottest Ap stars. Its abundance determinations are based on T_{eff}=18000°K and log g = 4.2. Of the elements studied, Mg, Si, and Eu are more overabundant in HD34452 than any of the cool Ap stars. The other elements agree quite well. For Eu, the only rare earth detected, this may be due in part to the difference of analysis. For Si, the lines used with the cool Ap stars give smaller abundances than the average for HD34452. The result for [Si/Mg] = +0.7 disagrees with that determined by Searle and Sargent (1964) which was +1.5 although the equivalent widths agree reasonably well. Previous studies agree with Tomley et al. Since the solar abundances and oscillator strengths are similar to this study, the difference may be caused by the adopted 8 km/sec microturbulent velocity.

When allowance is made for photometric pecularities, the abundances of the spectrum variables agree with those of cool Ap stars of similar pecularity type. Some of the abundance anomalies seen in HD34452 might appear in the cool Ap stars if they were hotter. The great elemental overabundances observed in spectrum variables may be a clue to distinguishing them from the non-variables or just an effect due to surface inhomogenities or analysis errors.

The surface maps of the spectrum variables HD125248 (Deutsch 1958), HD173650 (Rice 1970), and α^2CVn (Pyper 1969) show a patchy distribution of elemental abundances typically with the rare earths near the magnetic poles and the other varying elements near the magnetic equator. It is very peculiar to see similar abundance anomalies in the supposedly non-variable cool Ap stars. This study's cool Ap stars are not all seen pole-on since they consist of 21 out of the approximately 50 cool Ap stars whose apparent rotational velocities are known (Preston 1971d).

The non-variable sharp-lined cool Ap stars might all be spectrum variables with long periods. Preston (1970c) listed all sharp-lined cool Ap stars with known periods. Since then Wolff and Wolff (1971) found that HD118022 and HD137909 are periodic light variables. But the agreement of the abundances for HD176232 and HD204411 and of the line lists for HD137909 and HD201601 which were done using spectroscopic plates taken many years apart indicate that the periods for such variability in these stars have to be extremely long. Since the rotational period of HD137909 is 18 days and no spectrum variability is known for this star in this period, it is not a spectrum variable. Thus, at least one cool Ap star is not a spectrum variable. Although non-spectrum variables have abundances similar to spectrum variables, the distribution of the elements on their surfaces has to be much more uniform. The scale of non-uniformity has to be sufficiently small so that to a distant observer the distribution of elemental abundances is indistinguishable from complete uniformity.

Despite non-uniform elemental abundance distributions, spectrum variables appear to have similar abundance anomalies to cool Ap stars. Spectrum variables have a wide range of line strength behavior with only the rare earths always varying togehter. Undetected spectrum variables might have caused some scatter in the derived cool Ap star abundance anomalies although at least one cool Ap star is shown not to be a spectrum variable.

I. Implications of This Study's Results for the Theories of Ap Stars

Four types of theories have been advanced to explain the abundances of peculiar A stars: nuclear reactions on the stellar surface, nuclear reactions in stellar interiors followed by mixing or mass transfer, separation of elements by diffusion processes, and accretion of mass on the surface due to magnetic fields. Two boundary conditions apply (Searle and Sargent 1967):

1) The abundances are a surface phenomena. There are no giants with elemental abundances similar to those of Ap stars. As an A-type star evolves from the main sequence to the giant stage, its atmospheric structure changes from one basically in radiative to one in convective equilibrium. The abundance anomalies could easily be diluted in this process. Studies of clusters with Ap stars show that the material from which the stars formed did not have an abnormal composition. Furthermore, since the solar abundances are similar to those of recently formed A-type stars, the Ap stellar abundances have not greatly enriched the interstellar medium (see also bottom page 202).

2) The process which produces the abundance anomalies is related to the loss of angular momentum and the presence of the magnetic field. Slow rotational velocities and large magnetic fields distinguish magnetic Ap stars from other types of stars.

Table III-11 gives the mean overabundances of the cool Ap stars and the first three ionization potentials of the elements involved. The third ionization potentials of many rare earth elements are not known. They should be, however, similar for all these elements. The atomic energy level distributions of adjacent elements are somewhat alike. The difference in V and Cr overabundances has no obvious correlary in the ionization potentials. The Sr to Y jump might be related to the difference of third ionization potentials, but it is hard to see how since their fourth ionization potentials are similar. There is also no jump between the overabundances of Ca and Sc, elements which have a similar difference in third ionization potentials. This implies that values of the ionization potentials may not be as important as the flux in the continuum of these stars at the wavelengths of the elemental absorption edges.

The best determined properties of cool Ap stars are the abundance characteristics shown in Figures III-1, III-2, and III-7 which give [N/H], log N/H, and [N/Fe] as a function of atomic number and the range of these values (see also Table III-1). For example for Figure III-1, they can be summarized as 1) a systematic increase in overabundance with Z from Mg through the Fe peak, 2) a possible decline from Z=40 to Z=56, 3) a steep rise from Z=56 to Z=64, 4) a sudden increase between V

TABLE III-11: MEAN ELEMENTAL OVERABUNDANCES FOR THE COOL PECULIAR A STARS AND IONIZATION POTENTIALS

Element	Atomic Number	Ionization Potentials(eV) I	II	III	Mean [N/H]
Mg	12	7.64	15.03	80.12	-0.10±0.19
Si	14	8.15	16.34	33.46	+0.51±0.35
Ca	20	6.11	11.87	51.21	+0.62±0.43
Sc	21	6.54	12.80	24.75	+0.63±0.41
Ti	22	6.82	13.57	27.47	+0.78±0.37
V	23	6.74	14.65	29.31	+0.54±0.24 *
Cr	24	6.76	16.49	30.95	+2.02±0.51
Mn	25	7.43	15.64	33.69	+1.62±0.38
Fe	26	7.87	16.18	30.64	+1.06±0.33
Co	27	7.86	17.05	33.49	+1.58±0.56 *
Ni	28	7.63	18.15	35.16	+0.72±0.21 *
Sr	38	5.69	11.03	43	+1.89±0.80
Y	39	6.38	12.23	20.5	+0.24±0.27
Zr	40	6.84	13.13	22.98	+1.29±0.34 *
Ba	56	5.21	10.00	36	-0.17±0.82 *
La	57	5.61	11.06	19.17	+1.08±0.42 *
Ce	58	5.65	10.85	20	+1.90±0.29 *
Pr	59	5.42	10.55	21.62	+2.42±0.36 *
Nd	60	5.49	10.73		+2.47±0.71
Sm	62	5.63	11.07		+2.88±0.51 *
Eu	63	5.68	11.25	22	+3.85±0.72
Gd	64	6.16	12.1		+3.40±0.54
U	92	6	12:		+3.04±0.53 *

Note: * = not all stars included in the average.

and Cr and sudden decreases between Sr and Y, and Eu and Gd, and 5) the apparent universal nature of this overabundance curve for all cool Ap stars.

The abundances are not functions of the magnetic field strength or the apparent rotational velocity. Those of Fe, Cr, Mn, Nd, and Gd increase with effective temperature as probably do those of Mn, Y, and U. The Cr/Fe and the Nd/Fe ratios are also functions of the effective temperature. Certain abundance ratios such as log Cr/Ti and log Gd/Nd have preferred values. Some stars have effective temperatures derived in case 1 which are in good agreement with those initially derived from UBV photometry while others show a large discrepancy. A complete theory of Ap star abundance anomalies will explain these properties.

Fowler, Burbidge, and Burbidge (1955) suggested that the strong magnetic fields in Ap stars accelerate charge particles, particularly protons, and induce spallation reactions with the surface material. These reactions would enhance the abundances of certain elements and release neutrons whose capture would build heavy elements, for example, the rare earths. Spallation reactions cannot greatly enhance the abundances of already plentiful elements such as Fe and Si. Y has a normal abundance while the theory would by comparison with Sr expect to produce an excess. It cannot build the largest Sr abundances. Also the theory suggests that Ba through Sm be overabundant by 10^4 while Eu, Gd, and Dy should be overabundant by 10^3, contrary to what is observed.

Brancazio and Cameron (1967) modified this theory. Nuclear reactions due to protons with sufficient flux to induce spallation reactions lead to a progressive breakdown of the target material into H and He and, thus, they cannot create the overabundances. On the other hand, bombarding the surface material with a flux of pure alpha particles leads to a build-up of heavier elements. If equal fluxes of protons and alphas are involved, the destructive effect of the protons predominates. The maximum overabundance factors that these authors calculated are less than the observed mean overabundances for Si and Fe. Sr and Y should be overabundant together which is not observed. At maximum Fe abundance, the odd Z Fe peak elements should have similar abundances to the even Z Fe peak elements. This is not found. In addition, Fe and Si cannot be simultaneously at their maximum excesses since much of the excess Fe comes from the capture of α-particles from Si and neighboring elements.

We conclude that spallation processes did not produce the basic overabundances observed. However, the evidence for spallation reactions on the surface of HD201601 implies that in some cool Ap stars, they may have played a minor role in the production of the abundance anomalies. Perhaps they are partially responsible for the relatively mild abundance anomalies exhibited by this star.

As the surface nuclear reactions theory did not explain the observed abundances, Fowler, Burbidge, Burbidge, and Hoyle (1965) developed a theory in which nuclear reactions in the interiors build the heavy elements. Then by mixing or mass transfer from a companion, the processed material reaches the surface of the Ap star. However,

this material would tend to be He rich since nuclear reactions in the interior convert H into He. No He lines are observed in the spectra of the hottest program cool Ap stars. The predicted abundances are different from the observed, especially in regard to Cr/Mn (Clifford and Tayler 1965) for high temperature processing between 10^9 and 10^{10}°K where at suitable densities, the nuclear reactions may become so profuse that approximate statistical equilibrium occurs between the abundances of different nuclides (e-process). Truran and Cameron (1967) also disagree with Fowler et al. (1965) concerning the details of the nuclear physics.

If such a mechanism is to occur, then mass must be transferred to the surface, we will consider two basic cases 1) mass transfer from a companion and 2) mixing of the star. Guthrie (1967) and Van den Heuvel (1967) have discussed the first type of hypothesis. The latter believes that both Ap and Am stars were companions of supernovae. The differences in their chemical compositions excludes a common origin. Guthrie (1967) admits that peculiar A stars have a low percentage of spectroscopic binaries. But, he believes that the theory is possible for Ap stars while not for Am stars. For the Ap stars under consideration, the s-process products are probably exposed to an intense neutron flux in the core of the supernovae or in an envelope shock wave before being expelled in an explosion. The material from the Ba peak forms the rare earths (Guthrie 1969a). The expected abundances could not depend on the atmospheric parameters of the secondary and the amount of material captured depends on the

geometrical cross-section. This is an extremely inefficient process.

Tammann (1970) finds that the Galaxy has one supernovae every 26 years. They result from the explosions of stars of greater than 4 $M_{\odot}$. Guthrie (1967) believes that every supernovae produces one Ap star on the average although all Ap stars are not known to be binaries (Abt 1967). The excess abundances of the Ap stars are typical of the material expelled into the interstellar medium. However, their abundance anomalies are not at all like the solar abundances which are typical of the cosmic abundances. Cool Ap stars have Eu enrichments of at least 10^3. If their abundances are representative of all Ap stars, then the supernovae which produce the Ap stars consist of only 10^{-3} of all supernovae. Thus the number of required supernovae is larger than the observed number.

If there was mixing of the peculiar A stars, then eventually much of the processed material would be returned to the interstellar medium. Ten per cent of the upper main sequence stars are peculiar. Two per cent of the mass of the Galaxy is in stars with M_V=+0.5 or greater (Mihalas and Routly 1968). The mean lifetime of an A0 star is 5×10^8 years (Spitzer 1968) compared with 5×10^9 years since the sun formed. In that time there have been 10 generations of A stars. About 20 per cent of the galactic mass is in the interstellar medium (Middlehurst and Aller 1968). Let us assume that 70 per cent of the galactic mass has been part of the interstellar medium since the sun was formed. The material processed by the Ap stars is equal to 1/10 of that in the interstellar medium today. One-half of their mass is returned to the

interstellar medium since their masses are at least 2 $M_{\odot}$. Eu is enriched by at least 10^3 in the cool Ap stars. Suppose it is in all Ap stars. Then the youngest A stars should show Eu enrichments by about a factor of 14 over the solar values. However, the normal stars observed by Smith (1971) have essentially solar values of their Eu abundances.

Seeger, Fowler, and Clayton (1965) discuss the nuclear synthesis of heavy elements, those beyond the Fe peak, by neutron capture operating on Fe peak elements to produce the solar abundances. The Fe peak elements represent the end products of energy-generating processes via charged particle reactions. The heavy elements are synthesized usually by the chains of neutron capture on slow (s-process) and rapid (r-process) time scales. There is an additional way, the relatively inefficient p-process of proton addition or photoneutron emission. Its effects can be determined on the neutron-poor species which both the r- and s-processes bypass.

In the s-process, there is time for β decay to occur after each (n,γ) reaction and the resulting abundances are inversely proportional to the neutron capture cross-section while in the r-process (n,γ) and (γ,n) reactions compete and the final abundances of an isotope depend on the half-lives of its neutron rich precusors (Burbidge, Burbidge, Fowler, and Hoyle 1957). The neutron density is higher for the r-process than for the s-process. The Fe peak elements provide the seed nuclei for the s-process. If there is sufficient neutron exposure, then except near the ends of the neutron capture chains,

σN is constant where σ is the cross-section and N the resulting abundance. Guthrie (1969a) gives log $\Sigma 1/\sigma_i$, the expected relative abundances of the elements, as function of the atomic number Z for the s-process (Figure III-21). Compared with Figure III-2, there is a suggestion of fit with Sr, Y, and Zr, and none with the rare earths. Lines of Pb are not observed in the cool Ap stars. The s-process terminates at large atomic weights by alpha decay to Pb isotopes (Clayton and Rassbach 1967).

Seeger et al. (1965) deduced the isotopic solar system r-process contributions N_r by subtracting the s-process contributions from the observed isotopic abundances. Their calculations show that the main features of Figure III-22 can be explained by the r-process if the Fe peak elements are the main seed nuclei. The diagram is in disagreement with Figure III-2 as regards the rare earths, Sr, Y, and Zr. Since the solar and the Ap star abundances are quite different, the production of the Ap star abundance anomalies if they are produced by nuclear processes in stellar interiors is unlikely to occur similarly to the production of the solar abundances.

Now let us try to modify the results of the r- and s-processes which both produce Sr, Y, and Zr. The s-process follows a path in the N-Z plane near the line of beta-stability. It is very difficult to modify the abundances produced in this process. The r-process progenitors occur in the neutron rich area of this plane. The r-process products when they reach low neutron capture cross-section nuclei at magic neutron numbers (50, 82, 128, 184) decay by fast

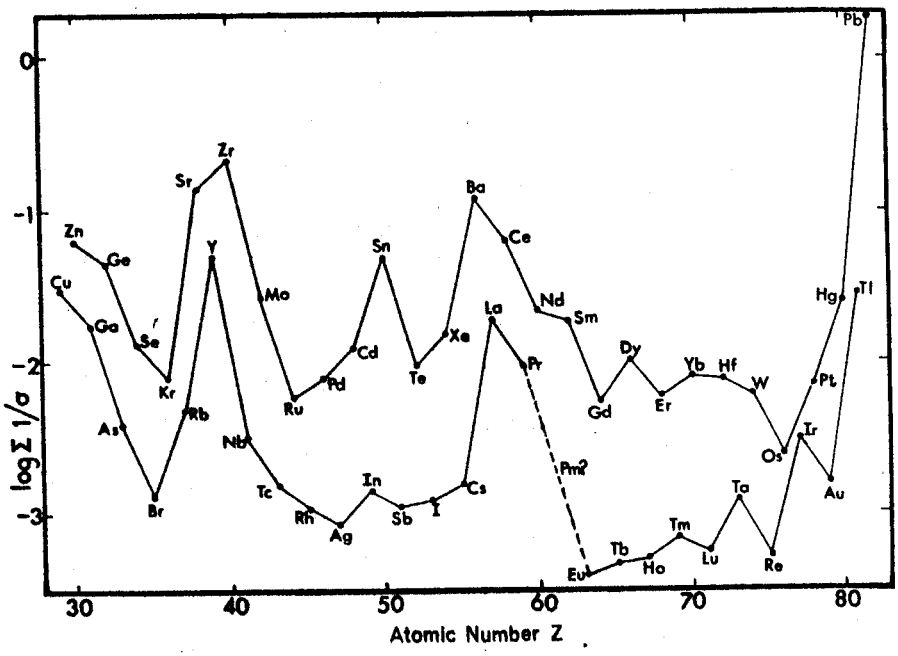

Fig. III-21. Summation of the reciprocal cross-sections for the s-process.

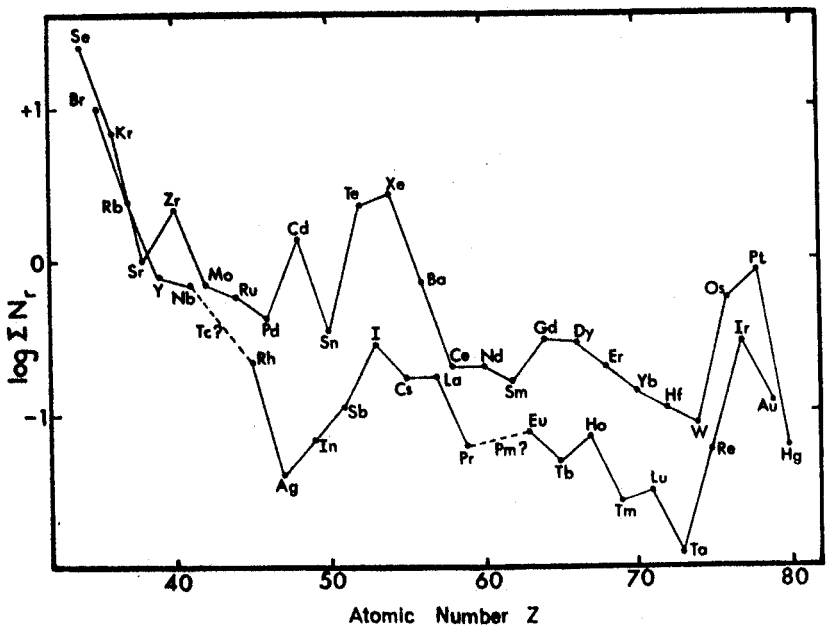

Fig. III-22. Logarithmic r-process abundances for the solar system.

Figures III-21 and III-22 are from Guthrie(1969a), page 548.

β-emission to less neutron-rich nuclei until capture again becomes more probable than β-decay (Allen, Gibbons, and Macklin 1971). The r-process peaks can be shifted by changing the neutron flux. Both processes can also work on the peaks built up by each other as well as on the Fe peak. If the r-process occurs after the s-, it will broaden the s-process peaks as well as displace their locations.

Confirmation of the identification of UII lines in cool Ap stars is very important for the theories of Ap star abundances. Their presence implies that the material has been produced by the r-process which means an exposure to a large neutron flux. This can occur only in massive objects, for example, supernovae.

Schramm and Fowler (1971) suggest that superheavy elements can be produced in explosive stellar events. There is thought to exist a relative region of nuclear stability for atomic masses near A=300, Z=114. After the termination of the r-process, the neutron-rich superheavy nuclei β-decay towards this island of stability. Eventually these nuclei assymetrically fission to atomic masses near A=126 (Sn, Te, I, Xe) and A=155 (Sm, Eu, Gd). The first region is one whose elements have lines which are difficult to detect while the latter is the rare earths. This mechanism may explain why Pd and Cd are seen in some cool Ap stars and the distribution of rare earth abundances whose maximum occurs at Eu for most cool Ap stars and at nearby elements for others. Changing the physical conditions during which these elements are produced may lead to shifts of the abundance maximum. This process might also reduce the r-process peaks near

A=130 and 195 by processing the material to higher A values. The abundances of the observed elements are likely to have been produced in several events with different physical conditions.

The r-process will also produce radioactive elements such as Th, U, Np, and Pu in addition to the rare earths. The production ratios for Th/U are near 2/3 (Seeger and Schramm 1970) if only ^{232}Th, ^{235}U, and ^{238}U are considered. If we allow for other U isotopes, this ratio more is like Th/U = 1/2. Let us determine whether ThII λ4019 should be detected. Its value of log gf is -0.80 compared with -0.24 for UII λ3860. The atomic structures of Th and U are not well known, but should be somewhat similar to each other and to the rare earths. The abundance and log gf differences shift log η by 0.86 and decrease log W at most by this amount if the line is on the linear part of the curve of growth. ThII λ4019 has a z value of 0.90 compared with 1.58 for UII λ3860. Thus the ThII line should not be detected in most cool Ap stars.

We have already noted difficulties in matching the Fe peak abundances. However, in part of the same stars which produce the superheavy elements by the r-process or in another star, additional Fe peak elements can be produced. So it may be possible to produce some of the elemental abundance anomalies in a supernovae. But there are the problems of those elemental abundances which are functions of the effective temperature and of the enrichment of the interstellar medium. Furthermore we cannot understand why Ap stars are slow rotators with strong magnetic fields.

Michaud (1970) considered the effects of radiative diffusion on the atmospheres of A-type stars. If the atmosphere has no currents faster than 10^{-3} cm/sec, then diffusion processes can be important. Gravitational settling leads to the underabundances of He, Ne, and O observed in the magnetic stars. In general, radiation pressure should lead to observations of overabundances of Mn, Sr, Y, Zr, and the rare earths at effective temperatures and gravities where they are seen in Ap stars. Si will be overabundant only if it has wide autoionization features. The abundance anomalies are expected to be functions of the effective temperature.

The radiation force transferred to a given element can be by photo-ionization (continuum absorption), line absorption, and auto-ionization. For the stars under consideration, there is little flux below the Lyman continuum. Photo-ionization will occur for those levels whose ionization potentials are less than 13.6 eV. Large radiation forces will push out elements whose ionization potentials are larger than 10.5 eV, but smaller than 13.6 eV in cool Ap stars, including C, P, Cl, Ca, Sc, As, Br, Sr, Y, Zr, Xe, Rn, and the rare earths. Ca, Sc, Sr, and the rare earths are overabundant in agreement with theory. C is not likely to be overabundant while Zr may be. Y is definitely not. The abundances of the other elements are unknown. If the relevant ionization potential is smaller than 10 eV or greater than 18 eV, the element will not absorb sufficient radiation to counter gravity. This is true for He, Li, Be, B, Ne, Na, Al, Ni, Cu, Ga, Se, Rb, In, Sb, Te, and Cs. Ni is overabundant in some cool Ap stars while

Ga and Se are likely to be in a few. The other elements have not been studied or have lines which are not observed. For the remaining elements the situation depends on the atomic structure. Line absorption can support the overabundances of elements heavier than the Fe peak. Light metals and Fe peak elements have to be supported by continuum absorption to have large overabundances. Si can have large overabundances if it has broad autoionization levels.

The diffusion hypothesis allows abundance anomalies to manifest themselves in 10^4 years. For an underabundance by a factor of 100 to be observed, the elements must settle down over 99% of the surface. The abundant, light, unionized elements, which have no properly placed continua and which do not have enough lines to be supported by them, should be most underabundant. Ionization will slow down this process. Mg should still be underabundant, but it is not in the cool Ap stars. This hypothesis predicts the Mn overabundances of the Mn stars, but not those of the cool Ap stars. Line absorption could also explain slight overabundances of other Fe peak elements; Ti and Fe are not affected by continuum radiation as much as Mn. Diffusion cannot produce large Cr absolute overabundances. Hence, this hypothesis cannot produce most of the observed overabundances of the Fe peak.

This theory also predicts Sr, Y, and Zr overabundances. Y is, however, normal in cool Ap stars. Also some dependence on effective temperature in Sr abundances might be expected, while none is observed. The atmospheres may not be sufficiently stable for this mechanism to operate. No predictions are made as to which rare earths should be

most overabundant; rather it seems that all rare earths should have the same abundances as seen in the Am stars. Michaud has not considered the effects of line blanketing in the rocket ultraviolet due to large elemental overabundances, especially those of the rare earths. Some Ap stars may be too bright in the far ultraviolet compared to normal A and B stars (see Schild and Chaffee 1971). For the above reasons, the theory in its present form is rejected and, at best, is incomplete.

Havnes and Conti (1971) suggest that the abundance anomalies result from a magnetic accretion process. The magnetic Ap stars selectively capture atoms from the ionized interstellar medium by their interaction with the rotating stellar magnetic field. The heavier elements have relatively small charge to mass ratios. Hence their ions penetrate close to the star where a further ionization may take place. Then the orbits are changed which results in their likely capture by the field. When this occurs the ions describe periodic orbits as they spiral along the magnetic field lines. The ions gradually diffuse from the field to the surface. The elemental abundances are initially concentrated at the magnetic poles. The relatively slow rotation of the magnetic stars results from the interaction of the magnetic field with the ionized interstellar gas.

This theory naturally results in spectrum variable production. One-quarter of the sharpest-lined cool Ap stars are known to be spectrum variables (Preston 1970c, 1971a). Havnes and Conti point out that elemental diffusion goes preferentially over the surface rather than deeper into the star because of the larger diffusion velocity at

smaller optical depths. The older magnetic stars would then have the most uniform distribution of elements on the surface and the longest rotational periods. It is also implied the greatest abundances. But from the results we have seen, it appears that some spectrum variables may have the largest elemental abundances.

The origin of the magnetic field is uncertain. A commonly accepted theory (Mestel 1967) suggests that it is fossil. Thus, the field originates with star formation. The massive clouds in spiral arms are those associated with this process (Field 1970). At birth, the magnetic stars may have already begun to have anomalous abundances.

The magnetic accretion model suggests that Mg will be near normal and Si may be somewhat overabundant which is as observed in the cool Ap stars. In addition the Fe group is expected to behave similarly to Si and together they should be enriched. Si, Ca, Sc, Ti, V, and Ni are enhanced by similar amounts, but Cr, Mn, and Fe are substantially more enhanced contrary to what is predicted. This hypothesis suggests that Sr and Y will be preferentially overabundant with respect to Zr, perhaps Sr with respect to Y, and this group as a whole greater enhanced than the Fe group. However, for the cool Ap stars, there are stars with greater Zr than Y overabundances. Sr is more overabundant than Y which is normal. The Sr overabundance is less than that of Cr but greater than that of the other Fe peak elements.

Magnetic accretion predicts great overabundances of the rare earths which are observed. However, no predictions are made as to which ones. Heavier elements should also be overabundant. Only for

a few stars are lines of Os and Pt seen. The Os overabundances are similar to those for Eu in HD5797 and HD118022. Thus, the detection of lines of these heavy elements is difficult even at the expected overabundances. In conclusion, this hypothesis explains some features of the abundance anomalies, but others it cannot. The diffusion of elemental abundances on the stellar surface has to be examined in far greater detail. But this theory does explain why Ap stars are slow rotators.

Thus, we are left without a theory of peculiar A stars. Nuclear reactions on the surface cannot produce the observed anomalies. Theories which produce the abundances in stellar interiors and deposit them on the surface by mixing or by supernovae companions are excluded by considerations of galactic enrichment. If the material is transferred from a companion, then we should observe some evidence of nuclear processing characteristic of the stellar interior. Nothing of the sort is observed. The magnetic Ap stars also have relatively few companions.

Processes based on atomic and atmospheric properties, such as the diffusion and magnetic accretion hypothesis, might lead to elemental abundance dependences on the effective temperature. However, both theories in their present form have difficulties. On the other hand, the similarity of the dependence of the Fe abundance on effective temperature for both the cool Ap and the Am stars implies a theory based on atmospheric and atomic properties if the cause of the Am abundance abnormalities is a subsurface elemental separation zone.

If the abundances of the interstellar medium have been modified but not enhanced by factors which would be detectable in the recently formed normal stars, then the observed abundances of the rare earths in the cool Ap stars which are not identical to the solar distribution can be more easily understood with the magnetic accretion process. Detailed consideration of the diffusive processes expected with this theory are necessary. However, how to reconcile this heuristic theory with the results of this study is beyond the scope of this discussion.

J. Summary of the Conclusions

The effective temperatures of the cool Ap stars obtained initially from UBV photoelectric data were modified by requiring that the derived Fe abundances from both FeI and FeII lines be equal. For some stars a discrepancy exists between the two estimates of effective temperatures. This may be partially due to line blanketing effects. The best previous determinations of effective temperatures support the adopted temperatures while those of other studies do not provide any evidence against them.

The abundances of the cool Ap stars are, in general, for every element studied similar to solar values or greater than them. Of the elements with the best determinations, Cr, Mn, Fe, Sr, Nd, Eu, and Gd are on the average overabundant by factors greater than 10. Si, Ca,

Sc, and Ti are overabundant by 3 to 6 times while Mg and Y have solar abundances on the average. The other Fe peak elements may also be significantly overabundant as well as Zr and the remaining rare earths. The situation for Ba is indeterminant. Lines appear which are consistent with an identification as UII. The derived mean overabundance is a factor of 1000.

All cool Ap stars show the characteristic abundance anomalies, although some to a greater degree than others. There are stars which tend to be at the top of all distributions of abundances while others are at the bottom. Those in the middle of the distributions are better mixed when the abundances of the different elements are considered.

When the abundances of this survey are compared with those of previous studies of normal and cool Ap stars reasonable agreement is found. The results of Sargent, Searle, and Lungershausen fit in well with this study although some of their conclusions are modified since a larger sample of cool Ap stars were considered, the most important of which is that cool Ap stars have abnormal Cr/Fe ratios. A few cool Ap stars are found which except for their values of [Cr/Fe] appear to be the cool extension of the classical Si stars. Arguments based on the presence of magnetic fields, spectrum variability, similar abundances, and paucity of binary companions in the literature suggest two subdivisions of the Ap stars 1) Mn stars and 2) Si and cool Ap stars. The discovery of the aforementioned stars strengthens this hypothesis.

The cool Ap stars studied are found to have abundances which are representative of their class. Their abundances cover part of the

range of variation known for the Si stars. Part of these differences may be due to analysis pecularities. The abundance differences found with the Mn stars are similar to those of other investigators. The abundances of spectrum variables tend to be in the upper part of the range of the cool Ap star abundances. α^2CVn and HD221568 both show Pr and Sm abundances far greater than any non-variable cool Ap star. It is speculated that perhaps such abundance differences distinguish the spectrum from the non-spectrum variables.

The abundances are found not to be a function of the magnetic field strength or the apparent rotational velocity. The Cr, Mn, Fe, Nd, and Gd absolute abundances increase with effective temperature as well as those of Cr and Nd with respect to Fe. The absolute Mn, Y, and U abundances show weaker but similar correlations. Other weaker correlations exist as well as diagrams with peculiar gaps in the abundance distributions or their ratios.

Significant abundance differences differentiate the cool Ap stars and the Am stars. There is a complete separation of abundance values for [Cr/Fe], [Nd/Fe], [Gd/Fe], [Y/Fe], [Cr/H], and [Gd/H]. Hence the mechanisms producing the abundance anomalies are different.

The results of low dispersion classification spectroscopy agree better with the appearance than the abundances. Strömgren photometric indices correlate poorly with the abundances. Thus, both methods pick out the Ap stars and their general type.

Certain ratios of elements close in atomic number such as Cr/V and Sr/Y prove for all known theories difficult to explain. Surface

nuclear reaction theories cannot build the proper overabundances of the Fe peak and have difficulties with conservation of nuclear material. Spallation reactions may play a minor role, however, in the production of the resultant abundance anomalies. Theories, which produce the anomalies by processing material in stellar interiors and then by transfer of mass from a companion or by mixing, are inconsistent with the observed enrichment of the interstellar medium since the sun was formed. The rare earths and U can be made if the r-process produces superheavy elements. In general, s-process abundances do not resemble those of the cool Ap stars.

Both the diffusion hypothesis and selective magnetic accretion in principle can explain why certain elemental abundances depend on the effective temperature while this is extremely difficult to do with nuclear theories. The diffusion hypothesis does not explain all the observed abundance anomalies. Magnetic accretion has similar difficulties. In addition, it cannot easily explain why the abundances are not correlated with magnetic field strength. Further theoretical studies are needed to explain these results and to extend the predictions of the various theories. My personal preference is for a theory of Ap star abundance anomalies based on atmospheric and atomic parameters, which takes into account the probable enrichment of the interstellar medium.

Appendix-Basic Data

This appendix contains most of the data upon which the results depend. Table A-1 contains for every line used in the abundance determination process the oscillator strength, log gf value; the excitation potential, χ; and the centroid of the σ components of the Zeeman pattern, z. Tables A-2 through A-24 are the effective temperature and Fe abundance determinations for the program stars. Then tables A-25 through A-54 give the abundance determinations for the other elements. Tables A-55 through A-57 show the equivalent widths and line qualities of CaII, MoII, and GdIII lines which were not converted into abundances. The last table, number A-58, contains the measured wavelengths of lines tentatively identified as those of UII.

Table A-1

Atomic Constants for Lines Used in Abundance Determinations

ion	mult.	λ(Å)	log gf	source	χ(eV)	z
MgI	15	4167.265	-0.82	SC	4.33	1.00
MgII	4	4481.129 } 4481.327	0.98	WS	{ 8.83 8.83	0.90 { 1.03 1.07
SiII	1	3853.657	-1.61	WS	6.83	1.07
		3862.592	-0.90	WS	6.83	0.84
CaI	2	4226.728	0.24	WS	0.00	1.00
	4	4425.441	-0.38	WS	1.87	0.50
		4434.960	-0.03	WS	1.88	1.00
		4435.688	-0.50	WS	1.88	1.00
		4454.781	-0.25	WS	1.89	1.17
	5	4283.010	-0.22	WS	1.88	1.50
CaII	1	3933.664	0.14	WS	0.00	1.33
ScII	7	4246.829	0.19	WA	0.31	1.00
	14	4400.355	-0.72	WA	0.60	1.08
		4415.559	-0.84	WA	0.59	0.67
	15	4314.084	-0.10	WA	0.62	1.12
TiI	42	4512.734	-0.25	CB	0.83	1.50
		4518.022	-0.14	CB	0.82	1.55
		4533.238	0.64	CB	0.84	1.40
		4534.782	0.41	CB	0.83	1.35
		4548.764	-0.18	CB	0.82	1.50
	44	4281.371	-1.05	CB	0.81	1.33
		4286.006	-0.12	CB	0.82	1.37
		4287.405	-0.14	CB	0.83	1.42
		4298.664	0.22	CB	0.81	0.83
TiII	31	4468.493	-0.65	WA	1.13	1.06
	40	4417.718	-1.18	WA	1.16	0.80
		4464.458	-1.66	WA	1.16	0.73
		4470.864	-1.80	WA	1.16	1.22
	41	4301.928	-1.11	WA	1.16	0.78

Table A-1, continued

ion	mult.	λ(Å)	log gf	source	χ(eV)	z	
TiII	51	4394.057	-1.47	WA	1.22	1.34	
		4418.340	-1.67	WA	1.23	1.27	
	60	4544.009	-2.08	WA	1.24	1.14	*
		4568.312	-1.93	WA	1.22	0.93	
	61	4395.848	-1.53	WA	1.24	1.22	
		4398.314	-2.09	WA	1.22	0.78	
		4409.220	-2.07	WA	1.24	1.48	
		4409.519	-2.07	WA	1.23	1.47	
		4411.936	-2.11	WA	1.22	1.33	
VI	22	4379.238	0.48	CB	0.30	1.23	
		4389.974	0.05	CB	0.27	1.07	
VII	25	4178.390	-1.66	WA	1.68	1.17	
		4202.350	-1.23	WA	1.70	1.25	
	37	4183.435	-0.77	WA	2.04	1.10	
		4205.080	-0.85	WA	2.03	1.00	
CrI	1	4274.803	-0.36	LL	0.00	1.96	
	10	4496.862	-1.19	AP	0.94	1.33	
		4545.956	-1.37	AP	0.94	1.92	
	21	4616.137	-1.21	AP	0.98	1.67	
	22	4359.631	-1.24	AP	0.98	1.25	
		4371.279	-1.25	AP	1.00	1.37	
		4384.977	-1.42	AP	1.03	1.42	
	276	4553.949	0.45	A	4.08	0.67	
CrII	18	4217.070	-2.38	WA	3.09	0.78	
	31	4246.410	-3.05	WA	3.84	2.10	
		4252.620	-1.85	WA	3.84	0.98	*
		4269.280	-2.06	WA	3.84	0.90	
		4275.570	-1.33	WA	3.84	0.90	
		4284.210	-1.64	WA	3.84	0.50	
	162	4224.850	-1.27	WA	5.31	0.80	

Table A-1, continued

ion	mult.	λ(Å)	log gf	source	χ(eV)	z	
MnI	22	4436.352	0.17	CB	2.91	1.50	
		4453.005	0.06	CB	2.93	1.50	
		4470.138	0.15	CB	2.93	1.20	
		4502.220	0.18	CB	2.91	1.50	
	23	4235.140	0.47	CB	2.91	1.10	
		4235.290	0.58	CB	2.88	1.22	
		4257.659	0.39	CB	2.94	1.33	
		4265.924	0.37	CB	2.93	1.47	
MnII	6	4283.772	-1.72	WA	5.37	1.00	
	7	4206.375	-1.13	WA	5.40	1.20	
	-	4239.210	-1.83	WA	5.37	1.50	
		4244.270	-1.63	WA	5.37	1.01	
		4281.940	-1.92	WA	5.37	2.17	
FeI	41	4404.750	-0.13	GW	1.55	1.25	
		4415.125	-0.54	AT	1.60	1.17	
	42	4202.031	-0.57	AF	1.48	1.15	
	68	4494.568	-1.05	AT	2.19	1.17	
		4528.619	-0.74	AF	2.17	1.25	
	152	4210.358	-0.88	AF	2.47	3.00	
		4299.242	-0.36	AF	2.41	1.50	
	350	4454.383	-1.15	AF	2.82	1.33	
	800	4219.364	0.08	AB	3.56	1.08	
	828	4484.227	-0.66	AF	3.59	1.25	
FeII	27	4303.167	-2.69	GB	2.69	1.11	*
		4385.381	-2.67	GB	2.77	1.33	
		4416.817	-2.75	GB	2.77	0.78	
	37	4491.401	-2.94	GB	2.84	0.40	
		4520.225	-2.76	BG	2.79	1.50	
		4582.835	-3.23	BG	2.83	1.50	
		4629.336	-2.44	BG	2.79	1.33	
	38	4508.283	-2.46	BG	2.84	0.50	
		4576.331	-3.10	BG	2.83	0.98	*
		4620.513	-3.47	BG	2.82	0.95	*

Table A-1, continued

ion	mult.	λ(Å)	log gf	source	χ(eV)	z
FeII	186	4635.328	-1.67	GB	5.93	1.07
CoI	18	3873.120	-0.31	CB	0.43	1.17
	31	3995.306	0.16	CB	0.92	1.22
NiI	86	4462.460	-0.41	GR	3.45	0.75
		4470.483	-0.13	GR	3.38	1.00
NiII	9	4244.800	-2.03	WA	4.01	0.72
GaII	-	4251.160	0.46	JS	14.10	0.75
SrI	2	4607.331	-0.57	CB	0.00	1.00
SrII	1	4215.524	-0.11	PE	0.00	1.33
	3	4161.798	-0.28	CB	2.93	1.33
YII	5	4398.020	-1.25	CB	0.13	1.00
	6	3950.350	-0.71	CB	0.10	1.25
		3982.590	-0.79	CB	0.13	1.08
ZrII	40	4317.320	-1.48	CB	0.71	1.14
	99	4179.810	-0.48	CB	1.66	0.90
BaII	1	4554.033	-0.55	CB	0.00	1.17
	4	4166.003	-0.24	CB	2.71	1.07
LaII	25	4322.510	-1.62	CB	0.17	1.00
	40	3988.510	-0.26	CB	0.40	1.33
	76	4619.870	-0.24	CB	1.75	0.67
	83	4230.950	-0.17	CB	1.95	1.00
CeII	1	4186.599	0.67	CB	0.67	1.10
		4306.724	-0.38	CB	0.51	0.95
		4562.360	-0.07	CB	0.47	0.84
		4628.160	-0.14	CB	0.47	0.85

Table A-1, continued

ion	mult.	λ(Å)	log gf	source	χ(eV)	z
CeII	2	4382.167	-0.17	CB	0.68	1.13
		4460.213	0.02	CB	0.47	0.67
		4560.959	-0.70	CB	0.68	1.50
	3	4450.732	-0.36	CB	0.68	1.64
		4483.900	-0.14	CB	0.86	1.61
	8	4227.746	-0.17	CB	0.69	1.50
	20	4463.410	-0.26	CB	0.95	0.90
	21	4270.716	-0.22	CB	0.95	0.72
	57	4486.909	-0.62	CB	0.29	0.85
	203	4214.041	-0.58	CB	0.60	1.09
	204	4270.189	-0.42	CB	0.55	0.98
PrII	4	4222.980	-0.36	CB	0.05	0.92
		4408.844	-0.84	CB	0.00	0.80
		4496.429	-1.01	CB	0.05	0.86
	8	4189.518	-0.22	CB	0.37	1.18
NdII	10	4303.573	-0.47	CB	0.00	0.74
		4358.169	-0.98	CB	0.32	1.09
SmII	22	4615.690	-1.57	CB	0.19	0.82
	32	4566.206	-1.41	CB	0.33	1.33
	36	4434.323	-0.75	CB	0.38	1.57
	37	4262.677	-0.84	CB	0.38	1.55
		4421.138	-1.01	CB	0.38	1.22
	41	4523.912	-1.72	CB	0.43	1.78
	45	4362.040	-0.96	CB	0.48	2.19
	49	4615.441	-1.42	CB	0.54	1.23
	50	4220.659	-0.89	CB	0.54	1.49
	53	4467.342	-0.39	CB	0.66	1.12

Table A-1, continued

ion	mult.	λ(Å)	log gf	source	χ(eV)	z
EuII	1	4205.050	-0.08	CB	0.00	1.62
	4	4435.580	-0.60	CB	0.21	1.88
	5	3907.100	0.03	CB	0.21	1.67
GdII	18	4167.159	-1.11	CB	0.42	unknown
	31	4498.276	-1.43	CB	0.43	2.11
	32	4215.023	-0.58	CB	0.43	1.34
	43	4316.052	-0.66	CB	0.66	1.75
	44	4506.333	-1.45	CB	0.50	1.50
	46	4204.857	-0.70	CB	0.52	1.58
		4253.366	-0.52	CB	0.55	1.92
	62	4483.328	-0.70	CB	1.06	1.32
	82	4582.380	-0.89	CB	1.25	1.28
	103	4406.670	-0.24	CB	1.42	1.82
HfII	72	4232.430	-0.09	CB	2.33	0.40
OsI	1	4420.468	-1.05	CB	0.00	1.58
UII	-	3859.580	-0.24	CB	0.03	1.58
		4241.670	-0.56	CB	0.63	0.52

Sources: A = personal guess
AB = average AF and BW
AF = Wolnik et al.(1970)
AP = Wolnik et al.(1968)
AT = average AF, GK, and BW
BG = Baschek et al.(1970)
BW = Bridges and Wiese(1970)
CB = Corliss and Bozman(1962)
GB = Groth(1961) after adding correction factor from BG
GK = Garz and Kock(1969)
GR = Garz et al.(1970)
GW = average GK and BW
JS = Jugaku et al.(1961)
LL = Lawrence et al.(1965)

Table A-1, continued

Sources(continued): PE = Penkin(1964)
SC = Schaeffer(1971)
WA = Warner(1967)
WS = Wiese et al.(1969)

Note: * = from Preston(1970a)

Note on Tables A-2 Through A-24

Tables A-2 through A-24 present the Fe abundances and effective temperatures. The upper part of each table gives the results derived from FeI lines while the lower part those from FeII lines. The columns contain the multiplet number from Moore(1945); the wavelength, λ, in $\mathring{A}$; the equivalent width, W, in $m\mathring{A}$; the reduced equivalent width, W_o, in $m\mathring{A}$, that which would result if the microturbulent velocity were zero; the line quality, qual.; and the abundances (log Fe/H) for cases 1, 2, and 3. For each ion, I give the logarithmic and arithmetic mean abundances. At the bottom of the table, the effective temperature is given for each case.

Table A-2

Effective Temperatures and Fe Abundance Determinations for HD2453

mult.	λ	W	W_o	qual.	abundance 1	2	3
FeI lines							
41	4404	145.6	89.9	A	-3.23	-3.50	-3.51
	4415	107.1	64.1	C	-3.44	-3.78	-3.71
42	4202	113.3	71.7	B	-3.06	-3.41	-3.37
68	4494	112.4	67.8	B	-2.55	-2.85	-2.75
	4538	119.3	68.2	B	-2.86	-3.16	-3.06
152	4210	100.8	44.8	A	-3.23	-3.46	-3.41
	4299	119.7	63.7	B	-3.20	-3.46	-3.43
350	4454	61.7	39.4	A	-2.96	-3.19	-3.13
800	4219	92.5	59.3	A	-3.16	-3.40	-3.31
828	4484	87.9	51.4	A	-2.75	-2.97	-2.87
			logarithmic mean:		-3.04	-3.32	-3.26
			arithmetic mean:		-2.97	-3.24	-3.16
FeII lines							
27	4303	197.1	151.6	B	-2.56	-2.81	-2.80
	4385	144.5	84.0	B	-3.39	-3.66	-3.70
	4416	170.8	147.2	A	-2.55	-2.81	-2.80
37	4491	125.8	116.5	C	-2.73	-3.02	-2.93
	4520	163.7	88.2	C	-3.32	-3.61	-3.55
	4582	117.1	60.4	B	-3.61	-3.89	-3.80
	4629	147.9	83.6	A	-3.76	-4.07	-4.00
38	4508	147.2	135.0	A	-3.02	-3.31	-3.26
	4576	155.0	112.3	A	-2.58	-2.92	-2.85
	4620	129.7	90.1	A	-2.59	-2.89	-2.85
186	4635	111.0	69.4	B	-3.17	-3.40	-3.31
			logarithmic mean:		-3.03	-3.31	-3.26
			arithmetic mean:		-2.85	-3.14	-3.09
			temperature:		10350°	9950°	9850°

Table A-3

Effective Temperatures and Fe Abundance Determinations for HD5797

mult.	λ	W	W_o	qual.	abundance 1	2	3
FeI lines							
41	4404	160.8	147.5	B	-3.14	-3.45	-3.41
	4415	119.8	106.0	C	-3.11	-3.45	-3.40
42	4202	162.3	151.7	C	-2.69	-2.91	-2.90
68	4494	132.0	116.8	B	-2.19	-2.53	-2.44
	4528	140.8	124.6	C	-2.40	-2.77	-2.66
152	4210	165.4	99.6	A	-2.43	-2.71	-2.62
	4299	141.0	119.5	E	-2.63	-3.02	-2.92
350	4454	69.4	54.3	B	-2.99	-3.32	-3.24
800	4219	140.9	129.3	B	-2.36	-2.64	-2.55
828	4484	80.9	64.2	B	-2.78	-3.11	-3.04
			logarithmic mean:		-2.67	-2.99	-2.92
			arithmetic mean:		-2.57	-2.88	-2.79
FeII lines							
27	4303	174.3	164.4	E	-2.61	-2.87	-2.90
	4385	175.9	161.4	A	-2.64	-2.93	-2.97
	4416	180.6	173.7	B	-2.49	-2.79	-2.81
37	4491	139.9	137.2	C	-2.74	-3.05	-2.94
	4520	152.9	130.7	B	-2.96	-3.20	-3.17
	4582	123.2	101.0	A	-2.86	-3.18	-3.09
	4629	191.3	177.1	A	-2.94	-3.28	-3.18
38	4508	165.2	162.0	B	-2.99	-3.25	-3.26
	4576	158.4	135.4	B	-2.56	-2.91	-2.82
	4620	132.5	121.6	A	-2.34	-2.69	-2.63
186	4635	139.4	126.7	A	-2.23	-2.51	-2.43
			logarithmic mean:		-2.67	-2.99	-2.93
			arithmetic mean:		-2.60	-2.92	-2.86
			temperature:		9600°	9200°	9150°

Table A-4

Effective Temperatures and Fe Abundance Determinations for HD8441

mult.	λ	W	W_o	qual.	abundance 1	2	3
FeI lines							
41	4404	80.1	80.1	B	-3.53	-3.85	-3.85
	4415	63.9	63.9	B	-3.58	-3.87	-3.87
42	4202	74.4	74.4	B	-3.14	-3.45	-3.47
68	4494	38.6	38.6	B	-3.46	-3.77	-3.74
	4528	47.1	47.1	B	-3.57	-3.83	-3.81
152	4210	50.2	50.2	B	-3.17	-3.41	-3.39
	4299	43.7	43.7	B	-3.88	-4.14	-4.12
350	4454	18.8	18.8	D	-3.67	-3.95	-3.87
800	4219	75.6	75.6	B	-2.79	-3.04	-3.00
828	4484	24.1	24.1	C	-3.59	-3.83	-3.80
			logarithmic mean:		-3.43	-3.70	-3.68
			arithmetic mean:		-3.32	-3.58	-3.55
FeII lines							
27	4303	88.4	88.4	B	-3.27	-3.53	-3.62
	4385	61.3	61.3	A	-3.98	-4.24	-4.29
	4416	87.8	87.8	A	-3.27	-3.53	-3.61
37	4491	86.1	86.1	C	-3.20	-3.50	-3.45
	4520	85.3	85.3	B	-3.40	-3.71	-3.67
	4582	70.4	70.4	B	-3.31	-3.63	-3.55
	4629	73.0	73.0	B	-4.05	-4.36	-4.32
38	4508	100.1	100.1	B	-3.45	-3.75	-3.71
	4576	83.6	83.6	A	-3.13	-3.43	-3.39
	4620	50.5	50.5	A	-3.69	-4.01	-3.94
186	4635	79.5	79.5	A	-2.90	-3.16	-3.08
			logarithmic mean:		-3.42	-3.71	-3.69
			arithmetic mean:		-3.31	-3.54	-3.57
			temperature:		10200°	9800°	9650°

Note: λ4454 is given one-half weight in the mean abundance averages.

Table A-5

Effective Temperatures and Fe Abundance Determinations for HD12288

mult.	λ	W	W_o	qual.	abundance 1	2	3
FeI lines							
41	4404	170.4	67.4	A	-3.62	-3.91	-3.89
	4415	137.5	58.5	C	-3.49	-3.78	-3.74
42	4202	166.5	72.1	B	-2.95	-3.23	-3.25
68	4528	128.7	53.6	C	-3.12	-3.41	-3.37
152	4210	93.5	42.1	C	-3.17	-3.43	-3.37
	4299	94.6	43.8	C	-3.63	-3.88	-3.87
800	4219	95.2	47.6	C	-3.34	-3.62	-3.56
			logarithmic mean:		-3.33	-3.61	-3.58
			arithmetic mean:		-3.26	-3.54	-3.52
FeII lines							
27	4303	242.5	127.6	E	-2.72	-2.99	-3.00
	4385	193.4	74.4	B	-3.57	-3.84	-3.88
37	4491	126.0	100.8	C	-2.89	-3.18	-3.10
	4520	199.1	68.2	B	-3.78	-4.10	-3.99
	4582	153.5	55.8	C	-3.69	-3.99	-3.88
	4629	164.4	61.6	C	-4.29	-4.60	-4.53
38	4508	166.0	128.7	B	-3.04	-3.33	-3.28
	4576	184.2	87.3	C	-2.97	-3.24	-3.21
	4620	138.3	64.3	B	-3.15	-3.47	-3.44
186	4635	159.7	68.0	B	-3.13	-3.40	-3.33
			logarithmic mean:		-3.33	-3.61	-3.56
			arithmetic mean:		-3.14	-3.42	-3.38
			temperature:		10600°	10150°	10000°

Table A-6

Effective Temperatures and Fe Abundance Determinations for HD18078

mult.	λ	W	W_o	qual.	abundance 1	2	3
FeI lines							
41	4404	175.7	116.4	B	-3.06	-3.35	-3.37
	4415	131.3	81.6	C	-3.19	-3.48	-3.50
42	4202	137.1	90.8	B	-2.90	-3.18	-3.21
68	4494	111.1	66.5	B	-2.78	-3.05	-3.03
	4528	137.4	80.4	B	-2.76	-3.05	-3.00
152	4210	123.5	49.6	A	-3.25	-3.50	-3.48
	4299	111.4	59.6	A	-3.53	-3.78	-3.76
350	4454	63.8	40.1	C	-3.10	-3.45	-3.33
800	4219	115.8	76.2	B	-2.68	-3.10	-3.08
828	4484	63.4	40.4	B	-3.21	-3.45	-3.40
			logarithmic mean:		-3.05	-3.34	-3.32
			arithmetic mean:		-2.97	-3.29	-3.25
FeII lines							
27	4303	169.4	121.9	C	-2.84	-3.10	-3.15
	4385	155.2	92.9	A	-3.24	-3.52	-3.60
	4416	159.8	134.3	A	-2.70	-2.96	-3.01
37	4491	109.6	100.6	C	-2.98	-3.28	-3.23
	4520	159.4	84.8	B	-3.44	-3.76	-3.73
	4582	130.8	67.1	A	-3.44	-3.75	-3.70
	4629	180.8	111.6	A	-3.36	-3.66	-3.63
38	4508	144.6	132.7	B	-3.09	-3.29	-3.35
	4576	151.8	108.4	A	-2.73	-3.03	-2.99
	4620	132.6	92.7	A	-2.64	-2.93	-2.88
186	4635	120.9	76.0	A	-2.99	-3.25	-3.24
			logarithmic mean:		-3.04	-3.33	-3.32
			arithmetic mean:		-2.95	-3.23	-3.23
			temperature:		10050°	9700°	9550°

Table A-7

Effective Temperatures and Fe Abundance Determinations for HD22374

mult.	λ	W	W_o	qual.	abundance 1	2	3
FeI lines							
41	4404	95.8	93.9	A	-3.85	-4.14	-4.10
	4415	76.2	74.0	B	-3.83	-4.11	-4.12
42	4202	50.6	49.1	A	-4.48	-4.73	-4.71
68	4494	56.6	55.0	C	-3.56	-3.89	-3.80
	4528	48.0	46.6	B	-4.15	-4.47	-4.36
152	4210	78.3	71.2	A	-3.05	-3.35	-3.29
	4299	73.8	71.0	B	-3.57	-3.91	-3.86
350	4454	36.2	35.6	B	-3.67	-3.94	-3.84
800	4219	75.9	73.7	B	-3.32	-3.56	-3.50
828	4484	48.5	46.6	B	-3.40	-3.70	-3.64
			logarithmic mean:		-3.69	-3.98	-3.92
			arithmetic mean:		-3.56	-3.82	-3.75
FeII lines							
27	4303	96.1	94.2	B	-3.33	-3.55	-3.65
	4385	81.0	78.6	A	-3.65	-3.90	-3.98
	4416	82.3	80.7	A	-3.53	-3.79	-3.87
37	4491	74.7	74.0	E	-3.75	-4.00	-3.92
	4520	88.8	87.1	B	-3.63	-3.93	-3.83
	4582	55.6	54.5	A	-4.04	-4.33	-4.22
	4629	92.8	91.0	B	-3.86	-4.19	-4.10
38	4508	86.6	85.7	A	-3.95	-4.25	-4.17
	4576	74.4	72.2	A	-3.61	-3.92	-3.86
	4620	53.1	51.6	B	-3.85	-4.17	-4.11
186	4635	64.3	62.4	C	-3.43	-3.66	-3.60
			logarithmic mean:		-3.69	-3.97	-3.94
			arithmetic mean:		-3.61	-3.92	-3.89
			temperature:		9450°	9100°	9050°

Table A-8

Effective Temperatures and Fe Abundance Determinations for HD50169

mult.	λ	W	W_o	qual.	abundance 1	2	3
FeI lines							
41	4404	190.2	92.8	A	-3.34	-3.58	-3.65
	4415	139.4	67.0	C	-3.53	-3.80	-3.82
42	4202	183.5	99.7	B	-2.71	-2.98	-3.02
68	4494	130.7	62.5	C	-2.84	-3.10	-3.08
	4528	154.2	70.1	B	-2.99	-3.23	-3.21
152	4210	109.7	44.6	C	-3.34	-3.56	-3.58
	4299	132.0	56.7	B	-3.56	-3.78	-3.80
800	4219	124.5	70.7	C	-2.93	-3.16	-3.15
828	4484	67.8	39.0	C	-3.17	-3.40	-3.40
			logarithmic mean:		-3.16	-3.40	-3.41
			arithmetic mean:		-3.05	-3.32	-3.32
FeII lines							
27	4303	241.7	176.4	C	-2.44	-2.68	-2.72
	4385	164.6	73.8	C	-3.67	-3.91	-3.98
	4416	189.8	139.6	B	-2.65	-2.90	-2.96
37	4491	114.3	97.7	C	-2.98	-3.28	-3.26
	4520	166.0	66.6	B	-3.89	-4.19	-4.13
	4582	170.8	68.0	B	-3.41	-3.69	-3.64
	4629	191.5	83.6	B	-3.80	-4.11	-4.06
38	4508	161.6	139.3	A	-3.03	-3.30	-3.28
	4576	176.1	100.1	B	-2.83	-3.11	-3.11
	4620	153.0	84.1	B	-2.78	-3.03	-3.03
186	4635	144.7	71.6	C	-3.12	-3.36	-3.28
			logarithmic mean:		-3.14	-3.41	-3.40
			arithmetic mean:		-2.94	-3.19	-3.21
			temperature:		10150°	9800°	9600°

Table A-9

Effective Temperatures and Fe Abundance Determinations for HD81009

mult.	λ	W	W_o	qual.	abundance 1	2	3
FeI lines							
41	4404	147.0	53.8	A	-4.96	-5.26	-5.23
	4415	132.5	54.3	C	-4.49	-4.82	-4.81
42	4202	158.3	63.8	C	-4.11	-4.44	-4.44
68	4494	142.1	56.2	C	-3.71	-4.03	-3.90
	4528	187.7	67.5	B	-3.68	-4.01	-3.90
152	4210	117.1	45.4	C	-3.92	-4.25	-4.18
	4299	198.9	65.2	C	-3.91	-4.21	-4.14
800	4219	108.6	49.6	C	-4.13	-4.42	-4.33
			logarithmic mean:		-4.11	-4.43	-4.37
			arithmetic mean:		-3.98	-4.31	-4.31
FeII lines							
27	4303	180.9	72.9	C	-3.75	-4.02	-4.08
	4385	186.3	65.8	E	-4.00	-4.26	-4.33
	4416	148.2	74.5	A	-3.71	-3.97	-4.04
37	4491	91.6	65.4	C	-3.97	-4.29	-4.20
	4520	146.6	52.9	C	-4.56	-4.89	-4.78
	4582	126.3	48.6	E	-4.24	-4.57	-4.44
	4629	130.4	50.7	C	-4.98	-5.31	-5.20
38	4508	119.1	77.3	C	-4.18	-4.50	-4.40
	4576	150.9	63.4	C	-3.93	-4.22	-4.16
	4620	117.2	53.0	C	-3.87	-4.19	-4.10
186	4635	77.4	40.5	E	-4.10	-4.35	-4.26
			logarithmic mean:		-4.12	-4.42	-4.36
			arithmetic mean:		-4.04	-4.30	-4.27
			temperature:		9300°	8900°	8900°

Table A-10

Effective Temperatures and Fe Abundance Determinations for HD89069

mult.	λ	W	W_o	qual.	abundance 1	2	3
FeI lines							
41	4404	104.3	79.0	B	-3.74	-4.10	-4.10
	4415	87.8	67.5	C	-3.69	-3.99	-3.98
42	4202	110.2	90.3	C	-2.99	-3.35	-3.33
68	4494	92.2	70.9	C	-2.75	-3.12	-3.04
	4528	75.7	55.7	C	-3.51	-3.81	-3.78
152	4210	104.2	52.1	A	-3.27	-3.59	-3.52
	4299	78.3	54.8	C	-3.72	-4.06	-4.00
350	4454	38.2	31.1	B	-3.43	-3.73	-3.68
800	4219	71.2	56.5	B	-3.49	-3.75	-3.72
828	4484	43.0	34.1	D	-3.44	-3.78	-3.73
			logarithmic mean:		-3.40	-3.72	-3.69
			arithmetic mean:		-3.27	-3.61	-3.57
FeII lines							
27	4303	117.4	96.2	E	-3.15	-3.44	-3.53
	4385	103.0	76.9	C	-3.62	-3.88	-3.95
	4416	106.2	94.8	A	-3.17	-3.45	-3.54
37	4491	89.4	85.1	C	-3.27	-3.62	-3.55
	4520	100.6	68.9	C	-3.89	-4.31	-4.14
	4582	101.0	68.7	B	-3.43	-3.84	-3.68
	4629	104.4	75.5	C	-4.04	-4.41	-4.32
38	4508	118.9	112.2	C	-3.34	-3.67	-3.62
	4576	110.7	93.0	C	-3.00	-3.34	-3.28
	4620	87.8	71.4	C	-3.16	-3.47	-3.42
186	4635	86.0	66.7	C	-3.26	-3.52	-3.43
			logarithmic mean:		-3.39	-3.72	-3.68
			arithmetic mean:		-3.30	-3.60	-3.53
			temperature:		9950°	9500°	9400°

Note: λ4484 is given one-half weight in the mean abundance averages.

Table A-11

Effective Temperatures and Fe Abundance Determinations for HD110066

mult.	λ	W	W_o	qual.	abundance 1	2	3
FeI lines							
41	4404	143.0	93.5	A	-3.36	-3.65	-3.69
	4415	118.7	76.6	B	-3.28	-3.60	-3.61
42	4202	136.4	96.7	B	-2.76	-3.07	-3.12
68	4494	117.2	74.2	B	-2.58	-2.86	-2.82
	4528	150.1	98.1	B	-2.40	-2.71	-2.70
152	4210	118.5	49.0	B	-3.25	-3.50	-3.50
	4299	128.9	71.6	E	-3.19	-3.40	-3.42
350	4454	57.6	38.1	A	-3.10	-3.40	-3.37
800	4219	113.3	79.8	B	-2.73	-3.01	-2.98
828	4484	69.2	43.5	B	-2.99	-3.35	-3.26
			logarithmic mean:		-2.96	-3.26	-3.25
			arithmetic mean:		-2.88	-3.14	-3.12
FeII lines							
27	4303	162.1	117.5	E	-2.90	-3.13	-3.20
	4385	158.9	100.6	B	-3.13	-3.39	-3.48
	4416	177.4	158.4	A	-2.52	-2.78	-2.80
37	4491	149.5	141.0	B	-2.57	-2.58	-2.79
	4520	165.2	93.3	C	-3.28	-3.60	-3.54
	4582	128.2	68.9	B	-3.37	-3.69	-3.66
	4620	163.7	100.4	A	-3.50	-3.82	-3.77
38	4508	144.7	134.0	A	-3.08	-3.39	-3.35
	4576	142.8	103.5	A	-2.78	-3.09	-3.06
	4620	139.7	102.0	A	-2.44	-2.77	-2.72
186	4635	117.9	73.7	B	-3.07	-3.32	-3.22
			logarithmic mean:		-2.97	-3.26	-3.24
			arithmetic mean:		-2.85	-3.14	-3.12
			temperature:		10100°	9700°	9550°

Table A-12

Effective Temperatures and Fe Abundance Determinations for HD111133

mult.	λ	W	W_o	qual.	abundance 1	2	3
FeI lines							
41	4404	123.4	73.5	B	-3.41	-3.73	-3.73
	4415	73.0	45.6	B	-3.85	-4.17	-4.15
42	4202	110.5	70.5	C	-2.97	-3.24	-3.27
68	4494	55.4	37.7	C	-3.27	-3.54	-3.51
	4528	71.4	44.1	B	-3.43	-3.68	-3.64
152	4210	76.4	39.4	B	-3.23	-3.49	-3.45
	4299	68.6	41.3	C	-3.70	-3.97	-3.93
350	4454	20.9	18.9	C	-3.34	-3.67	-3.60
800	4219	73.9	48.3	C	-3.30	-3.60	-3.53
828	4484	35.8	28.2	E	-3.14	-3.48	-3.41
			logarithmic mean:		-3.36	-3.66	-3.62
			arithmetic mean:		-3.31	-3.60	-3.58
FeII lines							
27	4303	157.7	110.0	C	-2.86	-3.16	-3.17
	4385	119.1	68.0	B	-3.72	-3.99	-4.05
	4416	137.6	109.6	C	-2.85	-3.14	-3.18
37	4491	116.4	98.6	C	-2.87	-3.17	-3.13
	4520	108.6	57.5	B	-4.04	-4.38	-4.29
	4582	92.2	50.6	B	-3.81	-4.13	-4.04
	4629	134.7	75.7	B	-3.89	-4.20	-4.14
38	4508	107.2	94.9	A	-3.45	-3.73	-3.70
	4576	120.9	82.2	A	-3.08	-3.37	-3.30
	4620	108.2	73.1	A	-2.94	-3.27	-3.20
186	4635	92.3	57.7	C	-3.44	-3.70	-3.62
			logarithmic mean:		-3.36	-3.66	-3.62
			arithmetic mean:		-3.17	-3.47	-3.43
			temperature:		10650°	10150°	10000°

Table A-13

Effective Temperatures and Fe Abundance Determinations for HD118022

mult.	λ	W	W_o	qual.	abundance 1	2	3
FeI lines							
41	4404	150.2	111.3	B	-3.18	-3.51	-3.50
	4415	110.6	78.4	C	-3.30	-3.65	-3.63
42	4202	109.6	80.6	C	-3.16	-3.51	-3.48
68	4494	123.8	89.7	C	-2.29	-2.64	-2.56
	4528	162.8	122.4	B	-2.18	-2.48	-2.43
152	4210	100.2	47.0	A	-3.37	-3.67	-3.60
	4299	108.2	67.2	E	-3.35	-3.67	-3.62
350	4454	62.1	41.7	C	-3.07	-3.42	-3.35
800	4219	110.4	84.3	B	-2.71	-3.02	-2.94
828	4484	89.4	59.2	C	-2.76	-3.01	-2.96
			logarithmic mean:		-2.94	-3.26	-3.21
			arithmetic mean:		-2.72	-3.04	-2.99
FeII lines							
27	4303	164.9	136.3	C	-2.73	-3.00	-3.04
	4385	155.0	111.5	B	-3.01	-3.29	-3.35
	4416	153.2	139.3	A	-2.67	-2.95	-2.99
37	4491	142.8	137.3	C	-2.60	-2.91	-2.86
	4452	155.7	101.8	B	-3.16	-3.52	-3.43
	4582	102.2	61.2	B	-3.66	-4.01	-3.88
	4629	154.4	108.0	A	-3.43	-3.76	-3.70
38	4508	161.6	155.4	B	-2.93	-3.28	-3.19
	4576	142.6	115.9	A	-2.65	-3.00	-2.92
	4620	114.1	88.4	B	-2.71	-3.07	-2.99
186	4635	118.2	87.6	B	-2.76	-3.02	-2.92
			logarithmic mean:		-2.94	-3.26	-3.21
			arithmetic mean:		-2.84	-3.15	-3.12
			temperature		10000°	9550°	9450°

Table A-14

Effective Temperatures and Fe Abundance Determinations for HD137909

mult.	λ	W	W_o	qual.	abundance 1	2	3
FeI lines							
41	4404	193.6	96.8	B	-3.55	-3.79	-3.81
	4415	175.0	88.4	C	-3.23	-3.52	-3.57
42	4202	195.3	111.6	C	-2.80	-3.07	-3.13
68	4494	155.4	75.1	C	-2.76	-3.05	-3.02
152	4210	186.4	56.1	C	-3.25	-3.51	-3.49
350	4454	88.8	45.3	C	-3.16	-3.40	-3.37
800	4219	140.0	74.9	B	-3.06	-3.28	-3.29
828	4484	91.6	47.0	C	-3.19	-3.40	-3.41
			logarithmic mean:		-3.12	-3.38	-3.39
			arithmetic mean:		-3.06	-3.32	-3.33
FeII lines							
27	4303	202.5	119.8	C	-2.89	-3.16	-3.24
	4385	204.7	99.4	C	-3.18	-3.45	-3.56
	4416	189.3	140.2	A	-2.70	-2.91	-3.02
37	4491	128.4	112.6	C	-2.88	-3.19	-3.15
	4520	222.7	96.4	B	-3.33	-3.62	-3.57
	4582	182.4	73.5	C	-3.34	-3.64	-3.61
38	4508	147.9	124.3	C	-3.25	-3.57	-3.50
	4576	167.8	95.3	B	-3.03	-3.32	-3.28
	4620	151.1	83.9	A	-2.91	-3.19	-3.14
186	4635	107.8	55.0	C	-3.59	-3.84	-3.79
			logarithmic mean:		-3.11	-3.39	-3.39
			arithmetic mean:		-3.03	-3.31	-3.31
			temperature:		9750°	9450°	9300°

Table A-15

Effective Temperatures and Fe Abundance Determinations for HD137949

mult.	λ	W	W_o	qual.	abundance 1	2	3
FeI lines							
41	4404	174.2	97.9	B	-4.25	-4.58	-4.58
	4415	142.4	79.6	E	-4.17	-4.51	-4.51
42	4202	184.6	121.4	C	-3.48	-3.81	-3.80
68	4494	180.2	107.3	C	-2.94	-3.25	-3.17
	4528	213.1	133.2	B	-2.97	-3.29	-3.21
152	4210	183.5	58.4	C	-3.89	-4.20	-4.17
800	4219	143.9	86.7	C	-3.46	-3.73	-3.67
828	4484	97.4	52.1	C	-3.71	-3.96	-3.96
			logarithmic mean:		-3.61	-3.92	-3.88
			arithmetic mean:		-3.38	-3.69	-3.65
FeII lines							
27	4303	177.7	114.6	C	-3.14	-3.44	-3.50
	4385	189.2	105.1	C	-3.31	-3.60	-3.67
	4416	152.6	114.7	B	-3.10	-3.42	-3.49
37	4491	96.0	83.5	C	-3.67	-3.97	-3.90
	4520	131.1	60.7	C	-4.48	-4.77	-4.70
	4582	140.5	64.2	E	-3.94	-4.21	-4.13
38	4508	122.2	105.3	C	-3.79	-4.11	-4.04
	4576	138.3	83.8	A	-3.54	-3.85	-3.78
	4620	134.0	81.7	C	-3.24	-3.54	-3.48
186	4635	87.6	50.3	C	-3.88	-4.11	-4.05
			logarithmic mean:		-3.61	-3.90	-3.87
			arithmetic mean:		-3.46	-3.78	-3.76
			temperature:		8850°	8450°	8450°

Table A-16

Effective Temperatures and Fe Abundance Determinations for HD165474

mult.	λ	W	W_o	qual.	abundance 1	2	3
FeI lines							
41	4404	118.1	52.3	B	-5.12	-5.39	-5.41
	4415	127.4	56.4	B	-4.57	-4.87	-4.93
42	4202	152.4	69.0	B	-4.09	-4.39	-4.39
68	4494	128.0	56.4	C	-3.86	-4.14	-4.04
	4528	185.8	75.5	B	-3.63	-3.91	-3.83
152	4210	130.7	47.4	C	-3.99	-4.31	-4.25
350	4454	34.8	27.4	W	-4.13	-4.45	-4.36
800	4219	102.6	51.0	A	-4.16	-4.46	-4.40
828	4484	70.5	39.2	C	-3.83	-4.11	-4.07
			logarithmic mean:		-4.09	-4.39	-4.35
			arithmetic mean:		-3.98	-4.27	-4.24
FeII lines							
27	4303	174.2	81.0	C	-3.59	-3.85	-3.94
	4385	153.1	62.0	C	-4.12	-4.36	-4.46
	4416	156.6	92.7	A	-3.35	-3.62	-3.71
37	4491	85.3	46.7	C	-4.04	-4.33	-4.26
	4520	121.2	65.6	B	-4.70	-5.03	-4.95
	4582	107.0	49.7	C	-4.34	-4.71	-4.60
	4629	103.6	46.7	A	-5.12	-5.46	-5.43
38	4508	116.2	84.2	C	-4.07	-4.38	-4.30
	4576	129.2	61.5	A	-3.99	-4.33	-4.26
	4620	107.2	53.3	B	-3.92	-4.24	-4.15
186	4635	71.3	39.8	C	-4.16	-4.40	-4.30
			logarithmic mean:		-4.08	-4.38	-4.35
			arithmetic mean:		-3.90	-4.18	-4.27
			temperature:		9150°	8750°	8750°

Note: λ4404, λ4454, and λ4629 are given one-half weight in the mean abundance averages.

Table A-17

Effective Temperatures and Fe Abundance Determinations for HD176232

mult.	λ	W	W_o	qual.	abundance 1	2	3
FeI lines							
41	4404	157.7	138.3	B	-4.34	-4.66	-4.66
	4415	133.4	115.0	C	-4.14	-4.46	-4.47
42	4202	115.5	98.7	C	-4.25	-4.55	-4.57
68	4494	104.8	85.2	B	-3.79	-4.07	-4.04
	4528	116.6	91.8	B	-3.99	-4.27	-4.25
152	4210	109.0	56.5	A	-4.42	-4.68	-4.70
	4299	103.4	76.6	E	-4.43	-4.69	-4.71
350	4454	55.4	42.3	C	-4.40	-4.66	-4.63
800	4219	105.3	90.0	B	-3.83	-4.05	-4.06
828	4484	40.2	32.7	C	-4.63	-4.89	-4.90
			logarithmic mean:		-4.22	-4.50	-4.50
			arithmetic mean:		-4.13	-4.41	-4.41
FeII lines							
27	4303	98.4	81.3	B	-3.77	-4.04	-4.13
	4385	98.4	74.0	B	-3.98	-4.26	-4.36
	4416	102.7	92.5	C	-3.57	-3.85	-3.93
37	4491	76.2	73.3	C	-4.06	-4.33	-4.31
	4520	84.3	60.2	C	-4.64	-4.89	-4.88
	4582	55.4	40.7	B	-4.80	-5.07	-5.02
	4629	108.7	83.0	B	-4.38	-4.67	-4.64
38	4508	92.5	87.3	C	-4.26	-4.54	-4.50
	4576	56.1	45.6	C	-4.78	-5.06	-5.00
	4620	72.4	59.8	C	-3.98	-4.24	-4.21
186	4635	47.3	38.1	C	-4.27	-4.45	-4.42
			logarithmic mean:		-4.23	-4.49	-4.49
			arithmetic mean:		-4.07	-4.34	-4.37
			temperature:		8200°	7800°	7800°

Table A-18

Effective Temperatures and Fe Abundance Determinations for HD191742

mult.	λ	W	W_o	qual.	abundance 1	2	3
FeI lines							
41	4404	146.5	130.8	A	-3.86	-4.17	-4.20
	4415	126.0	111.5	C	-3.63	-3.95	-4.00
42	4202	116.2	101.9	B	-3.65	-3.96	-4.02
68	4494	140.8	126.8	B	-2.66	-3.00	-2.96
	4528	127.8	110.2	C	-3.17	-3.50	-3.47
152	4210	145.0	82.9	A	-3.23	-3.54	-3.52
	4299	134.7	113.2	E	-3.28	-3.58	-3.61
350	4454	58.3	45.5	A	-3.81	-4.12	-4.10
800	4219	110.2	97.5	B	-3.26	-3.52	-3.48
828	4484	78.9	63.6	A	-3.32	-3.61	-3.64
			logarithmic mean:		-3.39	-3.70	-3.70
			arithmetic mean:		-3.20	-3.57	-3.54
FeII lines							
27	4303	139.3	129.0	C	-3.05	-3.34	-3.37
	4385	132.0	114.8	B	-3.11	-3.42	-3.54
	4416	122.5	114.5	A	-3.09	-3.39	-3.49
37	4491	108.2	105.0	C	-3.24	-3.59	-3.55
	4520	119.9	95.9	C	-3.62	-3.92	-3.88
	4582	89.6	67.9	B	-3.77	-4.07	-4.05
	4629	112.5	92.2	B	-4.03	-4.34	-4.30
38	4508	129.3	125.5	B	-3.54	-3.86	-3.80
	4576	101.8	89.3	B	-3.40	-3.72	-3.67
	4620	91.4	79.5	A	-3.24	-3.56	-3.53
186	4635	86.2	72.4	B	-3.28	-3.48	-3.41
			logarithmic mean:		-3.40	-3.70	-3.69
			arithmetic mean:		-3.32	-3.61	-3.55
			temperature:		8900°	8500°	8450°

Table A-19

Effective Temperatures and Fe Abundance Determinations for HD192678

mult.	λ	W	W_o	qual.	abundance 1	2	3
FeI lines							
41	4404	185.7	108.0	A	-2.93	-3.21	-3.20
	4415	117.0	63.6	B	-3.44	-3.76	-3.71
42	4202	164.2	100.7	C	-2.55	-2.81	-2.80
68	4494	117.4	63.1	C	-2.67	-2.93	-2.88
	4528	115.7	60.3	B	-3.05	-3.83	-3.30
152	4210	114.0	45.8	A	-3.20	-3.40	-3.38
	4299	123.2	59.2	B	-3.31	-3.56	-3.55
350	4454	65.0	39.2	B	-2.90	-3.16	-3.11
800	4219	108.7	62.8	A	-3.02	-3.26	-3.20
828	4484	83.1	46.4	C	-2.89	-3.07	-3.04
			logarithmic mean:		-3.00	-3.25	-3.22
			arithmetic mean:		-2.92	-3.17	-3.14
FeII lines							
27	4303	209.5	151.8	B	-2.55	-2.80	-2.82
	4385	156.4	80.2	A	-3.47	-3.73	-3.77
	4416	203.4	170.9	B	-2.40	-2.65	-2.67
37	4491	137.7	125.2	C	-2.62	-2.89	-2.85
	4520	172.0	80.0	C	-3.47	-3.78	-3.72
	4582	141.4	64.9	B	-3.43	-3.72	-3.66
	4629	176.1	88.9	B	-3.64	-3.94	-3.88
38	4508	154.7	138.1	B	-2.99	-3.27	-3.23
	4576	170.6	112.2	A	-2.65	-2.90	-2.88
	4620	152.3	97.6	A	-2.48	-2.75	-2.74
186	4635	123.7	68.7	C	-3.14	-3.40	-3.33
			logarithmic mean:		-2.99	-3.26	-3.23
			arithmetic mean:		-2.79	-3.05	-3.04
			temperature:		10400°	10000°	9850°

Table A-20

Effective Temperatures and Fe Abundance Determinations for HD201601

mult.	λ	W	W_o	qual.	abundance 1	2	3
FeI lines							
41	4404	143.6	128.2	C	-4.46	-4.79	-4.47
	4415	109.5	95.2	C	-4.45	-4.75	-4.78
42	4202	119.0	105.3	C	-4.22	-4.51	-4.53
68	4494	117.1	104.6	C	-3.51	-3.78	-3.75
	4528	146.6	130.9	C	-3.52	-3.81	-3.79
152	4210	122.4	68.0	C	-4.12	-4.37	-4.39
	4299	131.4	110.4	C	-3.89	-4.18	-4.14
350	4454	57.4	44.8	E	-4.35	-4.60	-4.60
800	4219	104.2	92.2	B	-3.81	-4.04	-4.05
828	4484	65.7	52.1	C	-4.16	-4.39	-4.36
			logarithmic mean:		-4.05	-4.32	-4.32
			arithmetic mean:		-3.96	-4.19	-4.17
FeII lines							
27	4303	98.7	85.1	B	-3.71	-3.98	-4.06
	4385	100.0	82.0	B	-3.81	-4.11	-4.17
	4416	91.2	83.7	B	-3.71	-4.01	-4.07
37	4491	76.3	73.4	C	-4.07	-4.34	-4.31
	4520	99.1	76.8	B	-4.16	-4.45	-4.42
	4582	79.5	59.8	C	-4.20	-4.46	-4.44
	4629	111.1	91.1	C	-4.25	-4.57	-4.49
38	4508	96.7	93.0	A	-4.17	-4.45	-4.40
	4576	84.9	73.8	B	-3.95	-4.22	-4.19
	4620	62.6	53.5	C	-4.18	-4.45	-4.41
186	4635	46.5	38.8	C	-4.25	-4.40	-4.39
			logarithmic mean:		-4.04	-4.31	-4.30
			arithmetic mean:		-4.00	-4.27	-4.26
			temperature:		8150°	7750°	7750°

Table A-21

Effective Temperatures and Fe Abundance Determinations for HD204411

mult.	λ	W	W_o	qual.	abundance 1	2	3
FeI lines							
41	4404	129.8	127.3	A	-3.37	-3.67	-3.68
	4415	98.3	96.4	C	-3.34	-3.64	-3.64
42	4202	79.4	77.1	B	-3.59	-3.88	-3.92
68	4494	66.0	64.1	C	-3.26	-3.58	-3.52
	4528	90.8	88.2	C	-3.02	-3.33	-3.32
152	4210	62.0	56.4	A	-3.43	-3.71	-3.70
	4299	95.3	92.5	E	-3.09	-3.37	-3.37
350	4454	43.5	42.2	B	-3.40	-3.70	-3.65
800	4219	74.4	72.2	B	-3.33	-3.56	-3.54
828	4484	50.1	48.6	C	-3.32	-3.61	-3.58
			logarithmic mean:		-3.32	-3.60	-3.59
			arithmetic mean:		-3.29	-3.58	-3.56
FeII lines							
27	4303	117.8	115.5	B	-2.99	-3.27	-3.36
	4385	100.4	97.5	B	-3.27	-3.54	-3.64
	4416	97.9	96.0	B	-3.21	-3.50	-3.60
37	4491	89.8	88.9	C	-3.32	-3.66	-3.59
	4520	106.8	103.7	B	-3.28	-3.62	-3.53
	4582	67.2	64.6	C	-3.69	-4.00	-3.93
	4629	109.4	106.4	B	-3.59	-3.92	-3.84
38	4508	124.7	123.5	B	-3.35	-3.67	-3.62
	4576	90.4	88.6	B	-3.22	-3.55	-3.47
	4620	77.5	76.0	B	-3.17	-3.49	-3.40
186	4635	69.7	67.7	C	-3.30	-3.54	-3.45
			logarithmic mean:		-3.31	-3.61	-3.58
			arithmetic mean:		-3.27	-3.55	-3.56
			temperature:		9550°	9150°	9050°

Table A-22

Effective Temperatures and Fe Abundance Determinations for HD216533

mult.	λ	W	W_o	qual.	abundance 1	2	3
FeI lines							
41	4404	83.7	62.5	A	-3.88	-4.25	-4.20
	4415	67.5	51.5	C	-3.83	-4.13	-4.12
42	4202	91.5	72.6	C	-3.07	-3.39	-3.36
68	4528	61.0	45.5	C	-3.50	-3.77	-3.75
152	4210	86.2	44.0	A	-3.22	-3.49	-3.46
	4299	78.4	54.8	B	-3.47	-3.74	-3.71
350	4454	30.9	26.4	B	-3.25	-3.55	-3.50
800	4219	58.4	45.6	C	-3.55	-3.81	-3.75
828	4484	34.3	28.8	C	-3.30	-3.59	-3.54
			logarithmic mean:		-3.45	-3.75	-3.71
			arithmetic mean:		-3.38	-3.67	-3.66
FeII lines							
27	4303	104.5	85.0	C	-3.31	-3.59	-3.65
	4385	94.6	69.6	B	-3.72	-3.99	-4.05
	4416	104.9	94.5	B	-3.12	-3.38	-3.45
37	4491	87.1	83.0	C	-3.21	-3.53	-3.47
	4520	103.5	71.3	C	-3.69	-4.00	-3.96
	4582	65.6	45.6	C	-4.01	-4.31	-4.26
	4629	110.8	81.5	A	-3.79	-4.10	-4.06
38	4508	106.5	100.5	A	-3.41	-3.69	-3.66
	4576	92.0	76.0	B	-3.29	-3.58	-3.54
	4620	68.0	54.0	B	-3.53	-3.86	-3.79
186	4635	98.4	78.1	C	-2.90	-3.18	-3.09
			logarithmic mean:		-3.45	-3.75	-3.72
			arithmetic mean:		-3.34	-3.62	-3.60
			temperature:		10400°	9950°	9800°

Table A-23

Effective Temperatures and Fe Abundance Determinations for ν Cap

mult.	λ	W	W_o	qual.	abundance 1	2	3
FeI lines							
41	4404	50.2	34.9	-	-4.64	-4.96	-4.89
	4415	35.1	27.6	-	-4.41	-4.74	-4.70
42	4202	32.9	26.3	-	-4.38	-4.70	-4.67
152	4235	17.9	16.3	-	-4.60	-4.90	-4.82
	4260	40.1	30.4	-	-4.47	-4.75	-4.68
800	4219	17.8	16.2	-	-4.34	-4.60	-4.55
			logarithmic mean:		-4.47	-4.78	-4.72
			arithmetic mean:		-4.46	-4.77	-4.71
FeII lines							
27	4303	66.6	41.6	-	-4.49	-4.76	-4.78
	4385	67.0	41.9	-	-4.53	-4.79	-4.79
	4416	60.4	40.0	-	-4.52	-4.78	-4.78
37	4491	49.7	34.8	-	-4.57	-4.86	-4.80
	4520	56.7	39.1	-	-4.64	-4.96	-4.86
	4582	33.3	26.6	-	-4.52	-4.64	-4.74
	4629	85.0	50.0	-	-4.66	-4.97	-4.89
38	4508	71.2	43.7	-	-4.80	-5.13	-5.04
	4576	55.8	37.7	-	-4.32	-4.65	-4.57
	4620	39.4	29.8	-	-4.19	-4.49	-4.42
186	4635	50.2	34.9	-	-4.10	-4.30	-4.30
			logarithmic mean:		-4.48	-4.74	-4.72
			arithmetic mean:		-4.43	-4.69	-4.71
			temperature:		10500°	10050°	9950°

Notes: λ4235: log gf=-0.25
λ4260: log gf=+0.04
The source of these values is Wolnik *et al.* (1970).

Table A-24

Effective Temperatures and Fe Abundance Determinations for o Peg

mult.	λ	W	W_o	qual.	abundance 1	2	3
FeI lines							
41	4404	77.2	46.5	B	-4.55	-4.84	-4.83
	4415	68.9	42.8	A	-4.25	-4.53	-4.54
42	4202	51.0	35.2	C	-4.40	-4.67	-4.68
68	4528	40.0	30.3	C	-4.07	-4.41	-4.35
152	4210	21.8	19.1	C	-4.12	-4.36	-4.35
	4235	49.0	34.0	C	-4.26	-4.55	-4.54
	4260	75.9	45.8	C	-4.26	-4.51	-4.48
	4299	42.6	31.8	C	-4.19	-4.54	-4.50
800	4219	28.0	23.3	C	-4.35	-4.59	-4.54
			logarithmic mean:		-4.27	-4.56	-4.53
			arithmetic mean:		-4.26	-4.55	-4.52
FeII lines							
27	4303	104.3	59.6	A	-3.98	-4.24	-4.29
	4385	98.7	56.7	A	-4.12	-4.39	-4.44
	4416	88.1	51.5	A	-4.21	-4.47	-4.52
37	4491	82.2	48.9	C	-4.22	-4.54	-4.48
	4520	81.4	48.4	C	-4.45	-4.74	-4.70
	4582	60.0	39.0	C	-4.25	-4.56	-4.52
	4629	93.2	54.2	C	-4.61	-4.92	-4.85
38	4508	92.6	53.8	B	-4.58	-4.91	-4.83
	4576	72.2	44.0	B	-4.25	-4.56	-4.49
	4620	60.9	39.3	B	-4.01	-4.33	-4.27
			logarithmic mean:		-4.27	-4.57	-4.54
			arithmetic mean:		-4.22	-4.52	-4.49
			temperature:		10150°	9750°	9600°

Notes: λ4235:log gf=-0.25
λ4260:log gf=+0.04
The source of these values is Wolnik et al.(1970).

Note on Tables A-25 Through A-54

Tables A-25 through A-54 give the abundance determinations for the elements other than Fe in order of atomic number. For each line, I give the wavelength, λ, in Å; the equivalent width, W, in mÅ; the reduced equivalent width, W_o, in mÅ; the line quality, qual.; and the deduced abundances for the effective temperatures of cases 1 and 2. For blended lines, I normally give, in addition, the wavelengths of the centroids. For each star, the arithmetic mean abundance is given. Some lines are given double or one-half weights in these mean abundance averages. This information is given in each table. In some tables, the following symbols are used: n.m. for not measured and : for uncertain determination.

Table A-25

Mg Abundances from MgI and MgII Lines

star	MgI λ4167 W	qual.	W_o 1	2	abundance 1	2	MgII λ4481 W	qual.	abundance 1	2
HD2453	80.7	C	58	57	-3.53	-3.78	531.2	B	-4.18	-4.23
HD5797	187.6	E	151	133	>-2.44	-2.66	628.6	B	-4.13	-4.18
HD8441	16.5	C	16.5	16.5	-4.47	-4.72	274.4	B	-4.84	-4.91
HD12288	n.m.						392.9	B	-4.44	-4.50
HD18078	42.7	C	28	28	-4.30	-4.49	346.7	B	-4.64	-4.69
HD22374	48.4	C	25	25	-4.62	-4.78	249.3	B	-5.05	-5.09
HD50169	67.0	W	43	40	-3.95	-4.19	364.9	B	-4.57	-4.63
HD81009	84.1	E	51	51	-4.29	-4.54	368.5	C	-4.69	-4.72
HD89069	74.9	C	62	58	-3.68	-4.02	446.9	C	-4.41	-4.47
HD110066	68.6	E	50	46	-3.83	-4.15	410.6	B	-4.46	-4.52
HD111133	41.2	E	24	25	-4.05	-4.30	368.7	B	-4.49	-4.56
HD118022	74.4	C	52	52	-3.84	-4.11	477.1	C	-4.34	-4.41
HD137909	127.7	C	71	72	-3.61	-3.76	437.6	C	-4.46	-4.50
HD137949	144.5	C	86	87	-3.80	-3.98	363.1	C	-4.74	-4.74
HD165474	61.3	C	42	43	-4.58	-4.78	263.1	C	-5.03	-5.06
HD176232	240.1	B	216	216	-2.66	-2.88	346.3	C	-4.74	-4.67
HD191742	134.8	A	110	111	-3.28	-3.49	401.2	B	-4.64	-4.65
HD192678	43.4	E	30	25	-4.05	-4.32	285.7	C	-4.78	-4.82
HD201601	222.0	C	201	201	-2.75	-2.98	407.1	C	-4.59	-4.50
HD204411	69.4	B	64	64	-3.86	-4.10	402.0	B	-4.56	-4.62
HD216533	104.6	C	83	82	-2.97	-3.26	453.0	B	-4.33	-4.40
ν Cap	23.4	-	23.4	23.4	-4.13	-4.38	389.9	-	-4.46	-4.52
o Peg	24.2	B	24.2	24.2	-4.31	-4.54	387.9	B	-4.51	-4.57

Note: The effects of line blending in MgI(15) λ4167.27 caused by GdII(42) λ4167.16 have only been partially corrected.

Table A-26

Si Abundances from SiII Lines

	SiII(1) λ3853.7			abundance		SiII(1) λ3862.6			abundance		mean Si abundance	
star	W	qual.	W_o	1	2	W	qual.	W_o	1	2	1	2
HD2453	100.9	C	83.4	-4.18	-4.20	108.7	A	94.5	-4.71	-4.72	-4.37	-4.39
HD5797	117.3	C	111.7	-3.81	-3.83	194.6	C	188.9	-3.82	-3.84	-3.81	-3.83
HD8441	55.9	C	55.9	-4.71	-4.72	67.2	C	67.2	-5.17	-5.18	-4.88	-4.89
HD12288	192.4	C	129.1	-3.54	-3.56	218.6	C	172.1	-3.89	-3.89	-3.68	-3.69
HD18078	103.4	C	85.5	-4.17	-4.18	153.2	A	138.0	-4.18	-4.19	-4.17	-4.18
HD22374	77.2	B	76.4	-4.35	-4.36	109.0	A	107.9	-4.56	-4.58	-4.44	-4.46
HD50169	229.0	C	180.3	-3.14	-3.16	282.7	C	257.0	-3.46	-3.47	-3.27	-3.29
HD81009	131.6	C	82.3	-4.26	-4.26	136.2	C	94.6	-4.76	-4.78	-4.44	-4.45
HD89069	92.2	C	85.4	-4.18	-4.19	111.8	C	106.5	-4.55	-4.57	-4.33	-4.34
HD110066	154.4	B	133.1	-3.53	-3.54	207.3	B	192.4	-3.76	-3.78	-3.63	-3.64
HD111133	100.9	C	83.4	-4.17	-4.19	136.1	C	121.5	-4.34	-4.35	-4.25	-4.26
HD118022	69.8	W	56.3	-4.72	-4.71	90.2	B	75.2	-5.03	-5.05	-4.85	-4.85
HD137909	95.9	C	71.6	-4.42	-4.42	105.6	A	83.8	-4.89	-4.91	-4.59	-4.60
HD137949	97.2	C	73.1	-4.41	-4.41	147.0	B	118.6	-4.47	-4.48	-4.44	-4.45
HD165474	95.5	C	67.3	-4.50	-4.50	116.7	A	88.4	-4.85	-4.87	-4.64	-4.65
HD176232	75.4	C	69.8	-4.46	-4.42	106.7	A	102.6	-4.68	-4.62	-4.56	-4.51
HD191742	116.8	C	111.2	-3.83	-3.86	163.8	B	157.1	-4.09	-4.11	-3.95	-3.97
HD192678	190.9	C	157.8	-3.29	-3.30	214.3	C	184.7	-3.80	-3.81	-3.47	-3.48
HD201601	84.1	C	80.1	-4.30	-4.24	115.7	A	112.3	-4.52	-4.47	-4.40	-4.34
HD204411	80.6	C	79.8	-4.30	-4.30	93.0	B	92.1	-4.78	-4.80	-4.48	-4.48
HD216533	101.4	C	93.9	-4.02	-4.03	112.5	A	107.1	-4.51	-4.53	-4.20	-4.21
ν Cap	84.1	-	64.7	-4.54	-4.54	117.7	-	89.2	-4.77	-4.80	-4.64	-4.65
o Peg	69.4	A	54.6	-4.73	-4.73	103.8	A	78.6	-4.95	-4.99	-4.83	-4.84

Table A-27

Ca Abundances from CaI Lines

mult.	λ	W	W_o	qual.	abundance 1	abundance 2	
HD2453							
2	4226	66.5	50.8	A	-5.33	-5.79	
4	4425	19.1	19.1	D	-4.53	-4.93	
	4455	37.4	31.4	C	-4.83	-5.24	
5	4283	32.4	27.4	C	-4.43	-4.84	
			mean abundance:		-4.77	-5.19	a,b
HD5797							
2	4226	82.8	74.6	A	-5.48	-5.93	
4	4425	17.1	17.1	D	-5.35	-5.73	
5	4283	29.7	26.5	B	-5.24	-5.63	
			mean abundance:		-5.38	-5.79	a,b
HD8441							
2	4226	37.3	37.3	C	-5.83	-6.33	
			mean abundance:		-5.83	-6.33	
HD12288							
2	4226	105.2	57.5	B	-4.88	-5.38	
5	4283	25.9	21.4	C	-4.38	-4.86	
			mean abundance:		-4.64	-5.13	a
HD18078							
2	4226	60.7	47.1	B	-5.79	-6.18	
4	4435	28.5	25.9	D	-5.01	-5.37	
5	4283	20.1	19.7	C	-4.93	-5.30	
			mean abundance:		-5.32	-5.78	a,b

Table A-27, continued

mult.	λ	W	W_o	qual.	abundance 1	abundance 2	
HD22374							
2	4226	55.9	54.8	B	-6.23	-6.59	
			mean abundance:		-6.23	-6.59	
HD50169							
2	4226	80.0	51.9	E	-5.58	-5.96	
4	4425	25.0	23.4	C	-4.62	-4.98	
			mean abundance:		-4.99	-5.37	a
HD81009							
2	4226	121.3	60.7	C	-6.22	-6.61	
4	4425	44.8	36.7	C	-5.16	-5.54	
	4455	120.8	57.3	E	-5.39	-5.75	
			mean abundance:		-5.59	-5.97	a
HD89069							
2	4226	37.4	34.0	C	-6.23	-6.74	
4	4435	26.2	24.5	E	-5.11	-5.62	
	4455	24.9	23.3	C	-5.43	-5.91	
5	4283	21.6	20.6	W	-4.95	-5.48	
			mean abundance:		-5.58	-6.08	a,c
HD110066							
2	4226	95.8	69.4	A	-5.10	-5.54	
4	4425	22.0	21.0	C	-4.72	-5.12	
	4435	47.1	38.6	C	-4.63	-5.07	
	4455	65.5	47.8	C	-4.73	-5.16	
5	4283	35.0	28.9	B	-4.66	-5.08	
			mean abundance:		-4.88	-5.21	a

Table A-27, continued

mult.	λ	W	W_o	qual.	abundance 1	abundance 2	
HD111133							
2	4226	24.6	23.2	C	-5.78	-6.30	
			mean abundance:		-5.78	-6.30	
HD118022							
2	4226	75.7	60.1	C	-5.48	-5.96	
4	4425	36.5	34.1	C	-4.52	-4.98	
5	4283	41.9	34.3	B	-4.64	-5.12	
			mean abundance:		-4.90	-5.37	a
HD137909							
2	4226	216.9	139.0	C	-4.03	-4.35	
4	4425	89.9	70.8	C	-3.98	-4.29	
	4435	161.3	89.1	C	-4.03	-4.21	
	4455	164.0	80.4	E	-4.46	-4.76	
5	4283	100.0	53.5	B	-4.43	-4.80	
			mean abundance:		-4.13	-4.42	
HD137949							
2	4226	293.4	252.9	C	-4.26	-4.67	
4	4425	114.6	96.3	C	-4.48	-4.80	
	4435	180.9	117.5	C	-4.52	-4.88	
	4455	283.3	216.3	E	-4.16	-4.50	
5	4283	104.0	57.3	C	-5.28	-5.64	
			mean abundance:		-4.42	-4.77	

Table A-27, continued

mult.	λ	W	W_o	qual.	abundance 1	abundance 2	
HD165474							
2	4226	145.1	72.9	C	-6.00	-6.38	
4	4225	47.2	39.3	C	-5.26	-5.63	
	4435	97.0	54.8	C	-5.28	-5.65	
	4455	116.8	61.8	C	-5.44	-5.77	
5	4283	67.0	41.6	C	-5.28	-5.72	
			mean abundance:		-5.44	-5.82	a
HD176232							
2	4426	266.5	256.2	C	-4.91	-5.23	
4	4425	106.2	102.1	C	-4.91	-5.14	
	4435	116.2	99.3	C	-5.29	-5.54	
	4455	152.0	126.6	C	-5.26	-5.50	
5	4283	99.6	75.4	C	-5.44	-5.73	
			mean abundance:		-5.11	-5.38	
HD191742							
2	4426	262.9	252.9	B	-4.22	-4.62	
4	4425	105.6	101.5	B	-4.35	-4.70	
	4435	140.8	125.7	C	-4.44	-4.78	
	4455	146.0	125.9	C	-4.91	-5.16	
5	4483	86.4	68.6	A	-5.02	-5.35	
			mean abundance:		-4.49	-4.84	
HD192678							
2	4226	69.2	49.4	C	-5.37	-5.69	
4	4455	20.0	19.0	D	-5.12	-5.40	
5	4283	24.3	22.1	C	-4.53	-4.84	
			mean abundance:		-5.00	-5.31	a

Table A-27, continued

mult.	λ	W	W_o	qual.	abundance 1	abundance 2	
HD201601							
2	4226	250.2	240.6	C	-4.98	-5.33	
4	4425	101.6	97.7	C	-5.00	-5.24	
	4435	111.9	107.1	C	-5.22	-5.45	
	4455	180.4	161.1	E	-5.02	-5.22	
5	4283	86.6	69.3	B	-5.60	-5.84	
			mean abundance:		-5.11	-5.37	
HD204411							
2	4226	124.0	121.6	B	-4.47	-4.86	
4	4425	68.0	67.3	C	-4.25	-4.71	
	4435	69.0	67.6	C	-4.59	-5.04	
	4455	104.1	102.1	C	-4.34	-4.77	
5	4283	65.4	63.5	A	-4.44	-4.89	
			mean abundance:		-4.39	-4.84	
HD216533							
2	4226	60.0	51.7	B	-5.28	-5.78	
4	4435	35.7	32.2	C	-4.50	-4.96	
5	4283	22.5	21.4	D	-4.49	-4.99	
			mean abundance:		-4.73	-5.21	a,b
ν Cap							
2	4226	33.5	28.9	-	-5.89	-6.25	
			mean abundance:		-5.89	-6.25	
o Peg							
2	4226	71.8	49.2	C	-5.63	-6.08	
			mean abundance:		-5.63	-6.08	

Notes: a. λ4226 is given double weight in the mean abundance averages

Table A-27, continued

except if its derived abundance is more than .75 dex smaller than any other CaI line abundance determination in which case triple weight is given.

b. D quality lines and those whose equivalent width is less than 20 mA are given one-half weight.
c. skip λ4283 in the mean abundance averages.
d. λ4226 is given triple weight.

Table A-28

Sc Abundances from ScII Lines

mult.	λ	W	W_o	qual.	abundance 1	abundance 2	
HD2453							
7	4246	102.7	68.5	A	-8.25	-8.50	
14	4400	49.9	35.9	C	-8.05	-8.29	
	4415	53.9	41.8	C	-7.80	-8.04	
15	4314	56.0	38.4	D	-8.48	-8.83	
			mean abundance:		-8.08	-8.32	a,b
HD5797							
7	4246	118.3	107.5	B	-7.88	-8.11	
14	4400	44.4	37.6	C	-8.31	-8.68	
	4415	50.0	45.5	C	-8.21	-8.36	
15	4314	49.9	41.6	E	-8.97	-9.17	
			mean abundance:		-8.07	-8.30	a,c
HD8441							
7	4246	39.5	39.5	C	-9.15	-9.39	
15	4314	10.2	10.2	D	-9.49	-9.74	
			mean abundance:		-9.24	-9.48	b
HD12288							
7	4246	149.1	70.7	C	-8.03	-8.36	
14	4400	92.4	46.2	D	-7.70	-7.92	
	4415	35.2	28.2	C	-7.97	-8.25	
			mean abundance:		-7.92	-8.19	B

Table A-28, continued

mult.	λ	W	W_o	qual.	abundance 1	abundance 2	
HD18078							
7	4246	64.1	44.2	B	-9.12	-9.31	
14	4400	31.0	27.7	C	-8.44	-8.65	
	4415	26.4	25.1	C	-8.39	-8.60	
			mean abundance:		-8.64	-8.84	a
HD22374							
7	4246	67.4	66.1	B	-8.88	-9.09	
14	4400	28.2	27.9	C	-8.79	-9.02	
	4415	30.6	30.3	C	-8.60	-8.79	
15	4314	48.4	47.0	D	-8.92	-9.08	
			mean abundance:		-8.86	-8.99	a
HD50169							
7	4246	98.4	54.4	C	-8.78	-8.99	
			mean abundance:		-8.78	-8.99	
HD81009							
7	4246	189.7	85.1	E	-8.45	-8.70	
14	4415	67.5	41.4	C	-8.41	-8.63	
			mean abundance:		-8.43	-8.66	
HD89069							
7	4246	73.0	59.3	C	-8.77	-9.04	
14	4415	22.9	21.6	C	-8.54	-8.80	
			mean abundance:		-8.68	-8.96	a

Table A-28, continued

mult.	λ	W	W_o	qual.	abundance 1	abundance 2	
HD110066							
7	4246	114.1	80.9	A	-8.08	-8.33	
14	4400	51.1	36.8	C	-8.14	-8.42	
	4415	33.5	28.4	B	-8.27	-8.50	
15	4314	53.4	57.9	E	-8.76	-8.99	
			mean abundance:		-8.17	-8.43	a,c
HD111133							
7	4246	51.4	37.5	C	-8.93	-9.23	
			mean abundance:		-8.93	-9.23	
HD118022							
7	4246	73.5	61.2	C	-8.68	-8.96	
14	4415	27.5	24.8	C	-8.42	-8.94	
15	4314	22.6	22.6	E	-9.21	-9.47	
			mean abundance:		-8.67	-8.94	a
HD137909							
7	4246	253.3	197.9	C	-7.03	-7.21	
14	4400	154.0	80.6	E	-7.21	-7.39	
	4415	107.2	72.4	B	-7.29	-7.48	
			mean abundance:		-7.19	-7.35	
HD137949							
7	4246	227.7	183.6	C	-7.63	-7.85	
14	4400	164.9	103.1	C	-7.27	-7.48	
	4415	94.6	69.6	C	-7.87	-8.08	
			mean abundance:		-7.52	-7.73	

Table A-28, continued

mult.	λ	W	W_o	qual.	abundance 1	abundance 2	
HD165474							
7	4246	159.0	79.5	C	-8.70	-8.90	
14	4400	67.4	38.7	E	-8.68	-8.90	
	4415	61.3	40.1	C	-8.53	-8.73	
			mean abundance:		-8.63	-8.84	
HD176232							
7	4246	51.8	42.8	C	-10.21	-10.35	
14	4400	28.6	25.1	C	-9.52	-9.72	
	4415	18.9	17.3	D	-9.60	-9.82	
			mean abundance:		-9.71	-9.91	b
HD191742							
7	4246	104.9	94.5	B	-8.49	-8.71	
14	4400	35.5	31.1	C	-9.01	-9.23	
	4415	50.0	45.5	C	-8.53	-8.74	
15	4314	89.5	75.8	C	-8.38	-8.58	
			mean abundance:		-8.54	-8.75	a
HD192678							
7	4246	101.8	61.7	C	-8.44	-8.62	
14	4400	39.1	29.8	E	-8.18	-8.37	
	4415	23.8	22.2	D	-8.26	-8.43	
15	4314	44.8	31.5	E	-8.74	-8.92	
			mean abundance:		-8.38	-8.56	b

Table A-28, continued

mult.	λ	W	W_λ	qual.	abundance 1	abundance 2	
HD201601							
7	4246	75.2	65.4	C	-9.63	-9.81	
14	4400	45.0	38.1	C	-9.23	-9.43	
	4415	36.0	33.6	B	-9.22	-9.41	
15	4314	42.8	36.3	E	-9.87	-10.06	
			mean abundance:		-9.41	-9.60	
HD204411							
7	4246	59.0	57.8	A	-9.08	-9.30	
14	4400	46.8	45.4	C	-8.30	-8.51	
	4415	27.6	27.3	C	-8.62	-8.86	
			mean abundance:		-8.64	-8.86	a
HD216533							
7	4246	56.3	45.0	C	-8.89	-9.17	
14	4415	15.0	14.4	C	-8.49	-8.74	
15	4314	23.2	20.7	C	-8.95	-9.29	
			mean abundance:		-8.82	-9.10	a,d
ν Cap							
7	4246	41.6	31.0	-	-9.16	-9.43	
			mean abundance:		-9.16	-9.43	
o Peg							
7	4246	62.2	39.9	A	-9.18	-9.42	
			mean abundance:		-9.18	-9.42	

Notes: a. λ4246 is given double weight in the mean abundance averages.
b. D quality lines are given one-half weight.
c. λ4314 is given one-half weight.
d. λ4415 is given one-half weight.

Table A-29

Ti Abundances from TiI Lines

mult.	λ	W	W_o	qual.	abundance 1	abundance 2	
HD2453							
42	4535	44.5	32.7	D	-5.01	-5.37	
			mean abundance:		-5.01	-5.37	uc
HD5797							
42	4512	55.8	42.6	B	-4.76	-5.11	
	4518	50.9	39.2	B	-4.94	-5.30	
	4533	119.0	97.5	C	-4.26	-4.60	
	4535	92.5	73.4	B	-4.56	-4.92	
	4549	69.6	53.1	D	-4.60	-4.90	
44	4281	19.4	17.6	C	-4.64	-4.97	
	4286	46.9	37.5	C	-4.93	-5.32	
	4287	67.7	52.9	B	-4.52	-4.85	
	4299	37.4	34.3	C	-5.39	-5.74	
			mean abundance:		-4.64	-5.00	a
HD12288							
42	4533	25.9	24.9	D	-5.29	-5.64	
			mean abundance:		-5.29	-5.64	uc
HD18078							
42	4512	21.9	18.9	C	-4.92	-5.21	
	4518	24.4	22.2	C	-5.01	-5.31	
	4535	21.2	18.4	D	-5.67	-6.00	
			mean abundance:		-5.08	-5.39	uc
HD22374							
42	4533	16.1	15.9	D	-6.54	-6.86	
	4535	15.1	15.0	D	-6.36	-6.66	
			mean abundance:		-6.44	-6.75	uc

Table A-29, continued

mult.	λ	W	W_o	qual.	abundance 1	2	
HD81009							
42	4533	55.7	35.5	E	-6.10	-6.44	
			mean abundance:		-6.10	-6.44	uc
HD110066							
42	4549	25.9	22.0	D	-4.95	-5.30	
			mean abundance:		-4.95	-5.30	uc
HD111133							
42	4535	15.2	14.5	D	-5.32	-5.76	
			mean abundance:		-5.32	-5.76	uc
HD137909							
42	4518	11.6	11.6	D	-5.65	-5.95	
	4533	122.4	53.2	E	-5.22	-5.49	
	4535	57.8	36.6	C	-5.47	-5.71	
	4549	41.8	30.3	C	-5.01	-5.28	
44	4299	30.3	25.3	B	-5.60	-5.78	
			mean abundance:		-5.36	-5.55	a
HD137949							
42	4533	52.9	34.2	E	-6.51	-6.89	
			mean abundance:		-6.51	-6.89	uc
HD165474							
42	4535	34.7	28.0	D	-6.19	-6.56	
44	4286	15.3	15.3	D	-6.03	-6.38	
	4287	17.8	17.8	D	-5.91	-6.28	
	4299	11.7	11.6	D	-6.56	-6.88	
			mean abundance:		-6.13	-6.47	uc

Table A-29, continued

mult.	λ	W	W_o	qual.	abundance 1	2	
HD176232							
42	4518	10.1	9.6	D	-7.14	-7.47	
	4533	39.8	31.8	E	-7.18	-7.50	
	4535	31.3	26.5	E	-7.10	-7.40	
44	4286	9.5	9.3	D	-7.15	-7.46	
	4287	11.6	10.9	D	-7.05	-7.37	
			mean abundance:		-7.13	-7.45	uc
HD191742							
42	4512	20.4	18.4	D	-6.04	-6.40	
	4534	31.9	27.3	C	-6.44	-6.80	
44	4299	11.2	11.0	D	-6.76	-7.15	
			mean abundance:		-6.46	-6.72	uc
HD192678							
42	4549	7.5	7.5	D	-5.30	-5.59	
44	4287	15.4	15.4	D	-4.91	-5.16	
			mean abundance:		-5.07	-5.32	uc
HD201601							
42	4533	51.6	40.3	W	-6.99	-7.30	
	4535	33.4	28.1	E	-7.14	-7.39	
			mean abundance:		-7.06	-7.34	uc
HD204411							
42	4512	13.5	13.4	D	-5.66	-6.01	
	4535	17.9	17.5	D	-6.18	-6.52	
	4549	12.7	12.6	D	-5.78	-6.12	
			mean abundance:		-5.82	-6.17	uc

Table A-29, continued

mult.	λ	W	W_o	qual.	abundance 1	abundance 2	
HD216533							
42	4549	22.7	22.2	D	-4.69	-5.06	
			mean abundance:		-4.69	-5.06	uc

Notes: All lines with equivalent widths less than 20mA or with D quality have one-half weight in the mean abundance averages.
uc = mean abundance averages are poorly determined.
a = B quality lines are given double weight.

Table A-30

Ti Abundances from TiII Lines

mult.	λ	W	W_o	qual.	abundance 1	abundance 2
HD2453						
31	4468	127.0	83.5	A	-6.29	-6.40
40	4418	104.8	78.2	A	-5.87	-6.08
	4464	89.1	68.0	E	-5.69	-5.88
	4471	84.6	50.4	B	-6.02	-6.24
51	4394	76.0	45.8	A	-6.41	-6.55
	4418	83.7	49.2	C	-6.14	-6.27
60	4544	69.5	43.4	C	-5.88	-6.04
	4568	49.4	36.6	A	-6.19	-6.37
61	4396	71.5	44.1	B	-6.37	-6.54
	4398	31.0	27.0	B	-6.25	-6.43
	4409	51.6	34.9	G	-6.05	-6.24
	4410	97.1	53.1	G	-5.58	-5.75
	4412	79.7	47.2	C	-5.71	-5.87
			mean abundance:		-6.02	-6.21
HD5797						
31	4468	261.6	256.5	B	-5.19	-5.41
40	4418	203.9	199.9	A	-4.91	-5.09
	4464	209.8	201.7	E	-4.43	-4.62
	4471	150.3	136.6	A	-4.72	-4.92
41	4302	256.6	251.6	E	-4.72	-4.92
51	4394	174.3	160.0	B	-4.74	-4.91
	4418	143.5	128.1	A	-4.80	-4.96
60	4544	138.3	123.5	C	-4.47	-4.64
	4568	105.3	94.0	A	-5.05	-5.22
61	4396	157.7	143.4	B	-4.79	-4.97
	4398	113.2	104.8	A	-4.66	-4.80
	4409	106.4	84.4	C	-5.06	-5.23
	4410	116.2	94.5	C	-4.83	-5.02
	4412	138.3	121.3	B	-4.43	-4.59
			mean abundance:		-4.72	-4.91

Table A-30, continued

mult.	λ	W	W_o	qual.	abundance 1	abundance 2	
HD8441							
31	4468	36.5	36.5	C	-7.63	-7.83	
40	4418	30.4	30.4	C	-7.22	-7.43	
	4464	22.5	22.5	C	-6.99	-7.16	
41	4302	40.4	40.4	C	-7.08	-7.24	
51	4394	23.9	23.9	C	-7.02	-7.17	
60	4544	16.8	16.8	D	-6.61	-6.78	
	4568	14.3	14.3	C	-6.84	-7.01	
61	4396	30.8	30.8	C	-6.77	-6.95	
	4409	17.1	17.1	D	-6.59	-6.77	
	4410	28.3	28.3	C	-6.30	-6.48	
	4412	15.9	15.9	D	-6.59	-6.76	
			mean abundance:		-6.79	-6.97	
HD12288							
40	4418	177.6	103.3	C	-5.16	-5.46	
	4464	124.9	69.4	C	-5.52	-5.74	
51	4394	108.8	47.7	B	-6.23	-6.42	
	4418	107.1	46.4	B	-6.06	-6.24	
60	4544	99.1	45.3	B	-5.73	-5.91	
61	4396	124.7	53.8	C	-5.98	-6.18	
	4398	51.5	33.7	C	-5.97	-6.16	
	4410	65.0	37.0	C	-5.90	-6.10	+
			mean abundance:		-5.77	-5.97	

Table A-30, continued

mult.	λ	W	W_o	qual.	abundance 1	abundance 2	
HD18078							
31	4468	95.0	59.7	A	-7.07	-7.24	
40	4418	80.2	58.5	C	-6.56	-6.72	
	4464	59.5	44.7	E	-6.48	-6.65	
	4471	39.7	30.3	C	-6.70	-6.86	
51	4394	31.4	26.6	B	-7.00	-7.16	
	4418	50.0	40.0	C	-6.47	-6.62	
60	4544	20.8	19.1	D	-6.49	-6.76	
	4568	26.8	24.6	B	-6.60	-6.74	
61	4396	61.2	49.8	C	-6.35	-6.49	
	4398	26.8	23.5	C	-6.47	-6.61	
	4410	38.2	27.6	B	-6.39	-6.53	+
	4412	44.7	32.4	B	-6.22	-6.38	
			mean abundance:		-6.50	-6.67	
HD22374							
31	4468	60.2	58.4	B	-7.38	-7.54	
40	4418	50.0	49.0	B	-7.11	-7.27	
	4464	26.0	25.7	E	-7.24	-7.41	
	4471	29.5	29.2	C	-7.01	-7.20	
41	4302	75.8	74.3	D	-6.41	-6.56	
51	4394	29.1	28.8	C	-7.20	-7.35	
	4418	40.9	39.7	C	-6.74	-6.89	
60	4544	29.7	29.4	C	-6.59	-6.74	
	4568	16.3	16.1	D	-7.08	-7.22	
61	4396	26.9	26.6	C	-7.19	-7.33	
	4398	13.4	13.4	D	-6.98	-7.10	
	4409	22.6	22.4	C	-6.76	-6.90	
	4410	35.4	35.0	B	-6.46	-6.60	
	4412	28.1	27.8	C	-6.60	-6.75	
			mean abundance:		-6.83	-6.98	

Table A-30, continued

mult.	λ	W	W_o	qual.	abundance 1	abundance 2	
HD50169							
31	4468	100.0	52.6	C	-7.22	-7.40	
40	4418	94.8	57.1	C	-6.52	-6.72	
	4471	42.8	31.0	W	-6.64	-6.80	
51	4394	54.0	34.4	C	-6.76	-6.92	
	4418	56.9	35.6	C	-6.54	-6.70	
60	4568	33.6	26.7	D	-6.55	-6.68	
61	4396	69.4	39.7	C	-6.58	-6.74	
	4398	14.6	14.6	D	-6.68	-6.82	
	4409	29.7	26.8	G	-6.38	-6.50	
	4410	83.5	42.6	G	-5.95	-6.10	
	4412	39.3	29.3	C	-6.27	-6.45	
			mean abundance:		-6.40	-6.59	
HD81009							
31	4468	183.2	74.5	C	-7.01	-7.18	
40	4418	159.0	79.5	C	-6.33	-6.51	
	4471	127.8	52.0	E	-6.55	-6.68	
51	4394	81.4	40.5	C	-6.98	-7.13	
	4418	83.0	41.1	C	-6.76	-6.91	
60	4544	73.8	39.0	E	-6.44	-6.59	
	4568	49.0	32.7	B	-6.74	-6.91	
61	4396	108.0	47.2	C	-6.73	-6.89	
	4410	54.2	35.0	G	-6.52	-6.68	+
			mean abundance:		-6.63	-6.79	

Table A-30, continued

mult.	λ	W	W_o	qual.	abundance 1	abundance 2
HD89069						
31	4468	86.4	64.0	B	-7.01	-7.20
40	4418	82.3	70.9	B	-6.26	-6.46
	4464	70.0	60.3	E	-6.10	-6.29
	4471	69.5	51.9	C	-6.19	-6.41
41	4302	98.1	86.8	C	-5.90	-6.08
51	4394	66.7	48.7	B	-6.48	-6.66
	4418	40.8	32.6	C	-6.70	-6.90
60	4544	39.1	31.8	C	-6.33	-6.52
61	4396	56.5	42.8	C	-6.58	-6.77
	4398	35.9	32.1	C	-6.29	-6.49
	4409	27.4	24.7	G	-6.50	-6.70
	4410	44.2	34.3	C	-6.26	-6.45
	4412	49.1	37.5	C	-6.13	-6.34
			mean abundance:		-6.34	-6.53
HD110066						
31	4468	132.7	91.5	B	-6.25	-6.45
40	4418	101.0	76.5	A	-6.05	-6.23
	4464	74.0	56.5	E	-6.10	-6.31
	4471	61.2	40.0	B	-6.43	-6.65
51	4394	65.8	41.4	B	-6.61	-6.78
	4418	57.4	38.8	A	-6.47	-6.65
60	4544	43.1	32.9	C	-6.23	-6.44
	4568	32.2	27.1	B	-6.56	-6.70
61	4396	66.9	42.6	B	-6.50	-6.70
	4398	38.0	31.1	B	-6.26	-6.46
	4409	29.2	27.0	C	-6.38	-6.55
	4410	75.6	44.7	C	-5.92	-6.10
	4412	56.2	37.5	C	-6.06	-6.25
			mean abundance:		-6.32	-6.47

Table A-30, continued

mult.	λ	W	W_o	qual.	abundance 1	abundance 2
HD111133						
31	4468	67.2	44.2	B	-7.22	-7.47
40	4418	48.0	37.2	C	-6.87	-7.10
	4471	28.3	24.0	E	-6.57	-6.85
41	4302	62.5	47.0	C	-6.63	-6.86
51	4394	29.5	24.2	C	-6.81	-7.02
	4418	43.7	31.9	B	-6.40	-6.64
61	4396	52.8	36.7	C	-6.43	-6.64
	4409	15.9	15.3	D	-6.49	-6.68
	4410	44.5	32.7	C	-5.99	-6.21
	4412	17.0	15.7	C	-6.45	-6.61
			mean abundance:		-6.50	-6.70
HD118022						
31	4468	122.2	92.6	A	-6.29	-6.48
40	4418	96.8	79.3	B	-6.03	-6.24
	4471	87.5	59.1	C	-5.96	-6.17
51	4394	75.2	48.5	A	-6.46	-6.64
	4418	70.6	47.4	B	-6.26	-6.48
60	4544	58.9	42.4	C	-6.05	-6.24
	4568	42.8	34.2	B	-6.41	-6.60
61	4396	75.6	51.8	C	-6.32	-6.49
	4409	46.9	34.0	G	-6.23	-6.45
	4410	79.6	49.1	G	-5.84	-6.04
	4412	62.3	42.1	C	-6.00	-6.19
			mean abundance:		-6.16	-6.34

Table A-30, continued

mult.	λ	W	W_o	qual.	abundance 1	abundance 2	
HD137909							
31	4468	218.6	139.2	B	-5.79	-5.91	
40	4418	191.5	141.0	B	-5.24	-5.36	
	4464	152.6	106.0	D	-5.13	-5.30	
	4471	156.8	74.0	C	-5.62	-5.81	
41	4302	184.4	136.6	C	-5.23	-5.43	
51	4394	117.6	54.7	B	-6.39	-6.50	
	4418	103.8	50.9	B	-6.29	-6.43	
60	4544	104.6	52.8	C	-5.84	-6.02	
	4568	64.5	40.3	B	-6.34	-6.50	
61	4398	67.7	43.4	C	-6.08	-6.22	
	4409	109.8	49.9	G	-5.93	-6.05	
	4410	131.0	56.7	G	-5.73	-5.84	
	4412	147.4	66.4	C	-5.40	-5.50	
			mean abundance:		-5.65	-5.80	
HD137949							
31	4468	178.3	116.5	C	-6.44	-6.63	
40	4418	130.0	91.5	C	-6.27	-6.45	
	4471	97.9	52.9	W	-6.67	-6.85	
41	4302	153.9	118.4	C	-5.91	-6.08	
51	4394	77.3	43.4	B	-7.08	-7.24	
	4418	56.2	36.3	E	-7.06	-7.22	
61	4396	102.7	55.5	C	-6.69	-6.83	
	4398	20.1	19.5	D	-7.00	-7.23	
	4410	64.7	38.3	G	-6.62	-6.76	+
	4412	125.5	63.4	E	-5.85	-6.00	
			mean abundance:		-6.33	-6.52	

Table A-30, continued

mult.	λ	W	W_o	qual.	abundance 1	abundance 2	
HD165474							
31	4468	151.3	69.4	A	-7.20	-7.37	
40	4418	164.1	97.1	C	-6.04	-6.22	
	4471	96.8	46.1	C	-6.73	-6.90	
51	4394	97.1	45.6	C	-6.91	-7.06	
	4418	59.4	36.7	C	-6.93	-7.10	
60	4544	66.5	38.2	C	-6.52	-6.68	
	4568	44.3	31.4	C	-6.83	-6.98	
61	4396	83.8	43.0	C	-7.07	-7.22	
	4398	38.1	28.9	C	-6.70	-6.85	
	4410	61.2	36.4	G	-6.59	-6.71	+
	4412	60.0	36.1	C	-6.52	-6.67	
			mean abundance:		-6.64	-6.79	
HD176232							
31	4468	113.7	97.1	B	-6.99	-7.14	
40	4418	96.6	80.5	C	-6.77	-6.92	
	4464	62.0	54.9	C	-7.00	-7.15	
	4471	53.6	41.6	C	-7.16	-7.38	
41	4302	101.7	91.6	C	-6.55	-6.71	
51	4394	87.3	66.1	C	-6.65	-6.77	
	4418	75.9	57.9	C	-6.68	-6.83	
60	4544	35.3	29.4	E	-7.11	-7.27	
	4568	21.2	19.4	C	-7.42	-7.68	
61	4396	56.4	48.6	B	-7.12	-7.28	
	4398	32.6	27.6	C	-7.12	-7.29	
	4409	51.7	38.9	G	-6.84	-7.02	
	4410	58.6	43.4	C	-6.73	-6.89	
	4412	76.5	57.5	C	-6.26	-6.41	
			mean abundance:		-6.82	-6.97	

Table A-30, continued

mult.	λ	W	W_o	qual.	abundance 1	abundance 2
HD191742						
31	4468	125.0	112.6	C	-6.45	-6.65
40	4418	75.5	68.0	A	-6.80	-6.98
	4464	83.9	77.0	E	-6.10	-6.28
	4471	60.2	48.2	B	-6.78	-6.96
51	4394	80.8	64.1	B	-6.46	-6.60
	4418	96.6	79.8	C	-5.81	-5.99
60	4544	49.2	40.3	C	-6.57	-6.73
	4568	37.5	33.5	C	-6.89	-7.04
61	4396	54.8	44.5	A	-6.97	-7.13
	4398	23.5	22.4	B	-6.95	-7.13
	4409	46.7	37.1	C	-6.63	-6.79
	4410	71.8	54.4	B	-6.13	-6.29
	4412	65.3	51.0	C	-6.20	-6.35
			mean abundance:		-6.43	-6.59
HD192678						
31	4468	136.6	79.0	B	-6.38	-6.55
40	4418	124.4	86.4	C	-5.65	-5.82
	4464	102.9	72.5	E	-5.54	-5.70
	4471	88.4	49.1	C	-6.04	-6.19
51	4394	90.2	48.2	B	-6.30	-6.42
	4418	77.1	44.1	C	-6.22	-6.33
60	4544	53.7	35.8	E	-6.03	-6.17
	4568	42.9	32.5	C	-6.28	-6.41
61	4396	101.6	55.2	C	-6.05	-6.17
	4398	38.1	31.2	C	-6.12	-6.26
	4409	44.1	32.1	G	-6.12	-6.26
	4410	108.8	53.3	C	-5.57	-5.69
			mean abundance:		-5.97	-6.12

Table A-30, continued

mult.	λ	W	W_o	qual.	abundance 1	abundance 2
HD201601						
31	4468	119.5	113.8	B	-6.71	-6.93
40	4418	95.2	87.3	B	-6.64	-6.80
	4464	53.6	48.3	E	-7.22	-7.36
	4471	68.8	55.5	C	-6.86	-7.01
41	4302	97.1	89.1	C	-6.60	-6.78
51	4394	53.4	42.0	B	-7.41	-7.57
	4418	55.1	43.7	C	-7.14	-7.29
60	4544	37.9	32.4	E	-7.04	-7.23
	4568	19.4	18.3	C	-7.57	-7.72
61	4396	49.9	40.6	C	-7.36	-7.53
	4398	16.2	15.6	E	-7.44	-7.62
	4409	35.4	29.3	G	-7.11	-7.28
	4410	44.3	35.4	G	-6.95	-7.13
	4412	47.2	37.8	C	-6.86	-7.02
			mean abundance:		-6.93	-7.11
HD204411						
31	4468	119.4	115.9	A	-6.16	-6.30
40	4418	104.0	102.0	A	-5.78	-5.95
	4464	66.4	65.1	E	-6.14	-6.30
	4471	52.2	50.7	B	-6.41	-6.60
41	4302	105.8	103.7	C	-5.70	-5.96
51	4394	76.7	74.5	A	-5.90	-6.05
	4418	73.4	71.3	B	-5.79	-5.95
60	4544	31.6	31.0	C	-6.52	-6.70
	4568	26.7	26.4	C	-6.79	-6.96
61	4396	74.5	72.3	C	-5.90	-6.05
	4398	36.0	35.3	C	-6.40	-6.58
	4409	47.3	45.5	C	-6.14	-6.30
	4410	51.3	49.3	C	-6.03	-6.19
	4412	56.7	55.0	C	-5.82	-5.99
			mean abundance:		-5.99	-6.16

Table A-30, continued

mult.	λ	W	W_o	qual.	abundance 1	abundance 2
HD216533						
31	4468	95.6	71.9	A	-6.57	-6.79
40	4418	66.9	57.2	C	-6.44	-6.65
	4471	43.0	34.1	C	-6.45	-6.67
51	4394	60.8	44.7	A	-6.40	-6.58
	4418	47.8	37.1	C	-6.38	-6.59
60	4544	39.0	31.7	E	-6.14	-6.33
	4568	23.8	21.3	C	-6.57	-6.74
61	4396	62.3	47.2	C	-6.27	-6.45
	4398	33.7	30.1	B	-6.14	-6.36
	4409	34.1	28.9	G	-6.20	-6.39
	4410	59.6	42.9	C	-5.83	-6.03
	4412	48.5	37.0	B	-5.94	-6.15
			mean abundance:		-6.21	-6.41
ν Cap						
31	4468	63.9	40.4	-	-7.40	-7.61
40	4418	36.6	28.4	-	-7.14	-7.37
41	4302	43.1	31.7	-	-7.10	-7.34
51	4394	16.7	15.5	-	-7.13	-7.31
			mean abundance:		-7.18	-7.39

Table A-30, continued

mult.	λ	W	W_o	qual.	abundance 1	abundance 2
o Peg						
31	4468	86.6	50.9	B	-7.28	-7.46
40	4418	77.6	46.7	C	-6.85	-7.04
	4464	37.8	29.1	C	-6.77	-7.00
41	4302	79.1	47.4	B	-6.86	-7.04
51	4394	41.6	31.0	A	-6.91	-7.03
	4418	25.1	21.5	C	-6.90	-7.05
61	4396	25.8	21.9	C	-7.03	-7.19
			mean abundance:		-6.94	-7.11

Notes: A and B quality lines are given double weight in the mean abundance averages.
D quality lines and those whose equivalent width is less than 20mA are given one-half weight.
+ = The blend contains both λ4409.220 and λ4409.519. The values given are for one component. The blend is given the weight of a single line.

Table A-31

V Abundances

ion	mult.	λ	W	W_o	qual.	abundance 1	abundance 2	
HD2453								
VII	37	4183	12.6	12.6	D	-8.08	-8.20	
			mean abundance:			-8.08	-8.20	uc
HD5797								
VII	25	4202	26.5	23.7	E	-7.77	-7.89	
	37	4183	30.9	27.8	D	-7.87	-8.00	
			mean abundance:			-7.82	-7.94	
HD8441								
VII	25	4202	17.1	17.1	E	-7.73	-7.87	
	37	4183	16.5	16.5	C	-7.99	-8.12	
			mean abundance:			-7.84	-7.98	
HD18078								
VII	25	4202	26.6	23.8	E	-7.58	-7.71	
	37	4183	33.5	27.2	C	-7.71	-7.84	
			mean abundance:			-7.64	-7.77	
HD50169								
VII	37	4183	13.4	13.1	W	-8.13	-8.22	
			mean abundance:			-8.13	-8.22	uc
HD81009								
VII	37	4183	47.0	31.8	E	-7.86	-8.00	
			mean abundance:			-7.86	-8.00	uc

Table A-31, continued

ion	mult.	λ	W	W_o	qual.	abundance 1	abundance 2	
HD89069								
VII	25	4202	28.2	24.7	W	-7.60	-7.76	
	37	4183	32.3	27.4	W	-7.75	-7.91	
			mean abundance:			-7.67	-7.83	uc
HD110066								
VII	25	4202	25.8	24.1	C	-7.60	-7.73	
	37	4183	35.6	29.2	C	-7.65	-7.80	
			mean abundance:			-7.62	-7.76	
HD111133								
VII	37	4183	19.2	19.1	D	-7.74	-7.92	
			mean abundance:			-7.74	-7.92	uc
HD137909								
VII	25	4178	31.1	25.5	D	-7.21	-7.33	
	37	4183	43.9	31.6	E	-7.72	-7.82	
			mean abundance:			-7.48	-7.59	a
HD137949								
VII	25	4202	40.8	30.7	W	-7.83	-7.98	
	37	4183	100.0	62.9	E	-7.16	-7.27	
			mean abundance:			-7.29	-7.41	a
HD165474								
VII	37	4183	30.0	24.6	D	-8.10	-8.24	
			mean abundance:			-8.10	-8.24	uc

Table A-31, continued

ion	mult.	λ	W	W_o	qual.	abundance 1	abundance 2
HD176232							
VI	22	4379	18.0	16.5	C	-7.51	-7.87
			mean abundance from VI:			-7.51	-7.87
VII	25	4178	23.6	21.3	C	-7.90	-8.05
		4202	36.4	30.3	E	-8.10	-8.23
	37	4183	51.0	41.5	C	-7.98	-8.10
			mean abundance from VII:			-7.99	-8.12
			mean abundance:			-7.81	-8.04
HD191742							
VII	25	4178	38.8	28.6	C	-7.43	-7.59
		4202	21.1	19.0	E	-8.13	-8.29
	37	4183	70.1	59.4	C	-7.23	-7.37
			mean abundance:			-7.46	-7.60
HD192678							
VII	25	4178	21.5	19.0	C	-7.17	-7.27
	37	4183	48.2	33.9	E	-7.43	-7.53
			mean abundance:			-7.28	-7.38
HD201601							
VI	22	4379	30.8	26.8	B	-7.26	-7.62
		4390	20.8	19.3	D	-7.06	-7.42
			mean abundance from VI:			-7.18	-7.54 a

Table A-31, continued

ion	mult.	λ	W	W_o	qual.	abundance 1	abundance 2	
HD201601(continued)								
VII	25	4178	47.1	42.9	C	-7.32	-7.47	
		4202	77.9	63.8	E	-7.14	-7.25	
	37	4183	75.2	64.3	C	-7.32	-7.42	
			mean abudance from VII:			-7.22	-7.37	
			mean abundance:			-7.20	-7.45	
HD204411								
VII	25	4202	17.7	17.7	D	-7.94	-8.09	
	37	4183	15.1	15.1	D	-8.23	-8.36	
			mean abundance:			-8.06	-8.20	uc
HD216533								
VII	25	4202	12.4	12.3	W	-7.81	-7.99	
	37	4183	16.0	14.7	D	-7.98	-8.13	
			mean abundance:			-7.89	-8.05	uc
ν Cap								
VII	32	4006	24.2	20.9	-	-8.48	-8.63	b
			mean abundance:			-8.48	-8.63	
o Peg								
VII	37	4183	17.6	16.1	C	-8.03	-8.15	
			mean abundance:			-8.03	-8.15	

Notes: a = W and D quality lines are given one-half weight in the mean abundance averages.
b = χ(eV)=1.82 and log gf=-0.22(Warner 1967).
uc = uncertain determination.
The mean abundance is determined using VI and VII line averages weighted by the number of lines measured.

Table A-32

Cr Abundances from CrI Lines

mult.	λ	W	W_o	qual.	abundance 1	abundance 2	
HD2453							
1	4275	178.0	82.4	A	-4.04	-4.36	
10	4497	98.4	55.6	C	-3.50	-3.82	
	4546	149.6	66.2	A	-3.01	-3.32	
22	4360	115.7	67.7	B	-2.94	-3.26	
	4371	113.9	63.3	C	-3.05	-3.38	
	4385	95.5	53.1	C	-3.32	-3.53	
			mean abundance:		-3.12	-3.43	
HD5797							
1	4275	220.0	193.0	B	-3.54	-3.79	
10	4497	146.8	129.9	A	-2.66	-2.97	
	4546	189.1	155.0	A	-2.16	-2.56	
21	4616	202.8	181.1	C	-2.23	-2.58	
22	4360	146.8	132.3	C	-2.49	-2.83	
	4371	112.2	93.5	C	-2.95	-3.28	
	4385	111.9	91.7	C	-2.82	-3.15	
			mean abundance:		-2.52	-2.84	a
HD8441							
1	4275	100.8	100.8	B	-3.83	-4.16	
10	4497	50.0	50.0	C	-3.77	-4.10	
	4546	59.0	59.0	B	-3.34	-3.67	
22	4360	43.8	43.8	C	-3.80	-4.10	
	4371	38.3	38.3	C	-3.94	-4.25	
	4385	28.8	28.8	C	-4.04	-4.36	
			mean abundance:		-3.66	-3.99	a,b

Table A-32, continued

mult.	λ	W	W_o	qual.	abundance 1	abundance 2	
HD12288							
1	4275	222.3	66.6	A	-4.22	-4.59	
10	4497	175.3	66.2	C	-3.01	-3.32	
	4546	154.0	52.6	C	-3.21	-3.55	
22	4360	121.4	52.3	C	-3.22	-3.56	
			mean abundance:		-3.24	-3.58	
HD18078							
1	4275	153.6	69.8	A	-4.61	-4.91	
10	4497	100.5	56.5	C	-3.68	-3.99	
	4546	70.8	39.8	B	-4.00	-4.34	
21	4616	148.5	71.1	C	-3.22	-3.51	
22	4360	117.9	68.9	B	-3.15	-3.43	
	4371	81.3	47.3	C	-3.79	-4.07	
	4385	56.7	37.1	B	-3.93	-4.20	
			mean abundance:		-3.55	-3.83	a
HD22374							
1	4275	122.0	117.3	A	-4.26	-4.52	
10	4497	81.2	78.8	B	-3.58	-3.85	
	4546	65.0	61.3	B	-3.86	-4.17	
22	4360	68.8	66.8	B	-3.72	-3.99	
	4385	58.1	55.9	B	-3.87	-4.14	
			mean abundance:		-3.81	-4.08	

Table A-32, continued

mult.	λ	W	W_o	qual.	abundance 1	abundance 2	
HD50169							
1	4275	201.0	70.1	A	-4.50	-4.80	
10	4497	144.7	63.7	C	-3.40	-3.70	
	4546	117.4	48.3	B	-3.71	-3.99	
21	4616	155.5	59.1	E	-3.48	-3.78	
22	4360	130.3	61.2	B	-3.29	-3.58	
	4371	99.8	48.0	E	-3.68	-3.97	
	4385	80.5	42.1	C	-3.71	-3.99	
			mean abundance:		-3.54	-3.83	a
HD81009							
1	4275	166.4	53.9	C	-5.68	-5.92	
10	4497	113.2	47.6	C	-4.57	-4.86	
	4546	84.5	41.0	C	-4.57	-4.89	
21	4616	105.1	44.2	E	-4.61	-4.95	
22	4360	112.3	48.0	E	-4.40	-4.74	
	4371	104.9	45.6	E	-4.45	-4.80	
			mean abundance:		-4.58	-4.91	
HD89069							
1	4275	132.5	83.9	B	-4.33	-4.72	
10	4497	87.1	63.1	E	-3.60	-3.96	
	4546	55.5	37.5	E	-4.15	-4.47	
22	4360	68.3	51.4	C	-3.73	-4.13	
	4371	79.3	57.5	C	-3.55	-3.93	
	4385	41.5	32.9	C	-4.14	-4.51	
			mean abundance:		-3.82	-4.19	

Table A-32, continued

mult.	λ	W	W_o	qual.	abundance 1	abundance 2	
HD110066							
1	4275	186.7	92.0	B	-4.05	-4.39	
10	4497	127.7	73.4	B	-3.17	-3.51	
	4546	144.7	66.4	A	-3.17	-3.51	
22	4360	116.2	72.6	B	-2.99	-3.34	
	4371	110.6	66.6	C	-3.16	-3.48	
	4385	99.6	56.3	B	-3.30	-3.65	
			mean abundance:		-3.18	-3.53	a
HD111133							
1	4275	99.1	49.3	A	-4.73	-5.12	
10	4497	65.7	41.1	C	-3.68	-4.06	
	4546	60.7	37.0	B	-3.63	-3.99	
22	4360	62.0	40.3	E	-3.57	-3.95	
	4371	54.8	36.8	E	-3.66	-4.00	
	4385	31.9	25.7	C	-3.82	-4.19	
			mean abundance:		-3.72	-4.08	a
HD118022							
1	4275	152.9	84.9	A	-4.26	-4.65	
10	4497	99.2	64.0	A	-3.52	-3.89	
	4546	109.0	57.7	B	-3.56	-3.92	
22	4360	75.5	51.0	C	-3.73	-4.10	
	4371	61.4	41.5	E	-4.01	-4.36	
	4385	69.1	44.3	C	-3.77	-4.12	
			mean abundance:		-3.68	-4.04	a

Table A-32, continued

mult.	λ	W	W_o	qual.	abundance 1	abundance 2	
HD137909							
1	4275	222.8	79.4	B	-4.62	-4.84	
10	4497	123.0	56.2	B	-3.96	-4.20	
	4546	133.4	53.6	C	-3.88	-4.11	
21	4616	174.6	67.4	C	-3.56	-3.83	
22	4371	94.8	47.2	C	-4.05	-4.28	
			mean abundance:		-3.91	-4.16	a
HD137949							
1	4275	177.1	70.6	C	-5.52	-5.83	
10	4497	127.9	63.6	C	-4.48	-4.78	
	4546	78.5	40.5	C	-4.89	-5.31	
21	4616	137.5	59.0	C	-4.56	-4.89	
22	4360	118.0	62.1	C	-4.33	-4.66	
	4371	70.6	40.8	E	-4.98	-5.32	
			mean abundance:		-4.65	-4.98	
HD165474							
1	4275	168.9	56.3	C	-5.69	-5.96	
10	4497	92.5	44.3	B	-4.76	-5.09	
	4546	89.3	41.0	C	-4.67	-5.02	
21	4616	119.6	44.3	C	-4.75	-5.08	
22	4360	109.6	49.9	C	-4.46	-4.80	
	4371	77.0	40.3	C	-4.75	-5.07	
	4385	79.7	40.7	D	-4.58	-4.90	
			mean abundance:		-4.71	-5.06	a,c

Table A-32, continued

mult.	λ	W	W_o	qual.	abundance 1	abundance 2	
HD176232							
1	4275	173.4	128.4	A	-5.18	-5.50	
10	4497	61.6	46.3	B	-5.51	-5.79	
	4546	73.0	45.9	C	-5.34	-5.63	
21	4614	89.7	59.8	C	-5.03	-5.30	
22	4360	67.5	51.9	C	-5.15	-5.44	
	4371	63.8	48.0	C	-5.26	-5.57	
	4385	59.4	44.3	C	-5.24	-5.53	
			mean abundance:		-5.24	-5.54	a,b
HD191742							
1	4275	190.4	160.3	A	-4.33	-4.68	
10	4497	103.9	85.2	A	-3.86	-4.20	
	4546	150.8	113.4	A	-3.23	-3.56	
21	4616	152.3	122.8	B	-3.27	-3.54	
22	4360	95.3	78.8	B	-3.83	-4.18	
	4371	105.7	87.4	B	-3.64	-3.97	
	4385	101.6	81.3	B	-3.60	-3.96	
			mean abundance:		-3.56	-3.88	
HD192678							
1	4275	201.0	81.0	A	-4.04	-4.26	
10	4497	135.4	67.0	A	-3.11	-3.33	
	4546	163.3	66.7	B	-2.95	-3.19	
21	4616	209.2	92.2	C	-2.46	-2.70	
22	4360	142.4	75.7	B	-2.67	-2.92	
	4371	132.5	65.6	E	-2.93	-3.18	
	4385	111.2	55.0	B	-3.11	-3.34	
			mean abundance:		-2.88	-3.12	a

Table A-32, continued

mult.	λ	W	W_o	qual.	abundance 1	abundance 2	
HD201601							
1	4275	134.6	100.4	B	-5.52	-5.84	
10	4497	82.2	64.7	E	-4.96	-5.24	
	4546	55.9	39.9	C	-5.59	-5.84	
21	4616	72.2	52.3	C	-5.31	-5.59	
22	4360	72.5	58.5	E	-4.98	-5.24	
	4371	54.2	42.3	C	-5.49	-5.78	
	4385	37.4	30.9	E	-5.70	-5.97	
			mean abundance:		-5.28	-5.58	b
HD204411							
1	4275	117.4	112.9	A	-4.20	-4.52	
10	4497	61.2	59.4	C	-4.02	-4.36	
	4546	54.3	50.7	B	-4.10	-4.40	
21	4616	63.5	60.5	C	-3.96	-4.26	
22	4360	68.6	66.6	C	-3.61	-3.96	
	4371	62.7	60.9	C	-3.79	-4.11	
	4385	42.2	41.0	C	-4.20	-4.57	
			mean abundance:		-3.97	-4.28	a,b
HD216533							
1	4275	127.2	79.5	B	-4.08	-4.43	
10	4497	77.6	56.2	C	-3.43	-3.80	
	4546	113.0	67.3	C	-2.96	-3.32	
21	4616	109.7	70.3	E	-2.96	-3.32	
22	4360	76.2	56.9	C	-3.25	-3.58	
	4371	75.3	54.2	C	-3.29	-3.64	
	4385	56.7	41.7	B	-3.49	-3.87	
			mean abundance:		-3.26	-3.62	a

Table A-32, continued

mult.	λ	W	W_o	qual.	abundance 1	abundance 2
ν Cap						
1	4275	12.1	11.6	-	-5.94	-6.27
			mean abundance:		-5.94	-6.27
o Peg						
1	4275	30.0	24.6	C	-5.82	-6.11
			mean abundance:		-5.82	-6.11

Notes: a. A and B quality lines except λ4275 are given double weight in the mean abundance averages.
b. λ4275 is given double weight.
c. D quality lines are given one-half weight.

Table A-33

Cr Abundances from CrII Lines

mult.	λ	W	W_o	qual.	abundance 1	abundance 2
HD2453						
18	4217	113.3	88.5	A	-4.16	-4.28
31	4246	148.2	64.4	B	-3.61	-3.69
	4253	172.1	134.1	B	-3.59	-3.68
	4269	177.7	148.1	B	-3.28	-3.38
	4276	153.2	120.6	B	-4.26	-4.36
	4284	146.4	135.6	C	-3.81	-3.89
162	4225	102.1	92.5	A	-3.94	-4.03
			mean abundance:		-3.68	-3.78
HD5797						
18	4217	146.4	139.4	B	-3.75	-3.87
31	4253	182.4	175.3	B	-3.48	-3.58
	4269	196.5	190.8	B	-3.17	-3.29
	4276	182.7	175.7	A	-4.00	-4.11
	4284	200.7	96.8	C	-3.56	-3.68
162	4225	144.3	137.4	A	-3.53	-3.61
			mean abundance:		-3.51	-3.63
HD8441						
18	4217	110.4	110.4	A	-3.87	-4.00
31	4246	71.9	71.9	C	-3.38	-3.50
	4253	116.3	116.3	C	-3.83	-3.91
	4269	87.0	87.0	C	-4.07	-4.18
	4276	101.0	101.0	B	-4.53	-4.65
	4284	98.0	98.0	C	-4.28	-4.38
162	4225	130.6	130.6	B	-3.48	-3.56
			mean abundance:		-3.77	-3.87

Table A-33, continued

mult.	λ	W	W_o	qual.	abundance 1	abundance 2
HD12288						
18	4217	167.0	146.5	B	-3.36	-3.50
31	4253	252.2	225.2	C	-2.98	-3.09
	4269	248.7	228.2	C	-2.77	-2.88
	4276	184.2	156.1	A	-3.88	-3.99
	4284	205.8	199.8	B	-3.30	-3.43
162	4225	169.6	146.2	C	-3.27	-3.34
			mean abundance:		-3.19	-3.30
HD18078						
18	4217	128.2	103.4	A	-4.01	-4.12
31	4246	120.9	54.7	C	-3.92	-4.00
	4253	154.2	116.0	B	-3.85	-3.96
	4269	154.7	122.8	A	-3.58	-3.69
	4276	148.3	115.9	B	-4.39	-4.48
	4284	136.9	125.6	C	-3.97	-4.06
162	4225	126.0	100.0	B	-3.88	-3.95
			mean abundance:		-3.88	-3.98
HD22374						
18	4217	80.0	78.4	A	-4.65	-4.75
31	4246	66.2	62.4	B	-3.84	-3.92
	4253	102.2	100.2	B	-4.20	-4.29
	4269	97.7	95.8	B	-4.07	-4.16
	4276	108.6	107.5	B	-4.63	-4.72
	4284	104.0	103.0	B	-4.38	-4.46
162	4225	73.8	72.4	A	-4.57	-4.63
			mean abundance:		-4.24	-4.32

Table A-33, continued

mult.	λ	W	W_o	qual.	abundance 1	abundance 2
HD50169						
18	4217	158.1	109.0	B	-3.90	-4.02
31	4246	199.6	66.1	C	-3.58	-3.68
	4253	212.5	146.5	C	-3.54	-3.62
	4269	200.9	144.5	C	-3.35	-3.44
	4276	183.3	125.2	B	-4.26	-4.35
	4284	161.4	140.3	C	-3.81	-3.89
162	4225	119.6	74.8	C	-4.39	-4.48
			mean abundance:		-3.76	-3.86
HD81009						
18	4217	111.9	58.3	E	-5.24	-5.35
31	4253	174.7	78.0	C	-4.67	-4.77
	4269	177.2	85.2	C	-4.31	-4.39
	4276	147.4	69.5	C	-5.43	-5.51
	4284	129.9	89.0	C	-4.66	-4.75
162	4225	107.6	55.5	E	-5.07	-5.14
			mean abundance:		-4.74	-4.82
HD89069						
18	4217	84.0	73.7	B	-4.61	-4.75
31	4246	82.0	49.4	C	-4.07	-4.20
	4253	146.7	132.2	C	-3.70	-3.82
	4269	128.8	116.0	B	-3.68	-3.78
	4276	114.4	96.0	C	-4.69	-4.79
	4284	115.3	109.8	E	-4.17	-4.29
162	4225	90.3	86.0	C	-4.16	-4.24
			mean abundance:		-4.00	-4.10

Table A-33, continued

mult.	λ	W	W_o	qual.	abundance 1	abundance 2
HD110066						
18	4217	154.4	134.3	E	-3.61	-3.76
31	4246	155.0	69.8	C	-3.48	-3.58
	4253	189.4	159.2	B	-3.45	-3.56
	4269	184.7	159.2	B	-3.24	-3.36
	4276	165.8	140.8	A	-4.13	-4.22
	4284	135.0	125.0	B	-3.96	-4.07
162	4225	130.1	106.6	A	-3.77	-3.86
			mean abundance:		-3.58	-3.70
HD111133						
18	4217	94.6	72.8	C	-4.44	-4.57
31	4246	110.0	51.6	C	-3.90	-4.00
	4253	139.6	103.4	C	-3.90	-3.98
	4269	143.9	113.3	C	-3.55	-3.66
	4276	119.5	90.5	C	-4.63	-4.74
	4284	106.6	101.5	E	-4.16	-4.24
162	4225	84.9	63.8	C	-4.58	-4.73
			mean abundance:		-4.01	-4.11
HD118022						
18	4217	98.0	82.4	A	-4.39	-4.51
31	4246	120.9	62.6	E	-3.72	-3.82
	4253	155.6	134.1	C	-3.67	-3.79
	4269	153.5	135.8	C	-3.46	-3.58
	4276	146.0	128.1	B	-4.26	-4.38
	4284	131.9	124.4	C	-3.99	-4.11
162	4225	100.4	83.7	C	-4.19	-4.28
			mean abundance:		-3.91	-3.98

Table A-33, continued

mult.	λ	W	W_o	qual.	abundance 1	abundance 2
HD137909						
31	4246	108.4	46.3	E	-4.23	-4.31
	4253	146.9	83.9	C	-4.44	-4.49
	4276	176.7	116.2	A	-4.46	-4.52
	4284	136.5	114.7	C	-4.16	-4.23
162	4225	115.6	73.2	C	-4.50	-4.55
			mean abundance:		-4.35	-4.42
HD137949						
18	4217	146.5	111.0	W	-4.25	-4.36
31	4269	154.6	108.6	C	-4.03	-4.10
	4276	162.4	116.0	C	-4.66	-4.75
	4284	101.7	85.5	C	-4.82	-4.90
162	4225	107.1	74.4	C	-4.61	-4.66
			mean abundance:		-4.39	-4.47
HD165474						
18	4217	97.9	55.9	E	-5.36	-5.47
31	4253	126.2	63.1	C	-5.10	-5.16
	4269	156.0	83.9	C	-4.38	-4.46
	4276	125.8	65.9	B	-5.56	-5.62
	4284	104.6	75.8	C	-4.99	-5.07
162	4225	111.8	62.8	C	-4.89	-4.94
			mean abundance:		-4.93	-5.00

Table A-33, continued

mult.	λ	W	W_o	qual.	abundance 1	abundance 2
HD176232						
18	4217	62.5	55.3	E	-5.62	-5.68
31	4246	38.2	30.6	C	-5.00	-5.06
	4253	84.8	71.9	B	-5.02	-5.06
	4269	88.8	77.2	C	-4.69	-4.73
	4276	74.1	63.3	C	-5.78	-5.83
	4284	80.0	75.5	B	-5.16	-5.19
162	4225	53.7	46.7	B	-5.46	-5.45
			mean abundance:		-5.13	-5.17
HD191742						
31	4246	93.7	62.9	B	-3.94	-4.01
	4253	149.6	139.8	B	-3.89	-3.97
	4269	146.3	138.0	C	-3.70	-3.78
	4276	161.4	153.7	A	-4.31	-4.40
	4284	142.1	139.3	C	-4.11	-4.19
162	4225	96.6	88.6	A	-4.29	-4.34
			mean abundance:		-3.98	-4.08
HD192678						
18	4217	124.6	90.3	A	-4.11	-4.19
31	4246	168.8	64.9	C	-3.55	-3.62
	4253	216.6	170.6	B	-3.31	-3.37
	4276	174.3	128.2	B	-4.17	-4.25
	4284	145.6	131.2	C	-3.84	-3.90
162	4225	146.0	109.0	B	-3.68	-3.74
			mean abundance:		-3.67	-3.73

Table A-33, continued

mult.	λ	W	W_o	qual.	abundance 1	abundance 2
HD201601						
18	4217	65.0	52.8	E	-5.71	-5.77
31	4246	29.6	26.0	C	-5.13	-5.18
	4253	87.6	77.5	C	-4.88	-4.92
	4269	63.5	56.2	C	-5.28	-5.32
	4276	71.6	63.4	C	-5.77	-5.83
	4284	74.8	71.2	C	-5.27	-5.31
162	4225	51.9	42.2	C	-5.57	-5.57
			mean abundance:		-5.27	-5.31
HD204411						
31	4246	31.0	29.8	C	-4.75	-4.84
	4253	82.4	80.8	B	-4.54	-4.64
	4269	91.1	89.3	B	-4.16	-4.25
	4276	93.0	90.3	A	-4.87	-4.97
	4284	111.9	110.8	B	-4.26	-4.35
162	4225	58.0	56.9	A	-5.00	-5.05
			mean abundance:		-4.47	-4.56
HD216533						
18	4217	100.4	91.3	B	-4.10	-4.21
31	4246	88.0	52.4	C	-3.92	-4.01
	4253	140.7	126.8	C	-3.65	-3.76
	4269	127.0	113.4	C	-3.61	-3.71
	4276	131.4	118.4	C	-4.28	-4.38
	4284	165.7	160.9	C	-3.56	-3.70
162	4225	109.8	105.6	B	-3.73	-3.82
			mean abundance:		-3.80	-3.90

Table A-33, continued

mult.	λ	W	W_o	qual.	abundance 1	abundance 2
ν Cap						
31	4276	30.3	24.4	-	-6.41	-6.51
	4284	34.0	27.0	-	-6.03	-6.13
162	4225	23.2	20.2	-	-5.84	-5.91
			mean abundance:		-6.04	-6.12
o Peg						
31	4253	28.7	23.7	B	-5.98	-6.08
	4269	33.9	26.9	C	-5.70	-5.78
	4276	46.9	33.3	B	-6.24	-6.30
	4284	45.9	32.8	A	-5.95	-6.04
162	4225	26.2	22.2	C	-5.84	-5.90
			mean abundance:		-5.96	-6.03

Notes: A and B quality lines are given double weight in the mean abundance averages while those of D and W quality are given one-half weight.

Table A-34

Mn Abundances from MnI Lines

mult.	λ	W	W_o	qual.	abundance 1	abundance 2	
HD2453							
22	4470	35.0	28.0	C	-5.02	-5.27	
	4502	40.6	30.3	C	-4.94	-5.19	
23	4258	40.6	30.8	D	-5.14	-5.40	
	4266	41.0	30.8	C	-5.12	-5.38	
			mean abundance:		-5.05	-5.29	
HD5797							
22	4453	73.0	56.2	E	-4.80	-5.11	
	4470	42.2	35.2	B	-5.31	-5.63	
	4502	67.5	51.1	B	-4.86	-5.19	
23	4258	66.5	52.8	C	-4.98	-5.28	
	4266	83.4	65.2	C	-4.58	-4.87	
			mean abundance:		-4.89	-5.20	
HD8441							
23	4258	10.1	10.1	D	-5.94	-6.22	
	4266	14.9	14.9	D	-5.72	-6.01	
			mean abundance:		-5.82	-6.10	uc
HD18078							
22	4436	49.1	33.6	D	-5.03	-5.26	
	4470	17.9	16.3	C	-5.51	-5.82	
	4502	44.8	32.0	C	-5.08	-5.31	
23	4258	35.4	27.9	C	-5.40	-5.64	
	4266	40.8	30.7	C	-5.31	-5.54	
			mean abundance:		-5.23	-5.47	
HD22374							
23	4235	16.8	16.7	G	-6.32	-6.60	
	4266	19.0	18.6	C	-6.12	-6.37	
			mean abundance:		-6.21	-6.47	

Table A-34, continued

mult.	λ	W	W_o	qual.	abundance 1	2	
HD50169							
23	4235	46.0	33.0	G	-5.34	-5.57	
			mean abundance:		-5.34	-5.57	uc
HD81009							
22	4435	23.8	23.8	E	-5.96	-6.26	
23	4235	34.3	28.8	G	-6.05	-6.36	
			mean abundance:		-6.00	-6.31	
HD89069							
22	4436	31.6	26.8	D	-5.27	-5.62	
	4470	34.0	28.6	C	-5.28	-5.58	
	4502	44.4	31.5	C	-5.19	-5.48	
23	4258	37.9	31.1	C	-5.28	-5.70	
	4266	52.2	39.0	B	-5.15	-5.46	
			mean abundance:		-5.22	-5.53	
HD110066							
22	4470	29.3	25.2	C	-5.26	-5.57	
	4502	37.9	28.9	B	-5.12	-5.39	
23	4258	27.2	22.9	C	-5.52	-5.81	
	4266	37.3	28.7	C	-5.32	-5.59	
			mean abundance:		-5.24	-5.52	
HD111133							
22	4502	21.4	18.6	D	-5.13	-5.40	
23	4235	45.6	36.2	G	-4.94	-5.25	
	4266	24.5	21.7	E	-5.23	-5.52	
			mean abundance:		-5.07	-5.37	

Table A-34, continued

mult.	λ	W	W_o	qual.	abundance 1	abundance 2	
HD118022							
22	4436	28.8	25.3	W	-5.28	-5.61	
23	4235	32.2	27.2	G	-5.59	-5.92	
	4266	24.0	22.6	E	-5.58	-5.90	
			mean abundance:		-5.46	-5.84	
HD137909							
22	4502	39.6	29.1	D	-5.35	-5.65	
23	4235	71.2	41.2	G	-5.36	-5.59	
	4258	14.1	14.1	D	-6.07	-6.30	
	4266	61.8	36.6	E	-5.38	-5.56	
			mean abundance:		-5.43	-5.65	
HD137949							
22	4453	52.1	34.1	E	-6.00	-6.31	
	4470	30.9	23.1	E	-6.23	-6.54	
23	4258	61.2	38.0	C	-6.00	-6.28	
	4266	43.4	31.0	C	-6.22	-6.49	
			mean abundance:		-6.10	-6.39	
HD165474							
23	4235	13.7	12.0	G	-6.74	-7.05	
	4266	29.7	27.0	D	-6.07	-6.37	
			mean abundance:		-6.39	-6.77	uc
HD176232							
22	4436	27.6	25.3	D	-6.59	-6.86	
	4453	24.0	23.3	D	-6.77	-7.04	
	4502	22.1	22.1	C	-6.80	-7.29	
23	4258	21.5	19.7	C	-7.01	-7.25	
	4266	22.9	22.0	B	-6.90	-7.17	
			mean abundance:		-6.80	-7.10	

Table A-34, continued

mult.	λ	W	W_o	qual.	abundance 1	abundance 2
HD191742						
22	4453	35.6	29.7	C	-6.09	-6.40
	4470	29.3	25.7	B	-6.12	-6.43
	4502	42.6	34.1	B	-5.86	-6.16
23	4258	27.7	24.3	B	-6.36	-6.67
	4266	37.9	31.3	C	-6.14	-6.43
			mean abundance:		-6.08	-6.39
HD192678						
23	4258	26.3	22.3	E	-5.36	-5.54
	4266	26.9	22.6	E	-5.34	-5.52
			mean abundance:		-5.35	-5.53
HD201601						
22	4436	39.2	31.9	E	-6.45	-6.71
	4453	32.8	27.8	D	-6.67	-6.84
	4470	29.2	25.6	C	-6.65	-6.91
	4502	26.9	24.5	C	-6.66	-6.91
23	4258	26.7	23.6	C	-6.92	-7.18
	4266	26.1	23.1	C	-6.91	-7.17
			mean abundance:		-6.69	-6.93
HD204411						
22	4436	20.3	19.9	C	-5.78	-6.07
	4453	19.8	19.4	E	-5.90	-6.20
	4502	24.1	23.6	D	-5.66	-5.96
23	4258	12.6	12.5	C	-6.27	-6.57
	4266	14.8	14.7	D	-6.17	-6.47
			mean abundance:		-5.90	-6.21

Table A-34, continued

mult.	λ	W	W_o	qual.	abundance 1	abundance 2
HD216533						
22	4453	27.7	24.7	E	-5.16	-5.45
	4470	18.8	17.9	D	-5.30	-5.59
	4502	27.2	24.1	C	-5.13	-5.35
23	4235	46.2	36.7	G	-5.08	-5.37
	4258	20.9	20.9	D	-5.41	-5.68
	4266	23.6	23.6	D	-5.29	-5.58
			mean abundance:		-5.17	-5.45

Notes: B quality lines are given double weight in the mean abundance averages while those whose equivalent widths are less than 20 mA are given one-half weight.
I have used the blend at λ4235 only when an additional line is needed to improve the abundance determination. In this case I have divided the total equivalent width by one-half and considered the result as one line with appropriate mean values.
uc = uncertain determination.

Table A-35

Mn Abundances from MnII Lines

mult.	λ	W	W_o	qual.	abundance 1	abundance 2
HD2453						
6	4284	42.5	32.9	C	-5.23	-5.28
7	4206	69.2	43.8	A	-5.47	-5.52
-	4239	40.4	30.4	C	-5.17	-5.22
	4244	45.9	34.5	C	-5.26	-5.31
	4282	62.8	36.9	C	-4.91	-4.96
			mean abundance:		-5.21	-5.26
HD5797						
6	4284	91.1	79.9	B	-4.05	-4.09
7	4206	143.2	130.2	A	-3.84	-3.91
-	4239	74.9	57.6	C	-4.52	-4.58
	4244	102.1	91.2	B	-3.89	-3.93
	4282	94.8	62.4	C	-4.30	-4.36
			mean abundance:		-4.00	-4.05
HD8441						
6	4284	22.1	22.1	C	-5.56	-5.59
7	4206	43.8	43.8	B	-5.49	-5.54
-	4239	17.4	17.4	D	-5.57	-5.64
	4244	17.6	17.6	D	-5.82	-5.86
			mean abundance:		-5.55	-5.60
HD12288						
7	4206	31.8	26.5	C	-5.95	-5.99
-	4244	37.7	28.8	D	-5.40	-5.45
			mean abundance:		-5.68	-5.73

Table A-35, continued

mult.	λ	W	W_o	qual.	abundance 1	abundance 2
HD18078						
6	4284	50.0	36.8	C	-5.15	-5.20
7	4206	70.4	44.6	C	-5.48	-5.53
-	4239	45.6	32.2	C	-5.15	-5.21
	4244	68.7	46.4	C	-4.97	-5.01
	4282	44.3	31.2	E	-5.11	-5.16
			mean abundance:		-5.13	-5.19
HD22374						
6	4284	15.5	15.3	D	-5.87	-5.90
7	4206	46.6	45.2	A	-5.55	-5.60
-	4244	19.1	18.9	C	-5.84	-5.87
			mean abundance:		-5.63	-5.70
HD50169						
7	4206	61.0	37.9	C	-5.65	-5.70
-	4244	25.2	19.1	E	-5.75	-5.79
	4282	32.4	28.4	Q	-5.17	-5.23
			mean abundance:		-5.53	-5.58
HD81009						
7	4206	44.2	31.6	C	-5.96	-6.01
-	4282	31.5	28.4	D	-5.29	-5.35
			mean abundance:		-5.62	-5.67

Table A-35, continued

mult.	λ	W	W_o	qual.	abundance 1	abundance 2
HD89069						
6	4284	56.3	45.4	C	-4.93	-4.99
7	4206	122.3	101.1	B	-4.14	-4.20
-	4244	65.1	52.1	B	-4.84	-4.89
	4282	66.4	41.5	E	-4.83	-4.90
			mean abundance:		-4.48	-4.54
HD110066						
6	4284	40.4	31.8	B	-5.29	-5.35
7	4206	80.7	50.7	C	-5.32	-5.37
-	4239	35.0	27.6	B	-5.29	-5.35
	4244	55.8	40.1	B	-5.13	-5.19
	4282	37.4	28.8	B	-5.17	-5.23
			mean abundance:		-5.22	-5.28
HD111133						
6	4284	49.5	36.7	C	-5.09	-5.14
7	4206	81.8	56.4	C	-5.08	-5.16
-	4239	37.3	28.9	C	-5.19	-5.25
	4244	70.4	47.9	C	-4.87	-4.92
			mean abundance:		-5.04	-5.10
HD118022						
6	4284	26.1	23.5	E	-5.54	-5.56
7	4206	57.6	42.0	E	-5.55	-5.62
-	4244	34.3	28.8	C	-5.46	-5.53
	4282	34.7	27.3	C	-5.21	-5.29
			mean abundance:		-5.42	-5.48

Table A-35, continued

mult.	λ	W	W_o	qual.	abundance 1	abundance 2	
HD137909							
7	4206	65.6	39.0	E	-5.66	-5.72	
-	4282	51.9	34.6	Q	-5.05	-5.10	
			mean abundance:		-5.36	-5.41	
HD137949							
-	4282	39.4	30.3	C	-5.30	-5.36	
			mean abundance:		-5.30	-5.36	
HD165474							
7	4206	26.0	22.8	D	-6.23	-6.28	
-	4244	9.8	9.8	D	-6.20	-6.23	
	4282	23.3	23.3	D	-5.46	-5.51	
			mean abundance:		-5.81	-5.85	uc
HD176232							
6	4284	6.8	6.6	D	-6.29	-6.31	
-	4239	9.9	9.9	D	-6.05	-6.09	
	4244	18.6	17.4	C	-6.00	-6.03	
			mean abundance:		-6.07	-6.10	
HD191742							
6	4284	35.8	32.0	C	-5.46	-5.51	
-	4239	38.5	31.6	D	-5.35	-5.41	
	4244	41.5	36.4	C	-5.40	-5.45	
	4282	39.4	31.3	D	-5.13	-5.19	
			mean abundance:		-5.33	-5.40	

Table A-35, continued

mult.	λ	W	W_o	qual.	abundance 1	abundance 2
HD192678						
6	4284	31.9	26.4	E	-5.41	-5.44
7	4206	30.8	25.2	C	-5.96	-6.04
-	4239	23.0	20.4	D	-5.48	-5.50
	4244	51.2	35.8	C	-5.19	-5.26
			mean abundance:		-5.43	-5.48
HD201601						
6	4284	11.8	11.3	C	-6.12	-6.15
-	4244	18.1	17.1	D	-6.02	-6.05
	4282	18.8	18.8	C	-5.69	-5.71
			mean abundance:		-5.88	-5.91
HD204411						
6	4284	18.6	18.4	C	-5.76	-5.80
7	4206	26.8	26.5	E	-6.08	-6.12
-	4244	11.7	11.6	D	-6.09	-6.13
			mean abundance:		-5.92	-5.96
HD216533						
6	4284	48.5	40.1	C	-5.02	-5.07
-	4244	41.6	34.7	B	-5.25	-5.31
	4282	45.2	32.8	C	-5.02	-5.08
			mean abundance:		-5.12	-5.19

Notes: A and B quality lines are given double weight in the mean abundance averages while those of D quality are given one-half weight.

Table A-36

Co Abundances from CoI Lines

	CoI(31) λ3995			abundance		CoI(18) λ3873			abundance		mean Co abundance	
star	W	qual.	W_o	1	2	W	qual.	W_o	1	2	1	2
HD2453	23.1	W	20.8	-5.99	-6.29	n.m.					-5.99:	-6.29:
HD5797	149.6	C	137.2	-4.13	-4.45	n.m					-4.13	-4.45
HD8441	6.5	D	6.5	-6.75	-7.10	n.m.					-6.75:	-7.10:
HD12288	n.m.					n.m.					-6.03ul	-6.57ul
HD18078	77.1	C	47.9	-5.43	-5.71	n.m.					-5.43	-5.71
HD22374	n.m.					n.m.					-6.90ul	-7.21ul
HD50169	70.8	C	40.9	-5.56	-5.83	n.m.					-5.56	-5.83
HD81009	55.5	D	34.9	-6.41	-6.78	n.m.					-6.41:	-6.78:
HD89069	67.4	C	51.8	-5.40	-5.77	n.m.					-5.40	-5.77
HD110066	71.9	E	46.1	-5.45	-5.76	n.m.					-5.45	-5.76
HD111133	58.1	B	39.2	-5.26	-5.60	n.m.					-5.26	-5.60
HD118022	45.8	C	35.2	-5.82	-6.19	n.m.					-5.82	-6.19
HD137909	90.0	W	48.4	-5.65	-5.89	n.m.					-5.65:	-5.89:
HD137949	91.8	C	52.2	-6.31	-6.64	n.m.					-6.31	-6.64
HD165474	n.m.					n.m.					-7.16ul	-7.45ul
HD176232	100.4	C	83.0	-6.05	-6.37	76.8	C	63.0	-6.38	-6.75	-6.18	-6.52
HD191742	n.m.					44.5	W	38.0	-6.49	-6.92	-6.49:	-6.92:
HD192678	101.9	B	57.2	-4.88	-5.11	71.1	E	43.9	-5.09	-5.31	-4.98	-5.20
HD201601	89.8	B	76.1	-6.25	-6.54	73.1	C	62.5	-6.45	-6.79	-6.34	-6.65
HD204411	33.1	C	32.4	-6.25	-6.61	42.2	E	41.0	-5.86	-6.21	-6.01	-6.37
HD216533	n.m.					n.m.					-6.17ul	-6.50ul
ν Cap	n.m.					n.m.					-6.31ul	-6.64ul
o Peg	n.m.					n.m.					-6.57ul	-6.89ul

Note: The upper limits, ul, are based on a 15mA equivalent width for λ3995 except for the normal stars where they are 10mA.

Table A-37

Ni Abundances from NiI Lines

	NiI(86) λ4470					NiI(86) λ4462					mean Ni abundance	
				abundance					abundance			
star	W	qual.	W_o	1	2	W	qual.	W_o	1	2	1	2
HD2453	29.7	C	25.6	-4.42	-4.67	n.m.					-4.42	-4.67
HD5797	n.m.					n.m.					-5.21ul	-5.47ul
HD8441	n.m.					n.m.					-4.86ul	-5.10ul
HD12288	n.m.					n.m.					-4.64ul	-4.88ul
HD18078	30.2	B	26.3	-4.57	-4.80	16.2	D	15.0	-4.63	-4.87	-4.59	-4.83
HD22374	n.m.					n.m.					-5.31ul	-5.56ul
HD50169	n.m.					n.m.					-4.88ul	-5.09ul
HD81009	16.2	W	16.2	-5.38	-5.65	n.m.					-5.38:	-5.65:
HD89069	24.2	D	21.4	-4.79	-5.06	n.m.					-4.79:	-5.06:
HD110066	29.5	B	25.2	-4.57	-4.82	n.m.					-4.57	-4.82
HD111133	29.3	Q	29.0	-4.15	-4.44	n.m.					-4.15:	-4.44:
HD118022	17.1	D	16.6	-4.93	-5.20	n.m.					-4.93:	-5.20:
HD137909	32.7	E	26.2	-4.74	-4.96	n.m.					-4.74	-4.96
HD137949	31.7	E	26.2	-5.38	-5.66	n.m.					-5.38	-5.66
HD165474	25.2	D	21.5	-5.31	-5.59	n.m.					-5.31:	-5.59:
HD176232	16.8	D	15.8	-6.16	-6.38	n.m.					-6.16:	-6.38:
HD191742	33.4	B	29.8	-5.28	-5.53	n.m.					-5.28	-5.53
HD192678	47.0	C	35.9	-4.09	-4.27	n.m.					-4.09	-4.27
HD201601	21.5	C	20.1	-6.04	-6.27	n.m.					-6.04	-6.27
HD204411	20.1	D	19.3	-5.09	-5.38	n.m.					-5.09:	-5.38:
HD216533	28.2	C	24.5	-4.42	-4.69	8.0	D	7.9	-4.74	-5.00	-4.50	-4.77
ν Cap	n.m.					n.m.					-4.90ul	-5.14ul
o Peg	n.m.					n.m.					-5.09ul	-5.32ul

Notes: D quality lines are given one-half weight in the mean abundance averages.
Upper limits, ul, are based on a 15mA equivalent width for λ4470 except for the normal stars where 10mA is used.

Table A-38

Ni Abundances from NiII Lines

star	NiII λ4245 W	W_o	qual.	abundance 1	2	
HD2453	25.7	22.7	C	-5.73	-5.75	
HD5797	35.8	33.8	C	-5.49	-5.55	
HD8441	n.m.			-5.99ul	-6.02ul	
HD12288	n.m.			-6.00ul	-6.00ul	
HD18078	n.m			-6.00ul	-6.03ul	
HD22374	n.m.			-6.07ul	-6.12ul	
HD50169	17.2	16.9	D	-5.94	-5.97	
HD81009	n.m.			-6.09ul	-6.16ul	
HD89069	22.4	21.1	E	-5.80	-5.86	
HD110066	27.1	23.6	B	-5.72	-5.76	
HD111133	n.m.			-6.00ul	-6.00ul	
HD118022	18.2	16.9	D	-5.94	-6.00	
HD137909	41.6	32.2	B	-5.51	-5.55	
HD137949	n.m.			-6.17ul	-6.24ul	
HD165474	n.m.			-6.10ul	-6.18ul	
HD176232	n.m.			-6.28ul	-6.34ul	
HD191742	48.8	44.8	B	-5.30	-5.36	
HD192678	n.m.			-6.00ul	-6.00ul	
HD201601	n.m.			-6.29ul	-6.35ul	
HD204411	16.6	16.1	D	-6.01	-6.07	
HD216533	37.0	33.6	C	-5.41	-5.46	
ν Cap	50.8	34.8	-	-6.80	-6.86	+
o Peg	16.4	15.3	C	-5.99	-6.02	

Notes: n.m. = not measured
ul = upper limit based on an equivalent width of 15 mA for λ4245
+ = measured NiII(11) λ4067.05. log gf=-0.59(Warner 1967).

Table A-39

Ga Abundances from GaII Lines

star	GaII λ4251 W	W_o	qual.	abundance 1	2
HD2453	8.1	7.8	D	-5.32	-5.10
HD111133	16.4	15.2	D	-4.87	-4.70

Table A-40

Sr Abundances from SrI Lines

star	SrI λ4607 W	W_o	qual.	abundance 1	2
HD2453	39.9	27.7	C	-4.38	-4.85
HD5797	45.0	37.2	C	-4.83	-5.34
HD8441	n.m				
HD12288	n.m				
HD18078	25.5	20.7	C	-4.98	-5.42
HD22374	n.m.				
HD50169	n.m				
HD81009	15.4	15.4	D	-6.09	-6.61
HD89069	n.m.				
HD110066	36.8	26.6	B	-4.71	-5.17
HD111133	28.5	22.4	C	-4.23	-4.81
HD118022	n.m.				
HD137909	50.5	31.4	C	-4.91	-5.29
HD137949	109.7	56.0	C	-4.86	-5.31
HD165474	41.8	26.8	E	-5.88	-6.34
HD176232	47.7	37.9	C	-6.47	-6.85
HD191742	91.9	75.3	C	-3.86	-4.45
HD192678	n.m.				
HD201601	52.6	42.8	C	-6.25	-6.65
HD204411	n.m.				
HD216533	11.6	11.6	E	-4.92	-5.49
ν Cap	n.m				
o Peg	n.m.				

Notes: n.m. = not measured.

Table A-41

Sr Abundances from SrII Lines

star	SrII(3) λ4161.8 W	qual.	W_o	abundance 1	2	SrII(1) λ4215.5 W	qual.	W_o	abundance 1	2	mean Sr abundance 1	2
HD2453	64.2	C	36.9	-7.14	-7.39	322.5	E	228.0	-6.44	-6.79	-6.66	-6.99
HD5797	124.7	E	105.7	-6.07	-6.34	764.5	B	764.5	-6.24	-6.60	-6.15	-6.45
HD8441	46.6	B	46.6	-6.89	-7.14	207.3	E	207.3	-6.87	-7.21	-6.88	-7.17
HD12288	n.m.					140.7	E	49.9	-8.35	-8.71	-8.35	-8.71
HD18078	103.5	C	54.2	-6.75	-6.98	488.0	C	447.7	-6.30	-6.63	-6.47	-6.77
HD22374	n.m.					67.8	C	65.2	-8.85	-9.23	-8.85	-9.23
HD50169	200.5	C	91.1	-5.85	-6.11	887.0	C	860.3	-5.63	-5.97	-5.73	-6.03
HD81009	120.9	C	44.4	-7.54	-7.74	388.5	E	388.5	-7.54	-7.90	-7.54	-7.81
HD89069	40.3	E	30.1	-7.64	-7.85	121.6	C	90.7	-7.95	-8.35	-7.77	-8.03
HD110066	115.6	C	61.8	-6.48	-6.76	608.8	E	591.1	-6.00	-6.40	-6.17	-6.54
HD111133	195.7	E	140.8	-5.04	-5.40	607.3	B	583.9	-5.58	-5.97	-5.23	-5.60
HD118022	87.7	E	51.9	-6.84	-7.14	318.2	C	300.2	-6.71	-7.10	-6.77	-7.12
HD137909	144.9	C	58.9	-6.78	-6.99	306.9	C	217.6	-7.21	-7.48	-6.94	-7.17
HD137949	217.8	C	140.5	-6.23	-6.50	941.7	C	905.5	-6.79	-7.13	-6.42	-6.71
HD165474	141.4	E	50.7	-7.43	-7.64	522.0	C	466.1	-7.08	-7.43	-7.22	-7.52
HD176232	148.0	C	125.4	-6.77	-6.96	730.7	C	730.7	-7.55	-7.81	-7.00	-7.20
HD191742	287.3	C	278.9	-5.58	-5.86	1747.8	B	1747.8	-6.17	-6.53	-5.78	-6.08
HD192678	21.4	E	18.1	-7.76*	-7.95*	73.0	E	38.0	-8.83	-9.15	-8.33	-8.55
HD201601	110.0	C	90.2	-7.14	-7.33	632.2	C	632.2	-7.71	-7.98	-7.34	-7.54
HD204411	21.8	C	21.8	-8.09	-8.40	114.8	C	111.5	-8.04	-8.44	-8.06	-8.42
HD216533	164.6	E	139.5	-5.20	-5.50	739.3	B	739.3	-5.56	-5.94	-5.34	-5.67
ν Cap	n.m.					52.7	-	32.3	-9.10	-9.45	-9.10	-9.45
o Peg	n.m.					115.4	B	58.3	-8.48	-8.77	-8.48	-8.77

Notes: * = one-quarter weight given in the mean abundance averages.
n.m. = not measured.

Table A-42

Y Abundances from YII Lines

mult.	λ	W	W_o	qual.	abundance 1	abundance 2	
HD2453							
6	3950	20.5	16.9	C	-8.53	-8.81	
	3983	23.7	19.4	C	-8.34	-8.65	
			mean abundance:		-8.42	-8.72	
HD5797							
6	3950	31.9	27.3	D	-8.54	-8.92	
			mean abundance:		-8.54	-8.92	uc
HD8441							
5	4398	19.2	19.2	C	-8.06	-8.33	
6	3950	23.6	23.6	C	-8.36	-8.65	
	3983	15.6	15.6	C	-8.59	-8.86	
			mean abundance:		-8.28	-8.56	
HD12288							
6	3950	34.2	23.3	C	-8.12	-8.44	
			mean abundance:		-8.12	-8.44	
HD18078							
5	4398	34.8	26.2	C	-7.93	-8.15	
6	3950	35.9	26.4	E	-8.35	-8.62	
	3983	31.1	24.5	E	-8.34	-8.59	
			mean abundance:		-8.15	-8.40	
HD22374							
5	4398	22.1	21.7	C	-8.49	-8.73	
6	3950	23.4	22.9	C	-8.81	-9.05	
			mean abundance:		-8.62	-8.86	

Table A-42, continued

mult.	λ	W	W_o	qual.	abundance 1	abundance 2
HD50169						
6	3950	36.3	24.9	C	-8.30	-8.61
			mean abundance:		-8.30	-8.61
HD81009						
5	4398	50.1	29.6	W	-8.32	-8.58
6	3950	72.7	35.5	C	-8.54	-8.81
	3983	56.7	31.9	D	-8.59	-8.86
			mean abundance:		-8.48	-8.75
HD89069						
5	4398	24.0	20.9	D	-8.18	-8.48
6	3950	14.6	13.3	W	-8.96	-9.27
	3983	28.8	24.6	D	-8.43	-8.73
			mean abundance:		-8.37	-8.72
HD110066						
6	3950	31.0	23.8	C	-8.45	-8.73
	3983	28.1	22.5	C	-8.40	-8.67
			mean abundance:		-8.42	-8.70
HD111133						
6	3950	25.3	20.2	E	-8.19	-8.57
	3983	23.1	19.1	E	-8.14	-8.50
			mean abundance:		-8.16	-8.53
HD118022						
5	4398	23.2	19.8	D	-8.18	-8.49
6	3950	29.5	23.4	C	-8.52	-8.82
	3983	12.1	11.1	D	-8.91	-9.22
			mean abundance:		-8.44	-8.75

Table A-42, continued

mult.	λ	W	W_o	qual.	abundance 1	abundance 2
HD137909						
5	4398	68.7	37.7	C	-7.74	-7.94
6	3950	79.7	40.1	C	-8.08	-8.26
	3983	29.7	22.2	C	-8.65	-8.84
			mean abundance:		-8.02	-8.18
HD137949						
5	4398	93.1	49.3	C	-7.95	-8.18
6	3950	116.2	56.1	C	-8.10	-8.35
	3983	53.2	33.9	E	-8.81	-9.03
			mean abundance:		-8.16	-8.40
HD165474						
5	4398	52.4	31.0	C	-8.36	-8.62
6	3950	77.9	38.0	B	-8.50	-8.79
	3983	52.6	31.1	C	-8.72	-8.96
			mean abundance:		-8.50	-8.77
HD176232						
5	4398	49.8	39.5	B	-8.62	-8.85
6	3950	49.5	38.1	B	-9.06	-9.30
	3983	53.2	41.9	C	-8.84	-9.06
			mean abundance:		-8.80	-9.03
HD191742						
6	3950	22.0	20.0	C	-9.33	-9.56
	3983	27.0	24.3	E	-9.13	-9.37
			mean abundance:		-9.22	-9.45

Table A-42, continued

mult.	λ	W	W_o	qual.	abundance 1	abundance 2	
HD192678							
6	3950	23.9	18.8	C	-8.37	-8.67	
			mean abundance:		-8.37	-8.67	
HD201601							
5	4398	77.6	63.6	C	-7.91	-8.11	
6	3950	79.4	62.5	B	-8.33	-8.54	
	3983	71.4	58.5	B	-8.36	-8.55	
			mean abundance:		-8.22	-8.42	
HD204411							
6	3950	12.6	12.5	D	-9.24	-9.52	
	3983	11.0	10.9	D	-9.23	-9.49	
			mean abundance:		-9.23	-9.50	
HD216533							
6	3950	18.9	16.7	D	-8.46	-8.83	
			mean abundance:		-8.46	-8.83	uc
o Peg							
6	3950	15.4	13.2	C	-8.84	-9.11	
	3983	18.3	15.2	C	-8.65	-8.92	
			mean abundance:		-8.74	-9.00	

Notes: B quality lines are given double weight in the mean abundance averages while those of D and W quality are given one-half weight.
uc = uncertain determination.

Table A-43

Zr Abundances from ZrII Lines

star	λ	W	W_o	qual.	abundance 1	abundance 2	mean abundance 1	mean abundance 2
HD50169	4317	14.3	12.2	D	-7.69	-7.91	-7.69:	-7.91:
HD81009	4317	30.0	21.0	W	-7.87	-8.09	-7.87:	-8.09:
HD89069	4317	25.5	21.8	D	-7.45	-7.72	-7.45:	-7.72:
HD137909	4317	69.6	37.0	C	-7.04	-7.21	-7.04	-7.21
HD137949	4317	43.1	28.7	W	-7.80	-8.06	-7.80:	-8.06:
HD165474	4317	46.8	28.5	W	-7.69	-7.91	-7.69:	-7.91:
HD201601	4317	18.4	16.9	E	-8.63	-8.81		
	4180	20.8	19.4	D	-8.95	-9.08	-8.71	-8.92

Note: HD201601 - λ4180 is given one-half weight in the mean abundance averages.

Table A-44

Ba Abundances from BaII Lines

star	λ	W	qual.	W_o 1	W_o 2	4554 blend λ	abundance 1	abundance 2	mean abundance 1	mean abundance 2
HD2453	4554	62.8	B	12.8	0.0	53.97	-8.93		-8.93:	
HD5797	4554	75.7	B	3.0	0.0	54.00	-10.24		-10.24:	
HD8441	4554	36.9	C	0.0	5.0	54.05		-9.88		-9.88:
HD12288	4554	45.4	C	0.0	0.0	53.95				
HD18078	4554	43.4	B	0.0	0.0	53.99				
HD22374	4554	32.5	C	0.0	0.0	53.97				
HD50169	4554	33.4	C	0.0	0.0	53.96				
HD81009	4554	52.5	C	19.8	19.1	54.00	-9.53	-9.97	-9.53:	-9.97:
HD89069	4554	27.9	D	0.0	0.0	54.01				
HD110066	4554	61.5	B	0.0	0.0	53.97				
HD111133	4554	21.3	C	0.0	0.0	54.00				
HD118022	4554	57.9	C	11.5	14.5	54.01	-9.32	-9.52	-9.32:	-9.52:
HD137909	4554	172.4	C	54.1	54.2	54.02	-7.83	-8.02	-7.83	-8.02
HD137949	4554	177.9	C	64.0	61.5	53.98	-8.35	-8.80		
	4166	81.2	E	36.3	36.3		-7.55	-7.77	-7.79	-8.03
HD165474	4554	60.8	B	21.9	22.1	54.03	-9.57	-9.97	-9.57	-9.97
HD176232	4554	66.8	C	31.8	31.8	54.03	-10.06	-10.39	-10.06	-10.39
HD191742	4554	146.0	A	79.5	79.5	54.01	-8.03	-8.37		
	4166	16.4	C	13.9	13.9		-8.44	-8.68	-8.19	-8.50
HD192678	4554	39.5	B	0.0	0.0	53.95				
HD201601	4554	155.6	C	109.4	107.8	54.00	-8.39	-8.69		
	4166	21.8	C	17.6	17.6		-8.74	-8.96	-8.53	-8.80
HD204411	4554	80.8	A	57.7	56.7	54.01	-7.81	-8.25	-7.81	-8.25
HD216533	4554	141.5	B	84.7	83.2	54.02	-6.50	-6.98		
	4166	14.8	C	12.6	12.6		-7.58	-7.79	-6.77	-7.26
ζ Cap	4554	18.0	-	13.2	13.2		-8.77	-9.18	-8.77	-9.18
ζ Peg	4554	76.0	B	36.2	36.2	54.02	-8.04	-8.38	-8.04	-8.38

Table A-45

La Abundances from LaII Lines

star	λ	W	W_o	qual.	abundance 1	abundance 2	mean abundance 1	mean abundance 2
HD2453	3988	11.7	9.8	D	-9.30	-9.53	-9.30:	-9.53:
HD5797	3988	68.3	49.5	E	-8.06	-8.31		
	4231	14.5	12.5	D	-8.69	-8.96	-8.19	-8.44
HD12288	3988	69.1	28.7	C	-8.31	-8.56	-8.31	-8.56
HD50169	3988	35.3	19.8	E	-8.93	-9.14	-8.93	-9.14
HD81009	4620	24.6	16.4	C	-8.77	-8.97	-8.77	-8.97
HD89069	3988	26.6	19.0	W	-9.10	-9.34	-9.10:	-9.34:
HD118022	3988	15.2	12.1	W	-9.36	-9.63	-9.36:	-9.63:
HD137949	3988	67.7	31.6	C	-9.22	-9.44		
	4322	49.9	26.7	C	-8.01	-8.29		
	4620	66.7	38.1	E	-8.09	-8.26	-8.21	-8.43
HD176232	3988	20.6	16.1	D	-10.24	-10.44	-10.24:	-10.44:
HD192678	3988	38.5	21.5	C	-8.71	-8.95	-8.71	-8.95
HD201601	3988	53.2	38.0	C	-9.31	-9.50		
	4322	21.2	17.2	C	-8.77	-8.91	-8.96	-9.11
HD216533	3988	46.2	29.4	D	-8.39	-8.65	-8.39:	-8.65:

Table A-46

Ce Abundances from CeII Lines

mult.	λ	W	W_o	qual.	abundance 1	abundance 2	
HD2453							
1	4307	25.5	17.7	D	-7.94	-8.22	
	4562	27.6	18.9	C	-8.21	-8.49	
	4628	20.5	15.2	C	-8.30	-8.57	
2	4460	18.9	15.0	C	-8.46	-8.73	
	4561	25.6	16.6	D	-7.58	-7.84	
3	4484	21.0	14.5	C	-8.12	-8.39	
8	4228	36.9	20.9	C	-7.88	-8.14	
20	4463	16.4	12.1	C	-8.08	-8.31	
57	4487	27.3	18.7	C	-7.75	-8.03	
203	4214	26.2	17.8	C	-7.65	-7.91	
204	4271	18.4	14.6	D	-7.99	-8.21	
			mean abundance:		-7.97	-8.21	
HD5797							
1	4562	23.7	19.1	D	-8.70	-8.94	
57	4487	31.0	24.2	D	-8.02	-8.28	
			mean abundance:		-8.24	-8.50	uc
HD8441							
1	4187	8.4	8.4	W	-9.29	-9.56	
			mean abundance:		-9.29	-9.56	uc
HD12288							
2	4460	13.8	10.9	D	-8.48	-8.75	
			mean abundance:		-8.48	-8.75	uc

Table A-46, continued

mult.	λ	W	W_o	qual.	abundance 1	abundance 2	
HD18078							
1	4187	18.4	13.8	D	-9.11	-9.33	
	4628	8.8	7.9	D	-8.87	-9.11	
3	4484	16.5	12.4	D	-8.40	-8.62	
8	4228	48.2	24.7	C	-7.91	-8.13	
			mean abundance:		-8.21	-8.43	uc
HD50169							
1	4628	19.7	14.2	W	-8.48	-8.72	
			mean abundance:		-8.48	-8.72	
HD81009							
1	4562	55.4	25.6	B	-8.61	-8.85	
	4628	99.1	38.4	B	-8.00	-8.24	
2	4382	73.7	29.5	E	-8.20	-8.41	
	4460	52.0	26.0	C	-8.67	-8.91	
	4561	55.3	23.9	C	-7.94	-8.15	
20	4463	69.2	29.4	E	-7.97	-8.20	
21	4271	53.8	26.5	C	-8.09	-8.27	
57	4487	62.0	27.7	C	-8.06	-8.31	
203	4214	30.9	17.8	C	-8.29	-8.48	
204	4270	55.7	25.6	E	-8.16	-8.40	
			mean abundance:		-8.16	-8.36	
HD89069							
1	4628	22.7	17.9	W	-8.47	-8.75	
			mean abundance:		-8.47	-8.75	uc

Table A-46, continued

mult.	λ	W	W_o	qual.	abundance 1	abundance 2
HD110066						
1	4187	45.6	26.2	C	-8.53	-8.78
	4307	16.1	12.8	D	-8.36	-8.60
	4562	31.0	20.5	C	-8.32	-8.58
	4628	30.2	20.1	C	-8.27	-8.53
2	4382	20.8	15.1	D	-8.32	-8.57
	4460	23.0	17.6	C	-8.49	-8.77
	4561	24.7	16.5	C	-7.76	-8.00
3	4451	18.4	13.3	D	-8.24	-8.46
	4484	26.7	17.1	C	-8.17	-8.42
8	4228	45.6	24.0	B	-7.90	-8.16
20	4463	26.9	18.4	C	-7.93	-8.19
21	4271	31.3	21.6	D	-7.81	-8.06
57	4487	29.0	19.7	D	-7.88	-8.14
203	4214	36.1	22.0	D	-7.64	-7.88
204	4270	30.4	20.1	E	-7.88	-8.15
			mean abundance:		-8.03	-8.29
HD118022						
1	4187	39.1	24.3	W	-8.68	-8.95
	4562	29.1	20.6	C	-8.38	-8.68
	4628	40.7	26.8	C	-8.07	-8.36
2	4382	10.9	9.2	D	-8.65	-8.90
	4460	33.8	24.5	D	-8.27	-8.57
3	4484	26.8	17.6	W	-8.20	-8.49
			mean abundance:		-8.30	-8.58

Table A-46, continued

mult.	λ	W	W_o	qual.	abundance 1	abundance 2
HD137909						
1	4187	94.3	40.0	C	-8.11	-8.32
	4562	87.8	40.8	B	-7.65	-7.86
	4628	126.1	57.8	B	-7.05	-7.31
2	4460	78.2	42.5	C	-7.65	-7.83
	4561	77.3	30.6	C	-7.41	-7.60
3	4484	64.3	27.0	C	-7.98	-8.15
8	4228	86.1	33.6	E	-7.71	-7.91
20	4463	83.8	38.6	C	-7.33	-7.50
57	4487	76.7	36.9	C	-7.35	-7.55
203	4214	40.5	22.0	B	-7.84	-8.03
204	4270	73.9	35.0	C	-7.42	-7.62
			mean abundance:		-7.49	-7.70
HD137949						
1	4187	101.7	40.2	W	-8.63	-8.83
	4562	64.4	34.3	A	-8.55	-8.74
2	4460	78.9	46.7	C	-8.05	-8.27
	4561	83.0	33.7	C	-7.79	-7.97
3	4484	48.0	23.2	W	-8.65	-8.85
57	4487	64.6	34.4	C	-8.03	-8.25
204	4270	45.6	25.3	C	-8.43	-8.66
			mean abundance:		-8.14	-8.34

Table A-46, continued

mult.	λ	W	W_o	qual.	abundance 1	abundance 2
HD165474						
1	4187	66.6	29.1	E	-8.96	-9.19
	4562	40.9	22.0	C	-8.85	-9.10
	4628	82.0	35.7	C	-8.22	-8.46
2	4382	42.2	21.5	E	-8.58	-8.80
	4460	36.3	21.6	C	-8.94	-9.19
	4561	45.0	21.1	C	-8.13	-8.33
3	4484	36.1	19.4	E	-8.64	-8.87
8	4228	41.3	20.9	E	-8.60	-8.80
20	4463	47.3	23.8	C	-8.29	-8.51
21	4271	34.2	20.4	C	-8.42	-8.65
57	4487	41.0	22.0	C	-8.40	-8.65
203	4214	30.8	18.2	C	-8.34	-8.54
204	4270	36.8	20.6	C	-8.46	-8.71
			mean abundance:		-8.46	-8.68
HD176232						
1	4187	35.2	24.8	C	-9.65	-9.89
	4307	18.0	14.8	D	-9.41	-9.60
	4562	10.7	9.6	D	-9.97	-10.16
	4628	18.9	15.5	D	-9.59	-9.81
2	4460	17.1	14.7	C	-9.80	-9.97
20	4463	16.8	14.1	D	-9.21	-9.38
57	4487	20.8	17.2	D	-9.16	-9.34
203	4214	15.0	12.4	D	-9.07	-9.26
			mean abundance:		-9.44	-9.63

Table A-46, continued

mult.	λ	W	W_λ	qual.	abundance 1	abundance 2	
HD191742							
1	4187	59.2	45.2	E	-8.42	-8.61	
	4562	25.8	20.6	C	-9.07	-9.31	
	4628	35.3	27.4	C	-8.73	-8.96	
2	4382	11.4	10.1	D	-9.20	-9.41	
	4561	33.1	22.1	D	-8.20	-8.43	
3	4484	23.1	17.0	C	-8.88	-9.11	
8	4228	47.4	31.2	C	-8.29	-8.47	
20	4463	38.4	29.8	C	-8.19	-9.39	
21	4271	37.1	31.2	C	-8.11	-8.31	
57	4487	40.0	31.7	C	-8.14	-8.35	
			mean abundance:		-8.38	-8.58	
HD201601							
1	4187	53.0	40.2	C	-8.95	-9.11	
	4307	25.7	20.4	E	-9.17	-9.33	
	4562	18.2	15.4	D	-9.69	-9.91	
2	4460	31.5	26.5	E	-9.29	-9.48	
	4561	18.1	14.4	D	-8.89	-9.07	
3	4484	29.5	20.2	E	-9.11	-9.28	
21	4271	13.5	11.9	D	-9.36	-9.51	
57	4487	27.2	21.8	D	-8.99	-9.15	
			mean abundance:		-9.12	-9.29	
HD216533							
1	4187	43.1	29.3	E	-8.19	-8.50	
	4628	24.6	19.1	W	-8.10	-8.43	
			mean -bundance:		-8.16	-8.48	uc

Notes: D and W quality lines are given one-half weight in the mean abundance averages.
uc = uncertain determination.

Table A-47

Pr Abundances from PrII Lines

mult.	λ	W	W_o	qual.	abundance 1	abundance 2	
HD8441							
4	4496	14.6	14.6	C	-7.74	-8.07	
			mean abundance:		-7.74	-8.07	uc
HD50169							
4	4223	15.9	12.2	E	-8.51	-8.81	
			mean abundance:		-8.51	-8.81	
HD110066							
4	4223	21.8	16.0	E	-8.36	-8.72	
			mean abundance:		-8.36	-8.72	
HD111133							
4	4223	13.6	11.1	D	-8.20	-8.56	
			mean abundance:		-8.20	-8.56	uc
HD118022							
4	4223	9.1	8.2	W	-8.83	-9.28	+
	4409	24.4	18.5	D	-7.92	-8.30	+
8	4190	17.5	17.5	C	-8.33	-8.72	
			mean abundance:		-8.24	-8.67	
HD137909							
4	4409	81.7	40.8	E	-7.21	-7.44	
			mean abundance:		-7.21	-7.44	uc

Table A-47, continued

mult.	λ	W	W_o	qual.	abundance 1	abundance 2	
HD137949							
4	4223	154.8	99.2	W	-7.11	-7.45	x
	4409	77.1	41.9	E	-7.83	-8.09	
8	4190	125.9	56.0	C	-7.73	-8.00	
			mean abundance:		-7.63	-7.90	
HD165474							
8	4190	55.2	25.3	C	-8.68	-8.95	
			mean abundance:		-8.68	-8.95	
HD201601							
4	4223	20.6	17.0	D	-9.71	-9.95	
	4409	80.9	70.3	E	-7.55	-7.77	x
			mean abundance:		-8.25	-8.46	uc
HD216533							
4	4223	10.2	9.2	D	-8.48	-8.83	
			mean abundance:		-8.48	-8.83	uc

Notes: uc = uncertain abundance determination
+ = one-half weight in the mean abundance averages
x = one-quarter weight

Table A-48

Nd Abundances from NdII Lines

	NdII(10) λ4303.6					NdII(10) λ4358.2					mean Nd abundance	
				abundance					abundance			
star	W	qual.	W_o	1	2	W	qual.	W_o	1	2	1	2
HD2453	82.3	B	53.1	-6.72	-7.04	n.m.					-6.72	-7.04
HD5797	112.8	B	105.4	-6.49	-6.82	55.9	C	42.0	-7.07	-7.47	-6.61	-6.95
HD8441	39.3	C	39.3	-7.30	-7.67	n.m.					-7.30	-7.67
HD12288	125.5	E	56.3	-6.43	-6.78	n.m.					-6.43	-6.78
HD18078	55.5	C	35.1	-7.63	-7.95	32.1	C	20.2	-7.62	-7.93	-7.62	-7.94
HD22374	38.7	C	37.6	-8.08	-8.34	n.m.					-8.08	-8.34
HD50169	79.2	C	41.2	-7.28	-7.57	27.4	C	17.3	-7.64	-7.95	-7.42	-7.72
HD81009	67.2	E	31.1	-8.46	-8.73	n.m.					-8.46	-8.73
HD89069	55.3	B	44.2	-7.34	-7.72	n.m.					-7.34	-7.72
HD110066	82.3	B	54.9	-6.86	-7.20	n.m.					-6.86	-7.20
HD111133	54.7	E	35.1	-7.14	-7.53	22.8	C	16.1	-7.33	-7.74	-7.22	-7.62
HD118022	49.2	E	35.7	-7.64	-8.06	27.1	D	18.8	-7.74	-8.10	-7.67	-8.08
HD137909	76.6	C	40.3	-7.67	-7.97	n.m.					-7.67	-7.97
HD137949	135.2	C	98.0	-7.16	-7.48	86.0	D	39.4	-7.76	-8.00	-7.28	-7.60
HD165474	40.3	E	22.6	-8.92	-9.27	n.m.					-8.92	-9.27
HD176232	23.6	C	17.1	-9.87	-10.12	n.m.					-9.87	-10.12
HD191742	62.7	B	54.5	-7.91	-8.19	n.m.					-7.91	-8.19
HD192678	113.9	B	74.0	-6.21	-6.53	37.2	C	21.1	-7.30	-7.62	-6.37	-6.69
HD201601	45.6	C	38.6	-8.96	-9.16	35.2	E	25.9	-8.80	-9.03	-8.90	-9.09
HD204411	29.8	C	28.6	-8.37	-8.67	n.m.					-8.37	-8.67
HD216533	69.6	C	57.0	-6.56	-6.93	n.m.					-6.56	-6.93
ν Cap	n.m.					n.m.					n.m.	n.m.
o Peg	n.m.					n.m.					n.m.	n.m.

Notes: B quality lines are given double weight in the mean abundance averages.
D quality lines are given one-half weight.
n.m. = not measured.

Table A-49

Sm Abundances from SmII Lines

mult.	λ	W	W_o	qual.	abundance 1	abundance 2
HD2453						
32	4566	13.8	10.8	D	-6.94	-7.26
37	4263	15.2	11.6	D	-7.42	-7.75
	4421	25.0	16.8	D	-7.03	-7.33
45	4362	22.9	14.9	D	-7.17	-7.50
53	4467	30.7	19.4	D	-6.80	-7.13
			mean abundance:		-7.02	-7.35
HD5797						
22	4616	12.6	11.2	D	-7.56	-7.96
32	4566	9.1	8.3	D	-7.70	-8.03
37	4421	9.2	8.4	D	-8.04	-8.38
41	4524	15.2	12.1	D	-7.12	-7.48
45	4362	26.0	17.7	D	-7.61	-8.03
53	4467	31.0	22.8	D	-7.28	-7.64
			mean abundance:		-7.46	-7.83
HD18078						
22	4616	18.5	14.1	D	-7.01	-7.34
49	4515	14.4	11.2	D	-7.02	-7.38
50	4221	27.7	17.7	D	-7.34	-7.62
			mean abundance:		-7.10	-7.45

Table A-49, continued

mult.	λ	W	W_o	qual.	abundance 1	abundance 2
HD110066						
37	4263	12.6	10.2	D	-7.70	-8.02
41	4524	23.5	15.6	C	-6.57	-6.90
45	4362	21.7	14.7	D	-7.38	-7.73
49	4615	24.6	16.6	D	-6.80	-7.16
50	4221	23.3	16.0	D	-7.43	-7.71
			mean abundance:		-7.03	-7.31
HD137909						
36	4434	121.1	40.6	C	-6.84	-7.11
41	4524	58.5	25.2	B	-6.47	-6.73
45	4362	65.7	26.1	C	-7.19	-7.42
			mean abundance:		-6.71	-7.00
HD137949						
36	4434	152.5	52.6	C	-7.24	-7.57
37	4263	43.4	22.0	C	-8.23	-8.57
	4421	94.7	40.5	E	-7.33	-7.66
41	4524	72.9	29.5	C	-7.07	-7.41
45	4362	131.8	41.1	C	-7.32	-7.68
50	4221	72.7	31.2	C	-7.84	-8.11
			mean abundance:		-7.37	-7.73

Table A-49, continued

mult.	λ	W	W_o	qual.	abundance 1	abundance 2	
HD176232							
32	4566	17.6	14.0	D	-8.60	-8.90	
36	4434	65.4	37.2	C	-8.24	-8.52	
37	4263	19.4	14.7	C	-9.09	-9.37	
	4421	36.5	24.3	D	-8.51	-8.79	
41	4524	32.0	20.4	C	-7.97	-8.26	
50	4221	16.9	13.4	D	-9.11	-9.40	
53	4467	32.2	22.7	C	-8.47	-8.76	
			mean abundance:		-8.33	-8.65	*
HD191742							
37	4263	13.7	11.8	D	-8.63	-8.97	
53	4467	37.5	27.0	D	-7.86	-8.09	*
			mean abundance:		-8.21	-8.47	uc
HD201601							
32	4566	24.0	18.6	D	-8.44	-8.73	
36	4434	67.5	41.9	C	-8.12	-8.40	
37	4263	16.6	13.9	D	-9.16	-9.45	
	4421	37.7	26.6	C	-8.46	-8.72	
41	4524	30.7	20.2	C	-8.02	-8.30	
45	4362	34.3	21.2	C	-8.78	-9.03	
50	4221	15.5	12.8	E	-9.18	-9.46	
53	4467	44.2	32.3	C	-8.12	-8.37	
			mean abundance:		-8.33	-8.60	*

Notes: * = D quality lines and those whose equivalent widths are less than 20mA are given one-half weight in the mean abundance average.
uc = uncertain determination.

Table A-50

Eu Abundances from EuII Lines

mult.	λ	W	qual.	W_o 1	W_o 2	measured blend λ	abundance 1	abundance 2
HD2453								
1	4205	249.5	C	122.9	115.5	05.03	-5.70	-6.13
4	4436	196.6	B	73.9	72.5	35.60	-5.59	-5.97
5	3907	113.4	B	47.2	47.2		-6.67	-7.04
					mean abundance:		-5.78	-6.16
HD5797								
1	4205	243.4	E	153.1	148.2	05.04	-6.19	-6.65
4	4436	168.6	C	127.6	126.8	35.54	-5.73	-6.17
5	3907	104.8	D	75.4	75.4		-6.76	-7.13
					mean abundance:		-5.98	-6.47
HD8441								
1	4205	36.0	E	24.0	24.0	04.99	-7.93	-8.30
4	4436	31.1	C	31.1	31.1	35.58	-7.03	-7.39
5	3907	34.7	C	34.7	34.7		-7.30	-7.67
					mean abundance:		-7.31	-7.65
HD12288								
1	4205	104.8	C	27.2	25.2	04.98	-7.47	-7.93
5	3907	66.2	W	26.9	26.9		-7.33	-7.73
					mean abundance:		-7.42	-7.85

Table A-50, continued

mult.	λ	W	qual.	W_o 1	W_o 2	measured blend λ	abundance 1	abundance 2
HD18078								
1	4205	88.1	C	30.6	30.6	05.03	-7.77	-8.10
4	4436	47.0	D	21.2	22.1	35.59	-7.57	-7.87
5	3907	40.0	D	21.8	21.8		-8.07	-8.40
					mean abundance:		-7.81	-8.08
HD22374								
1	4205	32.8	B	30.3	30.3	05.08	-8.37	-8.71
4	4436	12.6	D	11.1	11.6	35.68	-8.61	-8.98
					mean abundance:		-8.44	-8.82
HD50169								
1	4205	102.7	E	35.3	35.1	05.07	-7.48	-7.81
4	4436	63.2	C	24.3	25.1	35.64	-7.34	-7.66
5	3907	50.9	D	23.6	23.6		-7.89	-8.22
					mean abundance:		-7.47	-7.79
HD81009								
1	4205	279.8	E	49.4	50.0	05.00	-7.79	-8.19
4	4436	264.4	C	53.5	53.5	35.58	-7.04	-7.47
5	3907	274.9	C	73.9	73.9		-7.07	-7.53
					mean abundance:		-7.19	-7.62
HD89069								
1	4205	134.8	E	67.7	69.5	05.05	-6.69	-7.10
4	4436	121.8	B	61.7	62.1	35.60	-6.18	-6.63
5	3907	87.5	C	50.0	50.0		-7.00	-7.38
					mean abundance:		-6.49	-6.93

Table A-50, continued

mult.	λ	W	qual.	W_o 1	W_o 2	measured blend λ	abundance 1	abundance 2
HD110066								
1	4205	215.9	C	65.9	65.9	05.03	-6.60	-7.21
4	4436	156.2	C	57.0	52.5	35.61	-6.15	-6.55
5	3907	147.1	E	67.8	67.8		-6.40	-6.77
					mean abundance:		-6.34	-6.77
HD111133								
1	4205	63.1	W	25.6	25.6	05.03	-7.49	-7.92
4	4436	27.0	E	16.9	16.9	35.60	-7.27	-7.69
5	3907	25.0	E	16.4	16.4		-7.83	-8.25
					mean abundance:		-7.47	-7.89
HD118022								
1	4205	219.6	C	117.8	116.4	05.04	-6.05	-6.47
4	4436	136.4	C	53.8	53.8	35.60	-6.35	-6.78
5	3907	95.2	C	47.4	47.4		-6.96	-7.42
					mean abundance:		-6.32	-6.74
HD137909								
1	4205	651.5	C	474.6	472.8	05.02	-5.04	-5.33
4	4436	342.0	C	94.0	92.0	35.62	-5.86	-6.20
5	3907	250.6	E	111.9	111.9		-6.19	-6.50
					mean abundance:		-5.43	-5.73

Table A-50, continued

mult.	λ	W	qual.	W_o 1	W_o 2	measured blend λ	abundance 1	abundance 2
HD137949								
1	4205	501.7	C	277.1	277.1	05.01	-6.48	-6.90
4	4436	312.8	C	71.7	71.7	35.59	-7.13	-7.59
5	3907	240.2	C	130.5	130.5		-7.00	-7.43
					mean abundance:		-6.77	-7.20
HD165474								
1	4205	375.4	C	133.8	133.8	05.02	-6.78	-7.21
4	4436	250.4	C	53.1	53.6	35.60	-7.21	-7.64
5	3907	213.4	E	61.9	61.9		-7.45	-7.91
					mean abundance:		-7.05	-7.50
HD176232								
1	4205	106.0	E	40.0	42.0	05.06	-9.26	-9.59
4	4436	146.0	C	40.0	40.0	35.65	-8.64	-9.01
5	3907	70.5	C	41.2	41.2		-8.99	-9.41
					mean abundance:		-8.89	-9.27
HD191742								
1	4205	177.7	C	72.5	72.5	05.04	-7.68	-8.15
4	4436	176.7	B	71.1	71.7	35.65	-7.09	-7.53
5	3907	99.9	C	70.4	70.4		-7.57	-8.03
					mean abundance:		-7.38	-7.82
HD192678								
1	4205	116.2	C	0.0	0.0	04.98		
4	4436	34.2	E	17.8	17.5	35.63	-7.44	-7.79
					mean abundance:		-7.44	-7.79 uc

Table A-50, continued

mult.	λ	W	qual.	W_o 1	W_o 2	measured blend λ	abundance 1	abundance 2
HD201601								
1	4205	165.2	C	71.2	77.3	05.04	-8.53	-8.82
4	4436	179.0	C	75.7	76.1	35.63	-7.82	-8.19
5	3907	75.5	E	48.7	48.7		-8.84	-9.19
					mean abundance:		-8.19	-8.54
HD204411								
1	4205	15.6	D	0.0	0.0	05.08		
4	4436	61.1	C	5.8	8.7	35.66	-8.84	-9.07
					mean abundance:		-8.84	-9.07 uc
HD216533								
1	4205	98.9	C	49.2	49.2	05.07	-6.74	-7.15
4	4436	50.7	C	25.1	25.7	35.65	-7.11	-7.47
					mean abundance:		-6.89	-7.28

Note: uc = uncertain determination, probably represents an upper limit.

Table A-51

Gd Abundances from GdII Lines

mult.	λ	W	W_o	qual.	abundance 1	abundance 2	
HD2453							
32	4215	43.3	23.4	C	-7.47	-7.79	
46	4253	15.9	11.9	C	-8.18	-8.31	
103	4407	62.4	27.7	B	-7.01	-7.19	
			mean abundance:		-7.34	-7.54	
HD5797							
32	4215	75.5	52.8	E	-6.93	-7.25	
44	4506	26.7	19.2	C	-7.39	-7.69	
46	4253	9.1	8.1	D	-8.79	-9.08	
103	4407	101.1	62.4	C	-6.37	-6.65	
			mean abundance:		-6.78	-7.07	
HD8441							
32	4215	32.0	32.0	C	-7.21	-7.53	
82	4582	25.1	25.1	C	-6.80	-7.10	
103	4407	31.8	31.8	C	-6.93	-7.21	
			mean abundance:		-6.95	-7.25	
HD12288							
32	4215	67.9	27.9	D	-7.10	-7.48	
46	4253	18.0	12.8	C	-7.77	-8.17	*
103	4407	74.6	27.6	C	-6.74	-7.15	
			mean abundance:		-7.02	-7.34	

Table A-51, continued

mult.	λ	W	W_o	qual.	abundance 1	abundance 2
HD18078						
32	4215	34.0	20.2	E	-7.84	-8.13
82	4582	51.1	26.1	D	-6.86	-7.14
103	4407	57.3	26.2	C	-7.28	-7.53
			mean abundance:		-7.26	-7.53
HD22374						
32	4215	60.6	58.3	C	-6.91	-7.17
82	4582	27.2	25.2	C	-7.40	-7.66
103	4407	33.7	30.4	D	-7.53	-7.77
			mean abundance:		-7.15	-7.41
HD50169						
82	4582	76.0	31.1	Q	-6.56	-6.86
103	4407	71.6	28.2	Q	-7.11	-7.36
			mean abundance:		-6.76	-7.02
HD81009						
32	4215	78.4	29.7	E	-8.03	-8.30
62	4483	64.1	26.3	E	-7.73	-8.02
103	4407	44.6	21.0	E	-8.04	-8.30
			mean abundance:		-7.91	-8.19
HD89069						
32	4215	34.0	22.2	C	-7.85	-8.20
43	4316	20.2	14.9	D	-7.98	-8.32
46	4253	21.0	15.1	D	-8.18	-8.51
			mean abundance:		-7.94	-8.29

Table A-51, continued

mult.	λ	W	W_o	qual.	abundance 1	abundance 2
HD110066						
31	4493	16.3	12.2	D	-7.37	-7.68
32	4215	63.0	32.0	C	-7.30	-7.63
43	4316	71.1	31.5	E	-7.15	-7.46
44	4506	36.4	20.8	C	-6.94	-7.26
46	4253	18.9	13.4	D	-8.11	-8.44
62	4483	28.1	18.0	C	-7.47	-7.79
103	4407	83.6	34.7	B	-6.88	-7.17
			mean abundance:		-7.12	-7.46
HD111133						
82	4582	43.8	23.5	Q	-6.53	-6.91
103	4407	55.3	25.8	Q	-6.89	-7.24
			mean abundance:		-6.68	-7.05
HD118022						
32	4215	67.3	36.6	C	-7.17	-7.54
103	4407	57.7	28.3	C	-7.29	-7.54
			mean abundance:		-7.23	-7.54
HD137909						
31	4498	48.2	22.2	C	-7.23	-7.47
32	4215	103.2	39.7	E	-7.25	-7.50
44	4506	75.2	30.2	C	-6.84	-7.07
62	4483	85.1	34.0	C	-7.23	-7.27
103	4407	81.5	30.5	C	-7.30	-7.54
			mean abundance:		-7.14	-7.33

Table A-51, continued

mult.	λ	W	W_o	qual.	abundance 1	abundance 2
HD137949						
32	4215	74.6	33.2	E	-8.19	-8.43
44	4506	95.6	37.3	C	-7.21	-7.46
62	4483	107.4	43.0	C	-7.32	-7.57
103	4407	79.7	30.9	C	-7.88	-8.10
			mean abundance:		-7.49	-7.74
HD165474						
31	4498	20.6	14.1	D	-8.01	-8.31
32	4215	39.9	20.5	E	-8.53	-8.80
43	4316	54.3	23.7	E	-8.19	-8.49
62	4483	55.7	24.9	C	-7.91	-8.19
103	4407	47.5	21.9	W	-8.10	-8.35
			mean abundance:		-8.12	-8.40
HD176232						
32	4215	32.8	22.0	E	-9.09	-9.31
43	4316	23.6	16.7	D	-9.15	-9.31
44	4506	17.1	13.4	C	-8.61	-8.82
46	4253	21.4	15.5	C	-9.39	-9.59
62	4483	18.0	14.2	D	-9.01	-9.21
82	4582	37.0	24.0	D	-8.28	-8.47
103	4407	34.3	21.3	C	-8.62	-8.80
			mean abundance:		-8.74	-8.97

Table A-51, continued

mult.	λ	W	W_o	qual.	abundance 1	abundance 2	
HD191742							
103	4407	49.3	28.8	B	-7.97	-8.17	
			mean abundance:		-7.97	-8.17	
HD192678							
32	4215	58.0	27.5	C	-7.26	-7.55	
103	4407	98.7	36.3	C	-6.59	-6.88	
			mean abundance:		-6.81	-7.10	
HD201601							
31	4498	19.4	15.5	C	-8.61	-8.82	
32	4215	26.1	18.4	E	-9.29	-9.50	
43	4316	23.1	16.9	C	-9.15	-9.37	
46	4253	23.0	16.5	C	-9.38	-9.57	
103	4407	30.4	20.1	C	-8.69	-8.87	
			mean abundance:		-8.91	-9.11	
HD204411							
32	4215	8.6	8.3	D	-8.91	-9.09	
103	4407	24.2	21.6	Q	-7.85	-8.12	+
			mean abundance:		-8.42	-8.66	
HD216533							
32	4215	45.4	28.2	E	-7.23	-7.58	
43	4316	15.0	11.9	D	-7.75	-8.08	
103	4407	59.5	31.3	C	-6.82	-7.27	
			mean abundance:		-7.12	-7.47	

Table A-51, continued

Notes: One-half weight is given to lines of D and W quality in mean abundance averages.
* = one-half weight given.
+ = one-quarter weight given.

Table A-52

Hf Abundances from HfII Lines

star	λ	W	W_o	qual.	abundance 1	abundance 2
HD110066	4232	34.1	27.7	C	-8.27	-8.36

Table A-53

Os Abundances from OsI Lines

star	λ	W	W_o	qual.	abundance 1	abundance 2
HD5797	4420	46.4	29.4	D	-6.58	-6.94
HD118022	4420	24.6	16.7	W	-6.85	-7.24

Table A-54

U Abundances from UII Lines

	UII(-) λ3859.6					UII(-) λ4241.7					mean U abundance	
				abundance					abundance			
star	W	qual.	W_o	1	2	W	qual.	W_o	1	2	1	2
HD2453	82.7	E	32.3	-8.74	-8.93	5.8	D	5.7	-9.78	-9.95	-8.90	-9.09
HD5797	114.0	E	86.4	-7.87	-8.08	22.7	D	20.3	-9.26	-9.46	-8.04	-8.25
HD8441	33.2	E	33.2	-8.76	-8.97	n.m.					-8.76	-8.97
HD12288	n.m.					n.m.					n.m.	n.m.
HD18078	70.2	E	28.5	-9.09	-9.26	n.m.					-9.09	-9.26
HD22374	37.4	E	34.3	-9.12	-9.31	n.m.					-9.12	-9.31
HD50169	80.8	E	28.3	-9.04	-9.22	n.m.					-9.04	-9.22
HD81009	44.1	E	20.5	-9.86	-10.10	30.5	D	19.1	-9.47	-9.68	-9.69	-9.91
HD89069	56.1	E	29.5	-9.09	-9.32	n.m.					-9.09	-9.32
HD110066	72.0	E	29.6	-9.00	-9.22	16.2	D	14.6	-9.34	-9.54	-9.09	-9.30
HD111133	17.7	E	13.1	-9.60	-9.83	n.m.					-9.60	-9.83
HD118022	55.7	E	27.3	-9.17	-9.42	11.2	D	10.7	-9.60	-9.80	-9.27	-9.51
HD137909	68.4	E	26.0	-9.38	-9.52	57.2	C	33.1	-8.57	-8.70	-8.81	-8.94
HD137949	51.4	W	23.3	-9.97	-10.20	n.m.					-9.97	-10.20
HD165474	29.4	W	17.2	-10.15	-10.37	n.m.					-10.15	-10.37
HD176232	44.3	E	25.9	-10.20	-10.38	n.m.					-10.20	-10.38
HD191742	80.5	E	50.9	-8.86	-9.07	n.m.					-8.86	-9.07
HD192678	59.1	E	25.0	-9.09	-9.30	n.m.					-9.09	-9.30
HD201601	23.3	E	17.4	-10.65	-10.85	n.m.					-10.65	-10.85
HD204411	19.1	E	17.8	-9.88	-10.12	n.m.					-9.88	-10.12
HD216533	95.9	E	55.4	-7.94	-8.16	n.m.					-7.94	-8.16
ν Cap	n.m.					n.m.					n.m.	n.m.
o Peg	n.m.					n.m.					n.m.	n.m.

Notes: D quality lines are given one-half weight in the mean abundance averages.
n.m. = not measured.

Note on Tables A-55 Through A-58

Tables A-55 through A-57 give the equivalent widths, W, and the line qualities, qual., of CaII(1) λ3933.66, MoII(3) λ4363.64 and λ4433.50, and GdIII λ4202.52 which were not converted into abundances. Table A-58 gives the measured wavelengths of the UII lines after corrections have been applied for the radial velocity.

Table A-55

CaII(1) λ3933.664 Equivalent Widths

star	W(mÅ)	qual.
HD2453	364	C
HD5797	407	E
HD8441	214	E
HD12288	390	D
HD18078	365	W
HD22374	214	C
HD50169	1032	C
HD81009	1840	C
HD89069	287	C
HD110066	921	E
HD111133	198	C
HD118022	354	E
HD137909	-	*
HD137949	-	*
HD165474	-	*
HD176232	-	*
HD191742	-	*
HD192678	319	E
HD201601	-	*
HD204411	-	*
HD216533	414	E
ν Cap	539	-
o Peg	701	C

Note: * = equivalent width not measured due to extremely broad wings.

Table A-56

Measured Equivalent Widths of MoII Lines

star	λ(Å)	W(mÅ)	qual.
HD2453	4364	46.7	C
	4433	69.4	D
HD5797	4364	30.8	C
	4433	68.9	C
HD18078	4364	14.9	D
	4433	31.0	D
HD81009	4364	23.9	C
HD89069	4364	33.6	C
	4433	40.1	D
HD110066	4433	38.2	C
HD111133	4433	25.2	Q
HD191742	4364	43.0	B
	4433	56.5	C
HD192678	4364	11.3	D
	4433	47.0	C
HD210601	4364	26.4	C
HD204411	4364	14.7	D
	4433	9.4	D
HD216533	4433	36.8	Q

Table A-57

Equivalent Width Measurements of GdIII λ4202.521

star	W(mÅ)	qual.
HD2453	45.1	C
HD5797	93.2	C
HD8441	30.7	C
HD18078	88.1	C
HD22374	37.3	Q
HD50169	69.8	C
HD81009	66.7	E
HD89069	49.8	E
HD110066	66.6	B
HD111133	58.3	C
HD118022	66.0	C
HD137909	104.7	E
HD137949	57.1	W
HD191742	54.5	D
HD192678	77.0	C
HD204411	20.6	Q
HD216533	55.8	C

Table A-58

Measured Wavelengths of UII Lines

star	measured wavelength λ3854.66	λ3859.58	λ4241.67
HD2453	54.76br	59.63	41.68
HD5797	54.76br	59.63	41.65
HD8441	54.76	59.61	
HD12288	54.77	59.64	
HD18078	54.78br	59.67	
HD22374	54.77	59.66	
HD50169	54.80	59.61wk	
HD81009	54.81	59.61	41.67wk
HD89069	54.80br	59.63	
HD110066	54.68	59.63	41.65
HD111133	54.77	59.62	
HD118022	54.74	59.62	41.62wk
HD137909	54.80br	59.59wk	41.66
HD137949	54.78	59.69	
HD165474	54.75	59.68	
HD176232	54.78	59.66	
HD191742	54.77br	59.65	41.65:
HD192678	54.79br	59.64	
HD201601	54.57	59.64	
HD204411	54.80	59.67	
HD216533	54.79br	59.63	

Notes: br = broad feature
wk = weak feature
: = uncertain determination

REFERENCES

Abt, H. A. 1967, in The Magnetic and Related Stars, ed. by R. C. Cameron (Baltimore:Mono Book Corp.),p.173.

Abt, H. A., and Golson, J. C. 1962, Ap. J., 136, 25.

Adelman, S. J. 1968, Pub. A. S. P., 80, 329.

-----. 1972, in preparation(research done with A. R. Hyland).

Albertson, W. 1936, Ap. J., 84, 26.

Allen, B. J., Gibbons, J. H., and Macklin, R. L. 1971, Advances in Nuclear Physics, 4, 205.

Aller, L. H. 1960, Sky and Telescope, 19, 338.

-----. 1963, Astrophysics: The Atmospheres of the Sun and Stars(New York: Ronald Press Co.).

-----. 1968, Pro. Astron. Soc. Australia, 1(4), 133.

Aller, M. F., and Cowley, C. R. 1970, Ap. J. (Letters), 162, L145.

Auer, L. H. 1964, Ap. J., 139, 1148.

Auer, L. H., Mihalas, D., Aller, L. H., and Ross, J. E. 1966, Ap. J., 145, 153.

Babcock, H. W. 1947, Ap. J., 105, 105.

-----. 1958, Ap. J. Suppl., 3, 141.

-----. 1960, in Stars and Stellar Systems: Vol. 6, Stellar Atmospheres, ed. by J. L. Greenstein(Chicago:University of Chicago Press), chap. vii,p.282.

Baschek, B., Garz, T., Holweger, H., and Richter, J. 1970, Astr. and Ap., 4, 229.

Baschek, B., and Oke, J. B. 1965, Ap. J., 141, 1404.

Baschek, B., and Reimers, D. 1969, Astr. and Ap., 2, 240.

Baschek, B., and Searle, L. 1969, Ap. J., 155, 537.

Baxandall, F. E. 1913, Observatory, 36, 440.

Belopolshy, A. 1913, A. N., 196, 1.

Bidelman, W. P. 1966, in I. A. U. Symp. 26, Abundance Determinations in Stellar Spectra, ed. by H. Hubenet(New York:Academic Press),p.229.

-----. 1967, in The Magnetic and Related Stars, ed. by R. C. Cameron (Baltimore:Mono Book Corp.),p.29.

-----. 1971a(private communication).

-----. 1971b(private communication).

Bidelman, W. P., and Corliss, C. H. 1962, Ap. J., 135, 968.

Bonsack, W. K. 1961, Ap. J., 133, 551.

Brandi, E., and Jaschek, M. 1970, Pub. A. S. P., 82, 847.

Brancazio, P. J., and Cameron, A. G. W. 1967, Canadian J. Phys., 45, 3297.

Bray, R. J., and Loughhead, R. E. 1965, Sunspots(New York:J. Wiley and Sons,Inc.).

Bridges, J. M., and Wiese, W. L. 1970, Ap. J. (Letters), 161, L71.

Bunker, A. F. 1940, David Dunlap Obs. Pub., 1, 209.

Burbidge, E. M., Burbidge, G. R., Fowler, W. A., and Hoyle, F. 1957, Rev. Mod. Phys., 29, 547.

Burbidge, G. R., and Burbidge, E. M. 1955a, Ap. J., 122, 396.

-----. 1955b, Ap. J. Suppl., 1, 431.

-----. 1956, Ap. J., 124, 130.

Cameron, R. C. 1966, Georgetown Obs. Mono. No. 21.

Cannon, A. J. 1901, Ann. Harvard Coll. Obs., 28, 129.

Cayrel, R., and Jugaku, J. 1963, Ann. d'ap., 26, 495.

Chapelle, J., and Sahal-Brechot, S. 1970, Astr. and Ap., 6, 415.

Clayton, D. D., and Rassbach, M. E. 1967, Ap. J., 148, 69.

Clifford, F. E., and Tayler, R. J. 1956, Mem. R. A. S., 69, 21.

Code, A. D. 1960, in Stars and Stellar Systems: Vol. 6, Stellar Atmospheres, ed. by J. L. Greenstein(Chicago:University of Chicago Press, chap. ii,p.50.

Cohen, J. G. 1970, Ap. J., 159, 473.

Conti, P. S. 1969, Ap. J., 156, 661.

-----. 1970, ibid., 160, 1077.

Conti, P. S., and Strom, S. E. 1968a, Ap. J., 152, 483.

-----. 1968b, ibid., 154, 975.

Corliss, C. H. 1962, J. Res. N. B. S., 66A, 169.

Corliss, C. H., and Bozman, W. R. 1962, Experimental Transition Probabilities For Spectral Lines of Seventy Elements, N. B. S. Mono. 53(Washington, D. C.:U.S. Government Printing Office).

Cowley, A., Cowley, C., Jaschek, M., and Jaschek, J. 1969, A. J., 74, 375.

Cowley, C. 1970, Ap. Letters, 5, 149.

Crawford, D. L. 1963, Ap. J., 137, 530.

Crawford, D. L., and Barnes, J. V. 1970, A. J., 75, 978.

Crosswhite, H. 1968, Analysis in progress, Johns Hopkins University.

Curtis, C. W. 1952, J. Opt. Soc. Am., 42, 300.

Danziger, I. J. 1966, Ap. J., 143, 591.

Deutsch, A. J. 1954, Trans. I. A. U.(Cambridge, England:Cambridge University Press), 8, 801.

-----. 1956, Pub. A. S. P., 68, 92.

-----. 1958, in I. A. U. Symp. 6, Electromagnetic Phenomena in Cosmical Physics, ed. by B. Lehnert(Cambridge, England:Cambridge University Press),p.209.

Dieke, G. H., Crosswhite, H. M., and Dunn, B. 1961, J. Opt. Soc. Am., 51,

820.

Diringer, M. 1965, Ann. de Phys., Series 13, 10, 89.

Drawin, H. R., and Felenbok, P. 1965, Data for Plasmas in Local Thermodynamic Equilibrium(Paris:Gauthier-Villars).

Durrant, C. J. 1970a, M. N. R. A. S., 147, 57.

-----. 1970b, ibid., 147, 75.

Dworetsky, M. M. 1969, Ap. J. (Letters), 156, L101.

Eggen, O. J. 1967, in The Magnetic and Related Stars, ed. by R. C. Cameron(Baltimore:Mono Book Corp.),p.141.

Evans, J. C. 1966, Ph.D. thesis, University of Michigan.

Evans, J. C., and Elste, G. 1971, Astr. and Ap., 12, 428.

Faraggiana, R., and Hack, M. 1962, Mem. Soc. Astr. Italiana, 33, 90.

Field, G. B. 1970, Sixteenth Liege Symposium(June 1969), Institute D'astrophysique Liege,p.29.

Fowler, W. A., Burbidge, E. M., Burbidge, G. R., and Hoyle, F. 1965, Ap. J., 142, 423.

Fowler, W. A., Burbidge, G. R., and Burbidge, E. M. 1955, Ap. J. Suppl., 2, 167

Fred, M. 1971(private communication).

Garstang, R. H. 1964, Observatory, 84, 161.

Garz, T., Heise, H., and Richter, J. 1970, Astr. and Ap., 9, 296.

Garz, T., Holweger, H., Kock, M., and Richter, J. 1969, Astr. and Ap., 2, 446.

Garz, T., and Kock, M. 1969, Astr. and Ap., 2, 274.

Goldberg, L., Müller, E. A., and Aller, L. H. 1960, Ap. J. Suppl., 5, 1.

Grevesse, N., and Swings, J. P. 1969, Astr. and Ap., 2, 28.

Griem, H. R. 1964, Plasma Spectroscopy(New York:McGraw Hill Book Company).

Groth, H. G. 1961, Zs. f. Ap., 51, 231.

Guthnick, P., and Prager, R. 1914, Veroff. Berlin-Babelsberg, 1, 38.

Guthrie, B. N. G. 1967, Pub. of Royal Observatory, Edinburgh, 6, 145.

-----. 1969a, Astrophys. and Sp. Sci., 3, 542.

-----. 1969b, Observatory, 89, 224.

Hack, M. 1958, Mem. Soc. Astr. Italiana, 29, 263.

-----. 1960, ibid., 31, 279.

-----. 1968, Sky and Telescope, 36, 92.

Harris, D. L., III, Strand, K. A., and Worley, C. E. 1963, in Stars and Stellar Systems: Vol. 3, Basic Astronomical Data, ed. by K. A. Strand(Chicago:University of Chicago Press), chap. xv,p.273.

Havnes, O., and Conti, P. S. 1971, Astr. and Ap., 14, 1.

Hayes, D. S. 1970, Ap. J., 159, 165.

Hiltner, W. A. 1945, Ap. J., 102, 438.

Hyland, A. R. 1967, in The Magnetic and Related Stars, ed. by R. C. Cameron(Baltimore:Mono Book Corp.),p.311.

Iben, I. 1967a, Ap. J., 147, 650.

-----. 1967b, Ann. Rev. Astr. and Ap., 5, 571.

Jaschek, C., and Jaschek, M. 1967, in The Magnetic and Related Stars, ed. by R. C. Cameron(Baltimore:Mono Book Corp.),p.287.

Jaschek, M., and Malaroda, S. 1970, Nature, 225, 246.

Jugaku, J., and Sargent, W. L. W. 1968, Ap. J., 151, 259.

Jugaku, J., Sargent, W. L. W., and Greenstein, J. L. 1961, Ap. J., 134, 783.

Kiess, C. C., and Meggers, W. F. 1928, J. Res. N. B. S., 1, 641.

Kodaira, K. 1967, Ann. Tokyo Astr. Obs., Ser. II, 10, 157.

Kohl, K. 1964, Das Spectrum des Sirius λλ3100-8863 Å, Institut fur

Theoretische Physik und Sternwarte der Universitat Kiel.

Kuchowicz, B. 1970, Nature, 227, 156.

Kurucz, R. 1969a, in Proc. 3rd Harvard-Smithsonian Conf. Stellar Atm., ed. by O. Gingerich(Cambridge, Mass.:M.I.T. Press),p.375.

-----. 1969b, Ap. J., 156, 235.

Lambert, D. L. 1968, M. N. R. A. S., 138, 143.

Lambert, D. L., and Warner, B., 1968a, M. N. R. A. S., 140, 197.

-----. 1968b, ibid., 138, 181.

-----. 1968c, ibid., 138, 213.

Lawrence, G. M., Link, J. K., and King, R. B. 1965, Ap. J., 141, 293.

Lockyer, N., and Baxandall, F. E. 1906, Proc. Roy. Soc.(London), 77, 550.

Lundendorff, H. 1906, A. N., 173, 1.

Maestre, L. A., and Deutsch, A. J. 1961, Ap. J., 134, 562.

Martin, D. C. 1935, Phys. Rev., 48, 938.

Martin, W. C. 1959, J. Opt. Soc. Am., 49, 1071.

Maury, A. C. 1897, Ann. Harvard Coll. Obs., 28, 1.

Meggers, W. F. 1941, J. Opt. Soc. Am., 31, 39 and 605.

Meggers, W. F., Corliss, C. H., and Schribner, B. F. 1961, Tables of Spectral-Line Intensities, Vol. 1, N. B. S. Mono. 32-Part 1 (Washington, D. C.:U.S. Government Printing Office).

Meggers, W. F., Schribner, B. F., and Bozman, W. R. 1951, J. Res. N. B. S., 46, 85.

Mestel, L. 1967, in The Magnetic and Related Stars, ed. by R. C. Cameron(Baltimore:Mono Book Corp.),p.101.

Michaud, G. 1970, Ap. J., 160, 641.

Middlehurst, B., and Aller, L. H. 1968, in Stars and Stellar Systems: Vol. 8, Nebulae and Interstellar Material, ed. by B. Middlehurst and L. H. Aller(Chicago:University of Chicago Press),p.vii.

Mihalas, D. 1965, Ap. J. Suppl., 9, 321.

Mihalas, D., and Henshaw, J. L. 1966, Ap. J., 144, 25.

Mihalas, D., and Routly, P. M. 1968, Galactic Astronomy(San Francisco: W. E. Freeman and Co.).

Moore, C. E. 1945, A Multiplet Table of Astrophysical Interest(N. B. S. Tech. Note, No. 36).

-----. 1958, Atomic Energy Levels, NBS Circular 467, 3(Washington, D.C.: U. S. Government Printing Office).

-----. 1965, Selected Tables of Atomic Spectra, NSRDS-NBS 3, Section 1 (Washington, D. C.:U. S. Government Printing Office).

Morgan, W. W. 1933, Ap. J., 77, 330.

Müller, E. A. 1966, in I. A. U. Symp. 26, Abundance Determinations in Stellar Spectra, ed. by H. Hubenet(New York:Academic Press),p.171.

-----. 1967, paper presented at the Symposium on the Origin and Distribution of Elements, Paris.

Oke, J. B. 1964, Ap. J., 140, 689.

Oke, J. B., and Schild, R. E. 1970, Ap. J., 161, 1015.

Osawa, K. 1965, Ann. Tokyo Astr. Obs., 9, 123.

Osman, B. 1966, Ph. D. thesis, University of Paris.

Penkin, N. P. 1964, J. Q. S. R. T., 4, 41.

Peterson, B. A. 1966, Ap. J., 145, 735.

Peterson, D. M. 1970, Ap. J., 161, 685.

Popper, D. M. 1959, Ap. J., 129, 659.

Preston, G. W. 1967a, Ap. J., 150, 871.

-----. 1967b, in The Magnetic and Related Stars, ed. by R. C. Cameron (Baltimore:Mono Book Corp.),p.3.

-----. 1969, Ap. J., 158, 251.

-----. 1970a, ibid., 160, 1059.

-----. 1970b, in Stellar Rotation, ed. by A. Slettebak(Dordrecht, D. Publishing Company),p.254.

-----. 1970c, Pub. A. S. P., 82, 878.

-----. 1971a, Ap. J., 164, 309.

-----. 1971b, Ap. J. (Letters), 164, L41.

-----. 1971c, Pub. A. S. P., 83, 571.

-----. 1971d(private communication).

Preston, G. W., and Cathey, L. R. 1968, Ap. J., 152, 1113.

Preston, G. W., and Wolff, S. C. 1970, Ap. J., 160, 1071.

Przyblski, A. 1966, Nature, 210, 20.

Pyper, D. 1969, Ap. J. Suppl., 18, 347.

Rice, J. B. 1970, Astr. and Ap., 9, 189.

Ross, J. E. 1970, Nature, 225, 610.

Russell, H. N. 1927, Ap. J., 66, 307.

Sargent, A. I., Greenstein, J. L., and Sargent, W. L. W. 1969, Ap. J., 157, 757.

Sargent, W. L. W. 1964, Ann. Rev. Astr. and Ap., 2, 297.

-----. 1966, in I. A. U. Symp. 26, Abundance Determinations in Stellar Spectra, ed. by H. Hubenet(New York:Academic Press),p.247.

Sargent, W. L. W., and Burbidge, G. R. 1970, Comments Ap. Space Phys., 2, 172.

Sargent, W. L. W., and Searle, L. 1962, Ap. J., 186, 408.

-----. 1967, in The Magnetic and Related Stars, ed. by R. C. Cameron (Baltimore:Mono Book Corp.),p.209.

Sargent, W. L. W., Searle, L., and Jugaku, J. 1962, Pub. A. S. P., 74, 408.

Sargent, W. L. W., Strom, K. M., and Strom, S. E. 1969, Ap. J., 157, 1265.

Schaeffer, A. 1971, Ap. J., 163, 411.

Schild, R., and Chaffee, F. 1971, Ap. J., 169, 529.

Schild, R., Peterson, D. M., and Oke, J. B. 1971, Ap. J., 166, 95.

Schramm, D. N., and Fowler, W. A. 1971, Nature, 231, 103.

Searle, L., Lungershausen, W. T., and Sargent, W. L. W. 1966, Ap. J., 145, 141.

Searle, L., and Sargent, W. L. W. 1964, Ap. J., 139, 793.

-----. 1967, in The Magnetic and Related Stars, ed. by R. C. Cameron (Baltimore:Mono Book Corp.),p.219.

Seeger, P. A., Fowler, W. A., and Clayton, D. D. 1965, Ap. J. Suppl., 11, 121.

Seeger, P. A., and Schramm, D. N. 1970, Ap. J. (Letters), 160, L157.

Shenstone, A. G. 1938, Phil. Trans. Roy. Soc. London, A, 237, 453.

Smith, M. A. 1971, Astr. and Ap., 11, 325.

Spitzer, L. 1968, in Stars and Stellar Systems: Vol. 7, Nebulae and Interstellar Matter, ed. by B. M. Middlehurst and L. H. Aller (Chicago:University of Chicago Press), chap. i,p.1.

Stepien, K. 1968, Ap. J., 154, 945.

Stibbs, D. W. N. 1950, M. N. R. A. S., 110, 395.

Strom, S. E., Gingerich, O., and Strom, K. M., 1966, Ap. J., 146, 880.

Strom, S. E., and Strom, K. M. 1969, Ap. J., 155, 17.

Sugar, J. 1961, Johns Hopkins Spectroscopic Report No. 22.

-----. 1965, J. Opt. Soc. Am., 55, 33.

-----. 1969, J. Res. N. B. S., 73A, 333.

-----. 1970, J. Opt. Soc. Am., 69, 454.

Sugar, J., and Reader, J. 1965, J. Opt. Soc. Am., 55, 1286.

-----. 1966, ibid., 56, 1189.

Tammann, G. A. 1970, Astr. and Ap., 8, 458.

Tomkins, F. S., and Fred, M. 1949, J. Opt. Soc. Am., 39, 357.

Tomley, L. J., Wallerstein, G., and Wolff, S. C. 1970, Astr. and Ap., 9, 380.

Truran, J. W., and Cameron, A. G. W. 1967, in The Magnetic and Related Stars, ed. by R. C. Cameron(Baltimore:Mono Book Corp.),p.273.

Underhill, A. B. 1969, in Proc. 3rd Harvard-Smithsonian Conf. Stellar Atm., ed. O. Gingerich(Cambridge, Mass.:M. I. T. Press),p.207.

Urey, H. C. 1967, Quart. J. R. A. S., 8, 23.

Van den Heuvel, E. P. J. 1967, B. A. N., 19, 11.

-----. 1971, Astr. and Ap., 11, 461.

Van Kleef, Th. A. M. 1960, Proc. Ned. Akad. Wetenschap, 63B, 501.

Velasco, R., Iglesias, L., Gullon, M. N., and Diago, M. C. 1963, Appl. Optics, 2, 687.

Wallerstein, G. 1968, in Nucleosynthesis, ed. by W. D. Arnett, C. J. Hansen, J. W. Truran, and A. G. W. Cameron(New York:Gordon and Breach),p.29.

Wallerstein, G., and Conti, P. S. 1969, Ann. Rev. Astr. and Ap., 7, 99.

Wallerstein, G., and Hack, M. 1964, Observatory, 84, 160.

Wallerstein, G., and Merchant, A. E. 1965, Pub. A. S. P., 77, 140.

Warner, B. 1967, Mem. R. A. S., 70, 165.

-----. 1968, M. N. R. A. S., 138, 229.

Watson, W. D. 1970, Ap. J. (Letters), 162, L45.

Weast, R. C., ed. 1968, Handbook of Chemistry and Physics(Cleveland: Chemical Rubber Publishing Company).

Wiese, W. L., Smith, M. W., and Miles, B. M. 1969, Atomic Transition Probabilities, Vol. 2, NSRDS-NBS22(Washington, D. C.:U. S. Government Printing Office).

Wolff, S. C. 1967a, Ap. J. Suppl., 15, 21.

-----. 1967b, in The Magnetic and Related Stars, ed. by R. C. Cameron (Baltimore:Mono Book Corp.),p.363.

-----. 1969, Ap. J., 157, 253.

-----. 1971(private communication).

Wolff, S. C., Kuhi, L. V., and Hayes, D. 1968, Ap. J., 152, 871.

Wolff, S. C., and Wolff, R. J. 1971, A. J., 76, 422.

Wolnik, S. J., Berthel, R. O., Carnevale, E. H., and Wares, G. W. 1969, Ap. J., 157, 983.

Wolnik, S. J., Berthel, R. O., Larson, G. S., Carnevale, E. H., and Wares, G. W. 1968, Phys. Fluids, 11, 1002.

Wolnik, S. J., Berthel, R. O., and Wares, G. W. 1970, Ap. J., 162, 1037.

-----. 1971, Ap. J. (Letters), 166, L31.

Wright, K. O., Lee, E. K., Jacobson, T. V., and Greenstein, J. L. 1964, Pub. Dom. Ap. Obs. Victoria, 7, 173.

Wrubel, M. H. 1950, Ap. J., 111, 157.

Zirin, H. 1968, Ap. J. (Letters), 152, L177.